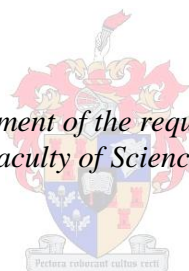


# **The Design and Synthesis of Novel HIV-1 Non-nucleoside Reverse Transcriptase Inhibitors**

by  
Nicole Pribut

*Thesis presented in fulfilment of the requirements for the degree of  
Master of Science in the Faculty of Science at Stellenbosch University*



Supervisor: Dr Stephen C. Pelly  
Co-supervisor: Prof Willem A. L. van Otterlo

March 2015

## **DECLARATION**

By submitting this thesis electronically, I declare that the entirety of the work contained therein is my own, original work, that I am the authorship owner thereof (unless to the extent explicitly otherwise stated) and that I have not previously in its entirety or in part submitted it for obtaining any qualification.

Date: December 2014

Copyright © 2015 Stellenbosch University

All rights reserved

## ABSTRACT

Since its discovery in the 1980's, HIV has affected the lives of millions of individuals around the globe. Despite obvious need and an enormous amount of research a cure has remained elusive due to the rapid onset of mutated forms of the virus. However, there has been considerable success in reducing viral levels of infected individuals through the use of highly active antiretroviral therapy (HAART). The first-line regimen HAART mainly targets reverse transcriptase (RT) through the employment of two nucleoside RT inhibitors (NRTIs) and a non-nucleoside RT inhibitor (NNRTI). NNRTIs target an allosteric pocket situated about 10 Å from the catalytic site and cause a conformational change in the enzyme upon binding, leading to the inhibition of viral replication. There are currently 5 FDA approved NNRTIs on the market which successfully inhibit viral replication, but the use of these drugs is becoming limited due to the onset of drug resistant strains of the virus.

In light of this need for the development of novel NNRTIs, we set out to explore new territory in NNRTI drug design with a goal of maintaining efficacy in the presence of both wild-type and mutated forms of HIV-1. To this end we designed three different NNRTI scaffolds along three different research thrusts.

The first of these focused on the synthesis of 15 novel flexible triazole containing compounds. With these compounds we sought to achieve  $\pi$ - $\pi$  stacking interactions with conserved amino acid residue Trp229 in the hope that we would be able to maintain efficacy in the presence of mutated forms of the virus. An additional feature included hydrogen bonding interactions to the backbone of Lys103. However, despite having thoroughly explored the triazole ring with multiple substitution arrangements, these compounds had very poor to no activity against whole cell HIV-1.

Secondly we focused on the synthesis of a 4-hydroxyindole scaffold as a potential NNRTI. The focus here was to achieve interactions to Trp229 and simultaneously achieve hydrogen bonding interactions to the backbone of Lys101 at the entrance of the pocket. This was a novel concept in this class of compounds. We were able to successfully synthesize the indole core as a proof-of-concept using the Knoevenagel-Hemetsberger method however; this compound had no activity against HIV-1.

Lastly, in our quest to synthesize a novel NNRTI that could maintain efficacy against HIV-1 we decided to attempt to improve upon the stability of a lead indole-based compound synthesized previously within our research group. The lead compound was found to be potent with an  $IC_{50}$  of 1 nM but was unstable in acidic media due to the presence of a methoxy functionality situated at the 3-position on the indole. We sought to overcome this issue by introducing a substituted aryl amine functionality at this position. We were successful in synthesizing our desired compound but unfortunately it was significantly less active against whole cell HIV-1 than the lead compound. However, we were not completely deterred as there are a number of unexplored bioisosteres as possibilities to improve upon the stability of the lead compound while maintaining its excellent activity profile.

## UITREKSEL

Sedert die ontdekking van die menslike immunitievirus (MIV) in die 1980's, het die virus al die lewens van miljoene mense wêreldwyd geaffekteer. Ten spyte van die ooglopende behoefte aan 'n geneesmiddel sowel as meer navorsing, bly 'n keermiddel sover onbekombaar as gevolg van die verskillende mutasies wat binne die virus gebeur. Ten spyte hiervan, was daar al heelwat sukses in terme van 'n verlaging van die virale vlakke in besmette individue deur die gebruik van hoogsaktiewe antiretrovirale terapie (HAART). As 'n eerste behandeling, teiken HAART meestal trutranskriptase (RT) deur die inspanning van twee nukleosied trutranskriptase inhibeerders (NRTIs) en 'n nie-nukleosied trutranskriptase inhibeerder (NNRTI). NNRTIs teiken 'n allosteriese leemte wat ongeveer 10 Å weg van die katalitiese posisie is en veroorsaak dan 'n konformasie verandering in die ensiem tydens die bindingsproses, wat dan lei tot die inhibisie van die virus se replikasie. Daar is tans 5 FDA goedgekeurde NNRTIs op die mark wat virale replikasie inhibeer, maar die gebruik van hierdie middels word alhoemmer belemmer as gevolg van die ontwikkeling van weerstandige stamme van die virus.

Met die oog op hierdie nood aan die ontwikkeling van nuwe NNRTIs, het ons gepoog om new gebiede te ondersoek in terme van die ontwerp van NNRTIs, met die doel om die effektiwiteit teen beide die wilde-tipe sowel as die gemuteerde vorme van HIV-1 te behou. Vir hierdie doeleindes het ons drie verskillende NNRTI steiers ontwerp, wat drie navorsingsdoeleindes na streef.

Die eerste van hierdie doeleindes was die sintese van 15 nuwe buigsame triasool-bevattende middels. Met hierdie middels het ons gepoog om  $\pi$ - $\pi$  pakkingsinteraksies te behaal met aminosuur residu, Trp229, en sodoende die effektiwiteit van die NNRTIs in die gemuteerde vorm van die virus te behou. 'n Additionele eienskap wat bygevoeg is, is 'n waterstof-bindingsinteraksie met die ruggraat van Lys103. Ten spyte van pogings om verskeie substitusie patrone om die triasool-ring te ondersoek, het hierdie middels baie swak tot geen aktiwiteit teen heel sel HIV-1 getoon nie.

Tweedens, was die fokus op die sintese van 'n 4-hidroksieindool steier as 'n potensiele NNRTI. Die fokus hier was om 'n interaksie met Trp229 te kry terselfdetyd as 'n waterstof-bindingsinteraksie met die ruggraat van Lys101, wat by die opening van die bindingssak is. Hierdie was 'n nuwe konsep vir hierdie klas van middele. Ons het die indool-kern van hierdie molekules suksesvol gesintetiseer deur middel van 'n Knoevenagel-Hemetsberger metode, maar ongelukkig het hulle geen aktiwiteit teen HIV-1 getoon nie.

Laastens het ons gepoog om 'n nuwe NNRTI te sintetiseer wat effektiwiteit teen HIV-1 behou, deur te probeer om vorderings te maak op die stabiliteit van 'n indool-gebaseerde hoof-middel wat al voorheen deur ons navorsingsgroep gerapporteer is. Hierdie hoof-middel het 'n IC<sub>50</sub> waarde van 1 nM gelewer, maar was onstabiel in suur medium as gevolg van die teenwoordigheid van 'n metoksie-groep in die 3-posisie van die indool. Ons het gepoog om hierdie probleem te oorkom deur 'n gesubstitueerde ariëlamien in hierdie posisie te plaas. Ons was suksesvol hierin, maar ongelukkig was die middel heelwat minder aktief teen die heel sel HIV-1 as die metoksie-weergawe. Ten spyte hiervan, is ons optimisties dat ons hierdie probleem kan oorkom, aangesien daar verskeie bioisostere is wat die stabiliteit van middel kan verbeter terwyl dit moontlik die effektiwiteit kan behou.



## ACKNOWLEDGEMENTS

### Personal Acknowledgements

Growing up my late grandmother always used to drill into my head that there was no such thing as “I can’t” and “it is impossible” and that everything could be achieved if you put your mind to it and worked hard for it. Admittedly there have been many a time where I seriously doubted these words but with patience and perseverance it turns out that the wise lady had a point. However, what she failed to mention is that everything is made easier with the help and support of the people around you.

It is on this note that I would firstly like to thank my supervisor, Dr Stephen C. Pelly for his unwavering support, patience and guidance throughout this project. Without which I would not have the confidence and skill in the lab that I feel I have today. Thank you for the innumerable laughs (not to mention beers) that have made many a frustrating day in the lab brighter. Your enthusiasm for medicinal chemistry is contagious.

To my co-supervisor, Prof Willem A. L. van Otterlo, thank you for the advice and input you have given in this project.

Thank you to Dr Jaco Brand and Ms Elsa Malherbe for all the NMR spectra, those 1D NOEs in particular. Thank you to CAF and Dr Marietjie Stander for the MS data.

I would also like to thank Dr Adriaan E. Basson at the National Institute for Communicable Diseases (NICD) for running all the biological assays for my compounds. I promise I’ll be sending you something exciting (by that I mean active) soon enough.

To the numerous members of the group of medicinal and organic chemistry (GOMOC) you are truly unique. It is not often that you end up with such a tight-knit group such as ours. I would like to give a special thank you to my lab partner in crime Tanya. Thank you for putting up with my mad ranting and raving. You have often helped me out more than you know and have definitely made working in the lab enjoyable. I dread the day you’ll leave me in that little lab all by myself.

Lastly and most importantly I have to give thanks to my family and friends (you know who you are) without you I would not be where I am today. Thank you for always having such a fierce and steadfast belief in me. Mom, without you I wouldn’t be who I am today. To my dad, thank you for the occasional whack on the head with a calculator encouraging me to broaden my mind and think out of the box. Devin, my big baby brother, I am your biggest fan! I know you will always have my back.

## **Acknowledgements for Funding**

Unfortunately, money does not grow on trees and without the proper funding this MSc would not be possible and I would probably still be waiting tables.

Therefore, I would like to thank the National Research Foundation (NRF) for their generous contribution in the form of a bursary.

DECLARATION.....	i
ABSTRACT.....	ii
UITREKSEL.....	iii
ACKNOWLEDGEMENTS.....	iv
Personal Acknowledgements .....	iv
Acknowledgements for Funding .....	v
Chapter 1: The Discovery of HIV as the Cause of AIDS, Global Impact and Treatment.....	1
1.1. Introduction to HIV .....	1
1.2. Mode of Infection.....	2
1.3. Antiretroviral Treatments.....	4
1.3.1. Nucleoside Reverse Transcriptase Inhibitors (NRTIs).....	5
1.3.2. Nucleotide Reverse Transcriptase Inhibitors (NtRTIs).....	7
1.3.3. Protease Inhibitors (PIs) .....	7
1.4. Newer Classes of Anti-retrovirals .....	9
1.4.1. Integrase Strand Transter Inhibitors (INSTIs).....	9
1.4.2. Fusion Inhibitors.....	10
1.4.3. Entry Inhibitors.....	10
1.5. Non-nucleoside Reverse Transcriptase Inhibitors (NNRTIs).....	11
1.5.1. Allosteric Inhibition of HIV-1 Reverse Transcriptase .....	11
1.5.2. First Generation NNRTIs .....	12
1.5.3. Second Generation NNRTIs .....	13
Chapter 2: Introducing Our Strategy.....	16
2.1. The emergence of drug resistance as a setback to controlling viral levels of infected individuals.....	16
2.2. Strategies employed in the design of novel NNRTIs to overcome resistance.....	17
2.2.1. A promising NNRTI candidate, lersivirine .....	17
2.2.2. Other examples of attempts to overcome resistance by targeting conserved residues within the NNIBP.....	19
2.3. Our Strategy.....	20
2.3.1. Synthesis of a small triazole library.....	21
2.3.2. An indole based scaffold designed to target Trp229 and Lys101 .....	21
2.3.3. An extension of previous work.....	22
Chapter 3: Synthesis of a Small Triazole Library .....	23
3.1. Establishing a Proof-of-Concept.....	23
3.2. The use of triazole rings in drug design.....	24
3.3. Introducing Click Chemistry.....	25

3.4.	Synthesis of Azide Fragments for Triazole Ring Synthesis.....	25
3.4.1.	Nucleophilic substitution reactions with sodium azide .....	25
3.4.2.	Employing a Modified Appel reaction for the synthesis of the desired azides from benzylic alcohols .....	27
3.5.	The Cu <sup>I</sup> Catalyzed Huisgen Cycloaddition Reaction.....	28
3.5.1.	Synthesis of the 1,4-triazole series of compounds .....	30
3.5.2.	Confirmation of regiochemistry .....	31
3.6.	Efficacy results of the 1,4-triazole series.....	33
3.7.	Attempts to introduce an ethyl chain onto the triazole ring.....	34
3.8.	The Ru <sup>II</sup> Catalysed Huisgen Cycloaddition Reaction.....	35
3.8.1.	Synthesis of <i>tert</i> -butyl(hex-3-yn-1-yloxy)dimethylsilane (38).....	37
3.8.2.	Synthesis of fully substituted triazole series of compounds .....	38
3.8.3.	Deprotection of fully substituted triazole compounds .....	39
3.8.4.	Employing NOE experiments to distinguish between the two regioisomers.....	39
3.9.	Efficacy results for fully substituted triazole compounds.....	42
3.10.	Synthesis of 2 <i>N</i> -triazole regioisomers 47 .....	44
3.10.1.	Attempts to synthesize 1,3-dimethyl-5-(pent-2-yn-1-yl)benzene (48).....	44
3.10.2.	Synthesis of 1-(3,5-dimethylphenyl)pent-2-yn-1-one (53).....	45
3.10.3.	Synthesis of (3,5-dimethylphenyl)(5-ethyl-2 <i>H</i> -1,2,3-triazol-4-yl)methanone (54) 46	
3.10.4.	Synthesis of (3,5-dimethylphenyl)(5-ethyl-2-(2-hydroxyethyl)-2 <i>H</i> -1,2,3-triazol-4-yl)methanone (42) .....	47
3.10.5.	Attempts to reduce the benzylic ketone to the corresponding alkane.....	47
3.10.6.	Confirmation of the structure of 2-(4-(3,5-dimethylbenzyl)-5-ethyl-2 <i>H</i> -1,2,3-triazol-2-yl)ethanol (47).....	49
3.11.	Efficacy results of 2-(4-(3,5-dimethylbenzyl)-5-ethyl-2 <i>H</i> -1,2,3-triazol-2-yl)ethanol (47) 51	
Chapter 4:	A Novel Concept - Targeting Trp229, Tyr188 and Lys101 .....	51
4.1.	Indole-based NNRTIs.....	51
4.2.	Introducing a novel concept .....	52
4.3.	Synthesizing the precursors for the Knoevenagel-Hemetsberger reaction.....	54
4.3.1.	Employing an Ullmann-type coupling reaction to form the biaryl aldehyde precursor.....	54
4.4.	Initial attempts to synthesize the indole product.....	56
4.4.1.	Employing the Knoevenagel condensation reaction to synthesize the acrylate precursor.....	56
4.4.2.	Describing the Hemetseberger indolization reaction. ....	58

4.5.	Functionalizing the 3-position of the indole.....	59
4.5.1.	The Friedel-Crafts acylation reaction.....	60
4.5.2.	Reduction of the ketone to the desired alkyl substituent.....	61
4.5.2.1.	Synthesis of ethyl-4-(3,5-dimethylphenoxy)-3-ethyl-1H-indole-2-carboxylate (79) .....	62
4.6.	Introducing a halogen at the 5-position in an attempt to improve activity.....	62
4.6.1.	Our attempts to introduce a fluorine onto the indole scaffold.....	63
4.7.	Analysis of the NOE results to determine the position of the fluorine.....	65
4.8.	Removal of the Boc protecting group and subsequent NMR analysis.....	66
4.9.	A study of the crystal structure reveals the cause of the observed anomalies in previous characterisation analyses.....	68
4.10.	Attempts to remove the ester functionality at position 2 using a quinoline/copper mediated decarboxylation reaction.....	70
4.10.1.	Synthesis of 4-(3,5-dimethylphenoxy)-1H-indole-2-carboxylic acid (88).....	70
4.10.2.	Synthesis of 4-(3,5-dimethylphenoxy)-1H-indole (89).....	71
4.11.	Efficacy results for the unfunctionalized 4-phenoxy indole (89).....	72
Chapter 5: The Design and Synthesis of a 3-Aminoindole-Based Scaffold as an Extension of a Lead Compound.....		73
5.1.	The rationale behind our design.....	73
5.2.	The paper behind our initial synthetic strategy.....	76
5.2.1.	Synthesis of ethyl 3-bromo-5-chloro-1H-indole-2-carboxylate (99).....	77
5.2.2.	Ullmann-type coupling in an attempt to obtain amine 100.....	78
5.3.	The search for an alternative aryl amination strategy.....	78
5.3.1.	Attempting a Buchwald-Hartwig Reaction procedure.....	78
5.3.2.	A final attempt to obtain compound 4 employing a coupling reaction procedure.....	80
5.4.	Changing direction in our synthetic strategy.....	80
5.4.1.	Synthesis of ethyl (4-chloro-2-cyanophenyl)carbamate (115).....	82
5.4.2.	Synthesis of diethyl 3-amino-5-chloro-1H-indole-1,2-dicarboxylate (116).....	82
5.5.	Functionalizing the Amine.....	83
5.5.1.	Synthesis of diethyl 5-chloro-3-(phenylamino)-1H-indole-1,2-dicarboxylate (117) 83	
5.5.2.	Synthesis of diethyl 5-chloro-3-(ethyl(phenyl)amino)-1H-indole-1,2- dicarboxylate (118).....	84
5.5.3.	An attempted deprotection to afford our target compound (5).....	84
5.5.4.	A last attempt to optimize the alkylation reaction.....	85
5.6.	Identifying the two products.....	87

5.6.1. Another attempt at the deprotection to yield ethyl 5-chloro-3-(ethyl(phenyl)amino)-1 <i>H</i> -indole-2-carboxylate (5).....	88
5.7. Efficacy results.....	88
Chapter 6: Conclusion.....	92
Chapter 7: Future Work.....	93
7.1. A revision of our 4-hydroxyindole target.....	93
7.2. Exploring a variety of bioisosteres to improve the stability of a lead compound.....	93
7.3. Getting creative and introducing an oxetane ring.....	95
Chapter 8: Experimental.....	96
8.1. General Procedures.....	96
8.1.1. Purification of Reagents and Solvents.....	96
8.1.2. Chromatography.....	96
8.1.3. Spectroscopic and physical data.....	96
8.1.4. Other general procedures.....	96
8.2. Experimental Procedures Pertaining to Chapter 3.....	97
8.2.1. Synthesis of (azidomethyl)benzene (7).....	97
8.2.2. Synthesis of 1-(azidomethyl)-3,5-bis(trifluoromethyl)benzene (9).....	97
8.2.3. Synthesis of 3-(azidomethyl)benzotrile (11).....	98
8.2.4. Synthesis of 1-(azidomethyl)-3,5-dichlorobenzene (14).....	98
8.2.5. Synthesis of 1-(azidomethyl)-3,5-dimethylbenzene (23).....	98
8.2.6. Synthesis of (1-benzyl-1 <i>H</i> -1,2,3-triazol-4-yl)methanol (29).....	99
8.2.7. Synthesis of 1-(azidomethyl)-3,5-bis(trifluoromethyl)benzene (30).....	99
8.2.8. Synthesis of (1-(3,5-dimethylbenzyl)-1 <i>H</i> -1,2,3-triazol-4-yl)methanol (31).....	99
8.2.9. Synthesis of 2-(1-(3,5-dimethylbenzyl)-1 <i>H</i> -1,2,3-triazol-4-yl)ethanol (32).....	100
8.2.10. Synthesis of 3-((4-(2-hydroxyethyl)-1 <i>H</i> -1,2,3-triazol-1-yl)methyl)benzotrile (33)	100
8.2.12. Synthesis of <i>tert</i> -butyl(hex-3-yn-1-yloxy)dimethylsilane (38).....	100
8.2.13. Synthesis of 2-(1-benzyl-4-ethyl-1 <i>H</i> -1,2,3-triazol-5-yl)ethanol (43A) and 2-(1-benzyl-5-ethyl-1 <i>H</i> -1,2,3-triazol-4-yl)ethanol (43B).....	101
8.2.14. Synthesis of 2-(1-(3,5-dichlorobenzyl)-4-ethyl-1 <i>H</i> -1,2,3-triazol-5-yl)ethanol (44A) and 2-(1-(3,5-dichlorobenzyl)-5-ethyl-1 <i>H</i> -1,2,3-triazol-4-yl)ethanol (44B).....	102
8.2.15. Synthesis of 3-((4-ethyl-5-(2-hydroxyethyl)-1 <i>H</i> -1,2,3-triazol-1-yl)methyl)benzotrile (45A) and 3-((5-ethyl-4-(2-hydroxyethyl)-1 <i>H</i> -1,2,3-triazol-1-yl)methyl)benzotrile (45B).....	102
8.2.16. Synthesis of 2-(1-(3,5-dimethylbenzyl)-4-ethyl-1 <i>H</i> -1,2,3-triazol-5-yl)ethanol (46A) and 2-(1-(3,5-dimethylbenzyl)-5-ethyl-1 <i>H</i> -1,2,3-triazol-4-yl)ethanol (46B).....	103
Unfortunately we were unable to isolate the desired 1,4-regioisomer 46B.....	103

8.2.17.	Synthesis of (3,5-dimethylphenyl)(5-ethyl-2 <i>H</i> -1,2,3-triazole-4-yl)methanone (54)	103
8.2.18.	Synthesis of (3,5-dimethylphenyl)(5-ethyl-2-(2-hydroxyethyl)-2 <i>H</i> -1,2,3-triazol-4-yl)methanone (55) .....	104
8.2.19.	Synthesis of 2-(4-((3,5-dimethylphenyl)(hydroxyl)methyl)-5-ethyl-2 <i>H</i> -1,2,3-triazol-2-yl)ethanol (56).....	105
8.2.20.	Synthesis of 2-(4-(3,5-dimethylbenzyl)-5-ethyl-2 <i>H</i> -1,2,3-triazol-2-yl)ethanol (47)	105
8.3.	Experimental Procedures Pertaining to Chapter 4 .....	106
8.3.1.	Synthesis of 2-(3,5-dimethylphenoxy)benzaldehyde (69) .....	106
8.3.2.	Synthesis of ethyl azidoacetate (64).....	106
8.3.3.	Synthesis of ( <i>Z</i> )-ethyl 2-azido-3-(2-(3,5-dimethylphenoxy)phenyl)acrylate (68)	107
8.3.4.	Synthesis of ethyl 4-(3,5-dimethylphenoxy)-1 <i>H</i> -indole-2-carboxylate (77).....	107
8.3.5.	Synthesis of 4-(3,5-dimethylphenoxy)-1 <i>H</i> -indole-2-carboxylic acid (88) .....	108
8.5.6.	Synthesis of 4-(3,5-dimethylphenoxy)-1 <i>H</i> -indole (89) .....	108
8.4.	Experimental Procedures Pertaining to Chapter 5 .....	108
8.4.1.	Synthesis of ethyl 3-bromo-5-chloro-1 <i>H</i> -indole-2-carboxylate (99).....	108
8.4.2.	Synthesis of ethyl (4-chloro-2-cyanophenyl)carbamate (115).....	109
8.4.3.	Synthesis of diethyl 3-amino-5-chloro-1 <i>H</i> -indole-1,2-dicarboxylate (116).....	109
8.4.4.	Synthesis of diethyl 5-chloro-3-(phenylamino)-1 <i>H</i> -indole-1,2-dicarboxylate (117)	110
8.4.5.	Synthesis of diethyl 5-chloro-3-(ethyl(phenyl)amino)-1 <i>H</i> -indole-1,2-dicarboxylate (118) .....	110
8.4.6.	Synthesis of ethyl 5-chloro-3-(ethyl(phenyl)amino)-1 <i>H</i> -indole-2-carboxylate (5)	111
Chapter 9:	References.....	111

## **Chapter 1: The Discovery of HIV as the Cause of AIDS, Global Impact and Treatment**

### **1.1. Introduction to HIV**

It was in the early 1980's that researchers discovered that a retrovirus was responsible for the onset of the acquired immuno-deficiency syndrome (AIDS). This retrovirus, believed to originate from a subspecies of Central West African chimpanzee *Pan troglodytes troglodytes*, was first isolated from a patient with lymphadenopathy suspected to have AIDS.<sup>1</sup> As a result, this retrovirus was originally called the lymphadenopathy-associated virus (LAV) but soon after came to be known as the human immunodeficiency virus (HIV) due to the fact that the presence of HIV went hand in hand with a notable decline in CD4 T-cells which play an important role in the adaptive immune response.<sup>2-4</sup>

This discovery of HIV as the cause of AIDS came unexpectedly during a time when many people thought that epidemic diseases did not afflict first world countries. Moreover, it was believed that AIDS was perhaps caused by autoimmunity to white blood cells, fungi or even chemicals.<sup>3</sup> <sup>5</sup>The discovery of HIV as the cause of AIDS was made possible due to the earlier discovery of the human T-cell leukemia virus (HTLV) types 1 and 2. The techniques for the identification and characterization of these retroviruses were made available with the discovery of reverse transcriptase by Temin and Baltimore almost ten years earlier in 1970. This led researchers to believe that AIDS would be caused by a retrovirus within the HTLV family. Although this theory was not entirely correct it did point researchers in the right direction for the discovery of HIV.<sup>3,5</sup>

Since this discovery HIV has earned the reputation as the most formidable pandemic affecting millions around the globe. The impact of HIV on society extends further than public health as it affects the economic growth, poverty, politics and society on a social level.<sup>6,7</sup> According to the World Health Organization (WHO) and UNAIDS 2013 global report there were in 2012 an estimated 35 million people living with HIV worldwide, with 70% of that population inhabiting Sub-Saharan Africa. They also reported an estimated 2.3 million new infections and 1.6 million AIDS related deaths in the same year.<sup>8</sup> In Sub-Saharan Africa, South Africa has the highest reported incidence of HIV in the world, with an estimated 6.1 million individuals infected with HIV.<sup>8</sup> The worst afflicted province is Kwazulu-Natal (KZN), which is probably linked to the high rate of unemployment, poverty and the social stigma often associated with infection.<sup>9</sup> HIV-related stigma and discrimination significantly hinders preventative measures as it often leads to the refusal of infected individuals to seek treatment, to adhere to the prescribed treatment and to disclose their HIV status to respective partners.<sup>6</sup> Of concern is that these statistics are conservative and it is estimated that in Sub-Saharan Africa more than half of the population living with HIV are unaware of their HIV status.<sup>10</sup>



## 1.2. Mode of Infection

Although it is possible to acquire HIV through several accidental modes of contact such as blood transfusion, sexual transmission still accounts for almost 80% of HIV infection.<sup>11</sup> One of the biggest travesties is mother-to-child transmission where during birth, blood contact with the infected mother may well lead to an infected infant.

For viral infection to occur the HI virus, which is enveloped in a viral envelope protein, targets the CD4 receptor molecule found primarily on T-lymphocytes, macrophages and dendritic cells.<sup>12</sup> The HI virus is then able to bind to the CD4 receptor with the aid of the viral envelope cell surface attachment glycoprotein gp120, which protrudes out from the viral envelope (Figure 1). The initial formation of the CD4/gp120 complex then allows for gp120 to associate with chemokine co-receptors, CCR5 or CXCR4, located on the host cell lipid membrane. The binding of gp120 with CD4 and the coreceptor triggers a conformational change in gp120 which exposes the viral transmembrane glycoprotein, gp41, which initiates the fusion of the viral envelope membrane with the plasma membrane of the host cell.<sup>12</sup> The fusion of viral and host cell membranes leads to the release of the viral nucleocapsid, which contains the viral RNA and enzymes, into the cytoplasm of the host cell.<sup>13</sup> After entry into the cytoplasm the viral capsid is removed and the viral core is released. At this point the enzyme reverse transcriptase transcribes the viral RNA into the complementary double-stranded viral DNA.<sup>13</sup>

The newly transcribed DNA is then transported into the nucleus of the host cell where the viral integrase catalyzes the incorporation of the viral DNA into the host cell genome.<sup>13</sup> The integrated viral DNA is now referred to as the “provirus” and can behave as a cellular gene and serve as a template for the transcription of new viral RNAs and mRNAs that are responsible for the translation of the structural, regulatory and accessory proteins needed for viral replication.<sup>13, 14</sup> The newly synthesized mRNA leaves the host nucleus and uses host ribosomes for the translation of non-functional precursor polyproteins Gag and Gagpol. The Gag precursor protein codes for all the structural viral proteins and the Gagpol precursor protein codes for the viral enzymes reverse transcriptase, integrase and protease.<sup>15</sup>

The Gag precursor polyproteins along with the newly transcribed viral RNA then target the host cell plasma membrane promoting encapsulation of the viral RNA and polyprotein precursors. This leads to the formation of new immature virus particles using the host cell plasma membrane to form the viral envelope. These immature progeny virions are then released from the host cell. During or after the budding of the progeny virion from the host plasma membrane, cleavage of the Gag and Gagpol polyprotein precursors by HIV protease generates the mature Gag and Gagpol proteins. This ultimately leads to virion maturation and the spread of infection to other host cells.<sup>13, 16</sup>

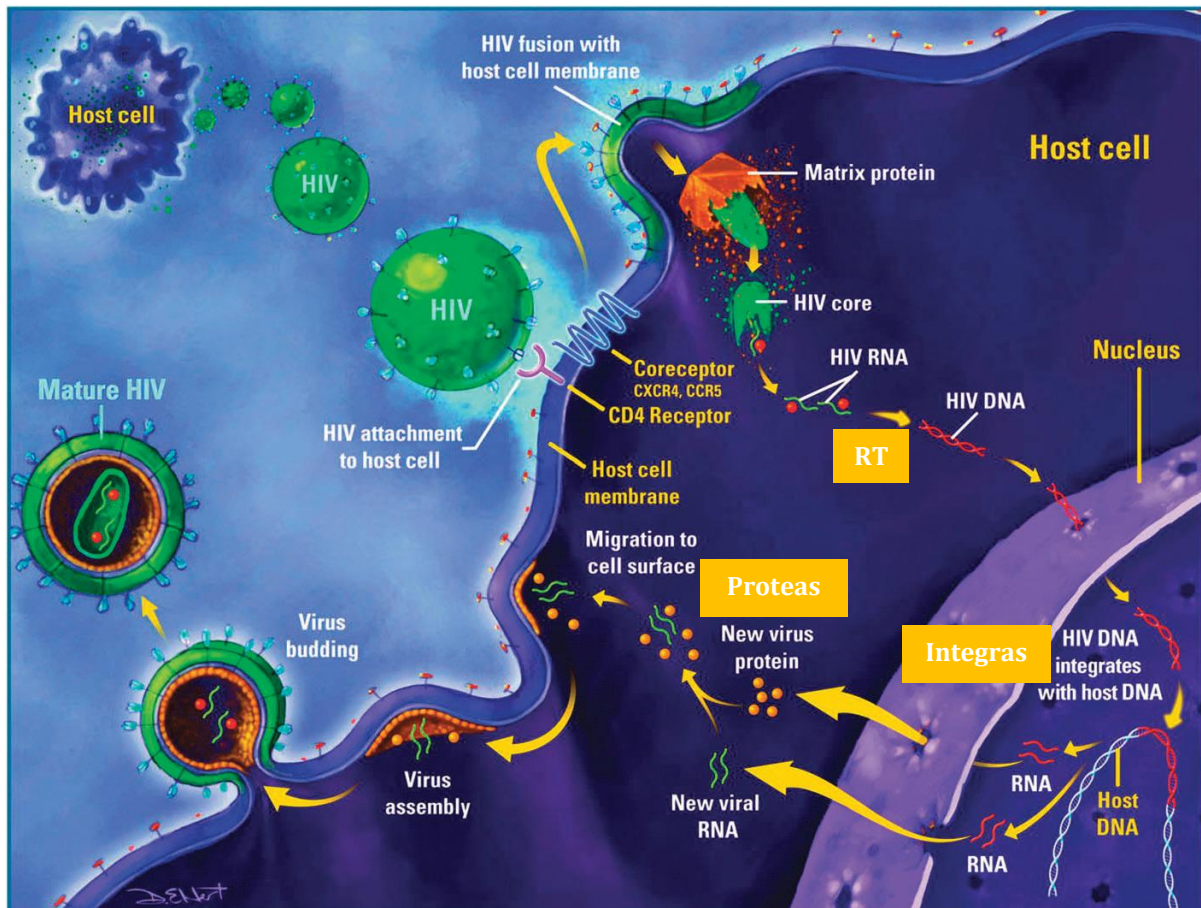


**Figure 1** HIV mode of infection and replication from Reynolds *et al.*<sup>14</sup>

With primary infection, viral replication occurs rapidly which results in a high incidence of viraemia. As the levels of HIV in the bloodstream increase, the number of CD4<sup>+</sup> T-cells decreases. At this point the majority of infected individuals show influenza-like symptoms. This is known as the acute stage of infection. Following this stage is the phase known as clinical latency, where viral levels in the bloodstream suddenly drop and CD4<sup>+</sup> T-cell levels rise. This is due to the fact that the immune system responds using CD8<sup>+</sup> T-cells and antibodies. Although viral levels drop at this stage, replication continues in viral reservoirs such as lymphoid organs. At the end of the clinical latency period, CD4<sup>+</sup> levels once again drop as the viral levels increase. The clinical latency period in the absence of treatment can last as long as 4 to 10 years. After the latency period, viral replication accelerates and a gradual decrease in the efficacy of the immune system is observed, resulting in the onset of opportunistic infections and it is at this point that the disease is regarded as having progressed to AIDS.

### 1.3. Antiretroviral Treatments

Although HIV has been fully characterized and its mode of infection and replication has been thoroughly studied, researchers have still not succeeded in creating a viable cure or vaccine against HIV. This can be attributed to the fact that HIV possesses a high mutation rate which makes it increasingly difficult to keep up with ever-changing therapeutic targets.<sup>17</sup> Despite this, researchers have had considerable success in reducing the viral load in infected individuals, thereby improving quality of life and preventing the onset of co-infections leading to the development of AIDS. This has been achieved through the use of highly active antiretroviral therapy (HAART), also known as triple therapy. As the latter suggests, this treatment makes use of a combination of three drugs, covering at least two classes of antiviral agents, to inhibit viral replication in infected individuals. The different classes are categorized according to their target for inhibition in the HIV replication cycle. Typically HAART consists of two nucleoside reverse transcriptase inhibitors (NRTIs) or nucleotide reverse transcriptase inhibitors (NtRTIs) in combination with either a non-nucleoside reverse transcriptase inhibitor (NNRTI) or a protease inhibitor (PI).<sup>18</sup>

The current first-line regimen recommended by the WHO in 2013 is to use the nucleotide reverse transcriptase inhibitor tenofovir disoproxil fumarate in combination with nucleoside reverse transcriptase inhibitor lamivudine and non-nucleoside reverse transcriptase inhibitor efavirenz.<sup>18</sup> The success of using HAART in the treatment of infected individuals has led to a decline of AIDS related deaths. The WHO has reported that AIDS related deaths are 2.3 million down from the number of deaths reported in 2005. Furthermore, the use of HAART has also led to a decline in the number of new infections to arise annually. In 2012 the number of new infections declined by 33% compared to the number of new infections in 2001.<sup>8</sup>

In the past, HAART was usually introduced for HIV infected individuals in the period between clinical latency and the development of AIDS.<sup>14</sup> In 2012, 9.7 million people were reported to be undergoing HAART which is an estimated 61% of those eligible for treatment. However, with the revision of the WHO guidelines this number dropped to only 34% of the population eligible for antiretroviral (ARV) treatment. This is due to the fact that the WHO has revised the recommended CD4 count for people living with HIV to be able to receive treatment. The new guidelines suggest that an infected individual with a CD4 count of  $\leq 500$  CD4 cells/mm<sup>3</sup> can initiate ARV treatment whereas previously only patients with a CD4 count  $\leq 350$  cells/mm<sup>3</sup> were eligible for ARV treatment.<sup>10</sup> Also, irrespective of the CD4 count, it has been ruled that HAART is to be initiated immediately for couples where the one partner is HIV positive, pregnant woman with HIV, individuals who also present coinfections such as tuberculosis and children under the age of 5 years.<sup>10</sup>

Currently 25 antiretroviral drugs have been approved by the Food and Drug Administration (FDA) for the use in the treatment of HIV infected individuals. These drugs fall into six categories and cover five therapeutic targets.<sup>19</sup>

### 1.3.1. Nucleoside Reverse Transcriptase Inhibitors (NRTIs)

The oldest class of antiretrovirals are nucleoside reverse transcriptase inhibitors (NRTIs) which target the polymerase active site of reverse transcriptase (RT). These molecules are analogues of naturally occurring nucleosides but they lack the 3' hydroxyl group required for the incorporation of nucleosides onto a growing DNA strand.<sup>20</sup> These NRTIs act as chain terminators and directly inhibit the transcription of viral RNA into the dsDNA required for HIV replication. However, NRTIs are regarded as prodrugs. This means that in order for these nucleoside analogues to be recognized by the DNA polymerase of RT and incorporated onto the propagating DNA chain, they have to first be activated to their triphosphate form by cellular kinases (Figure 2).<sup>20</sup> This requires three phosphorylation steps. Only once activated, can these analogues then compete with the naturally occurring nucleotides for incorporation onto the DNA strand.

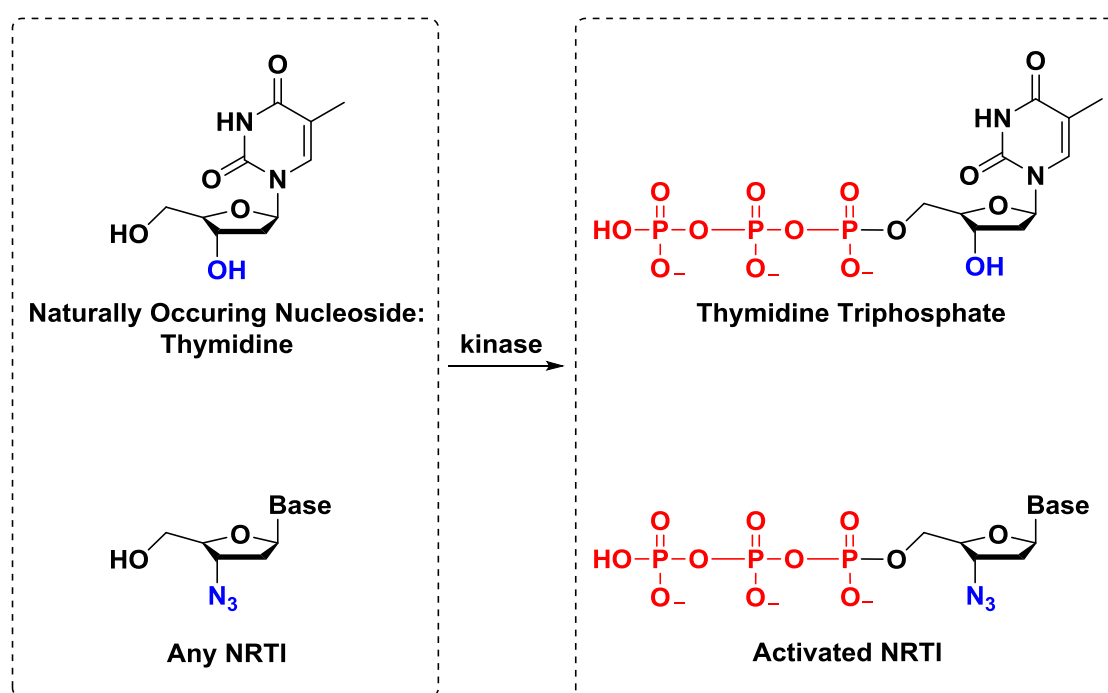


**Figure 2** Activation of nucleoside thymidine and an NRTI to the triphosphate form

3'-Azido-3'-deoxythymidine (AZT) or zidovudine (Retrovir®, Figure 3) which acts as a mimic of thymidine was the first drug to be approved by the FDA for the treatment of HIV in 1987. This discovery of AZT as a potent inhibitor of HIV, however, was a serendipitous one. AZT was originally synthesized in 1964 by Dr Jerome P. Horwitz as an anti-cancer agent but when tested in leukemic mice AZT was found to have no activity. As a result, AZT was for a while shelved and forgotten.<sup>21</sup> It was not until 1984 that AZT was rediscovered during a screening of a number of compounds against the Friend Leukemia Virus (FLV) and the Harvey Sarcoma Virus (HaSV), thought to be highly comparable to HIV. The results of this screening were exceptional as AZT was found to completely inhibit viral replication in both retroviruses and was soon after tested against HIV to give the same promising results. This chance discovery led to considerable expectation among researchers that this drug would allow for the eradication of HIV. This belief that AZT would be the 'wonder-drug' provided hope for many infected individuals worldwide.<sup>22</sup> However, due to the unforeseen onset of resistance the prescription of AZT only succeeded, on average, in prolonging the life of infected individuals by 18 months.<sup>23, 24</sup> This

meant that the search for a treatment against HIV, despite high expectations, had only just begun.

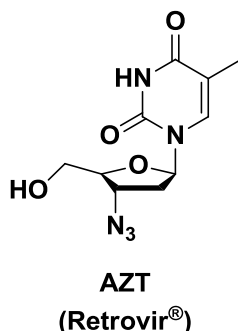


Figure 3 Azidothymidine (AZT)

In addition to AZT, six other NRTIs have been approved by the FDA for the treatment of HIV. These include lamivudine (Epivir<sup>®</sup>), emtricitabine (Emtriva<sup>®</sup>), zalcitabine (Hivid<sup>®</sup>), stavudine (Zerit<sup>®</sup>), didanosine (Videx<sup>®</sup>) and abacavir (Ziagen<sup>®</sup>) (Figure 4). These newer NRTIs often possess better long-term tolerability and safety. For example lamivudine, emtricitabine and tenofovir have none to almost no long-term adverse side effects.<sup>25</sup>

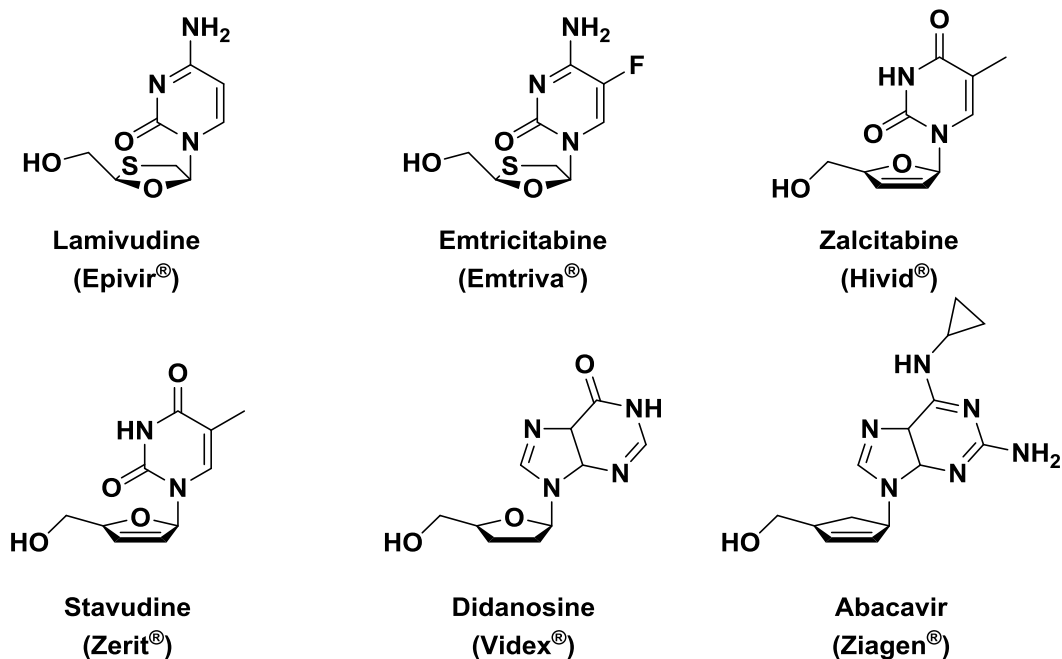


Figure 4 Some commercially available NRTIs

### 1.3.2. Nucleotide Reverse Transcriptase Inhibitors (NtRTIs)

Nucleotide reverse transcriptase inhibitors (NtRTIs) behave like NRTIs with regards to their mode of action. However, unlike NRTIs, they already contain one phosphonate group which cannot be cleaved by hydrolysis and, therefore, require only two phosphorylation steps to get to their active form.<sup>26</sup> This is highly advantageous as the first phosphorylation is the rate determining step *in vivo* and so by already incorporating one phosphonate group the process of converting the prodrug to the active triphosphate form is expedited. The only NtRTI that has been approved for the treatment of HIV is tenofovir disoproxil fumarate (Viread®, Figure 5) which is an adenosine nucleotide analogue. It is also the most widely prescribed drug in the treatment of HIV and is used in combination with other ARVs in both treatment naïve and treatment experienced patients.<sup>18</sup>

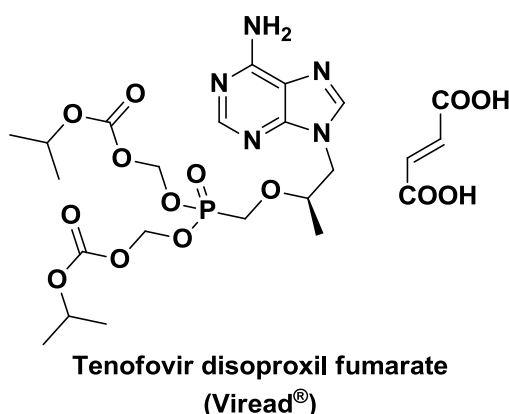
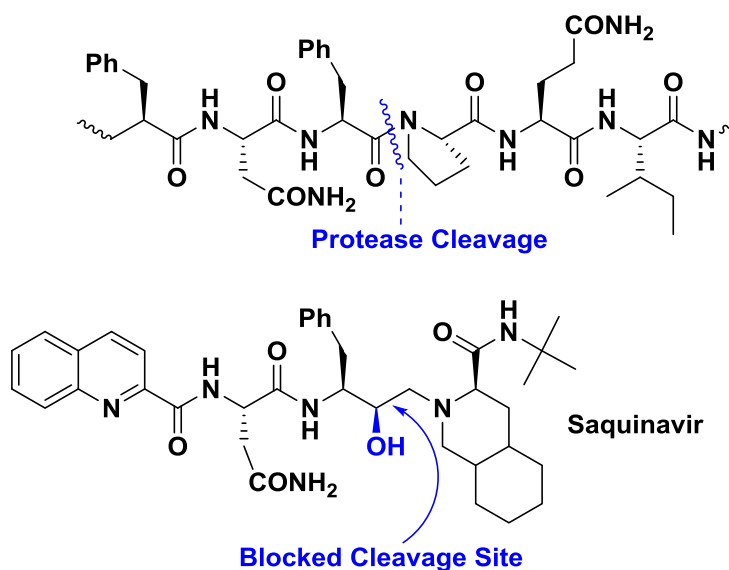


Figure 5

### 1.3.3. Protease Inhibitors (PIs)

Protease inhibitors are another class of therapeutic agents commonly used in HAART. HIV protease plays an important role in viral maturation as it is responsible for the generation of mature infectious HIV particles through the cleavage of viral Gag and GagPol precursor polypeptides into smaller proteins.<sup>15, 16</sup> Currently there are nine protease inhibitors (PIs) approved by the FDA for clinical use. PIs mimic the naturally occurring substrate of the HIV protease enzyme and can be divided into two categories, peptidomimetic inhibitors and non-peptidomimetic inhibitors, although the latter only refers to the PI tipranavir. The peptidomimetic PIs contain a hydroxyethylene core prohibiting cleavage of the PI by protease (Figure 6). As a result, competitive binding of the PI and subsequent failure to hydrolyse the drug results in deactivation of the enzyme.





**Figure 6** A representation of the protease cleavage site on a naturally occurring protease substrate (top) and the blocked site on protease inhibitor Saquinavir (bottom)

Saquinavir (Invirase®) was the first protease inhibitor approved by the FDA in 1995 (Figure 7).<sup>16</sup> Protease inhibitors that followed the approval of saquinavir were ritonavir (Norvir®) and indinavir (Crixivan®) in 1996. Ritonavir was poorly tolerated and was known to cause an elevation in cholesterol or triglycerides in the blood.<sup>25</sup> Ritonavir is now commonly used in combination with other PIs as a booster. Saquinavir, ritonavir and indinavir are all first generation PIs.

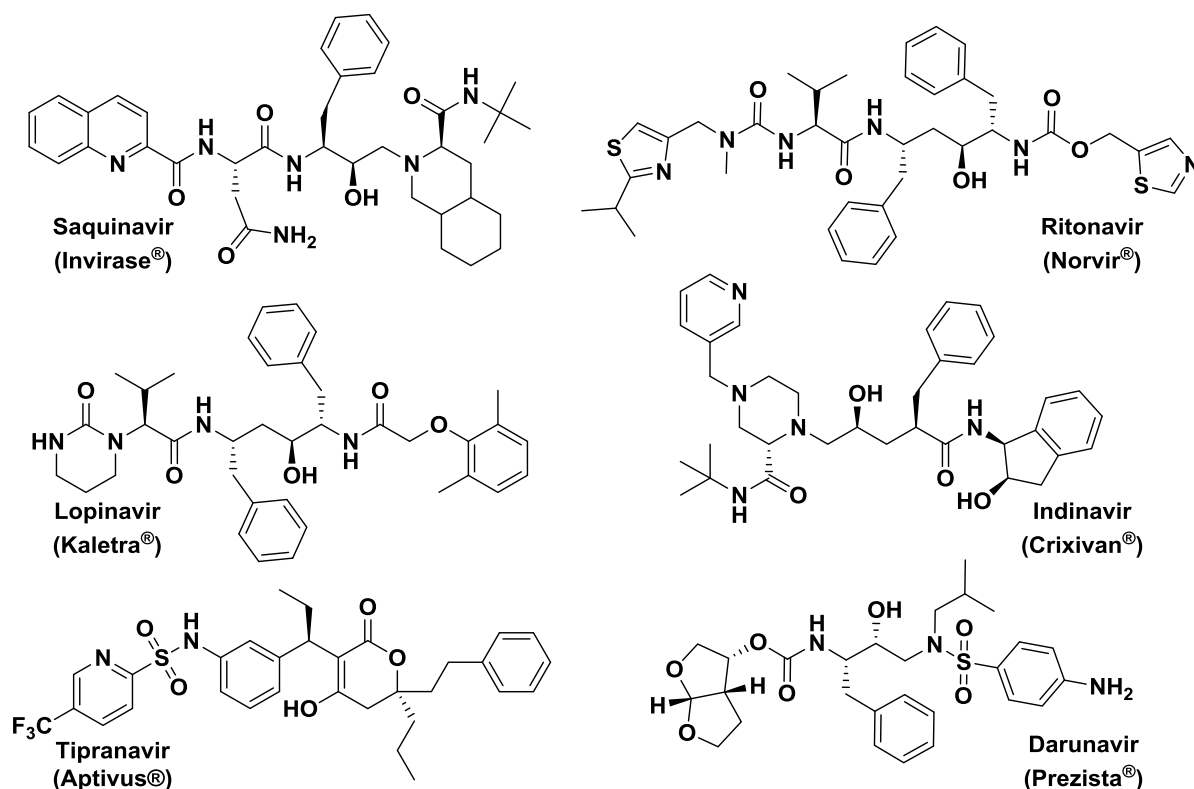


**Figure 7** Some commercially available PIs

Lopinavir (Kaletra®), darunavir (Prezista®) and tipranavir (Aptivus®) are all second generation PIs. Like most second generation inhibitors these PIs were developed to combat issues of resistance associated with earlier PIs.<sup>16</sup> Tipranavir is the only PI approved by the FDA that is non-peptidomimetic. Tipranavir is an important addition to the PI family as it has been shown to maintain efficacy against HIV strains that have resistance to other PIs.<sup>27</sup>

## 1.4. Newer Classes of Anti-retrovirals

### 1.4.1. Integrase Strand Transfer Inhibitors (INSTIs).

The newest class of antiretroviral drugs for the treatment of HIV infection are integrase inhibitors (Figure 8). These drugs target the integrase enzyme which catalyzes the insertion of the transcribed viral DNA into the genome of the infected host cell.

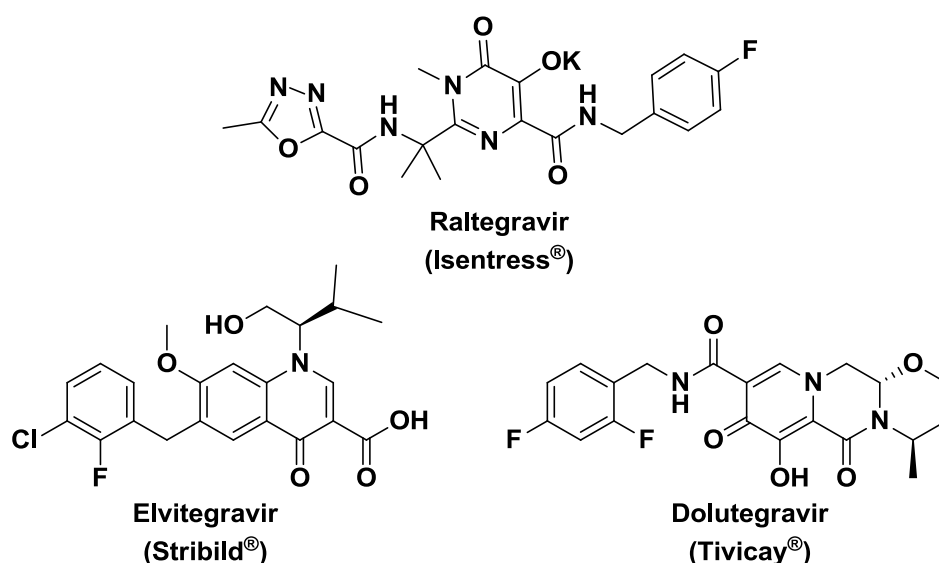


**Figure 8** The first three FDA approved INSTIs

Raltegravir (RAL, Isentress®) was the first integrase inhibitor approved for clinical use by the FDA in 2007.<sup>28</sup> This drug functions by blocking the active site of integrase and inhibiting strand transfer, thereby preventing the incorporation of the viral DNA into the host cell's genome.<sup>14, 29</sup> RAL, coadministered with an NNRTI or PI as a salvage therapy, is mostly given to treatment experienced patients where first line regimens have failed due to the onset of resistance and almost no treatment alternatives are available.<sup>29</sup> Unfortunately, RAL has a low genetic barrier to resistance and as a result, single point mutations can confer high level resistance. After the discovery of the first INSTI, further studies into this field led to the identification of elvitegravir (EVG, Stribild®) as another first generation INSTI. Like RAL, EVG was shown to be an effective INSTI in clinical trials but, unfortunately, also suffered a moderate genetic barrier to resistance.<sup>30</sup>

The moderate genetic barrier to resistance along with significant cross-resistance of first generation INSTIs led to the development of second generation INSTIs which would maintain efficacy in the presence of RAL and EVG resistant strains of the virus. The first of these to be



developed was dolutegravir (DTG, Tivicay®).<sup>31</sup> DTG is advantageous in that it can overcome resistance issues experienced by first generation INSTIs.<sup>32</sup>

### 1.4.2. Fusion Inhibitors

Enfuvirtide (Fuzeon®, Figure 9) is the first and only drug to be approved by the FDA as a fusion inhibitor. Enfuvirtide acts by binding to the transmembrane glycoprotein gp41, blocking the fusion of the viral envelope with the host cell plasma membrane.<sup>33</sup> It is a 36 amino acid synthetic peptide that stems from gp41.<sup>33</sup>

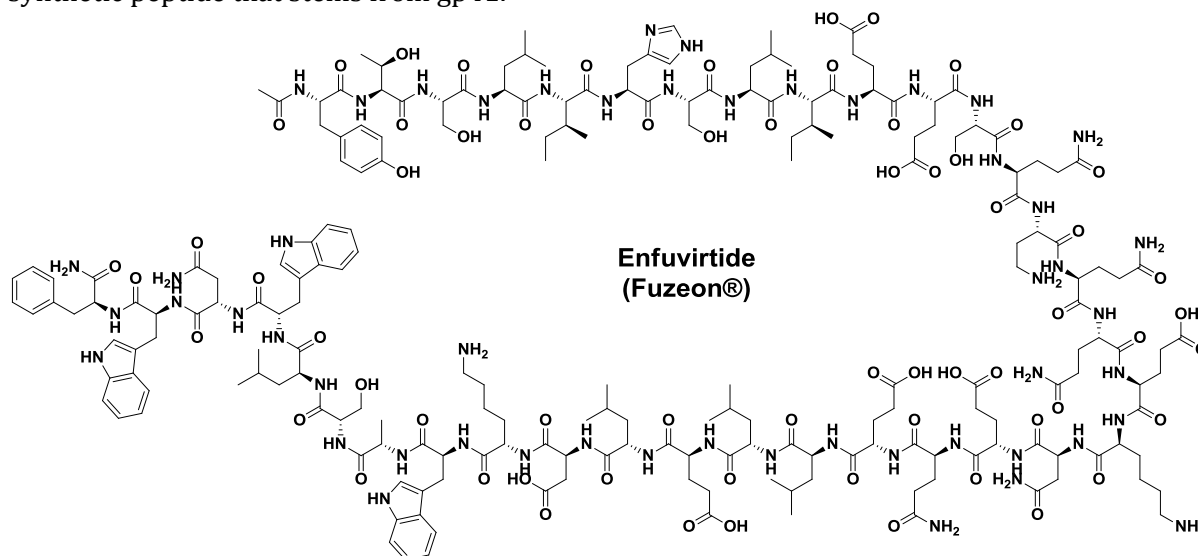


Figure 9

### 1.4.3. Entry Inhibitors

CCR5 is the predominant chemokine receptor targeted in early infection of HIV and is responsible for aiding the entry of HIV into the host cell. The chemokine co-receptor has become the latest target for antiviral therapy and is unique in the sense that this target is found on the host cell and is not a component of HIV.<sup>34</sup> Maraviroc (Selzentry®, Figure 10), which was approved for clinical use by the FDA in 2007, is the only small-molecule CCR5 chemokine receptor antagonist available on the market.<sup>34</sup> This drug inhibits HIV-1 entry into the host cell by blocking the interaction between the HIV-1 viral envelope and the chemokine receptor CCR5. However, maraviroc has little to no activity against the CXCR4 co-receptor or viruses that possess dual tropism.<sup>25</sup> Maraviroc is orally administered and only used for treatment experienced patients as a last resort.<sup>35</sup>

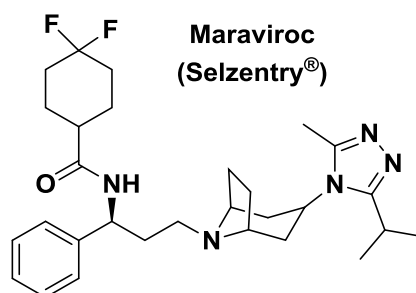
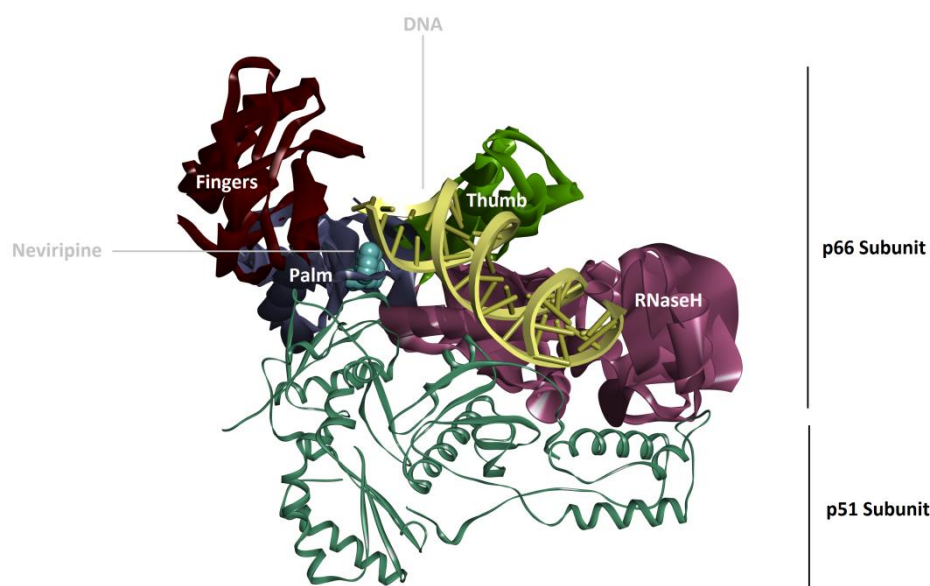


Figure 10 FDA approved entry inhibitor Maraviroc

## 1.5. Non-nucleoside Reverse Transcriptase Inhibitors (NNRTIs)

### 1.5.1. Allosteric Inhibition of HIV-1 Reverse Transcriptase

Reverse transcriptase plays a crucial role in the transcription of viral RNA into double stranded viral DNA and, as a result, is an important target for HIV replication inhibition. Reverse transcriptase is an asymmetric heterodimeric enzyme consisting of two subunits, p66 (66 kDa) and p51 (51 kDa) (Figure 11). The p51 and p66 subunits consist of the same amino acid sequence but possess differing tertiary structure.<sup>36</sup> The p66 unit comprises of the ribonuclease H (RNaseH) domain as well as four pol subdomains. The conformation of the p66 subunit is commonly likened to a right hand with three of the pol subdomains making up the fingers, palm and thumb. The palm domain contains the polymerase active site. The fingers subdomain holding down on the palm domain is the catalytic site. The fourth pol subdomain is called the connection domain, and lies between the RNaseH domain and the rest of the pol domain. The p66 domain has an open elongated conformation and plays a catalytic role in the enzyme. The p51 unit however, is more compact and seems to play a more structural role.<sup>36</sup>



**Figure 11** HIV-1 RT heterodimer (PDB structure 3v81). This image was prepared using Accelrys Discovery Studio 4.0.

There are two sites in RT that are targeted for the inhibition of transcription. The first is the catalytic site or polymerase active site where transcription of viral RNA into dsDNA occurs. This site is targeted by NRTIs. However, about 10 Å away from this catalytic site is a small, hydrophobic, allosteric pocket which is targeted by non-nucleoside reverse transcriptase inhibitors (NNRTIs). This allosteric pocket, known as the non-nucleoside binding pocket (NNIBP) is an elastic pocket which only forms upon binding of an NNRTI molecule.<sup>37</sup> This allows for vast structural diversity in the class of NNRTIs. This binding pocket is created by torsional rotation of the amino acids tyrosine 181 (Y181) and tyrosine 188 (Y188) from a “down” to an “up” position and the repositioning of the β-sheet containing amino acids tryptophan 229 (W229) and phenylalanine 227 (F227).<sup>38</sup>

NNRTIs are small, hydrophobic molecules that are noncompetitive inhibitors, and are highly selective for HIV-1 RT. Furthermore, their size and hydrophobicity allows these drugs to cross the blood-brain barrier (BBB). Unlike NRTIs, which are prodrugs, NNRTIs do not require preliminary activation by the phosphorylation of cellular kinases. Furthermore, they have a lower toxicity profile than NRTIs as they do not affect the activity of other cellular polymerases.<sup>39</sup>

### 1.5.2. First Generation NNRTIs

Early NNRTIs, such as nevirapine (Viramune®) and delavirdine (Rescriptor®) (Figure 12) are classified as “first generation” NNRTIs due to the fact that they possess rigid butterfly-like structures. Although initially they significantly reduce viral levels in infected individuals, after prolonged treatment single-amino acid mutations confer resistance. The most common single point mutations to confer resistance are K103N and Y181C. This low genetic barrier to resistance can be attributed not only to the rigidity of these structures but also on the fact that the binding of these compounds depend on being able to form  $\pi$ - $\pi$  interactions with amino acids Y181 and Y188, and these amino acids readily mutated to cysteine and leucine respectively. These mutations convert the aromatic tyrosine side chain to an aliphatic group, thereby, obliterating the important  $\pi$ - $\pi$  interactions between the inhibitor and the tyrosine side chain.<sup>40</sup>

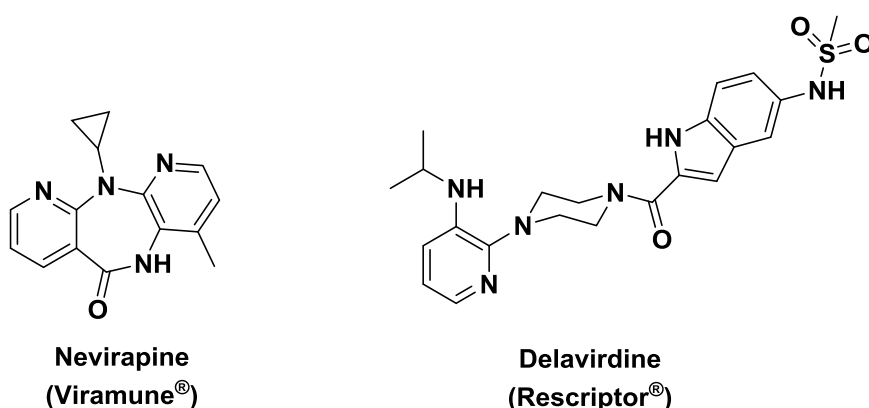
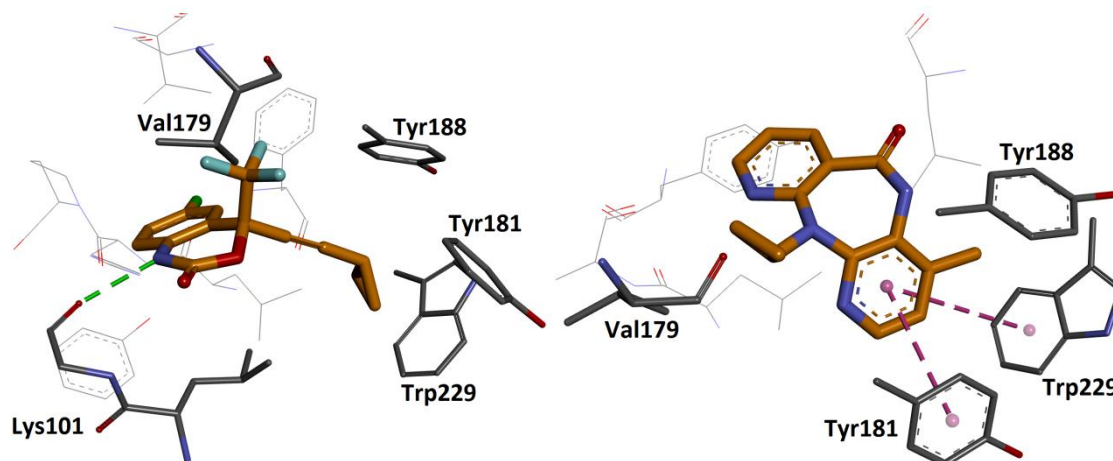


Figure 12 FDA licensed NNRTIs

### 1.5.3. Second Generation NNRTIs

Efavirenz (Sustiva®) is currently the most widely used component of first-line HAART. Although efavirenz has the rigidity associated with earlier NNRTIs, it is considered a second generation NNRTI. Efavirenz, unlike earlier NNRTIs, has a greatly improved resistance profile in comparison.<sup>41</sup> This can be attributed to the fact that the cyclopropyl moiety introduced in efavirenz, as opposed to the pyrimidine ring present in nevirapine, results in fewer interactions with Y181 and Y188 (Figure 13). Furthermore, there is the introduction of a hydrogen bond with the carbonyl oxygen on the backbone of lysine 101.<sup>41</sup>



**Figure 13** Comparative Binding mode of Efavirenz with no notable interactions with Tyr188 and Tyr181 (left) and Nevirapine which is reliant on  $\pi$ - $\pi$  interactions with the aromatic amino acid residues (right)

Second generation inhibitors such as etravirine (Intelence®) and rilpivirine (Edurant®) (Figure 14) are diarylpyrimidine (DAPY) NNRTIs and possess an element of conformational flexibility. Their considerable torsional flexibility allows for them to adopt a number of conformations enabling them to adapt to mutation induced changes in the allosteric pocket (Figure 15).<sup>37</sup> As a result, these second generation NNRTIs possess a higher genetic barrier to resistance and are resistant to a number of common clinical mutations that render “first generation” NNRTIs ineffective, such as the common K103N mutation. In fact three or more mutations are often required to render these second generation inhibitors ineffective. Unfortunately, this same feature of conformational adaptability also confers higher toxicity on these drugs due to off-target interactions.

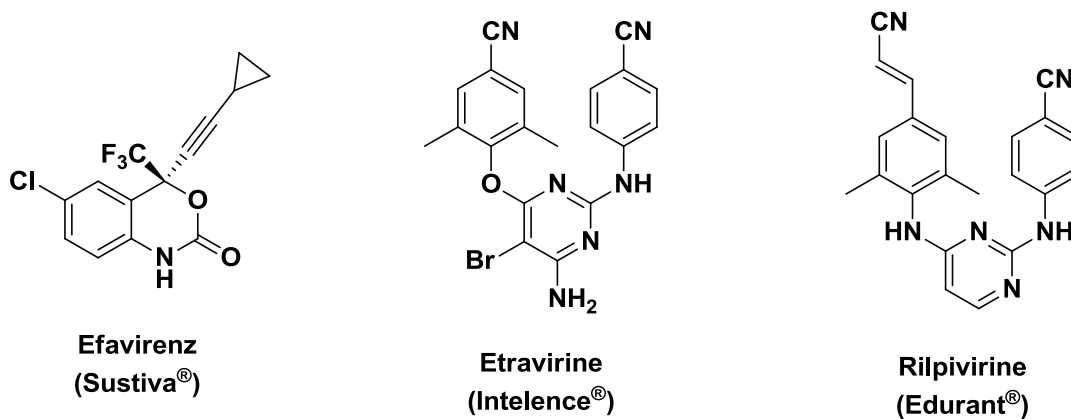


**Figure 14** FDA approved second generation NNRTIs

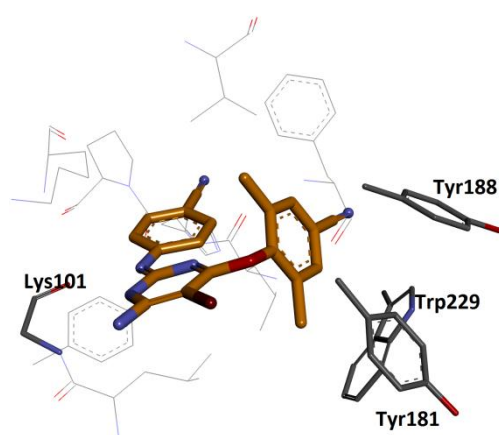


**Figure 15** The conformational flexibility of etravirine enables it to adopt multiple binding modes in the NNIBP

## Chapter 2: Introducing Our Strategy

### 2.1. The emergence of drug resistance as a setback to controlling viral levels of infected individuals

The biggest challenge to the success of clinically available NNRTIs in reducing the viral load effectively of infected individuals, is the onset of drug resistance. This issue is caused by the emergence of mutations immediately surrounding the NNIBP, which often directly leads to a decrease in the efficacy of a particular NNRTI.<sup>14</sup>

As mentioned in the previous chapter, first generation NNRTIs nevirapine and delavirdine are highly susceptible to the emergence of a wide range of single point mutations. Second generation NNRTIs efavirenz, etravirine and rilpivirine have a higher barrier to resistance and often require the presence of two or more mutated amino acid residues in the region of the NNIBP before significant resistance is observed.<sup>42</sup> The most common clinically relevant mutations that lead to the emergence of drug resistance are K103N, Y181C, Y188C/L, V106A/M, G180A/S and A98G.<sup>43</sup> There are three mechanisms by which these mutations can confer resistance. These include reducing the Van der Waals and  $\pi$ - $\pi$  stacking interactions between the inhibitor and the allosteric pocket, changing the hydrogen bonding character of the allosteric pocket and, finally, introducing steric clashes by altering the size of the amino acid residue side chains surrounding to the allosteric pocket.<sup>44</sup>

The most prominent and clinically relevant mutation is K103N, where Lys103 is replaced by Asn103, and this causes broad-spectrum resistance to most NNRTIs. Researchers have suggested that the K103N mutation causes resistance by stabilizing the closed NNRTI binding region in the absence of an inhibitor. As a result, a higher energy barrier is created for the binding of an inhibitor to the NNIBP, thereby reducing the activity of many NNRTIs.<sup>45</sup> Studies have shown that this occurs due to favourable hydrogen bonding interactions between the phenolic hydroxyl group of Tyr188 and the amide of Asn103.<sup>45</sup> However, it is unclear whether the stabilization of the apo-enzyme is the only mechanism by which this mutation leads to resistance. This doubt has been brought on by the ability of newer second generation NNRTIs such as etravirine to maintain activity against this mutation.<sup>46</sup> Other examples of less common mutations observed for amino acids surrounding the NNIBP include L100I, V106A and V108I.

As a result of this ongoing problem of the emergence of drug resistance, there is a continuous need to develop new NNRTIs. Therefore, understanding how these mutations confer resistance is vital in order to design NNRTIs that are able to overcome these issues.<sup>46</sup>

## 2.2. Strategies employed in the design of novel NNRTIs to overcome resistance

The mechanisms by which mutations confer resistance have been extensively studied. This has enabled researchers to design novel potential NNRTIs that overcome drug resistance. However, this success is often short-lived due to the inevitable re-emergence of resistance. There are two strategies often employed in the design of these novel NNRTIs. The first of which is for the inhibitor to possess an element of flexibility enabling it to adapt to conformational changes brought on by mutations in the NNIBP. Alternatively, one may set out to design novel inhibitors tailored for specific mutant strains.<sup>38</sup> Second generation NNRTIs etravirine and rilpivirine are examples of this strategy having been employed successfully.<sup>37</sup>

The second strategy is to target interactions between the inhibitor and highly conserved regions of the enzyme and minimize interactions to the more readily mutable amino acid residues.<sup>38</sup> These conserved residues which surround the binding site include Phe227, Trp229, Leu234 and Tyr318.<sup>47</sup> Mutations of these amino acid residues, particularly Trp229 and Tyr318, often lead to a decrease in viral fitness, and are therefore detrimental to viral replication and are not favoured.

Of these highly conserved residues, Trp229 is the most favoured residue for drug design. Trp229 forms part of the primer grip region (residues Phe227 to His235) of RT which sustains the primer terminus in the appropriate position for nucleophilic attack on incoming dNTPs.<sup>48</sup> Therefore, Trp229 is thought to be important for correct protein folding or for stabilizing the complex between RT and the template-primer. The effect of eight different mutations at position 229 on the enzymatic activity of RT and potential resistance to NNRTIs was studied by Pelemans *et al.*<sup>49</sup> Their studies showed that the presence of these mutations at position 229 in all cases severely compromised that enzymatic activity of RT and compromised the replicative ability of the virus. Only one mutation showed any significant resistance to NNRTIs while maintaining viral fitness.<sup>49</sup> Furthermore, any mutation of this amino acid residue *in vitro* or *in vivo* has not been observed under drug pressure, not even in combination with other mutations.<sup>49, 50</sup> This method of targeting conserved residue Trp229 has found success in a number of potential NNRTIs.

### 2.2.1. A promising NNRTI candidate, lersivirine

This design approach to overcome resistance found success in drug candidate lersivirine (Figure 16), which was until recently undergoing phase IIB clinical trials. The design of lersivirine resulted from lead optimization of capravirine which progressed to phase IIB clinical trials. Although capravirine was very effective, it suffered from rapid *in vivo* clearance due to the fact that it was prone to oxidative metabolism.<sup>51</sup> Lersivirine was designed to optimize the potency exhibited by capravirine and to maintain metabolic stability. In a 48 week double blind trial lersivirine was found to be as effective as efavirenz but was found to possess a better toxicological profile.<sup>52</sup> The attractiveness of lersivirine is also based on its unique mode of binding to the allosteric pocket of RT and its impressive resistance profile.<sup>53</sup>



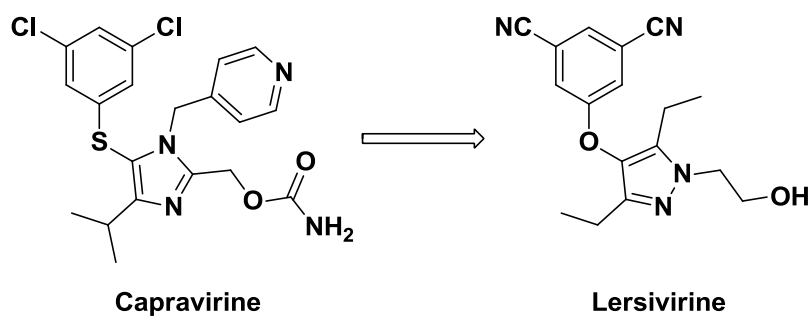
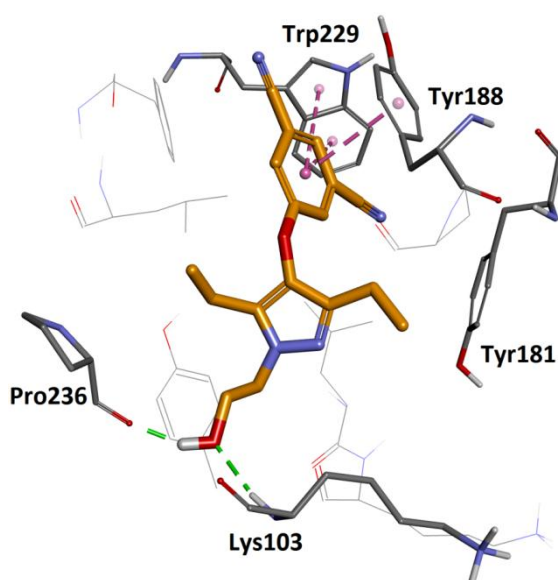


Figure 16

Lersivirine possesses an “upper” dicyanophenyl ring which forms edge-to-face  $\pi$ - $\pi$  interactions with immutable Trp229 and  $\pi$ - $\pi$  stacking interactions with Tyr188, as opposed to the more commonly targeted Tyr181.<sup>53</sup> Furthermore, this allows Tyr181 to adopt the energetically more favoured “down” orientation, as is found in the apo form of the enzyme.<sup>54</sup> All licensed drugs force Tyr181 into the “up” position, incurring a slight energy penalty. In addition lersivirine features hydrogen bonding between its hydroxyl functionality and the backbone of amino acid Lys103 (Figure 17).

This drug candidate was shown to be able to inhibit 60% of mutant strains of HIV. It maintained activity against 14 of 15 clinically significant single point mutations and against two double-mutations, Y181C/Y188C and V106A/Y181C.<sup>53</sup> Furthermore, the use of lersivirine in conjunction with other anti-HIV agents exhibits synergism.<sup>53</sup> Unfortunately, due to reasons not disclosed the development of lersivirine was recently halted.



**Figure 17** A representation of the unique binding mode of lersivirine in the NNIBP showing  $\pi$ - $\pi$  stacking interactions to Tyr188 and Trp229 and hydrogen bonding interactions to Lys103 and Pro236



### 2.2.2. Other examples of attempts to overcome resistance by targeting conserved residues within the NNIBP

Targeting conserved amino acid residues such as Trp229 has found considerable success in a number of other potential NNRTIs. Further examples of these include clinical candidates MK-4965 and MK-1438 (Figure 18). Like lersivirine, these biaryl NNRTIs maintain an element of flexibility and form  $\pi$ - $\pi$  stacking interactions with Trp229 and  $\pi$ - $\pi$  stacking interactions with Tyr188. Both MK-4965 and MK-1439 have broad spectrum antiviral activity at subnanomolar concentrations against wild-type HIV-1 and in the presence of mutations such as K103N and Y181C.<sup>55, 56</sup>

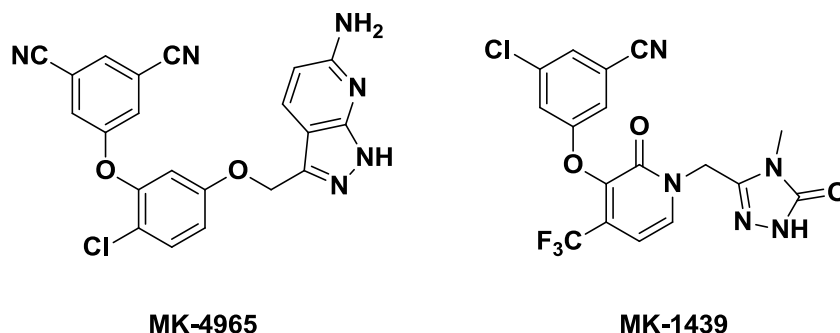


Figure 18

Another interesting NNRTI candidate is indazole **1** (Figure 19). Although this compound also targets the conserved residue Trp229 and forms hydrogen bonding interactions with the backbone of the NNIBP, it possesses a more rigid structure. Despite this, **1** still exhibits activity at nanomolar concentrations against wild-type HIV-1 and also maintains potency in the presence of mutations K103N and Y181C.<sup>57</sup>

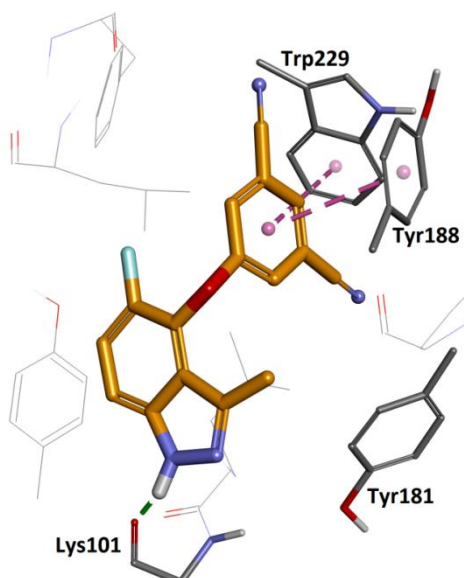
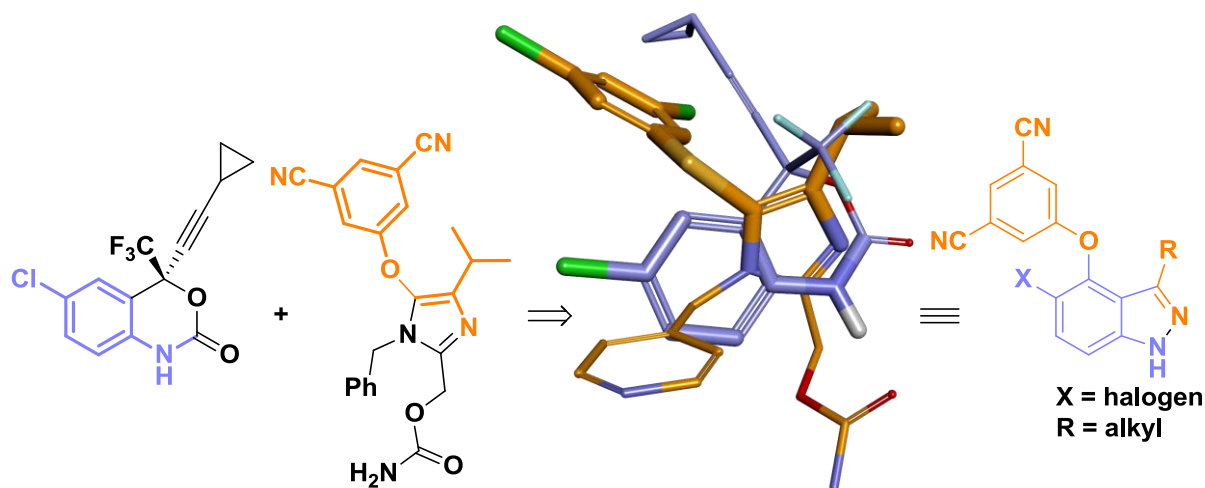


Figure 19 A representation of the binding mode of indazole **1** showing  $\pi$ - $\pi$  interactions with Trp229 and Tyr188 and hydrogen bonding interactions to Lys101.

This compound was designed through the use of molecular hybridization combining beneficial structural characteristics of efavirenz and capravirine (Scheme 1).<sup>57</sup> This was achieved by superimposing crystal structures of efavirenz and capravirine in the binding pocket and creating a hybrid from the two ligands by transposing the 3,5-disubstituted phenyl moiety of capravirine onto the the indazole core (distinct but similar to the bicyclic template of efavirenz).



**Scheme 1** Alignment and superimposition of the crystal structures of capravirine (orange) and efavirenz (blue) led to the hybridization of the two NNRTIs to yield indazole **1**. (Crystal structures taken from PDB structures 1EP4 and 1FK9)

### 2.3. Our Strategy

Drawing inspiration from the successes discussed previously, we sought to design and synthesize novel NNRTIs that could maintain efficacy in the presence of resistance strains of the virus. We envisaged that we could achieve this by introducing elements of flexibility to our compounds and improving binding affinity to the mutated NNIBP by targeting conserved residues such as Trp229. The aim of this MSc project can be divided into three different research thrusts. Below, these will be introduced briefly, but discussed in greater detail in subsequent chapters.

### 2.3.1. Synthesis of a small triazole library

The first of the three research thrusts focused on the synthesis of novel triazole-containing compounds **2** (Figure 20), the design of which was inspired by lersivirine. These small flexible biaryl compounds featured a *bis*-metasubstituted aryl ring to maintain  $\pi$ - $\pi$  stacking interactions with Tyr188 and  $\pi$ - $\pi$  edge-to-face interactions with Trp229. In addition, these compounds possess an appropriate substituent, such as a short alcohol chain on the triazole ring which would enable them to form hydrogen bonding interactions with the backbone of Lys103. For the construction of these triazole-containing compounds we would make use of the highly versatile click chemistry which could provide us with enough scope to synthesize a small library of compounds.

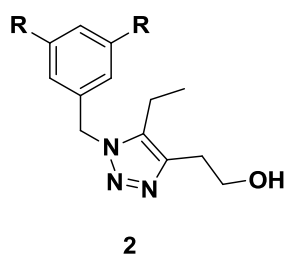


Figure 20

### 2.3.2. An indole based scaffold designed to target Trp229 and Lys101

The second research thrust focused on the design and synthesis of a novel indole based compound **3** (Figure 21) which also features  $\pi$ - $\pi$  interactions with Tyr188 and Trp229. In addition to these interactions we endeavour to extend to the entrance of the allosteric pocket with the appropriate functionality to introduce hydrogen bonding interactions with the backbone of Lys101. Other interactions include an ethyl chain to occupy the Val179 pocket, as well as a halogen at the 5-position shown to help improve potency of potential NNRTI candidates.<sup>57, 58</sup>

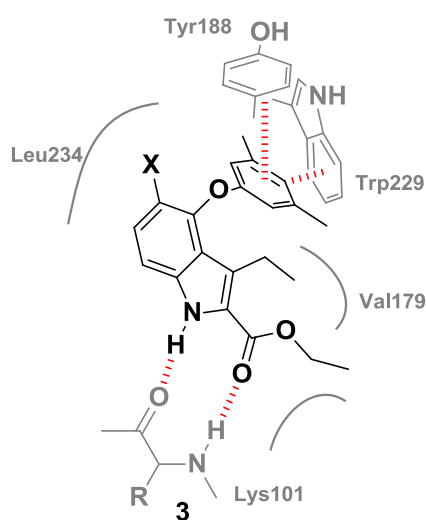


Figure 21

### 2.3.3. An extension of previous work

Finally the third research thrust is an extension of work done previously within our research group. Recently an indole based compound **4** (Figure 22) was synthesized in our laboratory and was found to be potent against HIV RT with an  $IC_{50}$  value of 1 nM. This compound was also found to maintain potency against the common and clinically problematic mutation K103N.<sup>59</sup> However, of concern was the fact that the compound appeared acid labile, and therefore in its current form would never be available in oral dosage form.

Our strategy involves improving the stability of this compound by replacing the methoxy functionality with a suitable bioisostere, such as the aryl amine for compound **5**. We wished to keep the  $\pi$ - $\pi$  stacking interactions to Tyr181 as this was shown to be imperative in maintaining activity against RT.<sup>59</sup> We also sought to maintain occupation of the Val179 pocket with an alkyl chain, as well as hydrogen bonding interactions to the backbone of Lys101.

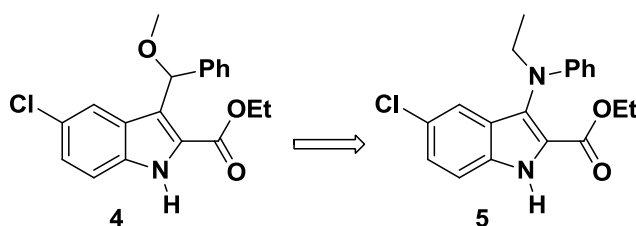
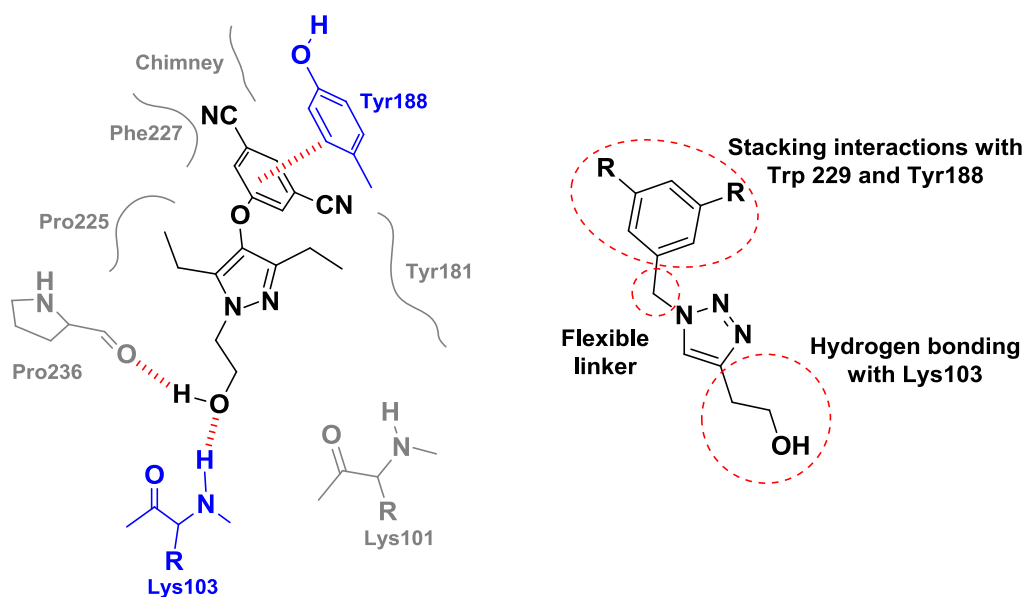


Figure 22

## Chapter 3: Synthesis of a Small Triazole Library

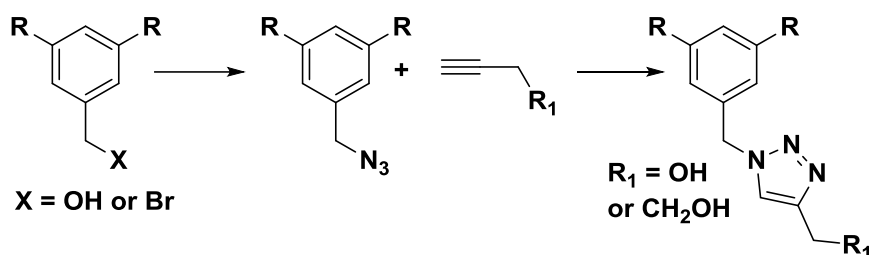
### 3.1. Establishing a Proof-of-Concept

We had decided that lersivirine was a suitable starting point for the design of our novel triazole containing potential NNRTIs due to its unique and impressive resistance profile. In order to establish a proof-of-concept, our first target series of biaryl compounds would consist only of a disubstituted triazole ring. This is as far from the structure of lersivirine (which consists of a fully substituted pyrazole ring) as we dared go as these compounds would only possess the structural features that were deemed important in the binding mode of lersivirine (Figure 23). These included a *bis*-meta-substituted aryl ring maintaining  $\pi$ - $\pi$  stacking interactions to conserved residue Trp229 and the less targeted Tyr188, as well as, an alcohol chain for maintaining hydrogen bonding interactions to Lys103. Furthermore, these compounds would possess an element of flexibility allowing for the rearrangement of the potential inhibitor within the binding pocket. For the linker atom we decided to replace the oxygen found in lersivirine with a carbon as this would not interfere with the conformation of our compounds and would also simplify the synthetic sequence.



**Figure 23** Binding mode of lersivirine showing  $\pi$ - $\pi$  stacking interactions with Tyr188 and hydrogen bonding interactions with Lys103 (left) and proposed scaffold for our triazole compounds (right).

The simplicity of this structure and the incorporation of the triazole ring would enable us to utilize the well-documented and established azide-alkyne Huisgen cycloaddition reaction (Scheme 2).<sup>60</sup> This reaction would, due to its versatility, facilitate the synthesis of a small library of simple regiospecific compounds and allow for us to explore the effects of varying substituents on the aryl ring, as well as varying lengths of the alcohol chain situated on the triazole ring.



**Scheme 2** Initial synthetic strategy leading to a series of disubstituted triazole compounds

### 3.2. The use of triazole rings in drug design

Heterocycles have been used extensively in the design and development of drug candidates, in fact it is estimated that approximately 80% of marketed drugs contain at least one heterocycle.<sup>61</sup> Heterocycles are popularly used as bioisosteric replacements for a large number of functional groups to improve potency and selectivity of drug candidates. They are also often employed to improve the pharmacokinetic and toxicological profiles of drug candidates by improving their lipophilicity, polarity and aqueous solubility.<sup>61</sup>

The use of triazole rings, in particular, as the heterocycle of choice in drug discovery has grown steadily over the last couple of years.<sup>60</sup> Although triazole rings do not occur in nature, they have been shown to exhibit several biological activities such as anticancer, antimalarial, antiviral and anti-inflammatory activities.<sup>62</sup> Triazole rings have become popular due to their ability to be employed as both hydrogen bond acceptor and donor, to be able to be involved in ring stacking interactions and, if not directly involved in any interactions, to act as a stable structural linking unit. Furthermore, triazole rings have been reported to be metabolically stable. *In vivo* they are not oxidized or reduced and cannot be cleaved hydrolytically.<sup>63</sup>

With regards to NNRTIs, the presence of a triazole ring is not altogether uncommon. However, unlike the 1,2,3-triazole moiety employed in our compounds, triazole containing NNRTIs discovered in the literature seem to only consist of the 1,2,4-triazole moiety, examples of which include RDEA806 (Figure 24). This compound was found to exhibit potent activity against HIV RT and maintain efficacy in the presence of the mutation K103N.<sup>56, 64</sup>

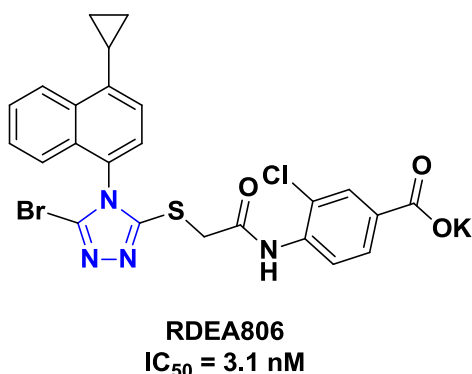


**Figure 24** RDEA206, an example of the use of a triazole ring in NNRTIs

### 3.3. Introducing Click Chemistry

The reactions for the synthesis of triazole rings such as the copper and ruthenium azide-alkyne catalyzed Huisgen cycloaddition reactions fall under the umbrella term click chemistry. The term click chemistry was first defined in 2001 by Sharpless *et al.* in a paper describing the synthesis of large molecules following nature's method of joining smaller units together using a heteroatom linker.<sup>65</sup> This is defined as a reaction that is versatile, makes use of readily available starting materials and reagents, provides good yields, is efficient and selective, can be carried out under mild and simple reaction conditions and requires minimal workup and purification.<sup>65</sup>

Reactions that meet these criteria include the hetero-Diels Alder reaction, ring opening reactions of strained heterocycles such as epoxides and aziridines, "non-aldol" type carbonyl chemistry such as the formation of ureas and thioureas and the copper or ruthenium catalysed Huisgen 1,3-dipolar cycloaddition reactions.<sup>63, 65</sup>

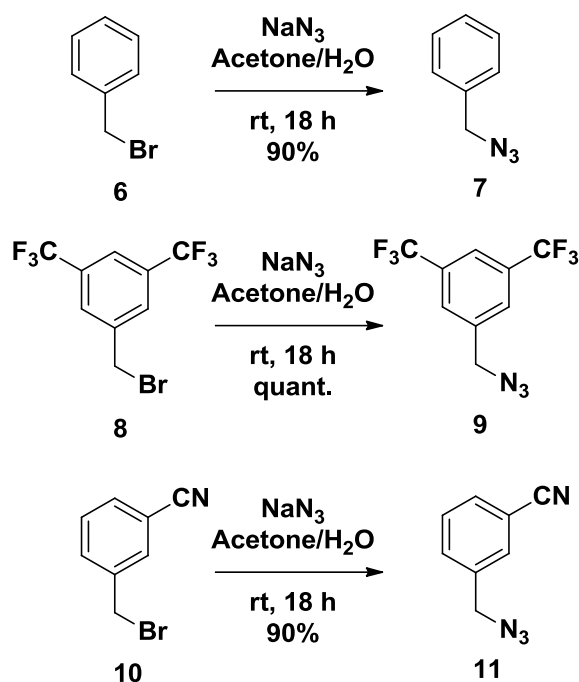
The Huisgen 1,3-dipolar cycloaddition of azides and alkynes is considered the "cream of the crop" of all click chemistry reactions. These reactions are popular due to the ease with which the azide and alkyne components can be introduced into the reaction and the stability that these components possess under standard synthetic conditions.<sup>65</sup> Another attractive feature of this reaction is the tolerance of this reaction to the presence of a variety of functional groups, with the exception of Michael acceptors and strained olefins.<sup>66</sup> The ease with which these reactions can be carried out simplifies synthesis and allows for faster and efficient lead discovery and optimization.<sup>67</sup>

### 3.4. Synthesis of Azide Fragments for Triazole Ring Synthesis

For the initial synthetic strategy we envisaged utilizing a variety of substituted benzylic azides with commercially available propargyl alcohol or 1-butyne-3-ol as the precursors for the azide-alkyne Huisgen cycloaddition reaction. The benzylic azides could be synthesized from available benzylic halides and alcohols. These included benzyl bromide **6**, 1-(bromomethyl)-3,5-bis(trifluoromethyl)benzene **8**, 3-(bromomethyl)benzonitrile **10**, (3,5-dichlorophenyl)methanol **12** and (3,5-dimethylphenyl)-methanol **22**.

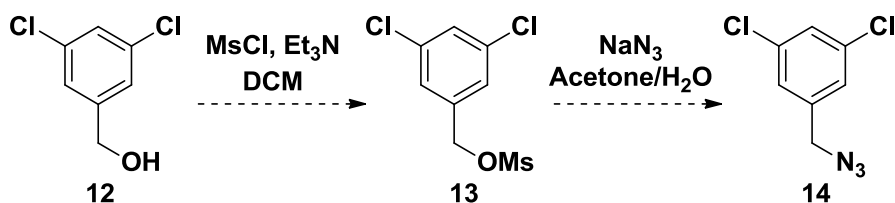
#### 3.4.1. Nucleophilic substitution reactions with sodium azide

The conversion of the benzyl halides to the corresponding benzyl azides could be carried out through the use of a simple and well documented substitution reaction with sodium azide. The respective benzyl halide along with 1.5 equivalents of sodium azide was taken up in a 4:1 mixture of acetone and distilled water and was carried out at ambient temperature for approximately 18 hours.<sup>68</sup> These reactions proceeded without incident and provided excellent yields as can be seen in Scheme 3 below.



Scheme 3

However, the benzyl alcohol precursors (for example **12**, Scheme 4) could of course not be converted to the azide by a simple nucleophilic substitution reaction. Therefore, we had to employ a different method. The most obvious route would be to convert the alcohol to a more suitable leaving group and only then carry out a nucleophilic substitution reaction with sodium azide. We envisaged that this could be achieved by simply converting the alcohol to methanesulfonate using methanesulfonyl chloride.



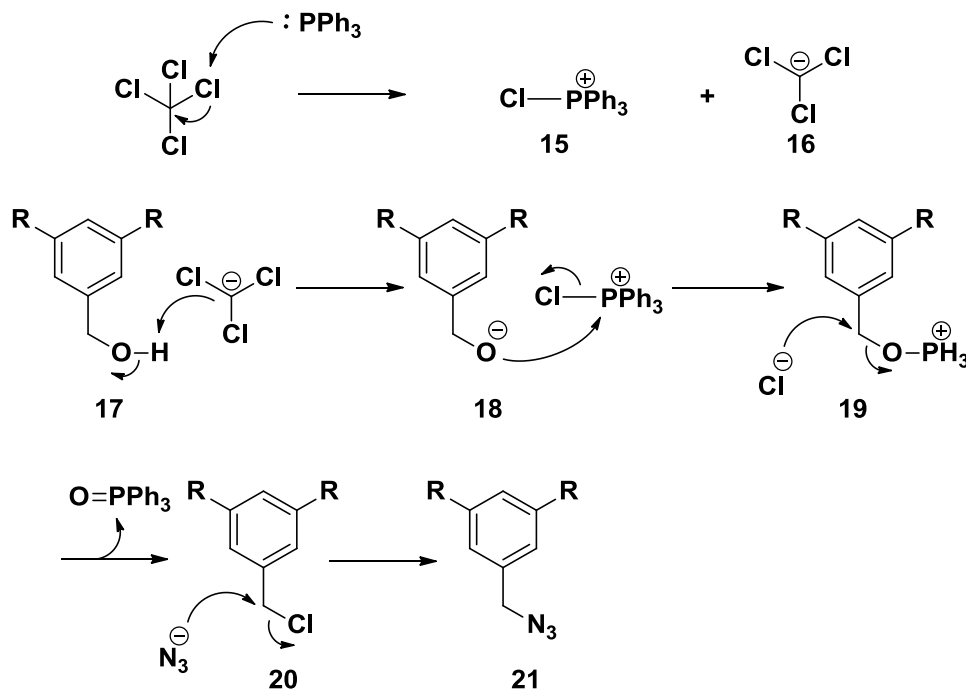
Scheme 4

This strategy was first attempted using 3,5-dichlorobenzyl alcohol **12** as the azide precursor. Precursor **12** was taken up in DCM with triethylamine as the base and methanesulfonyl chloride was added dropwise to this mixture at 0 °C.<sup>69</sup> However, when we analysed the <sup>1</sup>H NMR for the formed product the methyl signal associated with the methanesulfonate functionality was not observed. In fact the only observed signals corresponded to the starting material. As the isolated product could not be starting material due to the significant difference in the R<sub>f</sub> value we came to the conclusion that dimerization had occurred. We envisaged that this was due to the fact that unreacted benzyl alcohol rapidly displaced methanesulfonate **13** as it was forming. Despite attempts to optimize this reaction (which included omitting the triethylamine) we were unable to prevent dimerization from occurring. As a result, an alternative strategy for the conversion of the benzyl alcohol to the respective azide had to be considered.



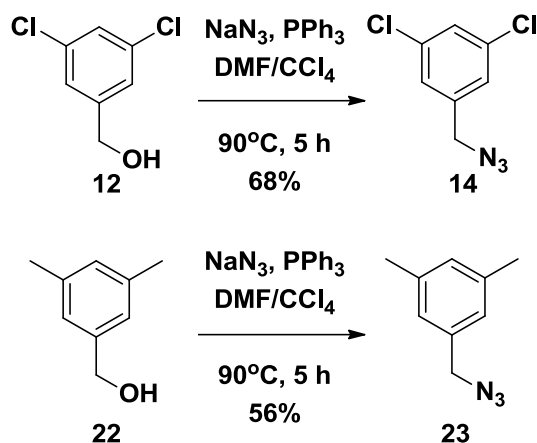
### 3.4.2. Employing a Modified Appel reaction for the synthesis of the desired azides from benzylic alcohols

Having studied the literature we envisaged that an Appel reaction could be the solution to our azide installation difficulties. This reaction, as discovered by Professor Ralph Appel, readily converts an alcohol to an appropriate halide.<sup>70</sup> In the case of converting an alcohol to a chloride, this is achieved through the use of triphenylphosphine and carbon tetrachloride as the chloride source. The mechanism for this reaction is presented in Scheme 5. The first step is the formation of the phosphonium chloride cation **15** and trichloromethanide **16**. The trichloromethanide anion deprotonates the alcohol **17** while the cation is then responsible for the phosphorylation of the newly formed anion **18** to the alkoxyphosphonium salt **19**. The driving force for this reaction is the formation of the strong P-O bond followed by the release of the relatively unreactive triphenylphosphine oxide.<sup>71</sup> The reason we called this a modified Appel reaction is due to the fact that sodium azide was also added to the reaction mixture resulting in a substitution of the newly formed benzylic chloride **20** with the desired azide **21**. The sodium azide was introduced into the reaction mixture prior to the addition of the chloride source. It was obvious that the presence of the charged azide ion in the reaction mixture meant that the less reactive alcohol was now unlikely to outcompete the azide in the displacement of the benzylic chloride and, as a result, dimerization would not occur.



Scheme 5 Proposed mechanism for a modified Appel reaction

Therefore, to a solution of the benzyl alcohol and sodium azide in DMF was added triphenylphosphine. The reaction mixture was then heated to 90 °C under reflux before carbon tetrachloride was added. The modified Appel reaction was carried out at this temperature for approximately 18 hours.<sup>72</sup> The yields for these reactions were moderate as shown in Scheme 6.



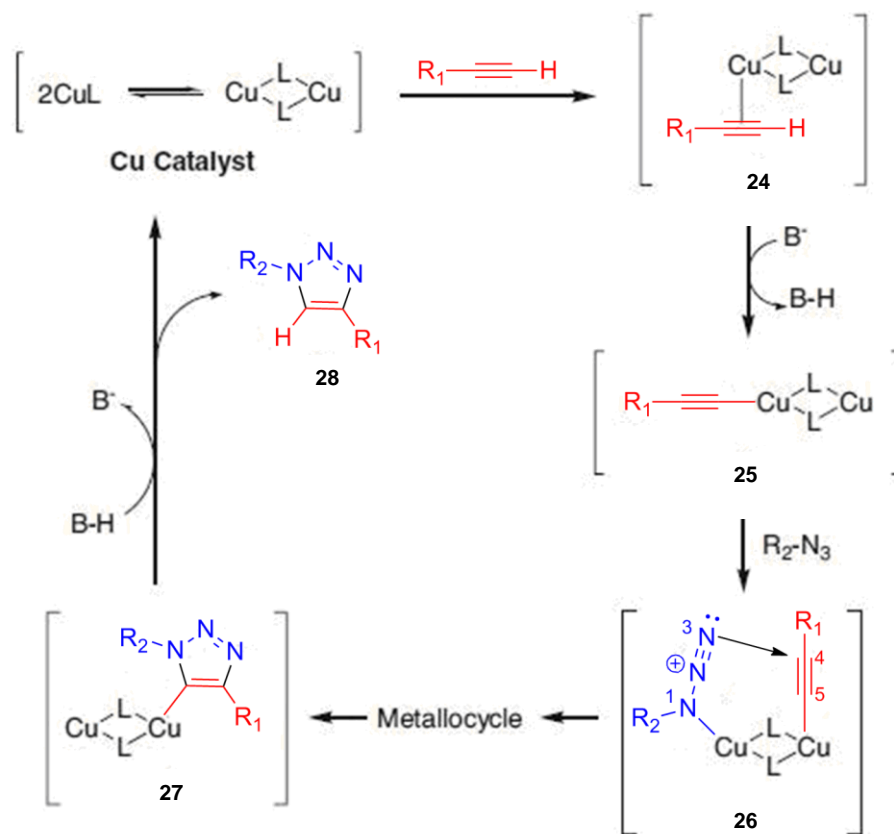
Scheme 6

All spectroscopic data for the azides synthesized coincided with the data reported in literature. With the alkynes and benzyl azides in hand we could begin the synthesis of our triazole library.

### 3.5. The Cu<sup>I</sup> Catalyzed Huisgen Cycloaddition Reaction

The Cu<sup>I</sup> catalyzed Huisgen cycloaddition reaction (CuAAC) is considered the most popular and versatile variant of Huisgen dipolar cycloaddition reactions. The advantages of the CuAAC reaction were first described in 2002 by the groups of Sharpless and Meldal independently.<sup>73,74</sup> These reactions which occur between azides and terminal alkynes are highly regiospecific forming the 1,4-triazole product exclusively. Furthermore, these reactions can occur in a variety of solvents and tolerate a range of pH values and temperatures.<sup>75</sup>

It is thought that the CuAAC reaction occurs in a stepwise manner (Scheme 7).<sup>75</sup> The first step of the CuAAC reaction involves the complexation of a Cu<sup>I</sup> dimer with the terminal alkyne to form an active Cu-acetylide species **25**. This step can be carried out with either a Cu(I) salt such as copper iodide in the presence of a nitrogen containing base such as 2,6-lutidine or DIPEA, or with Cu(I) generated *in situ* from a Cu(II) salt such as CuSO<sub>4</sub> in the presence of a reducing agent such as ascorbic acid or sodium ascorbate.<sup>73</sup> Reactions using Cu(I) generated from a Cu(II) source, despite Cu(I) sensitivity to oxygen, are generally carried out in water/alcohol mixture which precludes the requirement for the presence of any base.<sup>75</sup> The use of Cu(I) salts, however, can only be carried out under inert conditions and in organic solvents and so the presence of a base or the use of high temperatures is required for the formation of the active Cu-acetylide complex.<sup>76</sup> In this instance the deprotonation of the terminal alkyne facilitates the insertion of the Cu<sup>I</sup> into the terminal alkyne to form the active species **25**. The second step involves the displacement of one of the ligands of the copper complex by coordination of the azide forming a copper acetylide-azide complex **26**.<sup>75</sup> The formation of this complex activates the alkyne, making it more susceptible to nucleophilic attack by the distal nitrogen of the azide. This generates a metallocycle intermediate which positions the azide for triazole ring formation, ultimately leading to the formation of a copper-triazole derivative. Next protonation of the copper-triazole derivative **27** occurs followed by dissociation of the triazole product **28** and regeneration of the copper catalyst.<sup>75</sup>

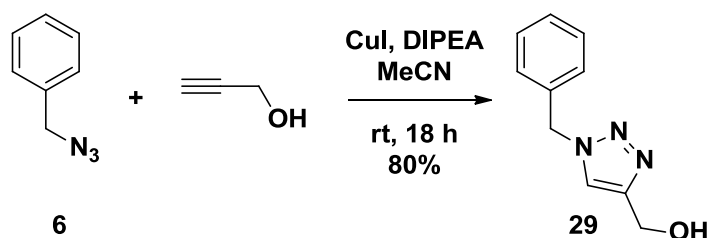


**Scheme 7** Proposed mechanism for CuAAC reaction adapted from Hein *et al.*<sup>77</sup>

For our purposes we chose a procedure which makes use of copper (I) iodide in acetonitrile and using DIPEA as the base. The use of DIPEA as a base in these reactions is thought to minimize the formation of unfavourable side products. Furthermore, the use of excess base has been shown to improve the yields of these reactions by possibly stabilizing the oxidation state of  $\text{Cu}^{\text{I}}$ .<sup>75</sup>

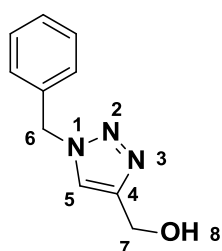
### 3.5.1. Synthesis of the 1,4-triazole series of compounds

For the synthesis of our first 1,4-triazole biaryl compound we made use of propargyl alcohol with benzyl azide **6** (Scheme 8). Both precursors were taken up in MeCN along with 2 equivalents of DIPEA. A catalytic amount of CuI was then added and reaction was run at room temperature for 18 hours.<sup>78</sup>



Scheme 8

Interestingly, our initial attempt at the CuAAC reaction was unsuccessful, however, the reason for this was quickly revealed. These reactions require concentrated conditions to proceed and in our initial attempts the reaction mixture was simply too dilute. The copper iodide does not dissolve in the MeCN but remains suspended and, as a result, the reaction needs to be as concentrated as possible in order for the reaction to occur. With this in mind, the procedure mentioned above was attempted once more using significantly less solvent and under these conditions the reaction proceeded without further complications. Purification by column chromatography yielded 80% of **29** as a white solid.



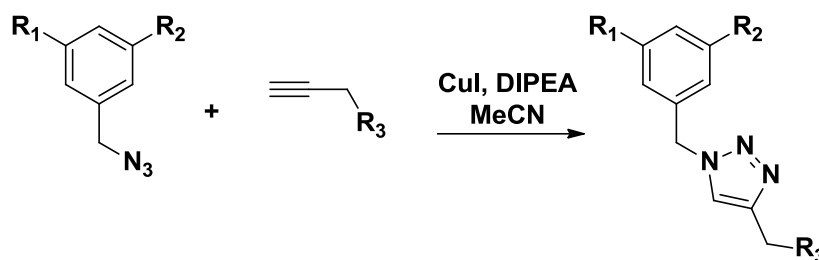
Analysis of the  $^1\text{H}$  NMR spectrum of **29** revealed that the CuAAC had been successful. Firstly the benzylic protons and the CH proton on the triazole ring were clearly accounted for. The protons at 6 appeared as a singlet at 5.46 ppm integrating for 2H, and proton 5 appeared as a singlet at 7.37 ppm integrating for 1H. The proton corresponding to the OH was also clearly observed as a broad triplet at 2.07 ppm. The methylene protons at 7 were observed as a doublet at 4.71 ppm integrating for 2H.

Confident that this synthetic strategy would work well with our other azide and alkyne precursors, we could continue synthesizing our small 1,4-triazole library.

Table 1 shows the triazole compounds successfully synthesized using this method. These compounds were also fully characterized and the characteristic signals observed in the  $^1\text{H}$  NMR spectrum of **29** were also observed for the newly synthesized compounds.

Interestingly, the yield obtained for the synthesis of compound **33** was relatively poor in comparison with the yields obtained for compounds **29** to **32**. However, the reason for this was not investigated.

Table 1



Compound	R <sub>1</sub>	R <sub>2</sub>	R <sub>3</sub>	%Yield
29	H	H	OH	80
30	CF <sub>3</sub>	CF <sub>3</sub>	OH	92
31	Me	Me	OH	98
32	Me	Me	CH <sub>2</sub> OH	86
33	H	CN	CH <sub>2</sub> OH	46

### 3.5.2. Confirmation of regiochemistry

Although literature clearly states that the CuAAC reaction exclusively synthesizes the 1,4-triazole regioisomer, we deemed it important to confirm this by additional spectroscopic studies. To this end, the nuclear Overhauser effect (NOE) would mostly likely be effective as it establishes the spatial proximity between protons.<sup>79</sup> By irradiating signals of interest and observing the through-space correlations to other signals the 3D structure of a small molecule can be confirmed. There are 2 options for NOE experiments, 1D and 2D NOE experiments can be carried out. We found that 1D NOE experiments were more sensitive and provided more information than the 2D NOE experiments.

For the purpose of confirming regiochemistry we selected the 3,5-dimethyl triazole derivative **32** with the longer alcohol chain. Using the <sup>1</sup>H NMR spectrum of **32** as a reference (Figure 25), we irradiated at the chemical shifts corresponding to protons on the methylene linker 6, the proton on the triazole ring 5 and the methylene protons on the alcohol chain represented as 7 and 8. If we had synthesized the desired 1,4-triazole ring we would expect to observe correlations between the protons 5 and 6, as well as between protons 5 and 7.

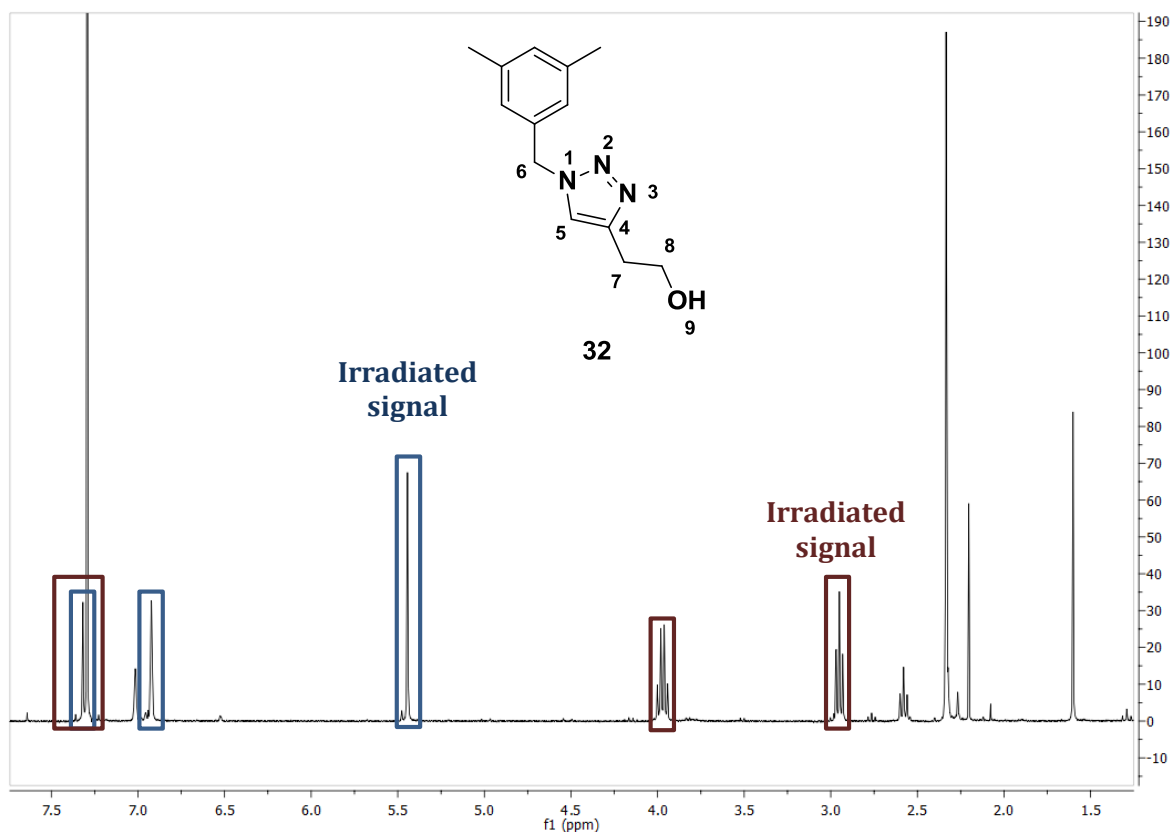


Figure 25  $^1\text{H}$  NMR spectrum of **32**

The blocks shown on the  $^1\text{H}$  NMR spectrum (Figure 25) correspond to the correlations observed between protons on the NOE spectrum. The blue blocks show the correlations observed when we irradiated at 5.44 ppm which corresponds to the methylene protons 6. Irradiation here showed clear correlations to the triazole proton 5 situated at 7.32 ppm, as well as the aromatic protons. However, no correlations were observed between protons 6 and those on the alcohol chain.

The red blocks are associated with the correlations observed when we irradiated at 2.95 ppm which corresponds to proton 7 on the alcohol chain. Irradiation at this peak shows clear correlations between protons 7 and 8 as would be expected, as well as between protons 7 and 5. No correlations are observed between protons 7 and 6.

If the undesired 1,5-regioisomer (Figure 26) had been synthesized we would have expected to observe correlations between methylene protons 6 and 7 as the alcohol chain would occupy the 5-position on the triazole ring as opposed to the 4-position. Consequentially we would not observe any correlations between the triazole proton, now proton 4 on the structure, and methylene protons 6. As our observations do not match those expected for the 1,5-regioisomer we could safely conclude that the CuAAC synthesis did provide us with the desired 1,4-triazole regioisomer.

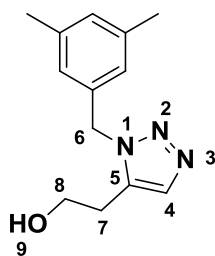


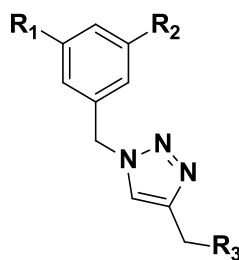
Figure 26

Having synthesized 5 different proof-of-concept 1,4-triazole compounds we could send them for biological evaluation.

### 3.6. Efficacy results of the 1,4-triazole series

Biological evaluation of our compounds was carried out by our collaborators at the National Institute for Communicable Diseases (NICD) in Johannesburg. Phenotypic and toxicity assays were carried out against wild-type HIV-1.<sup>80,81</sup> The results of these assays are shown in Table 2.

Table 2



Compound	R <sub>1</sub>	R <sub>2</sub>	R <sub>3</sub>	CC <sub>50</sub> (μM)	IC <sub>50</sub> (μM)
29	H	H	OH	>100	>83.5
30	CF <sub>3</sub>	CF <sub>3</sub>	OH	>53.4	>24.5
31	Me	Me	OH	>100	27.8
32	Me	Me	CH <sub>2</sub> OH	>100	>100
33	H	CN	CH <sub>2</sub> OH	>100	>83.5

We had hoped that these compounds would show some activity against HIV RT due to the fact that despite their simplicity, they still featured what we considered to be the structural characteristics of lersivirine imperative for its impressive activity profile (Figure 23). Although we expected that the activity would be less than that of lersivirine due to the simplified nature of their structures we did not expect that the 1,4-disubstituted triazole compounds synthesized would show such poor to no activity. We considered attributing the lack of activity to the oversimplification of these compounds and hypothesized that the triazole ring needed to be fully

substituted by introducing an alkyl chain, in particular an ethyl chain. This would bring the structure of our triazole compounds closer to the structure of lersivirine (Figure 27).

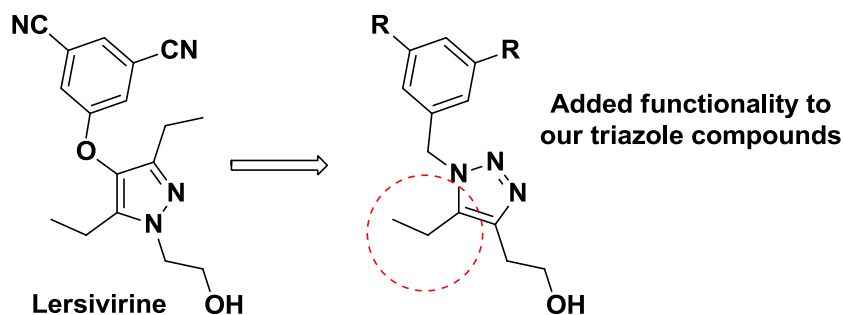
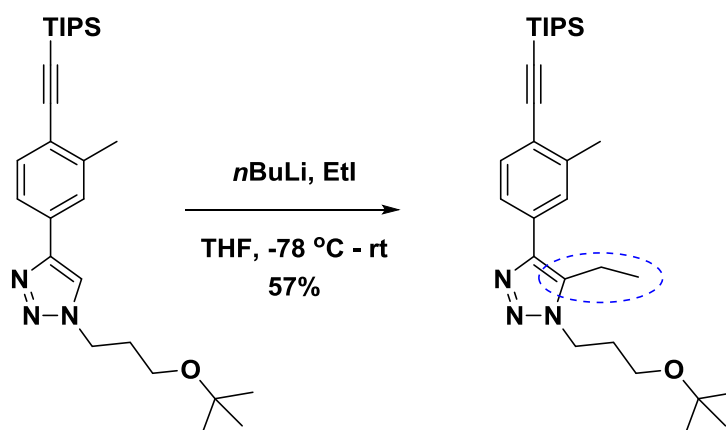


Figure 27

### 3.7. Attempts to introduce an ethyl chain onto the triazole ring

As previously mentioned,  $\text{Cu}^I$  catalysed Huisgen cycloaddition reactions are explicitly used for the reaction of azides with terminal alkynes. As a result, we could not use this method to synthesize the desired tri-substituted triazole rings using an internal alkyne and benzyl azide.

However, knowing how well these reactions worked in synthesizing the 1,4-triazole products we considered whether it would be possible to deprotonate the readily formed triazole ring at the 5-position and then introduce the desired ethyl chain onto the triazole ring using an appropriate alkyl halide. Only two papers were found that claimed to employ this method successfully. The papers by Ehlers *et al.* and Ohmatsu *et al.* reported a number of instances where they were able to lithiate a disubstituted 1,4-triazole ring using *n*-butyllithium and introduce an ethyl or methyl chain using ethyl or methyl iodide (Scheme 9).<sup>82,83</sup>

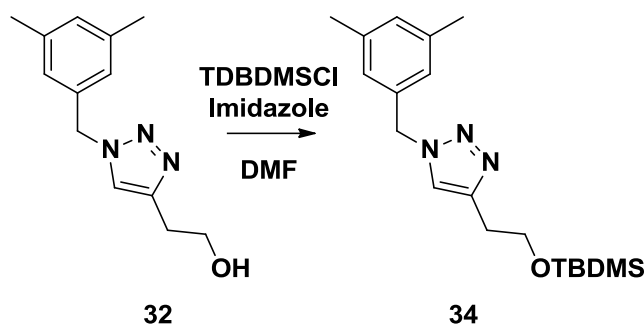


Scheme 9 Example of reaction carried out by Ehlers *et al.*<sup>82</sup>

Having decided to employ this methodology on our system, a first step required that we protect the alcohol on the ethyl chain. After careful consideration of the steps to follow, *tert*-butyldimethylsilyl (TBDMS) chloride was chosen for this purpose as it could be installed and removed selectively and under fairly mild conditions. Protection of the alcohol chain was easily obtained by the treatment of **32** with TBDMS-Cl in the presence of imidazole (Scheme 10). Purification by column chromatography yielded 88% of **34** as a white solid.

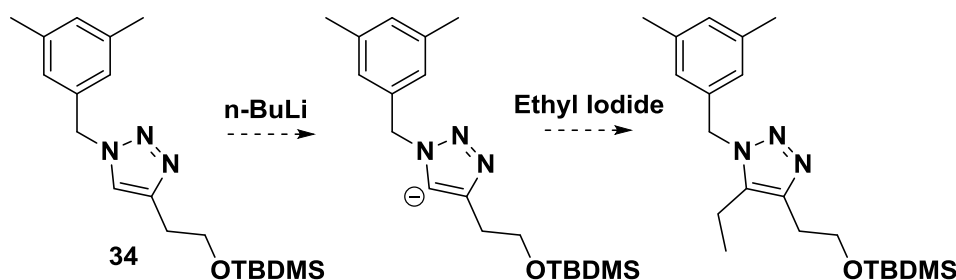


The appearance of two singlets at 0.87 ppm and at 0.00 ppm integrating for 9H and 6H respectively in the  $^1\text{H}$  NMR spectrum for **34** indicated that the protection of the alcohol with TBDMS-Cl had been successful.



Scheme 10

With the protected triazole compound in hand we could now attempt to install an ethyl chain onto the triazole ring using the strategy employed by Ehlers *et al.* and Ohmatsu *et al.*<sup>82, 83</sup> *n*-BuLi was added to **34** at  $-78^\circ\text{C}$  followed by the slow addition of iodoethane (Scheme 11). Unfortunately this reaction was not successful and produced numerous products, as determined by TLC. We therefore abandoned this methodology as a potential route, and thus returned to the possibilities available to us in the azide-alkyne cycloaddition reaction.



Scheme 11

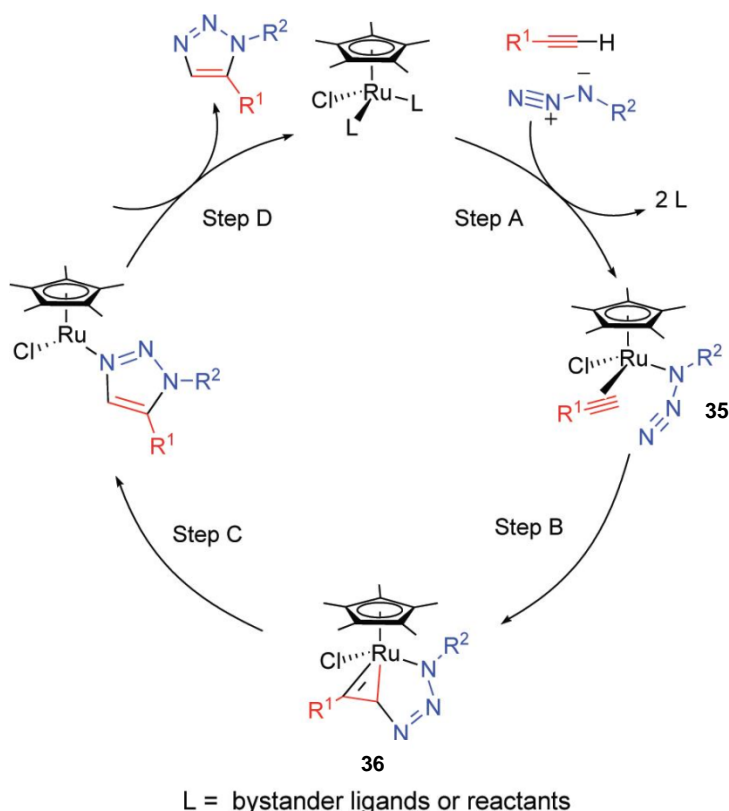
### 3.8. The Ru<sup>II</sup> Catalysed Huisgen Cycloaddition Reaction

The ruthenium catalysed azide-alkyne cycloaddition (RuAAC) reaction was first introduced by the groups of Fokin and Jia in 2005.<sup>84</sup> They discovered that the RuAAC reaction between terminal alkynes and azides selectively synthesises the 1,5-triazole regioisomer. Furthermore, the RuAAC reaction can overcome the limitations experienced by the CuAAC reaction and catalyse the cycloaddition of azides with internal alkynes.<sup>85</sup>

Ruthenium catalysed cycloaddition reactions are sensitive to the nature of the ligands associated with the ruthenium metal centre. In other words, the activity and regioselectivity of RuAAC reactions are dependent on nature of ligands.<sup>84</sup> In a paper by Boren *et al.* a number of ruthenium complexes were used as catalysts in a cycloaddition reaction between benzyl azide and phenyl acetylene to determine which ligands provided the most efficient and regioselective cycloaddition reaction.<sup>84</sup> They discovered that the ruthenium catalysts  $\text{Cp}^*\text{RuCl}(\text{PPh}_3)_2$ ,  $\text{Cp}^*\text{RuCl}(\text{COD})$  and  $[\text{Cp}^*\text{RuCl}]_4$  gave 100% conversion to the 1,5-regioisomer. However, the  $\text{Cp}^*\text{RuCl}(\text{COD})$  catalyst is more labile compared to ruthenium catalysts with phosphine ligands

and displaced more readily. This catalyst was also found to be particularly advantageous in reactions involving aryl azides and internal alkynes.<sup>85</sup> We had access to Cp\*RuCl(COD) and we decided to test if this would be the case for our own set of compounds.

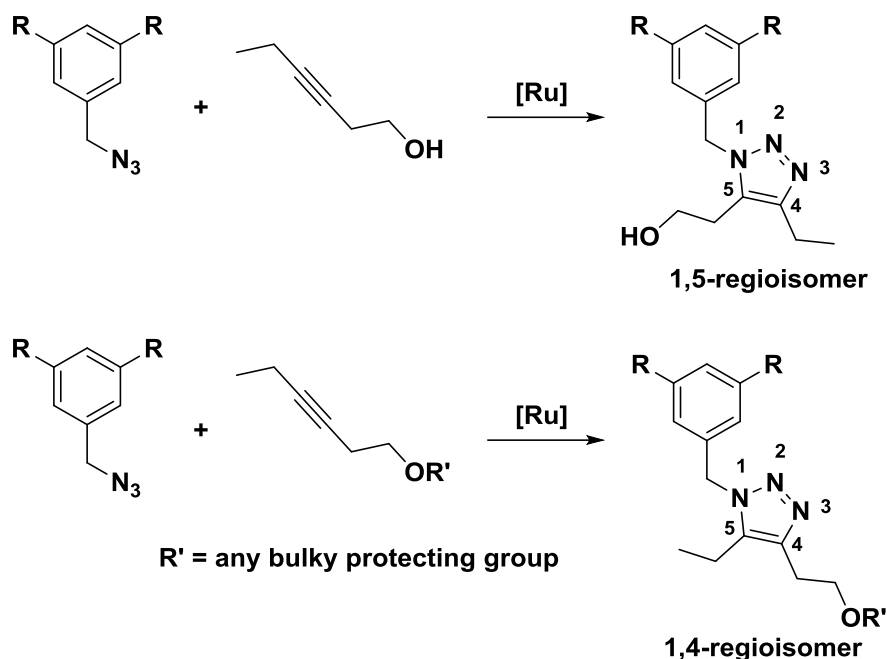
As the RuAAC reaction can occur with internal alkynes as well as terminal alkynes it is thought to be unlikely that ruthenium acetylides are involved in the catalytic cycle, unlike the formation of copper acetylide species in the CuAAC reaction. Ruthenium catalysis or cyclotrimerization using Cp\*RuCl(COD) proceeds *via* a ruthenapentamethylcyclopentadiene intermediate.<sup>85</sup> The first step in this catalytic cycle is the displacement of the spectator ligands by coordination of the alkyne and azide components to the ruthenium metal centre to yield the activated ruthenium complex **35** (Scheme 12). This is subsequently converted to the ruthenacyclopentadiene intermediate **36** *via* oxidative coupling of the azide and alkyne. This step is thought to control the regioselectivity of the reaction. The new C-N bond forms between the least sterically hindered and more electronegative carbon of the alkyne and the terminal nitrogen of the azide. This then undergoes reductive elimination, releasing the triazole product and regenerating the ruthenium catalyst.<sup>85</sup>



**Scheme 12** Proposed mechanism for RuAAC reaction adapted from Boren *et al.*<sup>85</sup>

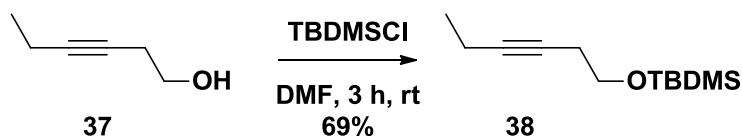
For our purposes the internal alkyne 3-hexyn-1-ol was commercially available. As this is an asymmetric alkyne there was the possibility of two regioisomers being formed when carrying out the RuAAC reaction. A study by Majireck and Weinreb reported that cycloaddition reactions with propargylic alcohols form exclusively the regioisomer where the alcohol chain is positioned at position 5 of the triazole ring, which in our case would be adjacent to the methylene linker (Scheme 13).<sup>86</sup> However, in an attempt to force the cycloaddition of the benzyl azide with 3-hexyn-1-ol to generate rather the desired regioisomer where the alcohol chain

occupies the 4-position of the triazole ring we considered introducing more bulk on the alcohol. We thought to achieve this by introducing a large protecting group on alcohol.



Scheme 13

### 3.8.1. Synthesis of *tert*-butyl(hex-3-yn-1-yloxy)dimethylsilane (38)



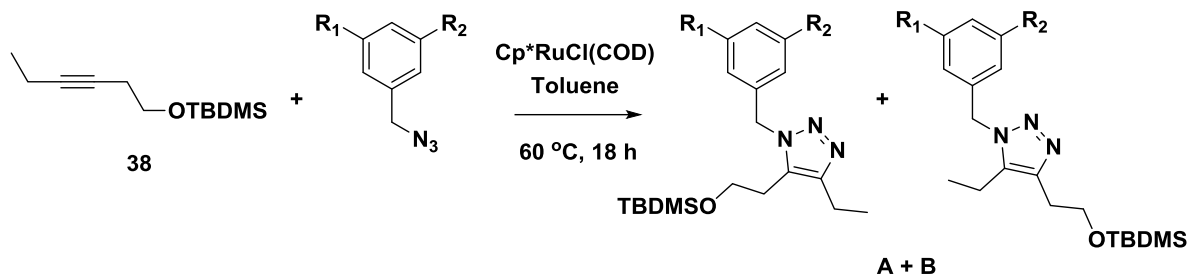
Scheme 14

Protection of the alcohol was easily achieved by stirring a solution of 3-hexyn-1-ol with *tert*-butyldimethylsilyl chloride and imidazole in DMF at room temperature for approximately 3 hours. After a simple workup and purification by column chromatography the product was obtained in 69% yield as a colourless oil.

Analysis of the  $^1\text{H}$  NMR spectrum clearly showed the presence of singlets at 0.88 ppm and 0.05 ppm which integrated for 9H and 6H respectively. These singlets correspond to the *tert*-butyl and dimethyl functionalities respectively.

### 3.8.2. Synthesis of fully substituted triazole series of compounds

With the protected alcohol **38** in hand we could proceed with the ruthenium catalysed cycloaddition reaction (Scheme 15). Toluene was the solvent of choice due to its high boiling point in case a higher activation was necessary. To ensure that the reaction conditions were inert the toluene was degassed for 10 min with nitrogen. The alkyne **38** and benzyl azide **5** were then added after which a second degassing was carried out. Finally the ruthenium catalyst  $\text{Cp}^*\text{RuCl}(\text{COD})$  was added and the reaction was heated to 60 °C and left for 18 hours.



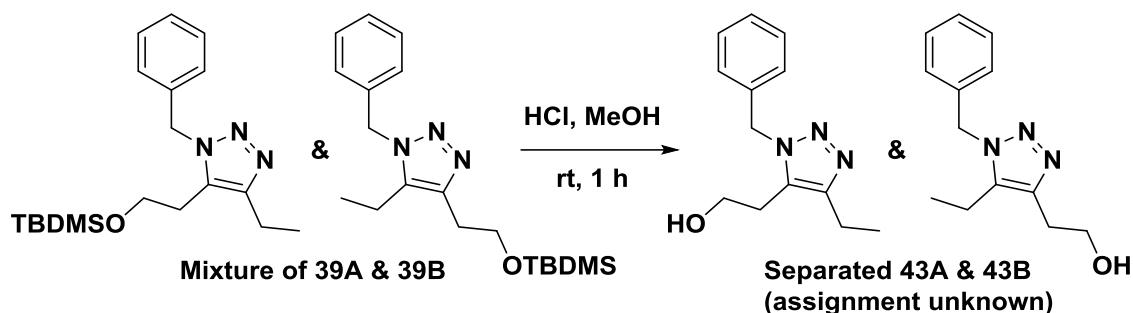
Scheme 15

We noticed when analysing the TLC that two products had formed. We expected that these products corresponded to the regioisomers represented in Scheme 15. As both products had very similar R<sub>f</sub> values we decided to keep the products combined and carry out the deprotection on the combined material. In doing so we hoped that removing the protecting group would result in a better separation of the two products allowing for easier purification and characterisation.

Table 3

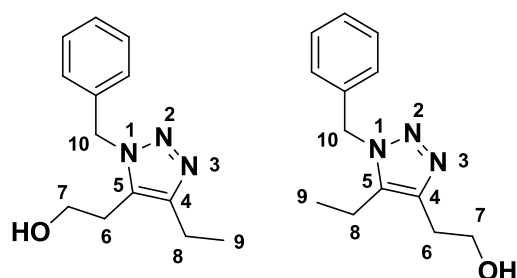
Compound	R <sub>1</sub>	R <sub>2</sub>
39A & 39B	H	H
40A & 40B	Cl	Cl
41A & 41B	H	CN
42A & 42B	Me	Me

### 3.8.3. Deprotection of fully substituted triazole compounds



Scheme 16

The combined products **39A** and **39B** were taken up in methanol and 3 equivalents of 6N HCl was added at 0 °C. The deprotection was carried out at room temperature for approximately 1 hour and as hoped, separation of the alcohols **43A** and **43B** was then possible by conventional chromatography.



Analysis of the  $^1\text{H}$  NMR spectrum of both products **A** and **B** revealed similarities between the two spectra that reinforced our hypothesis that two regioisomers had been formed. In both spectra signals were observed for protons 6, 7, 8 and 9, as well as for the methylene linker 10. However, the chemical shifts for these signals differed between the two spectra. The signals at chemical shifts corresponding to the aromatic region of the two compounds remained unchanged.

### 3.8.4. Employing NOE experiments to distinguish between the two regioisomers

In order to unambiguously assign compounds **43A** and **43B** as the 1,4- or 1,5-regioisomers (with regards to the position of the alcohol chain on the triazole ring) we once again employed the use of  $^1\text{H}$  NOE. Here we focused on the possibility of correlations between the methylene linker and the two substituents on the triazole ring (Figure 28).

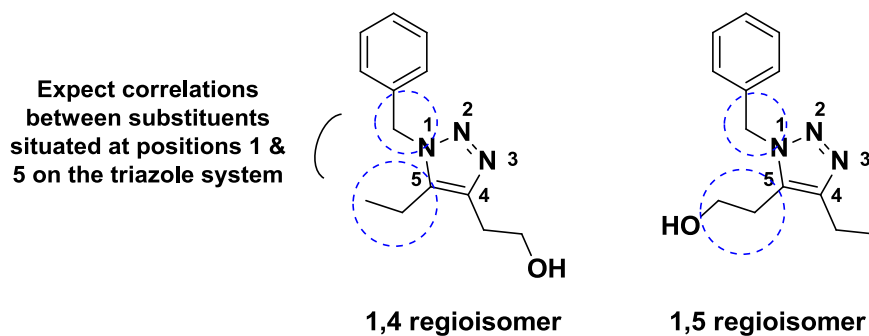


Figure 28

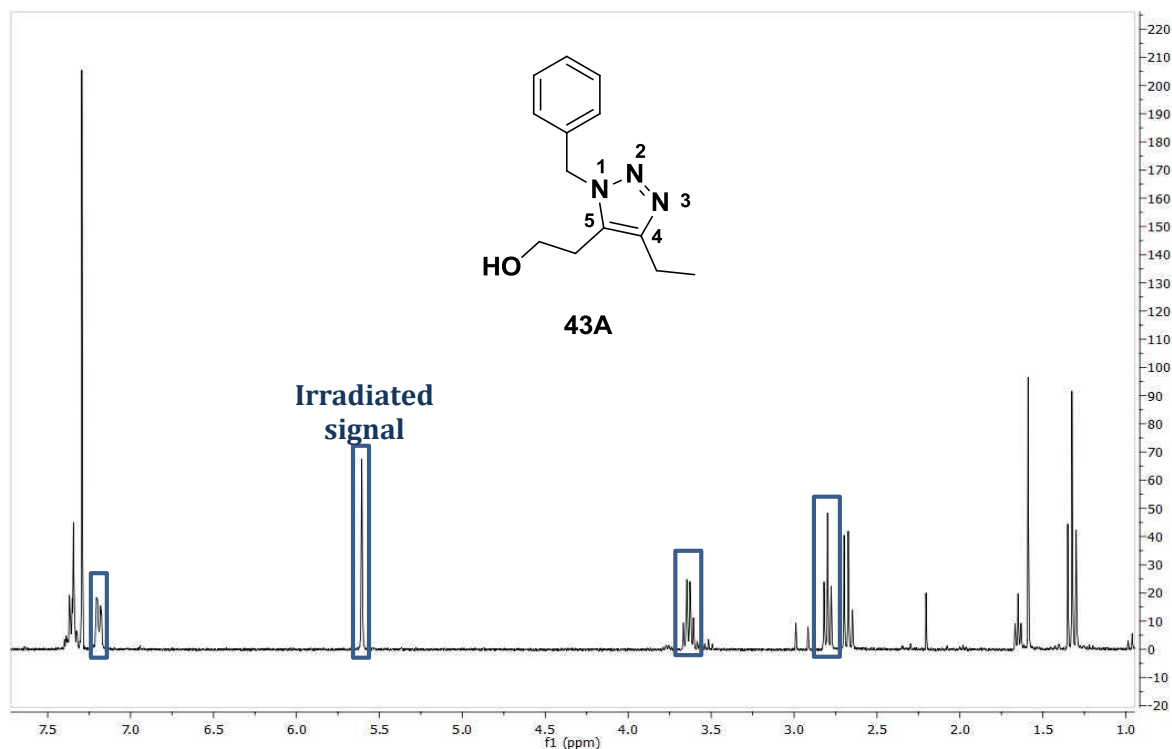


Figure 29

For both compounds, we irradiated at the chemical shifts corresponding to the methylene linker in the hope that the correlations observed in the one spectrum would allow us to unambiguously assign the regiochemistry. This would provide us with a clear indication which substituent on the triazole ring is adjacent to the methylene linker for each regioisomer. For the product **A**, irradiation at 5.56 ppm revealed clear correlations to signals at 2.74 ppm, 3.64 ppm and 7.14 ppm represented by the blue blocks on the <sup>1</sup>H NMR spectrum (Figure 29). The signal at 7.14 ppm corresponds to the aromatic protons and so a correlation between these protons and those on the methylene linker is to be expected for both compounds and is unhelpful. However, the observation of the signals at 2.74 ppm and 3.64 ppm is somewhat more helpful. Both of these signals are triplets and integrate for 2H. Both signals, therefore, correspond to the ethyl alcohol chain on the triazole ring. From these observations it is clear that the first product **A** corresponds to regioisomer where the ethyl alcohol chain is situated at position 5 of the triazole ring and the ethyl chain is at the 4-position.

For the second product **B** we would expect to see correlations between the protons on the methylene linker and the protons on the ethyl chain. We again irradiated at the signal corresponding to the protons of the methylene linker at 5.52 ppm. Here we saw clear correlations to signals at 1.00 ppm, 2.57 ppm and 7.20 ppm also represented by the blue blocks on the <sup>1</sup>H NMR spectrum (Figure 30). Once again the signal at 7.14 ppm corresponds to the aromatic protons. The signal at 1.00 ppm is a triplet and integrates for 3H, whereas the signal at 2.57 ppm is a quartet and integrates for 2H. These signals, therefore, correspond to the ethyl chain on the triazole ring. Again from these observations we were able to prove that the second product **B** was the regioisomer where the ethyl chain was now situated at the 5-position.

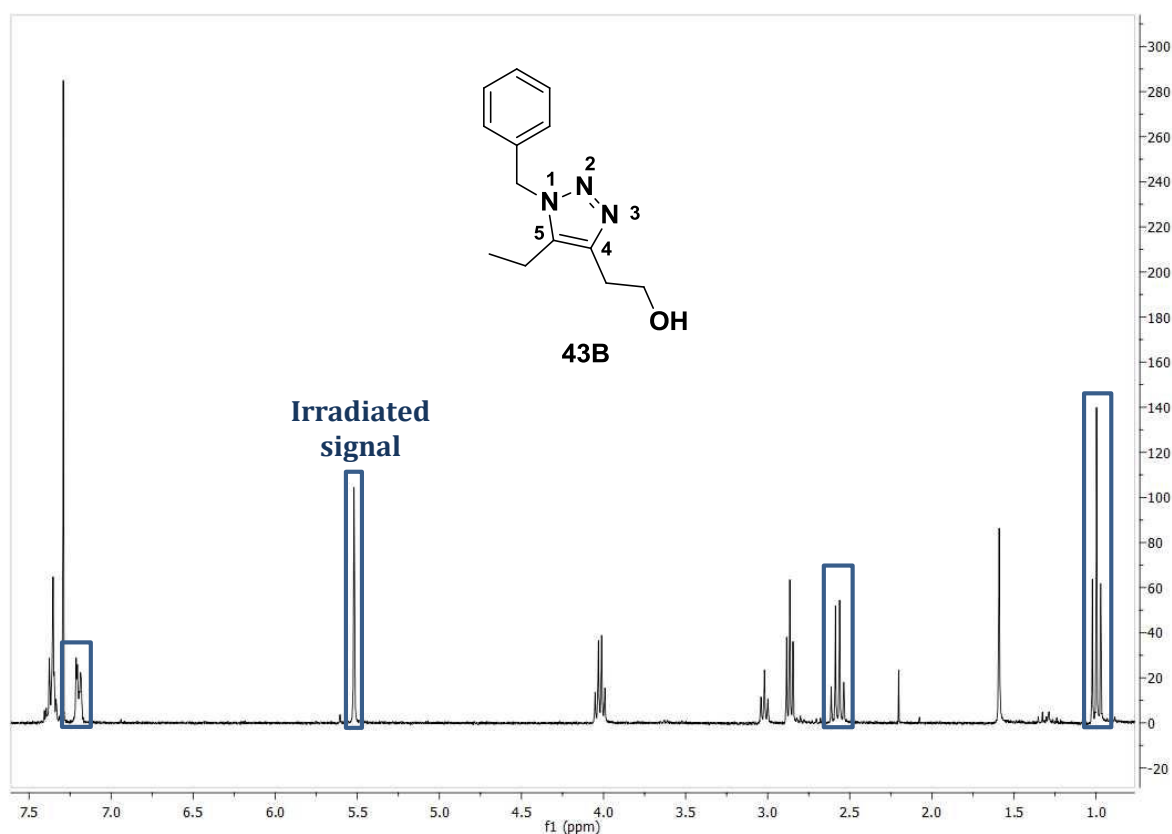


Figure 30

Along with these two fully substituted triazole compounds, a further 5 were successfully synthesized (Table 4) using the exact same synthetic method. As with **43A** and **43B** the yields for these reactions were poor, but enough product was obtained for characterization purposes and for testing. Unfortunately compound **46B** proved to be an exception as although we suspected we had formed both regioisomers we were unable to isolate both products as there was too little of **46B** to isolate.

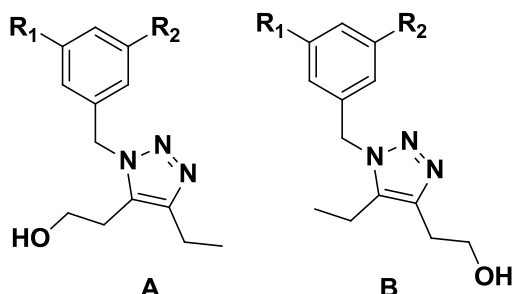
Table 4

Compound	R <sub>1</sub>	R <sub>2</sub>	%Yield	
			A	B
<b>43</b>	H	H	22	9
<b>44</b>	Cl	Cl	37	12
<b>45</b>	H	CN	29	13
<b>46</b>	Me	Me	29	-

### 3.9. Efficacy results for fully substituted triazole compounds

The set of 1,4- and 1,5-triazoles were sent to the National Institute for Communicable Diseases (NICD) for evaluation against wild type HIV in a whole cell assay and the results are presented in Table 5 below.

Table 5



#	R <sub>1</sub>	R <sub>2</sub>	CC50 A (μM)	IC50 A (μM)	CC50 B (μM)	IC50 B (μM)
43	H	H	>100	>100	>100	>100
44	Cl	Cl	>100	72.6	>100	45.2
45	H	CN	>100	>100	>100	>100
46	Me	Me	>100	>100	-	-

Once again these compounds were found to be inactive against HIV with the exception of **44A**, and **44B** which were found to be weakly effective. This was a surprising discovery due to the similarity between these compounds and lersivirine.

At this point we hypothesized that the underlying issue with regards to these compounds is a structural one. A paper by Mowbray *et al.* describing the synthesis of a series of pyrazole compounds leading to the discovery of lersivirine showed that the presence of two ethyl chains on the pyrazole ring presented the best efficacy results.<sup>51</sup> We termed these ethyl chains the upper and lower arms of lersivirine (Figure 31).

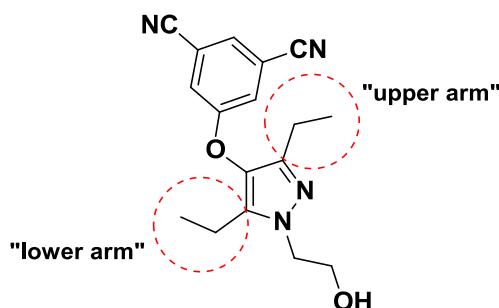
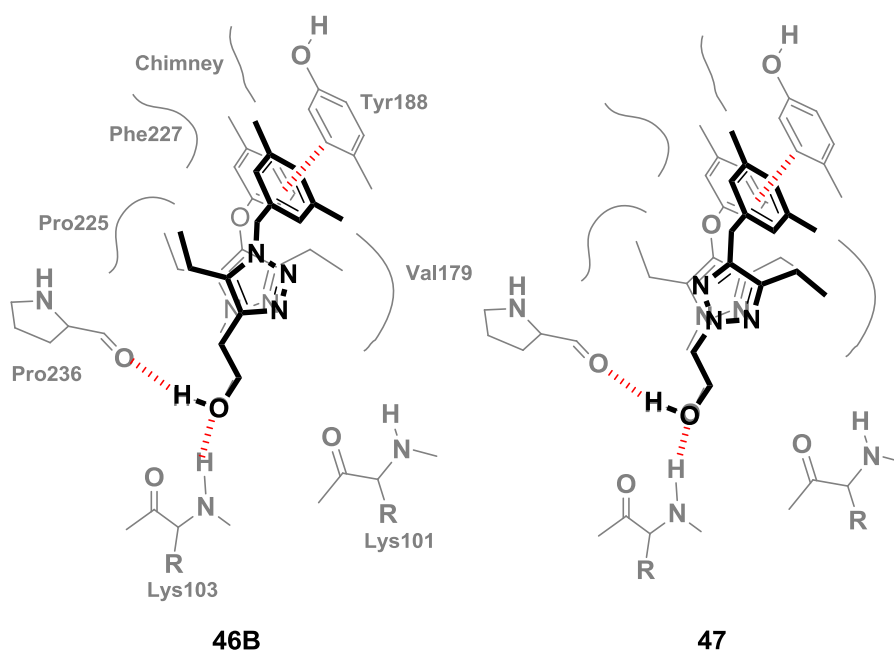


Figure 31

If we made the assumption that our 1,4-triazole compounds (compounds **B**) bind to the allosteric pocket in a similar manner to lersivirine, then the ethyl chain on our compounds



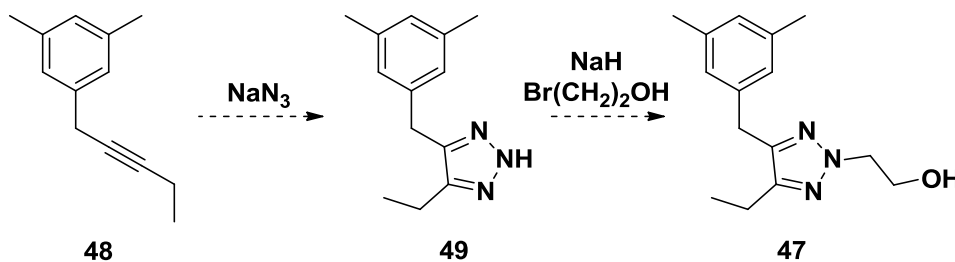
would occupy the position of the “lower” arm on the ring towards the back of the allosteric pocket (Figure 32, left). Unfortunately, due to the nature of the triazole ring we could not introduce a fourth substituent so that our structures could closely mimic the fully substituted pyrazole ring of lersivirine. We hypothesized that perhaps we had focussed on the wrong ethyl chain and, as a result, the ethyl chain should occupy the position of the “upper” arm of lersivirine (Figure 32, right), thereby, occupying the Val179 pocket. In order to achieve this we would need to revise the layout of our triazole scaffold as it is impossible to have the ethyl chain in the upper region using the benzylic azide precursors we had been using throughout the synthesis of our small triazole library. We would need to synthesize the less conventional 2*N*-substituted triazole regioisomer **47**. The synthesis of 2*N*-substituted triazole rings can only occur between terminal and internal alkynes and unsubstituted azides such as sodium azide.<sup>87</sup>



**Figure 32** Comparison of the proposed binding modes of **46B** and **47** with lersivirine

### 3.10. Synthesis of 2*N*-triazole regioisomers 47

To obtain the desired 2*N*- triazole regioisomer (Scheme 17), the alkyne would have to be built onto the benzyl moiety as opposed to the azide as was done previously. From here we envisaged that we could form the 2*N*-triazole ring with sodium azide and then introduce an alcohol chain at the 2*N* position using 2-bromoethanol. For the purpose of being able to make a direct comparison with the triazole compounds synthesized previously we would utilize the 3,5-dimethyl aryl moiety.

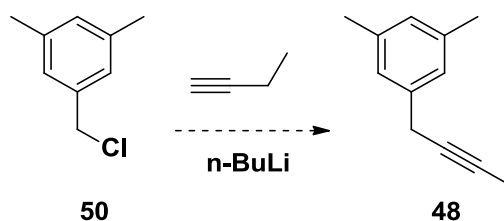


Scheme 17 proposed route to the 2*N*-regioisomer

#### 3.10.1. Attempts to synthesize 1,3-dimethyl-5-(pent-2-yn-1-yl)benzene (48)

In the synthesis of **48**, our initial strategy was to quite simply use the alkynyl anion as the nucleophile, and react it with benzyl chloride (Scheme 18). To our surprise there was very little literature precedence for such a strategy, especially with regards to the usage of short chain alkynes. However, we decided to attempt this synthetic route regardless as all the starting materials were readily available. As a slight technical difficulty, 1-butyne has a low boiling point and so it was imperative that all reactions were carried out below 8 °C.

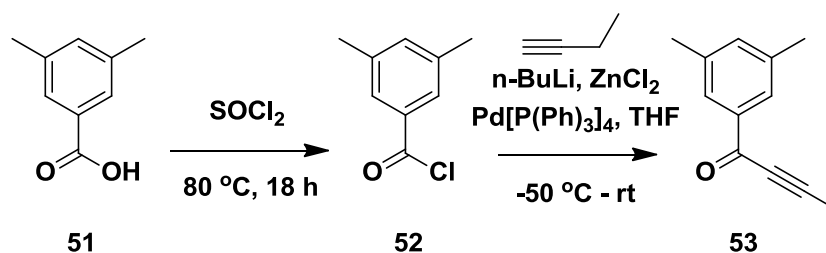
Unfortunately, our first attempt to synthesize the alkyne **48** by carrying out a simple nucleophilic substitution reaction with 3,5-dimethylbenzyl chloride, *n*-BuLi and 1-butyne was unsuccessful.



Scheme 18

A survey of the literature revealed a slightly more complex procedure which involved a copper promoted coupling reaction between terminal alkynes and benzyl halides.<sup>88</sup> The paper that reported this procedure focused largely on the coupling of benzyl halides with alkyl propiolates with the use of copper iodide, potassium carbonate and tetrabutylammonium iodide. However, they did report using the same reaction conditions for the coupling of benzyl chloride with hexyne. Unfortunately in our hands, this reaction did not proceed at all.

## 3.10.2. Synthesis of 1-(3,5-dimethylphenyl)pent-2-yn-1-one (53)

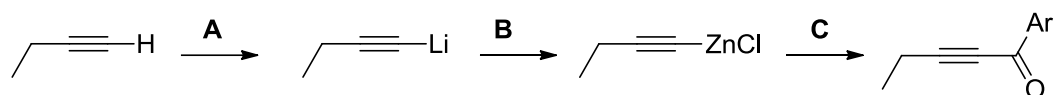


Scheme 19

Having been unsuccessful in our previous attempts, we now directed our attention to the fact that in stark contrast to the sparse amount of literature describing reactions involving alkylyl anion nucleophilic substitution onto benzyl chlorides, the literature describing the same substitution reaction onto acyl chlorides was far more abundant. Therefore, we considered this same strategy with the knowledge that we could remove the ketone at a later stage in the synthesis. This procedure was reported by Verkruijsse *et al.*<sup>89</sup> Here they report preparation of acetylenic ketones through an alkynylzinc chloride intermediate.

However, we first had to synthesize 3,5-dimethylbenzoyl chloride **52** from 3,5-dimethylbenzoic acid **51** (Scheme 19). This reaction was proceeded without incident by heating the benzoic acid in excess of thionyl chloride under reflux at 80 °C for 18 hours. The thionyl chloride was removed and the resulting 3,5-dimethylbenzoyl chloride was taken crude to the next step.

With the benzoyl chloride in hand we could carry out the procedure outlined by Verkruijsse *et al.* (Scheme 20).<sup>89</sup>



Scheme 20

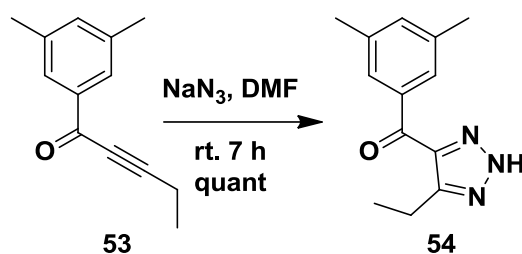
The first step in this reaction sequence was to lithiate the alkyne (Step A). However, as 1-butyne is a gas at 8 °C great care had to be taken to ensure that the reaction was kept at a low temperature at all times. In order to ensure that we were, in fact, working with a sufficient amount of 1-butyne, we decided to first condense the butyne gas by releasing the gas into a round bottomed flask that was cooled to about -50 °C. We attempted to condense an excess amount of the butyne gas as we would control with stoichiometry of the reaction with n-BuLi. The formation of a clear liquid at the bottom of the flask indicated that we had successfully collected 1-butyne and could, therefore, proceed with the reaction. From here the 1-butyne was carefully diluted with cold THF. This was followed by the addition of n-BuLi, all the while ensuring that the addition of solvent and reagents was slow enough so as not to heat up the 1-butyne. Once we had lithiated the alkyne we warmed the reaction to 0 °C before adding the zinc chloride, forming the alkynylzinc chloride intermediate (Step B). In order for the alkynylzinc chloride to react with the benzoyl chloride a catalytic amount of Pd[P(Ph)<sub>3</sub>]<sub>4</sub> had to be added to the reaction mixture preceding the addition of the benzoyl chloride. This, according to Verkruijsse *et al.*<sup>89</sup> would activate the carbonyl for attack by the alkynyl intermediate. Furthermore, they reported that without the presence of catalyst this reaction would not occur

but rather result in a number of side products.<sup>89</sup> Finally 3,5-dimethylbenzoyl chloride could be added (Step C) resulting in the formation of the desired acetylenic ketone **53**.

By monitoring the reaction on TLC, it was observed that almost immediately after the addition of 3,5-dimethylbenzoyl chloride it had appeared that the reaction had gone to completion. As we were unsure of the stability of **53** we decided to take the product into the next reaction crude.

### 3.10.3. Synthesis of (3,5-dimethylphenyl)(5-ethyl-2H-1,2,3-triazol-4-yl)methanone (**54**)

With the alkyne **53** in hand, we could directly synthesize the 4,5 disubstituted triazole ring **54** using sodium azide (Scheme 21). It is in this step that the importance of the carbonyl group adjacent to the alkyne is made clear. According to literature, cycloaddition reactions between internal alkynes and unsubstituted azides often require high temperatures and give low yields. However, the presence of an electron withdrawing group adjacent to the alkyne improves the reactivity of the alkyne.<sup>90</sup>

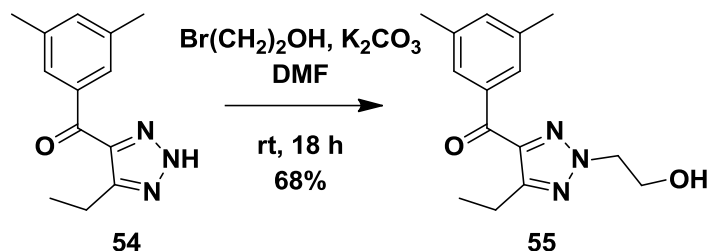


Scheme 21

The crude alkyne **53** was taken up in DMF with 1,2 equivalents of sodium azide and the reaction was carried out at room temperature for approximately 7 hours. The reaction mixture was then acidified and the product was purified by column chromatography to yield **54** as a yellow solid.

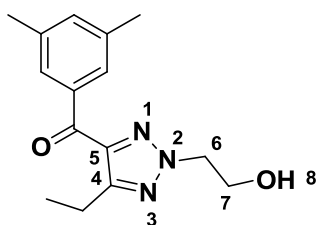
Unfortunately, analysis of the  $^1\text{H}$  NMR spectrum did not reveal any additional additional signals in comparison to **53** as the NH signal was not observed. However this phenomenon seemed to be in accordance with literature. Fortuitously the correct number of carbons in the  $^{13}\text{C}$  NMR spectrum along with the significant difference in  $R_f$  value between compounds **53** and **54** indicated that we had achieved the desired product **54**. At this point we decided that we would only know for sure once we had attempted subsequent steps in the reaction synthesis.

### 3.10.4. Synthesis of (3,5-dimethylphenyl)(5-ethyl-2-(2-hydroxyethyl)-2H-1,2,3-triazol-4-yl)methanone (**42**)



Scheme 22

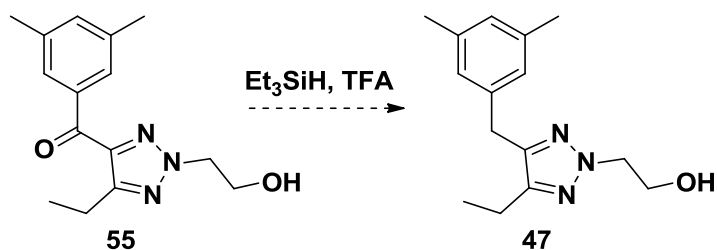
Having synthesized the triazole ring **54**, we were now in a position to introduce the final substituent required on our scaffold. The addition of the alcohol chain onto the triazole compound **54** was carried out using 2 equivalents of potassium carbonate and 1.5 equivalents of bromoethanol in DMF.<sup>91</sup> The reaction was carried out at ambient temperature for approximately 18 hours. Purification using column chromatography yielded 68% of **55** as a yellow solid.



We were able to establish the presence of the alkyl chain through analysis of the  $^1\text{H}$  NMR spectrum for **55**. Two multiplets at 4.62 ppm and 4.17 ppm were observed, both of which integrated for 2H. These correspond with protons at positions 6 and 7 of the alkyl chain. The presence of the alcohol was also observed due to the presence of a small triplet at 2.83 ppm integrating for 1H.

### 3.10.5. Attempts to reduce the benzylic ketone to the corresponding alkane

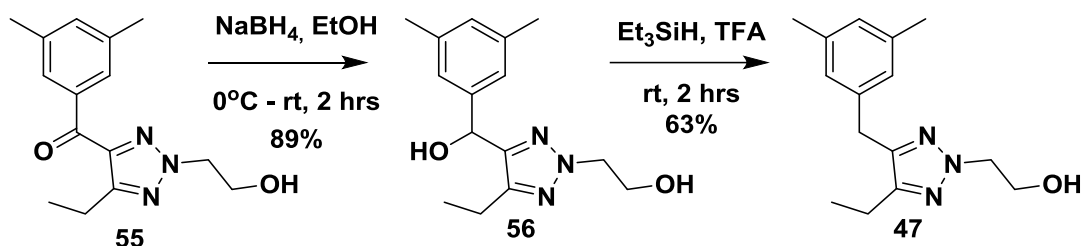
Once the fully substituted triazole ring was in hand the next step was to remove the benzylic ketone functionality to relinquish the desired methylene linker. The reduction of a ketone located between a phenyl group and heteroaromatic ring to the corresponding alkane had been successfully executed on a different scaffold within our research group and, as a result, we thought to use the same synthetic strategy on our scaffold.<sup>59</sup> The reduction was carried out employing trifluoroacetic acid and a large excess of triethylsilane (Scheme 23). However, on our scaffold this reaction resulted in incredibly poor yields, making even characterization difficult.



Scheme 23

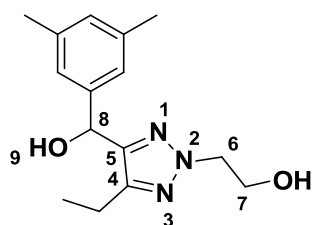
After searching through the literature, however, we were able to find a possible alternative strategy to optimize this reaction. The literature revealed that the above mentioned reduction proceeds *via* the corresponding secondary alcohol, which is then eliminated in the presence of

TFA to form a stabilized carbonium ion. The triethylsilane then acts as a hydride donor.<sup>92</sup> Considering the mechanism by which this reaction occurred we envisaged that perhaps we could optimize this reaction by first reducing the ketone to the alcohol and then carrying out the reduction of the alcohol using triethylsilane and TFA (Scheme 24).<sup>93</sup> A possible complication that we considered was that after reducing the ketone to the secondary alcohol, we would have two hydroxyl functionalities on our scaffold **56**. Although this problem could be readily solved by selectively protecting the primary alcohol, literature suggested that this precaution would not be necessary. A paper by Gevorgyan *et al.* suggested that reduction of a primary alcohol with triethylsilane would require the presence of a strong Lewis acid.<sup>94</sup>



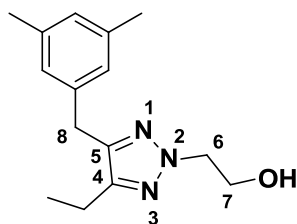
Scheme 24

With this in mind we proceeded with the reduction of the ketone without taking the precautionary measure of first protecting the primary alcohol. To this end, sodium borohydride was added to **55** in ethanol at  $0^\circ\text{C}$  after which the reaction was allowed to proceed at room temperature. The starting material was consumed within 2 hours. The crude product **56** required no purification and was obtained in 89% yield as a white solid.



Analysis of the  $^1\text{H}$  NMR spectrum of **56** confirmed that the reduction of the benzylic ketone to the alcohol had been successful. The benzylic proton 8 was identified at 5.87 ppm as a doublet integrating for 1H.

Having disposed of the ketone functionality, reduction of the resulting secondary alcohol was carried out without taking the precautionary measure of first protecting the secondary alcohol. To this end **56** was stirred with trifluoroacetic acid and an excess of triethylsilane. The reaction was run for 2 hours at room temperature, worked up and purified by column chromatography to yield **47** in 63% yield as a white solid.



Analysis of the  $^1\text{H}$  NMR spectrum for **47** revealed that the doublet observed for **56** was no longer present. However, a singlet at 3.92 ppm integrating for 2H was now observed which corresponded to the protons 8 on the methylene linker of **47**.

### 3.10.6. Confirmation of the structure of 2-(4-(3,5-dimethylbenzyl)-5-ethyl-2*H*-1,2,3-triazol-2-yl)ethanol (**47**)

Having arrived at our desired compound **47**, an important consideration is the fact that there are indeed three possible regioisomers upon substitution of the triazole ring with the alcohol chain (Figure 33). The first of which is the desired 2*N*-triazole, however, the 1,4- or 1,5-triazole regioisomers were also possibilities. In order to confirm that the isolated product was the desired regioisomer we decided to conduct NOE experiments. The 1,5-regioisomer was thought to be unlikely due to the fact that this would be a sterically crowded system, especially given that the presence of the carbonyl in **55** would result in a preferred co-planar ring system.<sup>87</sup> According to literature the preferred regioisomer is, in all likelihood, the 2*N*-triazole regioisomer.<sup>87</sup> In terms of the 1,4-triazole regioisomer we would expect to see correlations between the ethyl chain and the alcohol chain.

Figure 33 shows the 2*N*-, 1,5- and 1,4-triazole regioisomers respectively. The blue circles represent the correlations we would expect to observe when we look at the results of the NOE experiment.

If we had indeed synthesized the desired 2*N*-regioisomer then we would expect to observe through-space correlations between the protons on the methylene linker and those on the ethyl chain. However, we would also expect no correlations between either the methylene linker protons or ethyl chain protons and the ethyl alcohol chain.

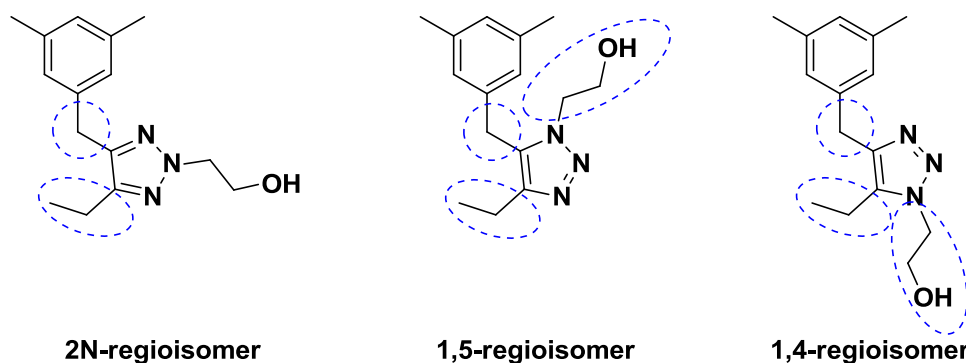


Figure 33 Possible regioisomers

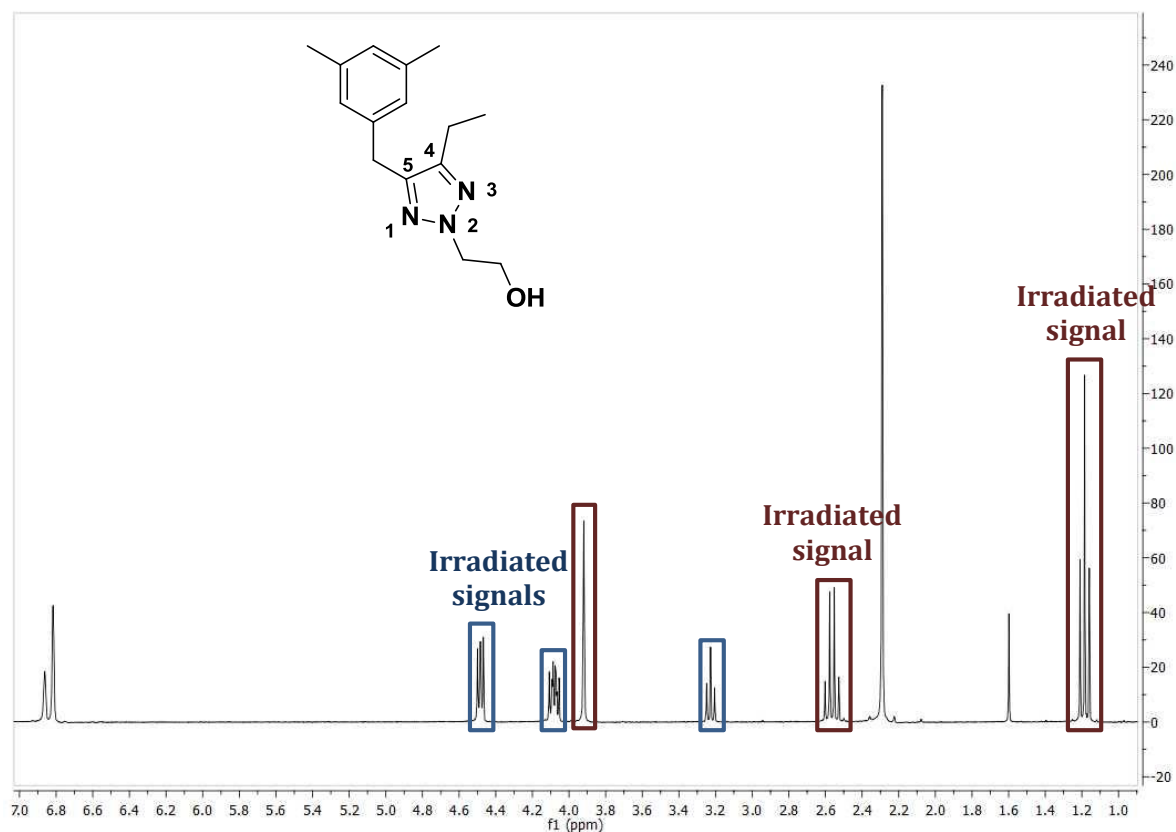


Figure 34

Analysis of the 1D NOE spectra revealed that interactions were indeed observed between the methylene linker and the ethyl chain as expected. Irradiation of the ethyl chain revealed through-space correlations to the methylene linker, however, no further coupling was observed (represented by the red blocks). Furthermore, irradiation of the methylene groups on the ethyl alcohol chain revealed no correlation to any other group on the triazole ring (represented by the blue blocks). We assume that this is due to the fact that at the 2*N*-position of the triazole ring the ethyl alcohol chain is too far away for any correlations to the rest of the molecule to be observed. We can, therefore, conclude that we did indeed synthesize the desired regioisomer. Satisfied that we had synthesized the desired 2*N*-regioisomer we sent **47** for biological evaluation.



### 3.11. Efficacy results of 2-(4-(3,5-dimethylbenzyl)-5-ethyl-2H-1,2,3-triazol-2-yl)ethanol (**47**)

Having arrived at our target compound **47**, we could now evaluate this triazole scaffold system for efficacy against HIV. The graph below shows the activity results of compound **47** (Figure 35). The similarity of the two curves indicated that the EC<sub>50</sub> value was similar to the CC<sub>50</sub> which, in essence, meant that the little activity we did see was not a result of HIV inhibition but rather reflected the toxicity of this compound at these concentrations. As a result, we could conclude that the new scaffold **47** was not active against HIV RT.

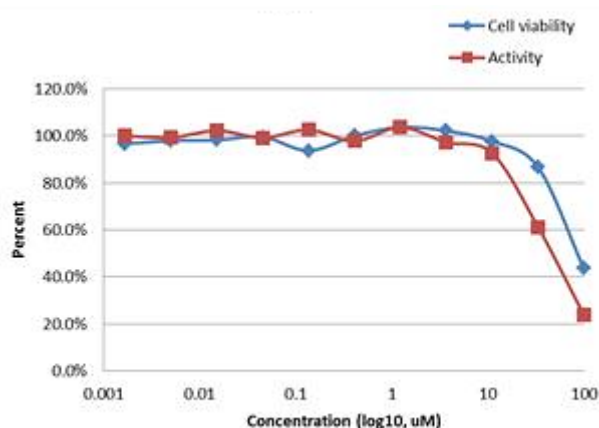


Figure 35

Altogether a library of 15 triazole containing compounds was successfully synthesized but, despite their structural similarity to lersivirine, possessed little to no activity against HIV.

However, we were able to thoroughly explore the possibility of 1,2,3-triazole compounds as novel scaffolds by introducing all possible regioisomers of this moiety. By doing so we were able to conclude that the 1,2,3-triazole functionality is not a suitable scaffold for the synthesis of novel NNRTIs of this scaffold format.

## Chapter 4: A Novel Concept - Targeting Trp229, Tyr188 and Lys101

### 4.1. Indole-based NNRTIs

There have been a number of instances in literature where different research groups employed an indole scaffold, in the development of novel NNRTIs. In most cases the indole was shown to serve as an auspicious scaffold as many of these candidate NNRTIs were shown to possess excellent activity against HIV RT. In 1993 Williams *et al.* reported the development of 5-chloro-3-(phenylsulfonyl)indole-2-carboxamide **57** (Figure 36) which was shown to be potent against HIV RT with an  $IC_{50}$  value of 3 nM and was also shown to exhibit significant activity against clinically important mutations such as K103N and Y181C.<sup>95</sup> Following the development of NNRTI **57**, a number of research groups developed novel NNRTIs with an indole core, which, like compound **58** resulted as a derivation of **57** in order to improve its resistance profile.<sup>96</sup> Recently however, researchers focused on the development of indole based NNRTIs with a phosphorous in place of the sulphur, such as compound **59**, which displayed significantly improved activity against HIV-RT.<sup>97</sup> IDX-899 **60** was developed by Indenix Pharmaceuticals as a promising drug candidate with a high genetic barrier to resistance and with an  $IC_{50}$  value of 1.2 nM against wild type RT.<sup>98</sup> This NNRTI made it to phase IIB clinical trials but unfortunately, development was halted due to adverse effects.<sup>99</sup>

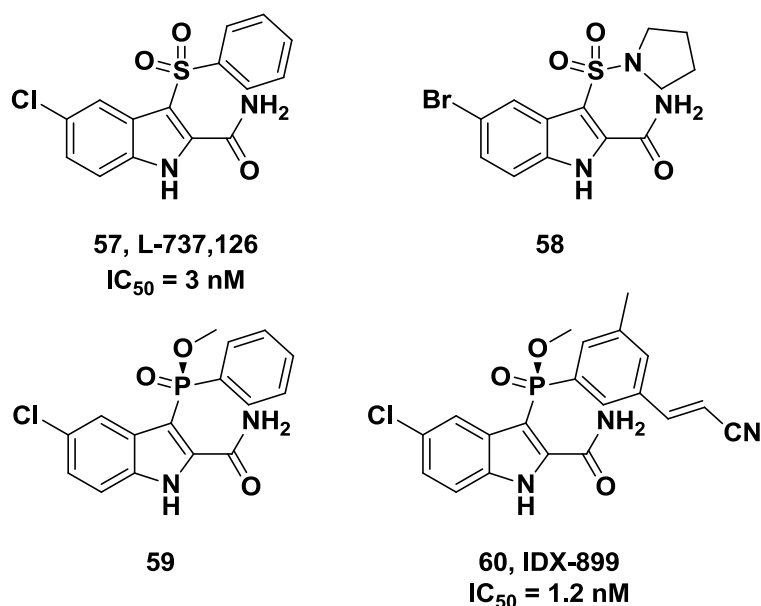


**Figure 36** Some examples of indole based scaffolds employed in the development of novel NNRTIs

## 4.2. Introducing a novel concept

The strategy for the design of our novel indole compound **62** involved combining elements of these indole scaffolds **61** with that of an indazole containing NNRTI **1** (Figure 37). Thus in a molecular hybridization approach, we envisaged that we would be able to retain the beneficial indole scaffold **61**, but shift the aryl functionality to the 4-position as is found on **1** thereby arriving at **62**.

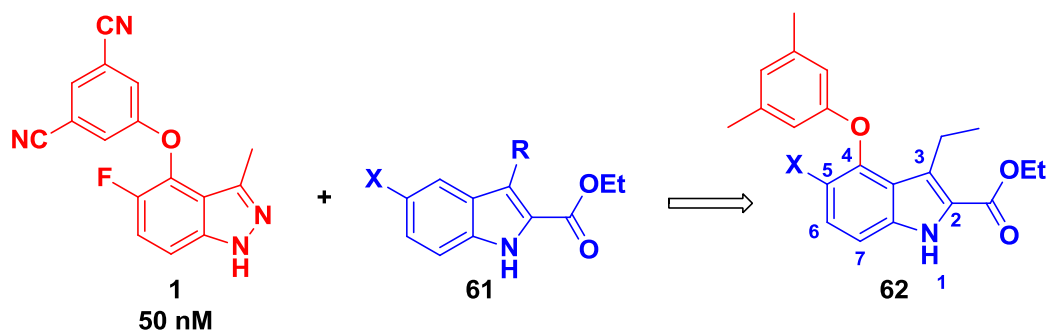


**Figure 37** Combining structural elements of two NNRTI scaffolds to create the indole template **62**

By doing so we would be able to achieve  $\pi$ - $\pi$  stacking interactions with the conserved amino acid residue Trp229 (Figure 38), as well as Tyr188. Furthermore, by maintaining a suitable carbonyl containing functional group, such as an ester, at the 2-position of the indole we would be able to simultaneously achieve hydrogen bonding interactions with the backbone of Lys101 at the entrance of the allosteric pocket. This concept is completely novel as no other NNRTIs within this category have accomplished interactions to both Tyr188 and Lys101. Additional features of our design would include an alkyl group at position 3 to occupy the Val179 pocket and a halogen at the 5-position. Both of these additional structural features have been shown to be imperative to the activity of a number of NNRTIs.<sup>58</sup> As a proof-of-concept and as a starting point in our synthesis we decided that we would employ methyl groups on the aryl ring at position 4 as opposed to the nitrile groups used for compound **1**, as this would simplify synthesis without altering the binding mode.

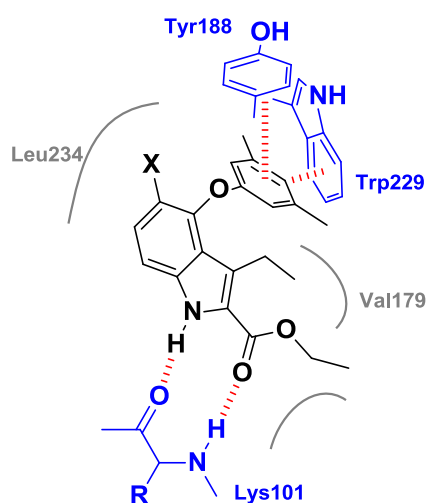
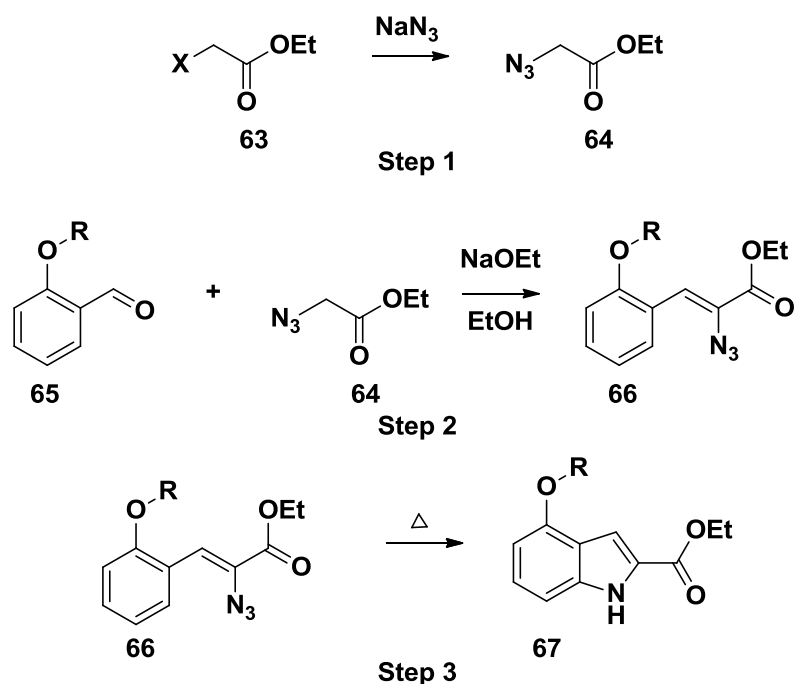


**Figure 38** Predicted binding mode of compound **62** in the NNIBP showing key interactions to Trp229, Tyr188 and Lys101

For the synthesis of compound **62** we originally considered functionalizing commercially available 4-hydroxy indole. However, as we would have to introduce the ester onto the 2-position we strategized that perhaps a more practical strategy would be to construct the indole with the ester functionality already in place. Fortunately, having combed through the literature, the synthesis of a 4-hydroxy indole scaffold was well documented by a number of research groups in a number of applications.<sup>100, 101</sup> They employed the Knoevenagel-Hemetsberger reaction sequence which would not only provide the indole with the hydroxyl functionality in the 4-position but also an ester at the 2-position. This synthetic method was therefore ideal for our purposes.

The Knoevenagel-Hemetsberger reaction sequence (also known as the Hemetsberger-Knittel reaction sequence) is considered a critical workhorse process particularly in an industrial setting and is popular due to the simplicity by which the indolization reaction can occur.<sup>102</sup> This process is divided into three consecutive steps (Scheme 25). Step 1 involves the synthesis of an alkyl azidoacetate **64** from an alkyl haloacetate **63** with sodium azide. This step is followed by a base-promoted Knoevenagel condensation reaction between the alkyl azidoacetate **64** and an aryl aldehyde **65** to form the intermediary  $\alpha$ -azido- $\beta$ -arylacrylate **66**. Finally, step 3 involves formation of the indole **67** through thermolysis of the  $\alpha$ -azido- $\beta$ -arylacrylate **66**.<sup>102</sup>



**Scheme 25** The three steps required for the Knoevenagel-Hemetsberger reaction sequence to form our desired functionalized indole system.

### 4.3. Synthesizing the precursors for the Knoevenagel-Hemetsberger reaction

The two precursors required for the synthesis of our proof-of-concept indole **62** includes ethyl azidoacetate **64** as this would provide the desired ethyl ester functionality at position 2 of the indole and a 2-phenoxy benzaldehyde **69** which would provide us with the hydroxyl functionality at the desired 4-position of the indole (Figure 39). With regards to the benzaldehyde we decided, for the sake of simplicity, to introduce the 3,5-dimethyl aryl group onto the benzaldehyde at the very beginning of our synthetic strategy. Literature has shown that a variety of groups at this position, regardless of the size is well tolerated.<sup>101</sup> As 2-bromobenzaldehyde **70** and 3,5-dimethylphenol **71** were readily available we envisaged we could couple the two reagents using an Ullmann reaction.

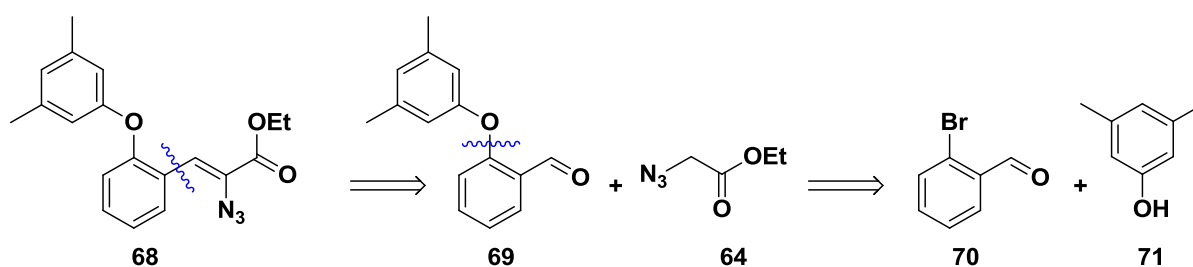


Figure 39

#### 4.3.1. Employing an Ullmann-type coupling reaction to form the biaryl aldehyde precursor

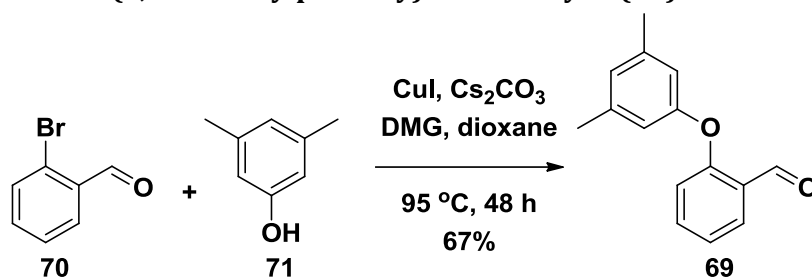
The Ullmann coupling reaction was discovered by Fritz Ullmann and has the reputation of being the most practical and useful method for the synthesis of aryl C-N, C-C and C-O bonds, particularly in industry, although it has been mainly used for the synthesis of biaryl ethers.<sup>103</sup> However, the synthetic scope was relatively limited as these reactions suffered from the use of harsh conditions and high temperatures (125 °C - 250 °C) as well as the use of stoichiometric amounts of copper catalyst required to obtain satisfactory yields.<sup>103, 104</sup>

It was only in 2001 that the introduction of an improved copper-ligand system arose as a solution to these drawbacks. This new method was discovered by the research groups of Taillefer and Buchwald, which led to a resurgence in the use of Ullmann-type reactions.<sup>104</sup> This development enabled for the reactions to occur at milder conditions (90 °C - 110 °C) and allowed for the use of only catalytic amounts of copper.<sup>105</sup> A study by Marcoux *et al.* showed that cesium carbonate seemed to be the base of choice for these reactions, as it substantially improved yields in comparison to other carbonate bases.<sup>106</sup> Furthermore, the choice of copper catalyst appeared to be less essential to the success of the reaction.<sup>103, 106</sup>

Ma *et al.* reported that CuI in the presence of the ligand *N,N*-dimethylglycine hydrochloride was an efficient system to catalyse Ullmann-type coupling reactions between aryl halides and phenols in good to moderate yields at 90 °C.<sup>107</sup> This was an extension of work done previously where this system was used successfully for Ullmann-type aryl amination reactions. The reaction was found to be tolerant of both electron-rich and electron-poor aryl halides, however, sterically hindered phenols give lower yields.<sup>107</sup> Due to the fact that the reagents for this

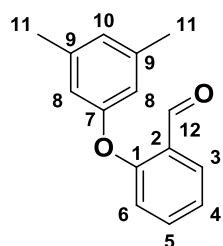
strategy were readily available and inexpensive, we decided to employ this procedure for the coupling of 3,5-dimethylphenol to 2-bromobenzaldehyde.

#### 4.3.1.1. Synthesis of 2-(3,5-dimethylphenoxy)benzaldehyde (69)



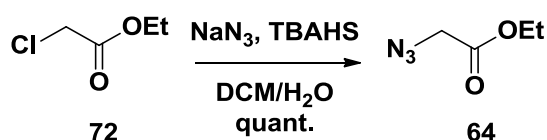
Scheme 26

For our first attempt at synthesizing the benzaldehyde **69** we employed the procedure reported by Ma *et al.*<sup>107</sup> This entailed using a small excess of phenol **71** (1.3 eq) in the presence of  $\text{Cs}_2\text{CO}_3$ , CuI and DMG in dioxane (Scheme 26). However, this reaction never seemed to go to completion and due to the similarity in  $R_f$  value between the product **69** and benzaldehyde **70** we were unable to isolate the pure product. As the starting material was likely to interfere with the subsequent condensation reaction we decided that we would attempt to optimize the reaction by first increasing the amount of 3,5-dimethylphenol introduced in the reaction. Therefore, we attempted to perform the coupling reaction with bromobenzaldehyde **70** in the presence of 4 equivalents of phenol. Through monitoring the TLC we were able to observe that by increasing the amount of phenol we were able to push the reaction to completion. A base wash with NaOH was required to remove excess phenol, as this provided complications when attempting to purify the product using column chromatography. This reaction produced **69** as a yellow oil and gave moderate to high yields.



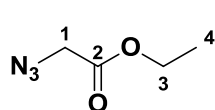
In the  $^1\text{H}$  NMR spectrum the characteristic aldehyde signal **12** was observed as a singlet at 10.52 ppm. Two broad signals at 6.83 and 6.69 ppm integrated for 1H and 2H respectively corresponding to the 3,5-dimethyl aryl ring protons **8** and **10**. Mass spectral analysis reported a mass of 227.1076 amu which corresponds with the expected mass of 227.1072 amu.

#### 4.3.1.2. Synthesis of the second required precursor ethyl 2-azidoacetate (64)



Scheme 27

The synthesis of ethyl azidoacetate was carried out with ease using a nucleophilic substitution reaction. Ethyl chloroacetate **72** was taken up in DCM and water in the presence of tetrabutylammonium hydrogen sulphate as a phase transfer catalyst and sodium azide.

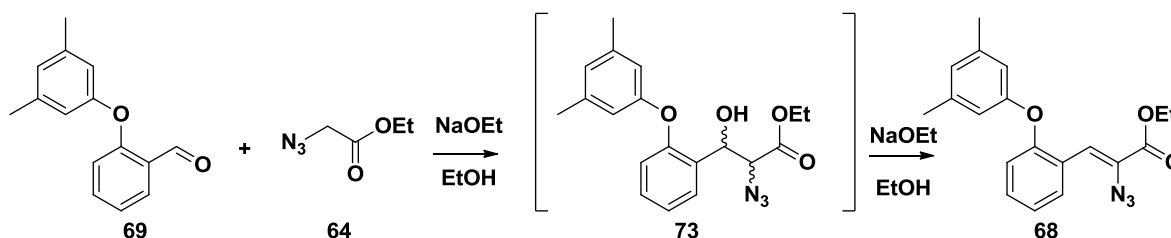


The  $^1\text{H}$  NMR and  $^{13}\text{C}$  NMR data obtained coincided with the NMR data reported in literature.<sup>108, 109</sup> The signal for the methylene protons at position 1 integrates for 2H and is observed as a singlet at 3.86 ppm and the ethyl chain signals at 4.23 and 1.28 ppm integrate for 2H and 3H respectively. For the  $^{13}\text{C}$  NMR spectrum signals are observed at 168.3, 61.8, 50.2 and 14.0 ppm. Unfortunately, the sample decomposed when sent for MS analysis, which was not surprising for this azide.

#### 4.4. Initial attempts to synthesize the indole product.

##### 4.4.1. Employing the Knoevenagel condensation reaction to synthesize the acrylate precursor

The Knoevenagel condensation reaction between the aryl aldehyde **69** and alkyl azidoacetate **64** occurs through an azido alcohol intermediate **73** (Scheme 28). This intermediate then undergoes an elimination to yield the acrylate product **68**.<sup>110</sup>

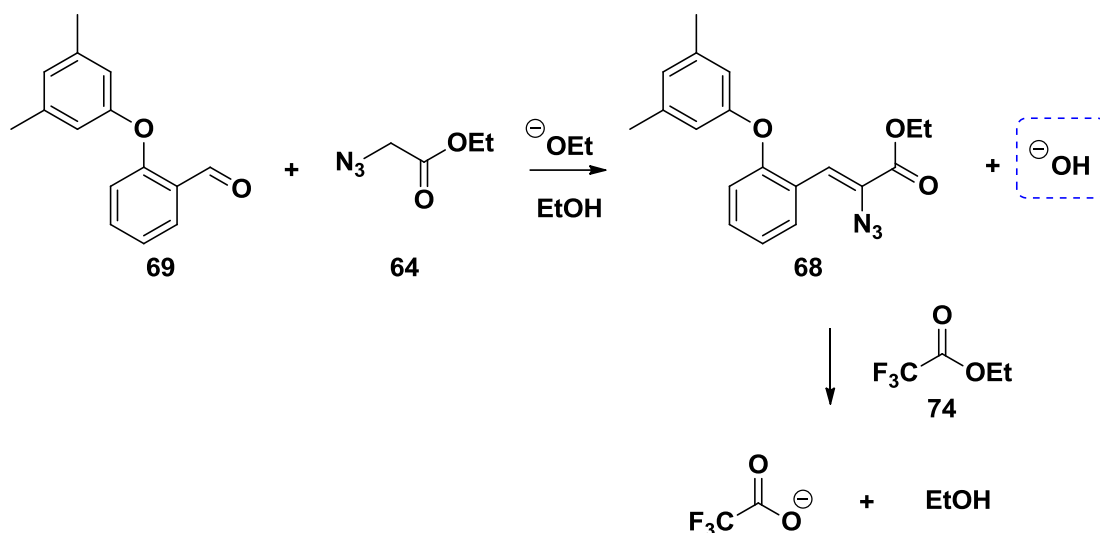


Scheme 28 Knoevenagel condensation reaction

Initially we attempted a procedure for the Knoevenagel condensation reaction reported by Coowar *et al.*<sup>100</sup> Sodium ethoxide was synthesized *in situ* from sodium in ethanol, and a mixture of azido ethylacetate **64** and benzaldehyde **69** in EtOH and THF was added to the reaction mixture. Unfortunately, using this method we were unable to isolate any of the desired products and monitoring the reaction by TLC revealed that numerous products were forming.

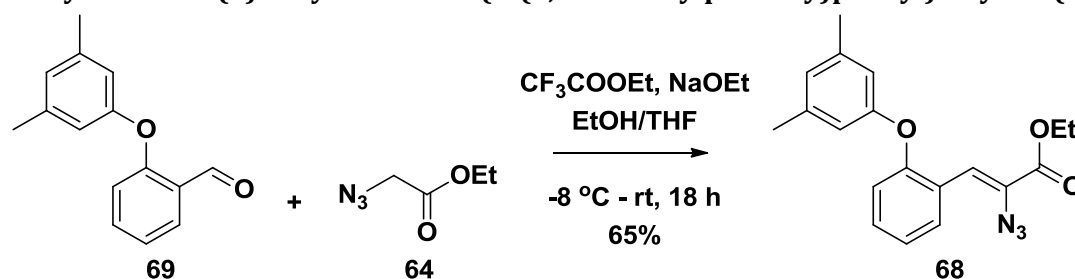
However, upon returning to the literature we discovered that this undesirable result could be explained. In a paper by Heaner *et al.*, it was reported that low yields were not uncommon with the synthesis of  $\alpha$ -azido- $\beta$ -arylacrylate and that there are two principal reasons behind the poor results for this reaction.<sup>102</sup> The first suggests that the ethyl azidoacetate is unstable and decomposes in the presence of base which, as a result, then interferes with the condensation process. Secondly the hydroxide by-product that had been eliminated after the condensation reaction can result in the hydrolysis of the ester group of the azido acetate **64**, the azido alcohol intermediate **73**, as well as the acrylate product **68**.<sup>102</sup>

It was reported that to overcome these complications and to maximize yields was to introduce a sacrificial electrophile, such ethyl trifluoroacetate **74**, to the reaction (Scheme 29).<sup>102</sup> The sacrificial electrophile which, by definition has to be highly electrophilic, is introduced in the condensation reaction to react with the hydroxide by-product before it is able to hydrolyse the ester functionality of the desired  $\alpha$ -azido- $\beta$ -arylacrylate product. The reaction between the hydroxide and the ethyl trifluoroacetate produces a weak unreactive base. Furthermore, the sacrificial electrophile does not interfere with the reaction process as it does not contain an acidic proton.<sup>102</sup>



**Scheme 29** A schematic representing the role of the sacrificial electrophile

#### 4.4.1.1. Synthesis of (Z)-ethyl 2-azido-3-(2-(3,5-dimethylphenoxy)phenyl)acrylate (**68**)

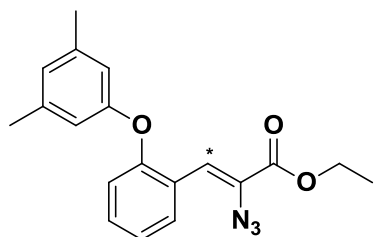


**Scheme 30**

In our first attempt at the modified reaction we used 3 equivalents of the ethyl trifluoroacetate to 1 equivalent of the benzaldehyde **69**, along with 4 equivalents of ethyl azidoacetate and 4 equivalents of base. This reaction yielded product **68** (Scheme 30) but only at a disappointing 43% yield. However, we found that if we increased the amount of the sacrificial electrophile to be equal to the equivalence of ethyl azidoacetate employed in the reaction we were able to improve the yields to above 60%. With the conditions of this experiment having been optimized we were able to continue with the reaction sequence.

The stereochemistry of the acrylate product was of importance as both the *E* and *Z* isomers could potentially be synthesized. It was imperative that the *Z* configuration be attained as the *E* configuration would not allow for the cyclization to occur and form the desired indole. A study carried out by Heaner *et al.* discovered that only one isomer was observed in the  $^1\text{H}$  NMR spectra for all the acrylate products that they had synthesized.<sup>102</sup> Using density functional theory calculations they discovered that the *Z*-isomer is the preferred configuration as it is more thermodynamically stable than the *E*-isomer. Further study showed that the *Z* configuration had all the atoms in one plane whereas the *E* configuration, due to the steric clash between the ester functionality and the aryl group on either side of the alkene, lead to a distorted and unfavourable non-planar structure.<sup>102</sup>

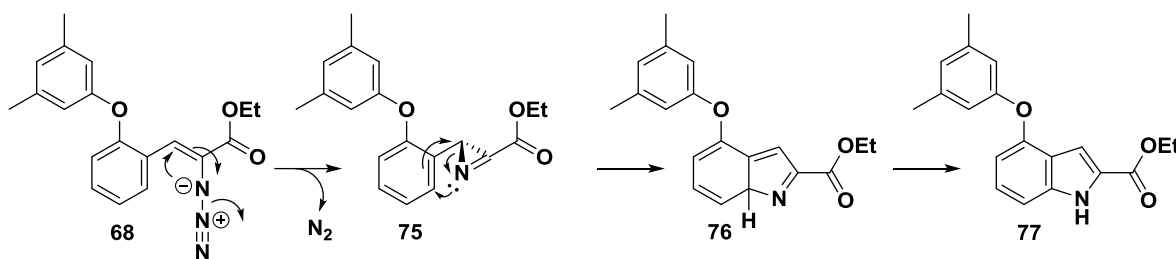




In accordance with literature the presence of only one vinyl proton in our  $^1\text{H}$  NMR was indicative of the fact that only the one stereoisomer was synthesized. The vinyl proton (\*) was represented by a singlet at 7.35 ppm. Mass spectral analysis provided a mass of 360.1314 amu ( $M+\text{Na}$ ) which coincided with the calculated mass of 360.1324 amu.

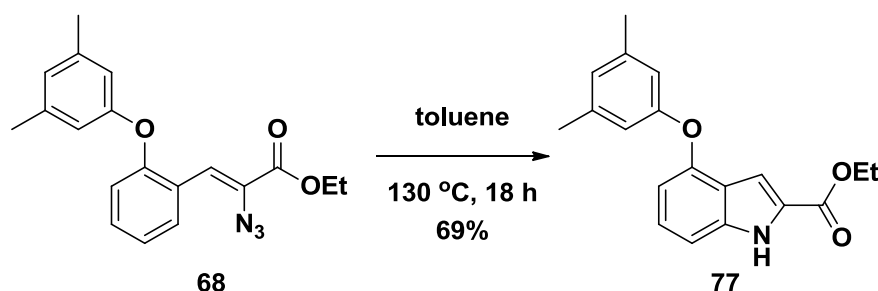
#### 4.4.2. Describing the Hemetsberger indolization reaction.

The Hemetsberger indolization reaction is typically carried out at high temperatures in non-polar, high boiling solvents such as xylene, mesitylene and toluene.<sup>102</sup> The reaction is believed to proceed *via* the formation of an azirene intermediate **75** (Scheme 31) which is accompanied by the release of nitrogen gas. Cyclization then occurs to form intermediate **76** which then undergoes tautomerism forming the more stable 5-membered ring **77**.<sup>111</sup> Fortuitously, the phenoxy functionality is *ortho* to the reacting vinyl azide, and therefore blocks the possibility of obtaining two products which would certainly be a problem if this group were rather *meta* to the vinyl azide.



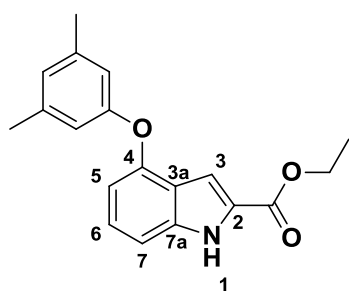
**Scheme 31** Proposed mechanism for the Hemetsberger reaction adapted from Heaner *et al.*<sup>102</sup>

#### 4.4.2.1. Synthesis of ethyl 4-(3,5-dimethylphenoxy)-1H-indole-2-carboxylate (**77**)



Scheme 32

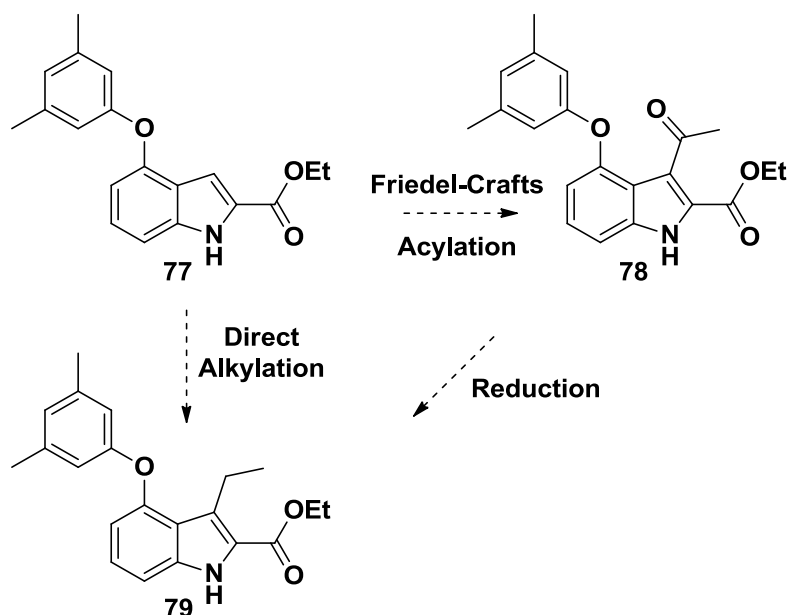
In our attempt at the Hemetsberger indolization reaction to form indole **77**, the azido acrylate **68** was taken up in toluene, and then added to a second volume of toluene refluxing at 130 °C. Monitoring the reaction by TLC revealed that after approximately 18 hours, the indole **77** had formed.



The observation of a broad singlet at 8.94 ppm integrating for 1H, was indicative that the formation of the indole had occurred successfully. This singlet correlates to the N-H of the indole. Furthermore, a notable signal shift was observed for protons 3 and 7. Spectral mass analysis provided a mass of 310.1444 amu which corresponds to the calculated mass of 310.1443 amu.

#### 4.5. Functionalizing the 3-position of the indole

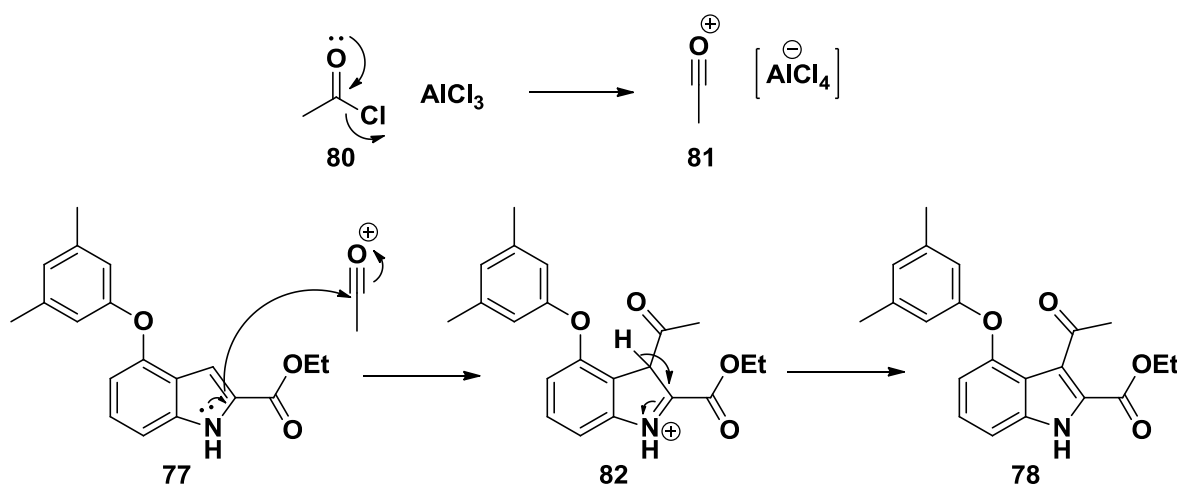
Having successfully synthesized the desired scaffold **77**, we could now attempt to functionalize the 3-position of the indole. In this instance, we sought to functionalize this 3-position with an ethyl chain to occupy the Val179 pocket in the NNIBP. This has been shown to have an influence on the activity of a compound in wild-type HIV-1 as well as in mutant strains of the virus.<sup>58</sup> We envisaged that the best method to achieve functionalization at this position would be to first acylate the indole, yielding **78** (Scheme 33), and subsequently reduce the carbonyl down to the corresponding alkyl chain resulting in indole **79**. Although we did consider directly alkylating the indole product **77** using, for instance, a Grignard reagent as a base. However, we decided against this strategy as we were concerned about the formation of a mixture of products due to the alkylation occurring at other points on the indole scaffold such as at the N position on the indole. Fortunately, the selective acylation of indoles at the 3-position is prevalent in literature. The most common method employed to acylate this position of the indole is to carry out a Friedel-Crafts acylation reaction.<sup>112</sup> This would result in the ketone **79** which, as we had discovered in the previous chapter regarding the biaryl triazole containing species, could subsequently be reduced with TFA and triethylsilane to yield the alkyl chain.



Scheme 33 Two probable synthetic pathways to the synthesis of indole **79**

#### 4.5.1. The Friedel-Crafts acylation reaction

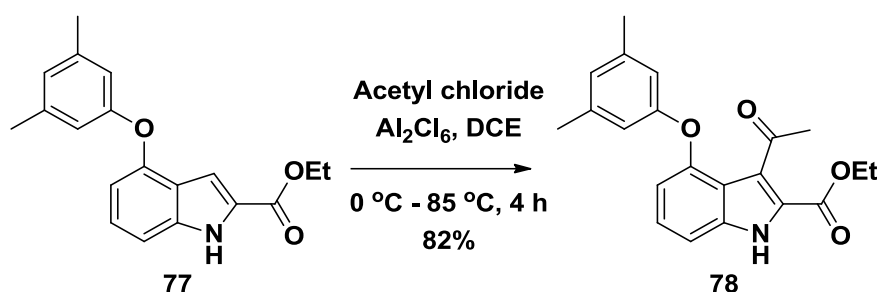
For the Friedel-Crafts reaction mechanism the acid chloride **80** and aluminium chloride forms a relatively stable acylium complex **81** which acts as an effective electrophilic reagent in the acylation process (Scheme 34).<sup>113</sup> This occurs through a halogen exchange between the acid chloride and aluminium chloride. The oxonium cation of the acylium complex that is formed is widely accepted as the primary acylating agent.<sup>114</sup> The  $\pi$  electrons of the indole then act as a nucleophile, attacking the acylium complex, in the process disrupting the aromaticity of the indole giving the cation intermediate **82**. Subsequent elimination of the proton from the  $sp^3$  carbon bearing the acyl group to form indole **78** then serves as the final step in the Friedel-Crafts acylation reaction.



Scheme 34 The mechanism for the Friedel-Crafts acylation reaction

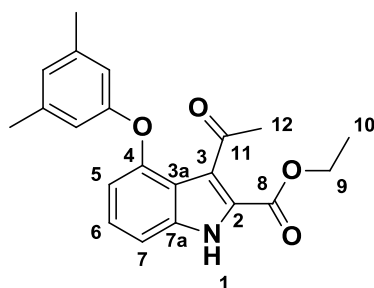
The Friedel-Crafts acylation of indoles takes place mainly at the 3-position, being the most nucleophilic site on the indole provided the nitrogen is not an anion.<sup>115</sup> However, it is possible that direct attack of the indole nitrogen can occur, leading to side products, although this is usually in minor quantities.<sup>112</sup> Normally protection and deprotection steps may circumvent this complication, however, the presence of the electron withdrawing ester functionality at the 2-position means that this is not a necessity and, as a result, acylation at the 3-position can occur without competition from the NH site and at high yields.<sup>116</sup> This observation is further justified by successful acylation of the 3-position of ethyl 2-indolecarboxylates carried out by our research group just recently.<sup>59, 117</sup> As a result, we expected acylation of the 3-position of our indole system to be carried out without incident.

#### 4.5.1.1. Synthesis of ethyl-3-acetyl-4-(3,5-dimethylphenoxy)-1H-indole-2-carboxylate (78)



Scheme 35

Treatment of the indole **77** with aluminium chloride and acetyl chloride in a Friedel-Crafts acylation proceeded without incident and the reaction provided yields of 70% and higher of the acylated product **78**, which could be rapidly purified by column chromatography.

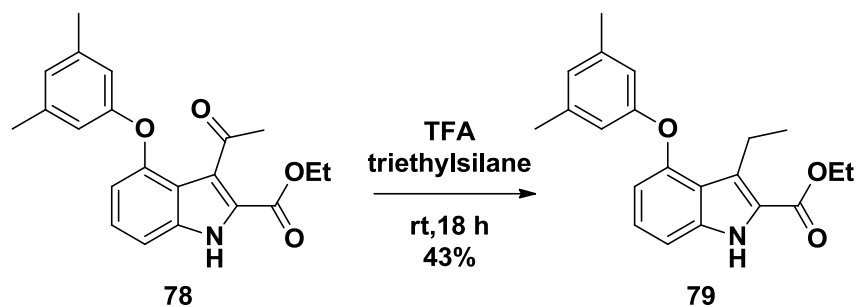


The presence of a singlet at 2.64 ppm in the <sup>1</sup>H NMR spectrum was indicative of the fact that the introduction of the ketone onto the indole had been successful. This peak integrated for 3H correlating to the methyl peak 12. Furthermore, analysis of the <sup>13</sup>C NMR spectrum showed that the characteristic ketone (carbon 11) signal was observed at 198.09 ppm.

#### 4.5.2. Reduction of the ketone to the desired alkyl substituent

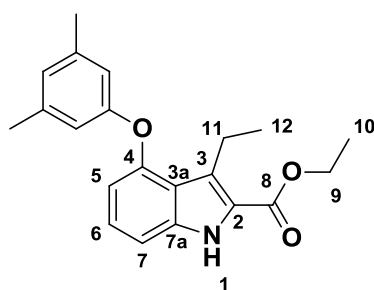
With the required number of carbons attached at the 3-position of the indole **78**, we could now proceed to defunctionalize the ketone, leading to the desired ethyl substituent.

#### 4.5.2.1. Synthesis of ethyl-4-(3,5-dimethylphenoxy)-3-ethyl-1H-indole-2-carboxylate (**79**)



Scheme 36

This method of reducing the ketone to the alkane has been employed successfully in our previous section (Chapter 3), although in this particular case we found it unnecessary to first reduce the carbonyl to the alcohol. Treatment of ketone **78** with TFA and TMS resulted in the alkane **79** being produced in moderate yields.



Analysis of the  $^1\text{H}$  NMR provided the evidence that the reduction of the ketone to the alkyl chain had been carried out successfully. The two methyl signals 10 and 12 overlap to give a complex signal at 1.40 ppm integrating for 6H. This, as well as the presence of two quartets at 4.41 and 2.89 ppm both integrating for 2H provided evidence for the presence of an ethyl chain on the indole scaffold.

With the compound **79** successfully synthesized, we were now in a position to evaluate its efficacy against whole cell HIV, and to this end it was handed over to our collaborators at the NICD. However, it was completely inactive against HIV RT. Nevertheless we did not despair and instead hypothesized that perhaps the inactivity had to do with the lack of a halogen at the 5-position of the indole. We made this hypothesis due to the fact that a halogen is always present on all indole based compounds synthesized both in our group and those in literature that have moderate to good activity against HIV (Figure 36). In fact, we discovered that there was an abundance of literature which supported this theory.

#### 4.6. Introducing a halogen at the 5-position in an attempt to improve activity

Having studied the literature we were able to establish precedence that the presence of a halogen at the 5-position of the indole can increase the activity of a compound significantly.<sup>57, 58</sup> A paper by Jones *et al.* reported the synthesis of a series of indazole containing NNRTIs, also with a phenoxy functionality at the 4-position such as compound **1** mentioned previously. They reported the activities of their indazole compounds with and without a halogen at the 5-position (compounds **83**, **84** and **1**, Figure 40). They reported that by introducing a fluorine at the 5-position of their indazole compound to give **1** they had managed to improve on the activity of the indazole compound by almost 7 fold. However, when they introduced a chlorine at this

position (**84**) the activity of these compounds decreased due to a steric clash caused by the large chlorine atom forcing the biaryl ether into a non-ideal configuration for binding.<sup>57</sup>

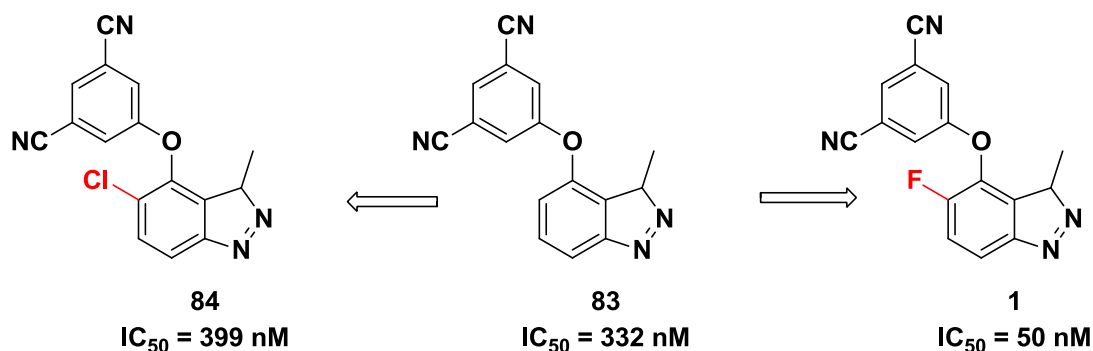


Figure 40 The influence of introducing a halogen on some indazole NNRTIs<sup>57</sup>

From these results and due to the similarity between our indole structure and their indazole structures, we decided that we would also attempt to introduce the smaller fluorine atom on our own indole based compounds at the 5-position.

#### 4.6.1. Our attempts to introduce a fluorine onto the indole scaffold

Unfortunately there was little precedence for adding a halogen onto the 5-position of the indole and, as a result, we had to employ the methods reported by Jones *et al.* in the synthesis of their indazole series.<sup>57</sup>

For the fluorination reaction Jones *et al.* reported the use of Selectfluor as the fluorinating agent (Figure 41).<sup>57</sup> This reagent has become a popular source of electrophilic fluorine due to its stability and relatively low toxicity in contrast with fluorine gas which was originally used as a source of electrophilic fluorine.<sup>118</sup>

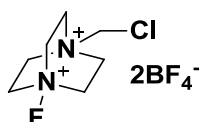
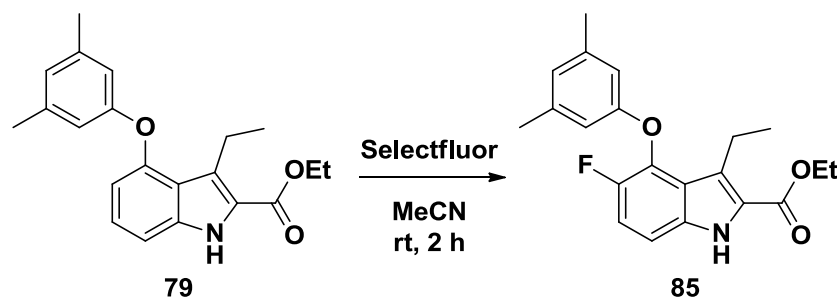


Figure 41 Selectfluor

For the fluorination of our indole **79** we envisaged that the electron donating phenolic functionality at the 4-position of the indole would promote fluorination at position 5, which is *ortho* to the phenoxy functionality. Furthermore, we hoped that selective fluorination at this position would be promoted due to fact that the 2 and 3-positions of the indole are occupied by the ester group and ethyl chain respectively.

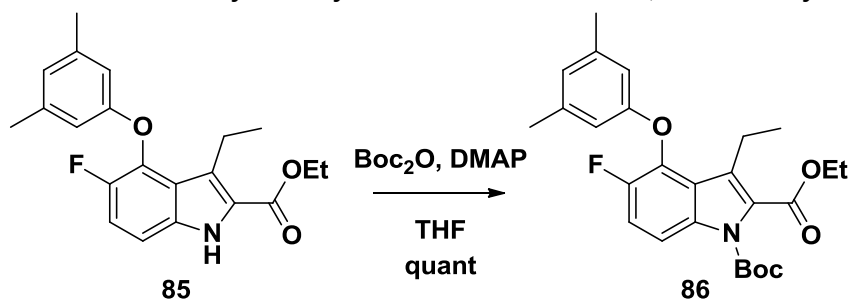
#### 4.6.1.1. Synthesis of ethyl-4-(3,5-dimethylphenoxy)-3-ethyl-5-fluoro-1H-indole-2-carboxylate (**85**)



Scheme 37

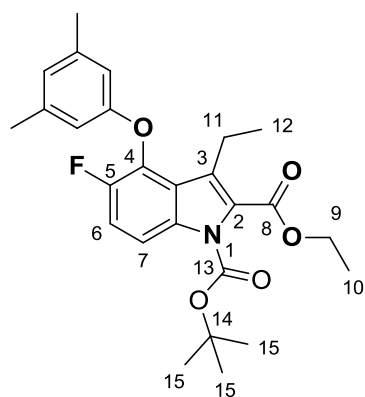
For our first attempt at the fluorination reaction we added selectfluor to a solution of the indole **79** suspended in acetonitrile. The reaction was only carried out for 2 hours due to the formation of a number of additional products. However, using column chromatography we were able to isolate what appeared to be the indole product **85**. Unfortunately, at this point, we ran into some complications with regards to the purification of this compound as the  $R_f$  of the fluorinated indole **85** and the unfluorinated indole **79** were very similar. In an attempt to purify this compound we decided to carry out a Boc protection reaction. We envisaged that by protecting the indole with a Boc group we may achieve a better separation between indole products **85** and **79**. Furthermore, we realized that by introducing a Boc protecting group onto the indole, we would be provided with an opportunity to run an NOE experiment in order to verify the fluorination position.

#### 4.6.1.2. Synthesis of 1-tert-butyl 2-ethyl-5-fluoro-1H-indole-1,2-dicarboxylate (**86**)



Scheme 38

We were able to carry out the Boc protection on the crude indole **85** in the presence of DMAP in THF. As we had hoped, purification of the protected indole **86** afforded a better separation between the fluorinated and non-fluorinated products.



We were able to establish that the reaction had taken place by analysing the  $^1\text{H}$  NMR spectrum. The absence of the broad NH peak in the  $^1\text{H}$  NMR spectrum indicated that the protection reaction had been carried out successfully. This observation was further justified by the presence of the singlet at 1.68 ppm which

integrated for 9H corresponding to the methyls 15 belonging to the Boc group.

#### 4.7. Analysis of the NOE results to determine the position of the fluorine

NOE experiments were carried out on our protected indole in the hope that we would be able to determine where the fluorine atom was situated by irradiating signals corresponding to the Boc *tert*-butyl groups, the indole aromatic protons and the protons on the upper aryl ring (Figure 42). The rationale here was that if the fluorination had occurred at the desired position then ideally we would be able to observe correlations between the methyl protons on the protecting group and the protons on the aromatic ring but we would not observe any correlations between the upper aryl ring protons and the aromatic protons on the indole.

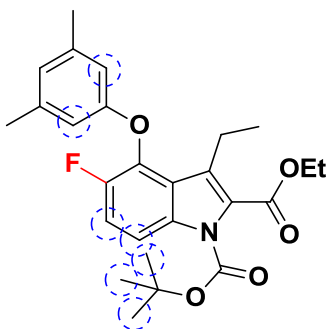


Figure 42

When we analysed the NOE results we did not observe any through-space correlations between the protons on the upper aryl ring and the protons on the indole which was expected should the fluorination have occurred at the correct position on the indole. However, when the signals of the Boc *tert*-butyl protons were irradiated no correlations to the aromatic protons were observed either which was odd.

Indeed, instead of the expected correlations between these signals we were presented with some unusual and rather perplexing observations. On closer inspection of the NOE results we discovered correlations between the indole aromatic protons (6 and 7 supposedly) and the protons on the ethyl chain 11 and 12 (Figure 43). This observation seemed highly unlikely as we expected the ethyl chain to be far enough from the aromatic protons for no correlations to be observed. In addition, one of the indole protons was clearly a singlet, and this did not correlate with our anticipated structure.



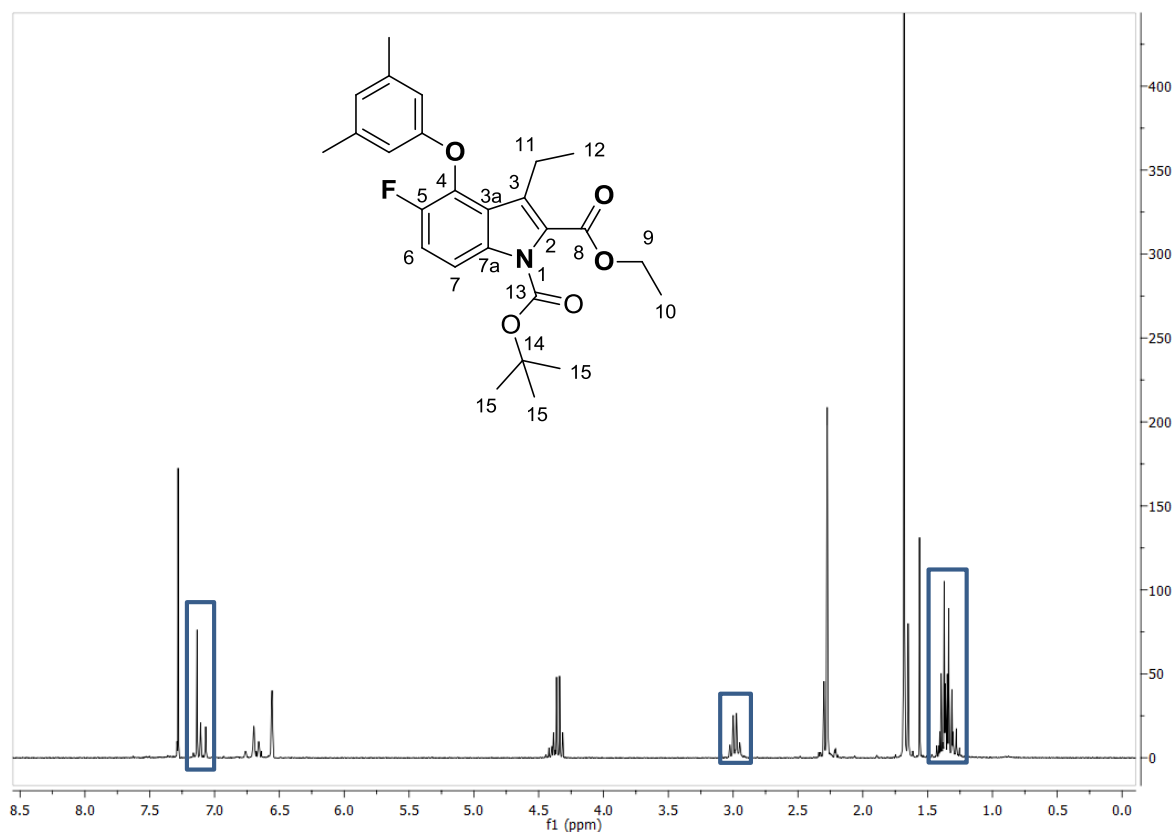
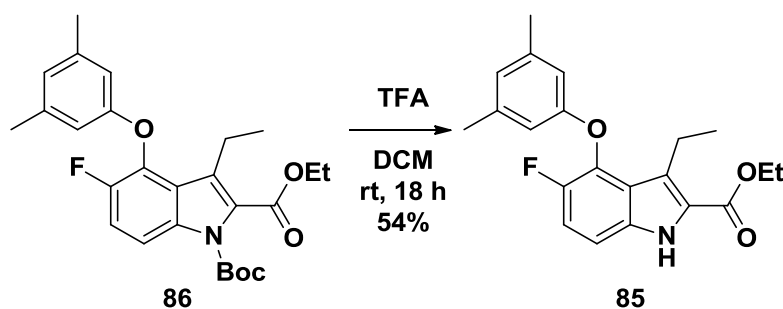


Figure 43

At this point we decided that we would remove the Boc group to obtain a more polar sample which would be more likely to crystallize and be amenable to X-ray analysis.

#### 4.8. Removal of the Boc protecting group and subsequent NMR analysis



Scheme 39

The Boc protecting group on compound **86** was readily removed in the presence of an excess of trifluoroacetic acid in DCM. Once the reaction had run to completion, as monitored by TLC, the solvent was removed *in situ* and the product **85** was recrystallized from diethyl ether to yield the product as a white solid in a moderate yield, but excellent purity, thereby providing an opportunity for careful NMR analysis.

If the fluorination had occurred in the correct position then the only aromatic signals we would observe would coincide with the upper aryl ring and with the two vicinal protons free from

substitution on the indole aromatic ring (Figure 44). Furthermore, for the two vicinal protons we would expect to observe two signals each existing as a doublet both with similar, if not the same, J coupling values.

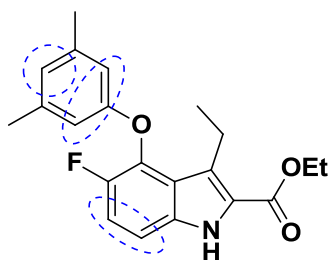


Figure 44

At first glance it appeared that all was in order as all the expected aromatic signals appeared to be present (Figure 45). The  $^1\text{H}$  NMR did reveal two aromatic signals belonging to the protons on the indole ring. The signal at 7.11 ppm presented as a doublet and the other at 7.05 ppm as a doublet of triplets which we thought could be attributed to some long range coupling to the indole NH. Furthermore, both of these aromatic signals integrated for 1H. However, on closer inspection we realized that the J coupling values of the two signals differed significantly which could not be possible.

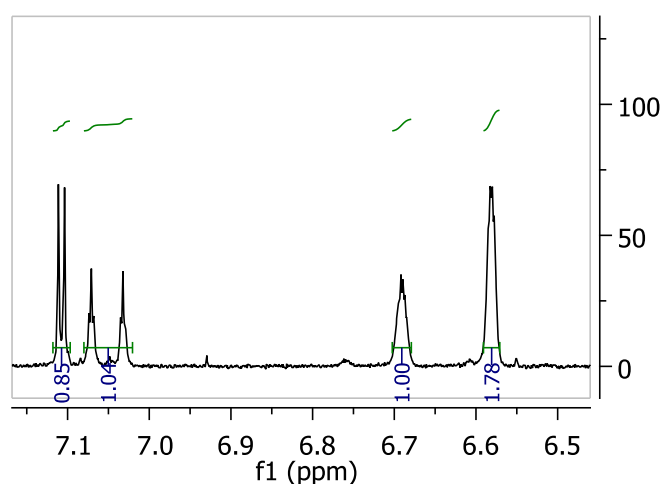
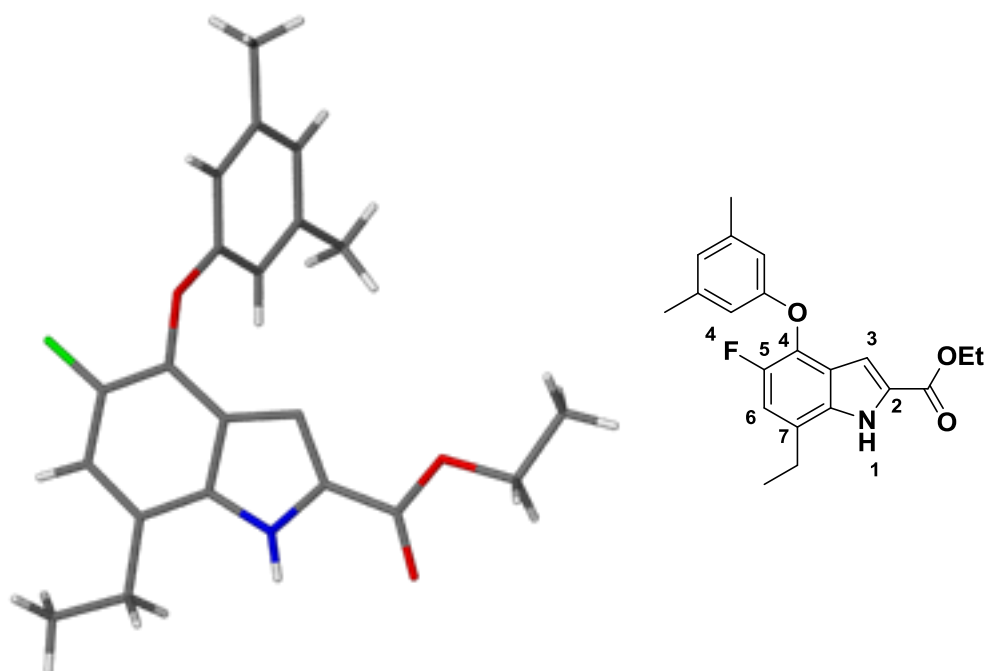


Figure 45

We realized at this point that the only way we would be able to properly explain the anomalies observed in the NOE spectrum of **86** and in the  $^1\text{H}$  NMR spectrum of **85** would be to obtain a crystal structure of our compound.

#### 4.9. A study of the crystal structure reveals the cause of the observed anomalies in previous characterisation analyses.

Fortunately, after some experimentation we were able to recrystallize **85** and obtain crystals of sufficient quality for X-ray analysis. The crystal structure we obtained was astounding as we had not predicted the observed results. To our astonishment the crystal structure showed that although the fluorine was situated at the desired position on the indole, the ethyl chain was not. Instead of at the 3-position as has always been the case when working with indoles in the past, the ethyl chain had been introduced onto the 7-position of the indole (Figure 46).



**Figure 46** The crystal structure obtained of compound **85**. This image was prepared using XSeed v2.05.

Although these results we obtained were unexpected, we were able to rationalize this phenomenon. Firstly, unlike previous indole compounds synthesized within our group, our indole scaffold possessed the phenoxy functionality situated at the 4-position of the indole which would be *ortho/para* directing on the aromatic ring. We had already established that without the phenoxy functionality at the 4-position, acylation does occur at the 3-position, even with the presence of the ester at the 2-position.<sup>117</sup> Therefore, we hypothesized that the presence of the phenoxy group is enough to alter the most nucleophilic site on the indole from the usual 3-position, to the observed 7-position.

In addition to explaining the anomalies observed in the NOE and NMR experiments, this phenomenon could explain why the indole **79** that we had sent for biological evaluation previously had been found to be inactive against whole cell HIV-1. We considered the possibility that the presence of the ethyl chain at the 7-position (**87**) led to steric clashes with the allosteric

pocket due to the presence of Tyr318 and other amino acid residues crowding that region (Figure 47).

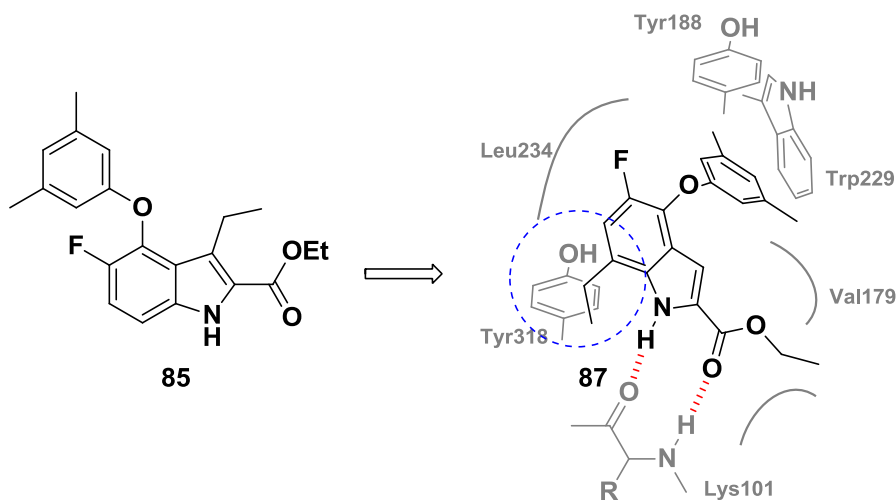


Figure 47

At this point, we took a measure of comfort in the fact that there could be a plausible explanation to the lack of activity of our compound. In order to establish whether our theory was founded, we decided to send our indole product **77**, without the ethyl chain situated at the 3-position, for biological evaluation (Figure 48). Fortunately, the obtained crystal structure assured us that at least the ester and phenoxy functionalities were situated in the desired positions on the indole. We envisaged that this scaffold would serve as a suitable proof-of-concept to indicate whether our aim to target both Trp229 and Lys101 was possible. To this end we sent this compound for biological evaluation. However, to our dismay the results obtained from the assays carried out on this compound indicated that it was also completely inactive against whole cell HIV. Even without the necessary halogen at the 5-position we would have expected the compound to have had some activity against HIV!

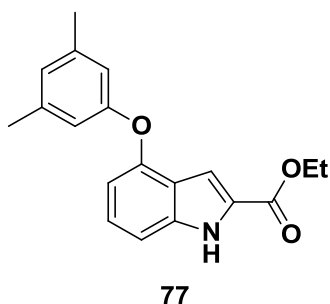


Figure 48

Unfortunately, these results seemed to imply that it may not be possible to achieve interactions with both Trp229 and Tyr188, as well as the backbone of Lys101 using a relatively rigid scaffold like the indole.

In order to test this theory we decided to synthesize the corresponding indole analogue without the ester at the 2-position.

#### 4.10. Attempts to remove the ester functionality at position 2 using a quinoline/copper mediated decarboxylation reaction

To remove the ester functionality from the 2-position we would need to carry out a decarboxylation reaction. However, this would require that the ester first be converted to the carboxylic acid. Fortunately, there were a large number of examples in literature where a decarboxylation reaction was successfully carried out on the 2-position of an indole with varying substituents on differing positions on the indole. These procedures often entailed heating the indole under reflux in a high boiling point solvent such as quinoline and in the presence of a copper source such as copper powder or copper oxide.<sup>100, 119.</sup>

##### 4.10.1. Synthesis of 4-(3,5-dimethylphenoxy)-1H-indole-2-carboxylic acid (88)

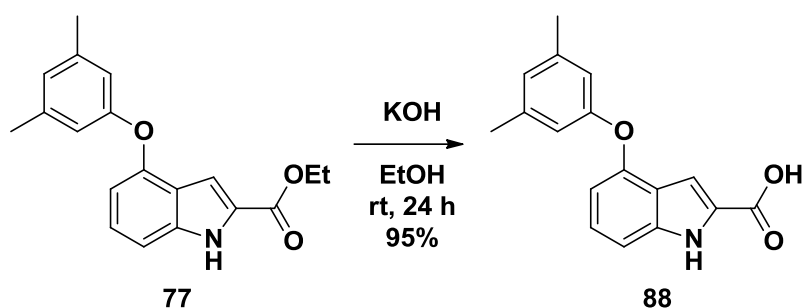
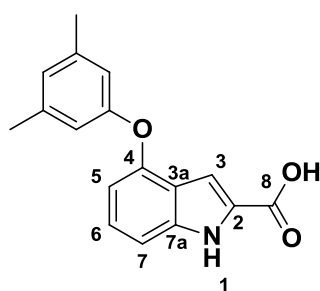


Figure 49

In order to carry out the decarboxylation reaction, the ester had to be hydrolysed to the carboxylic acid given that very little literature precedence existed for direct decarboxylation from the ester. The hydrolysis of the indole ester was carried out with ease using an excess of potassium hydroxide in ethanol. Once all the starting material had been consumed the product was isolated without the need for further purification resulting in 95% of yellow solid as the product.



The disappearance of the protons corresponding to the ethyl chain of the ethyl ester was indicative that the hydrolysis had been successful. Mass spectral analysis confirmed absence of the ethyl ester reporting a mass of 282.1122 amu corresponding to the expected mass of 282.1130 amu.

#### 4.10.2. Synthesis of 4-(3,5-dimethylphenoxy)-1*H*-indole (**89**)

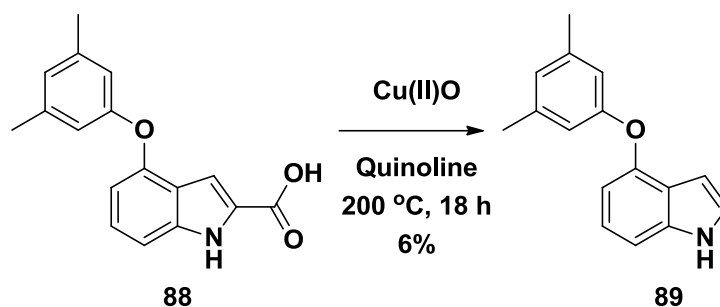
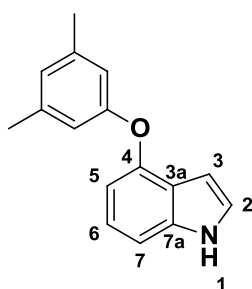


Figure 50

Having successfully hydrolysed the ester to the acid we could continue with the quinoline/copper mediated decarboxylation reaction. The indole was dissolved in quinoline with a catalytic amount of copper oxide and was heated to  $200\text{ }^\circ\text{C}$ . Unfortunately, the decarboxylation reaction afforded a very poor yield of only 6%. However, this was nevertheless enough product to send for biological evaluation. Our strategy at this point was to first evaluate the efficacy of **89** and if found to show promise in its HIV inhibition, then we would return to optimize this reaction.



Analysis of the  $^1\text{H}$  NMR spectrum revealed that the carboxylic acid had been successfully removed. This conclusion was made due to the observation of a new complex signal in the aromatic region of the spectrum which integrates for 1H. This signal corresponds to proton 2 of the indole. Unfortunately, the yield was so poor that we were unable to get further characterization data.

#### 4.11. Efficacy results for the unfunctionalized 4-phenoxy indole (**89**)

Having arrived at the 4-phenoxy indole scaffold **89** we could evaluate whether the presence of the ester at the 2-position of the indole was in fact detrimental to the activity of our desired compound. Compound **89** was handed to our collaborators at the NICD for biological evaluation.<sup>80, 81</sup> However, even without the ester, our 4-phenoxy indole scaffold was completely inactive against whole cell HIV. Although results gave an average IC<sub>50</sub> value of 3.41  $\mu$ M and an average CC<sub>50</sub> value of 7.86  $\mu$ M.

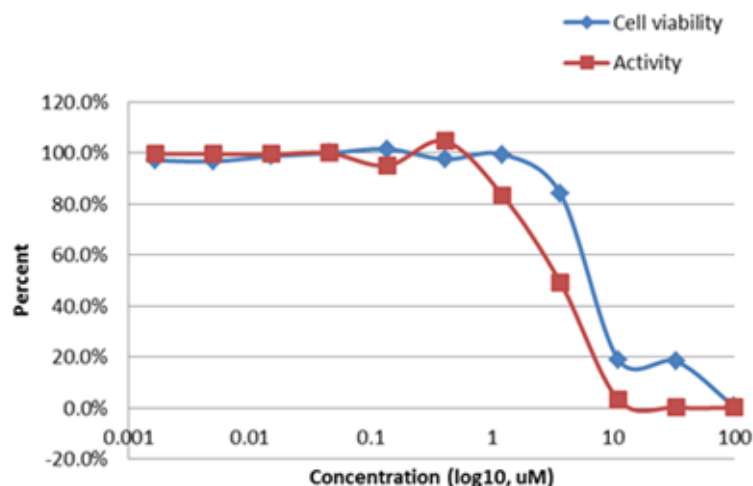


Table 6 Activity results for compound **89**

Although our indole scaffold **89** was still missing some of the desired substituents such as an ethyl chain at position 3 and a halogen at position 5, both of which were considered to be imperative for activity against HIV RT, the lack of activity of **89** was surprising. This is especially the case when one considers that without the ester present our scaffold (**89**) was becoming increasingly similar to the structure of indazole compound **1** (Figure 51).<sup>57</sup> At this point we had decided not to pursue this scaffold, as the scaffold was now moving away from the novelty we had hoped to achieve by targeting the region of Trp229 and Lys101 simultaneously.

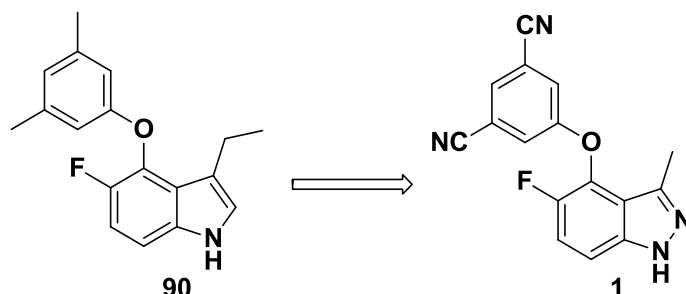
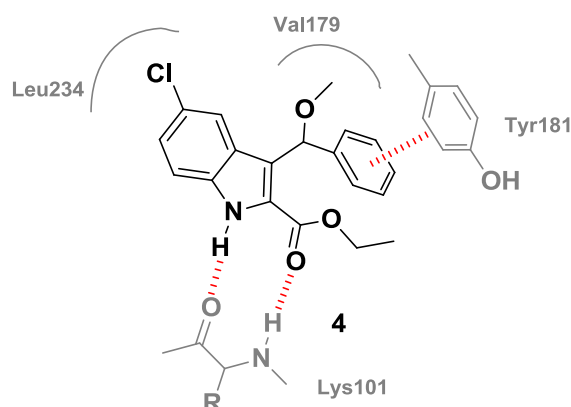


Figure 51

## Chapter 5: The Design and Synthesis of a 3-Aminoindole-Based Scaffold as an Extension of a Lead Compound

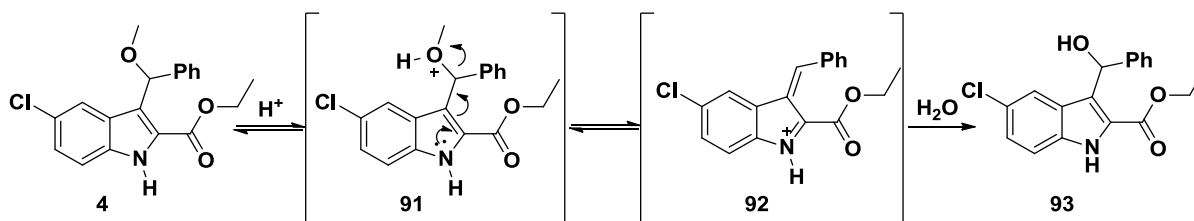
### 5.1. The rationale behind our design

Recently in our research group, a particularly potent methoxy-indole based compound **4** was synthesized (Figure 52).<sup>59</sup> Not only was this compound potent against HIV RT with an IC<sub>50</sub> value of 1 nM but was also found to maintain potency against problematic resistant strains of the virus, in particular the troublesome K103N mutation.<sup>59</sup>



**Figure 52** Representative schematic of **4** in the binding pocket showing  $\pi$ - $\pi$  stacking interactions with Tyr188 and hydrogen bonding interactions to the backbone of Lys101.

Unfortunately, problems with the stability of this compound ensured that **4**, as it was, could not advance to drug candidate level. It was identified that the cause of the instability was the methoxy functionality occupying the Val179 pocket. In an acidic environment the methoxy functional group could be activated through protonation converting it into a good leaving group. The protonated methoxy functionality is subsequently eliminated to form the reactive electrophile **92** (Scheme 40). *In vivo* this reactive species **92** is vulnerable to nucleophilic attack by water which would afford the hydroxyl product **93**. Furthermore since **93** is actually a precursor in the synthetic route to obtaining **4**, its HIV activity has already been established and it is a very poor inhibitor.<sup>59</sup> Therefore, inadvertent conversion of **4** to **93** *in vivo* is a serious problem.



**Scheme 40**

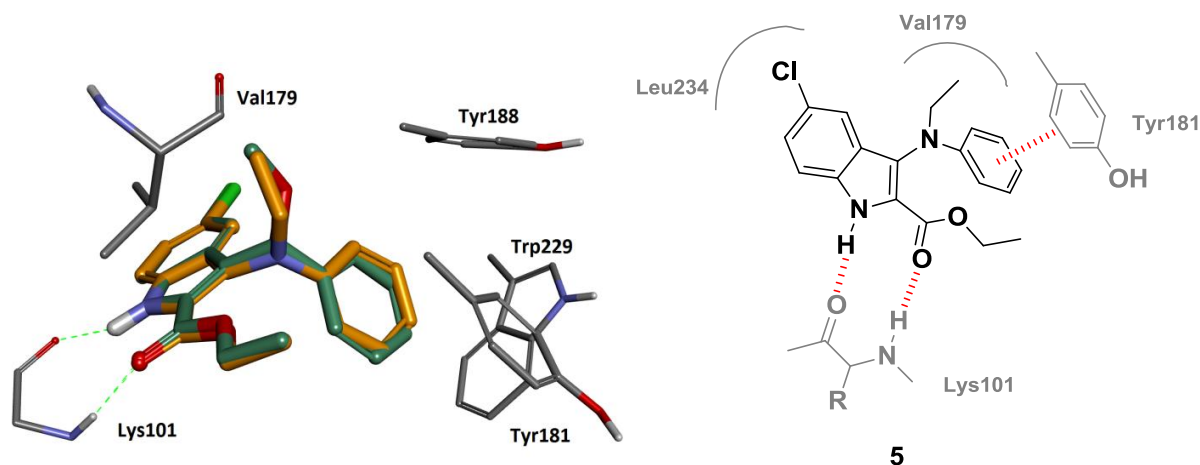
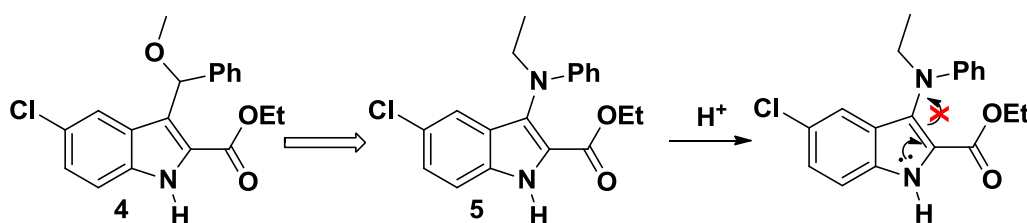
In order to combat this issue of instability we envisaged a strategy to replace the methoxy with a suitable and much more stable bioisostere. It was imperative that the choice of bioisostere



## Chapter 5: The Design and Synthesis of a 3-Aminoindole-Based Scaffold as an Extension of a Lead Compound

would be well accommodated within the Val179 pocket so as not to alter the binding orientation of the compound in the NNIBP. Furthermore, we wished to maintain the presence of the phenyl group at the 3-position of the indole as the  $\pi$ - $\pi$  stacking interactions with Tyr181 were discovered to be essential for the activity of the compound.<sup>117</sup>

To this end an amine-based compound **5** was envisaged which appeared to mimic **4** in terms of pharmacophoric features, but did not possess a labile leaving group (Scheme 41). Molecular modelling studies were undertaken using Accelrys Discovery Studio software, with CDocker as the main docking tool, in order to compare the predicted binding mode of a **5** against the lead compound **4**.<sup>120</sup> We proposed that by replacing the methoxy with an aryl amine we would remove the potential for elimination to occur as the reactive species formed in the case of **1** could not exist for the amino compound **5**. The modelling results suggested that our proposed compound **5** bound to the NNIBP in a manner very similar to that of the lead compound **4** (Figure 53). The ethylamine functionality was well accommodated in the Val179 pocket and hydrogen bonding interactions were maintained to the backbone of Lys101 as were the  $\pi$ - $\pi$  stacking interactions with Tyr181 and the proposed inhibitor **5**.

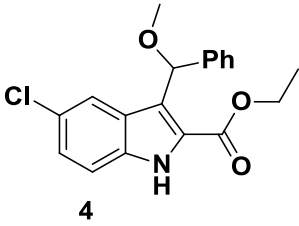
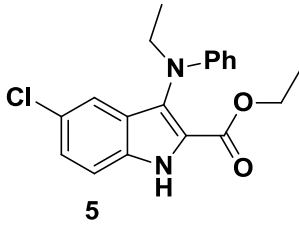


**Figure 53** Overlay of target compound **5** (orange) and lead compound **4** (green) (left) and schematic representing the binding mode of compound **5** in the binding site (right).

These results were further supported by the CDocker energy scores calculated (Table 7). Both of these energy scores represent the receptor-ligand interaction energy with the CDocker Energy score taking into account the internal ligand strain energy. By comparing the scores between compounds **4** and **5**, we found that the energy values were very close. This further supported the theory that compound **5** bound to the NNIBP in a similar fashion to the lead compound **4**.

## Chapter 5: The Design and Synthesis of a 3-Aminoindole-Based Scaffold as an Extension of a Lead Compound

Table 7

Compound		
CDOCKER Energy (kcal/mol)	-52.059	-55.5512
CDOCKER Interaction Energy (kcal/mol)	-49.4207	-56.8945

The promising docking results along with the proposed enhanced stability of the 3-amino indole derivative **5** was certainly encouraging. However, despite these promising results, we were nevertheless wary of a possible problem with respect to the required binding orientation of the nitrogen compound **5**. The energetically favoured orientation of the nitrogen attached to an aromatic ring system is to adopt an  $sp^2$  hybridised trigonal planar arrangement to facilitate p-orbital overlap with the adjacent aromatic ring (Figure 54). However, modelling studies show that the required binding configuration of the compound is such that this conjugation can only occur partially, if at all, as the p-orbital of the nitrogen appears to be out of plane with either of the adjacent aromatic systems.

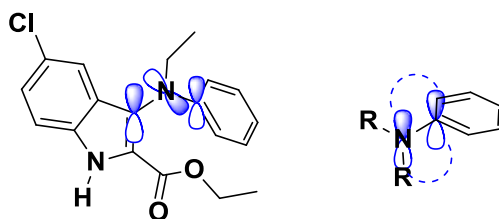
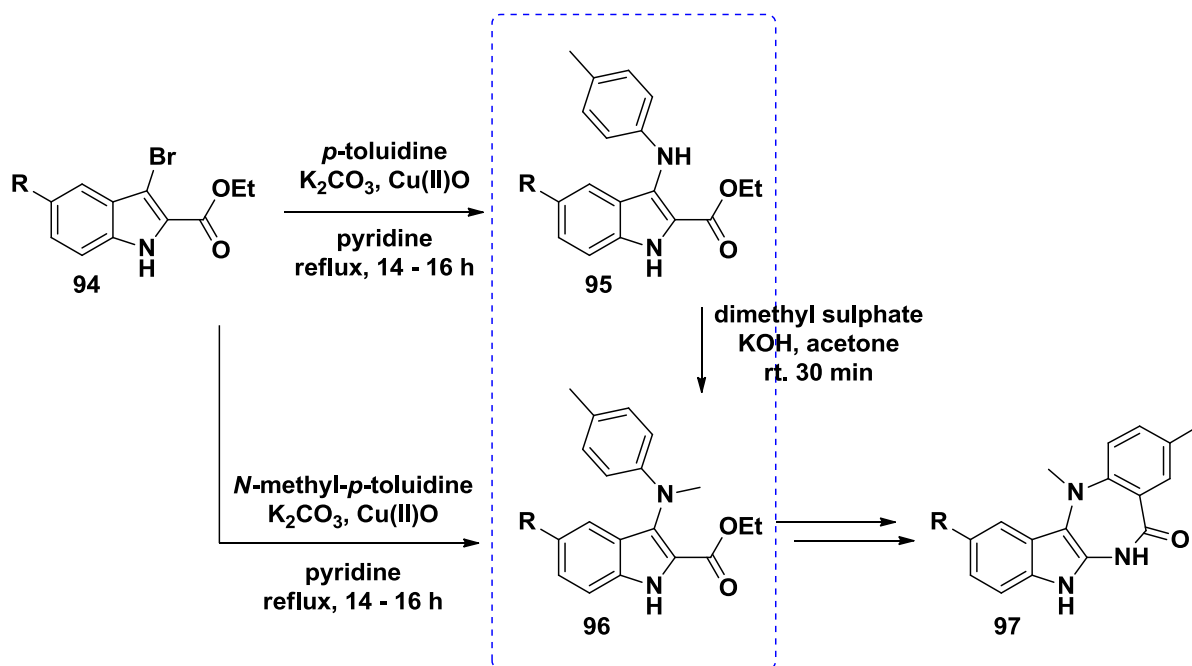


**Figure 54** The binding configuration of compound **4** (left) compared to a more preferable configuration with the nitrogen in the same plane as the adjacent phenyl ring (right).

With this concern in mind we embarked upon a search to see if there was indeed precedence for this binding configuration. Indeed a search of the protein data bank (PDB) revealed compounds which similarly possessed nitrogens with only partial  $sp^2$  character. Therefore, we considered it worth the risk to synthesize this compound and investigate its activity in comparison to the lead compound.

## 5.2. The paper behind our initial synthetic strategy

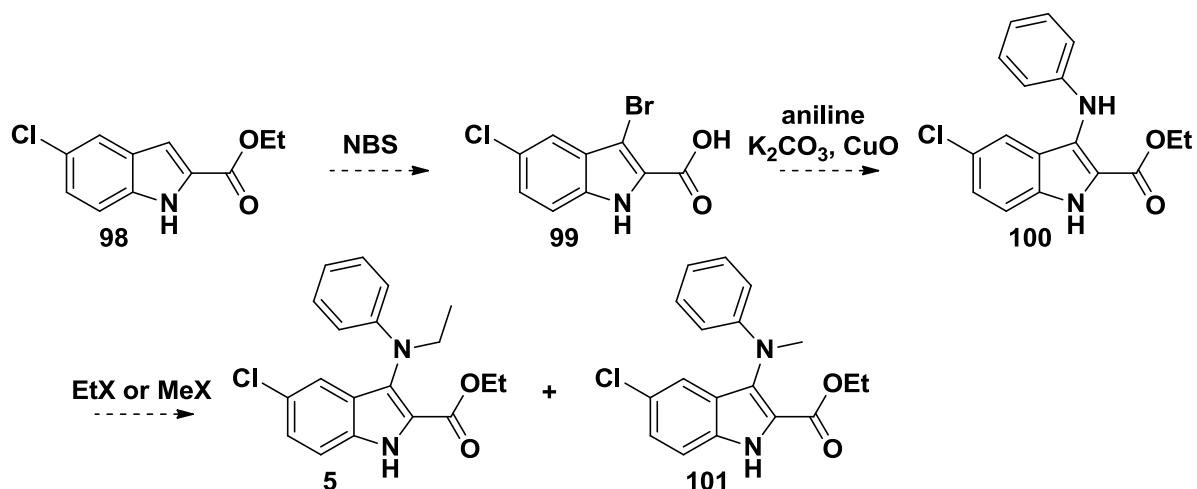
Having identified the desired target molecule **5**, we now embarked upon developing a synthetic strategy. To our surprise, the preparation of similar compounds had already been published. A paper by Hiremath *et al.* was discovered which described the preparation of 3-amino indole **96** as a precursor in the synthesis of antibacterial agents such as indolobenzodiazepinone derivative **97**.<sup>121</sup> The synthetic procedure (Scheme 42) involved a copper catalysed coupling between brominated indole **94** and an aniline to afford indole precursors **95** and **96** in moderate yields.<sup>121</sup>



Scheme 42

Compound **96** which is similar in structure to our target compound could be synthesized either by directly coupling the brominated indole **94** with substituted aniline, *N*-methyl-*p*-toluidine or by alkylating indole compound **95**, itself having been obtained by coupling **94** with *p*-toluidine. This conveniently discovered methodology certainly seemed suitable for our purposes and we decided to make use of the latter option, as we envisaged that the less sterically demanding aniline could potentially be more reactive in the coupling reaction. Furthermore, this route would allow us to finally alkylate the nitrogen with either methyl or ethyl substituents, providing more scope for potential NNRTI derivatives (Scheme 43). To this end we envisaged that commercially available ethyl 5-chloro-indole-2-carboxylate **98** could be brominated exclusively at the 3-position to afford **99**, which would be amenable to the coupling reaction with aniline yielding **100**. Subsequently alkylation could provide the methyl and ethyl derivatives **5** and **101** respectively.

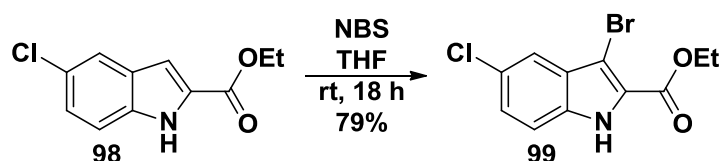
## Chapter 5: The Design and Synthesis of a 3-Aminoindole-Based Scaffold as an Extension of a Lead Compound



Scheme 43 Initial synthetic strategy

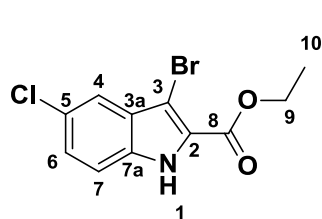
With our synthetic strategy in hand we could initiate attempts to synthesize our target compound 5.

## 5.2.1. Synthesis of ethyl 3-bromo-5-chloro-1H-indole-2-carboxylate (99)



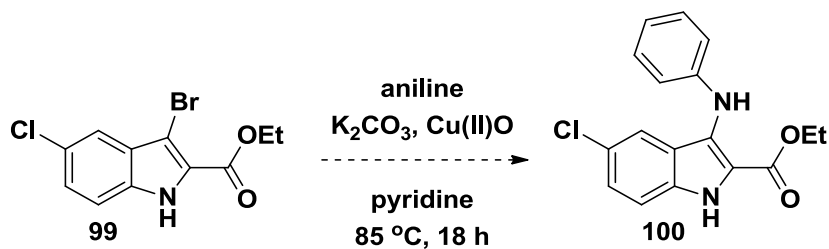
Scheme 44

The first step in our synthetic strategy involved the bromination of ethyl 5-chloro-1H-2-carboxylate **98** to afford compound **99**. Fortunately, there is an abundance of procedures in the literature for the selective bromination of ethyl indole-2-carboxylates at the 3-position. This was easily attained using *n*-bromosuccinimide and afforded high yields.



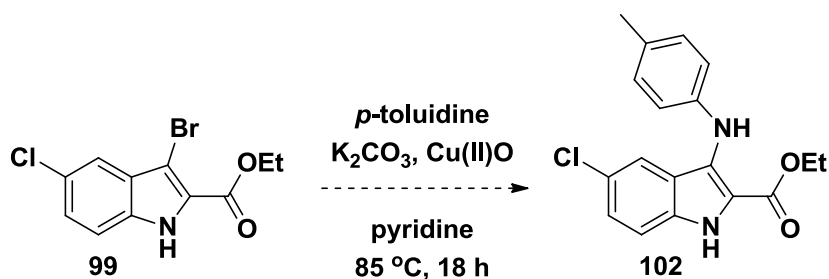
Analysis of the  $^1\text{H}$  NMR revealed only three aromatic signals corresponding to protons 4, 6 and 7. The singlet corresponding to proton 3 was not observed. Furthermore, analysis of the mass spectrum confirmed that the bromination had occurred as the results revealed a mass of 301.9591 amu which coincided with the calculated mass of 301.9583 amu.

### 5.2.2. Ullmann-type coupling in an attempt to obtain amine 100



Scheme 45

Having successfully synthesized the brominated indole **99** we hastened to attempt the coupling reaction using the conditions laid out by Hiremath *et al.* This entailed heating under reflux a mixture of **100**, aniline, potassium carbonate and cupric oxide in pyridine.<sup>121</sup> However, in our hands this reaction would not proceed. Therefore, we attempted to repeat the exact reaction as carried out by the authors (Scheme 46) employing *p*-toluidine. Despite several attempts at this strategy, the coupling product **102** still proved to be unobtainable.



Scheme 46

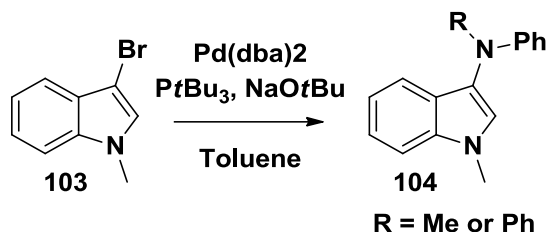
### 5.3. The search for an alternative aryl amination strategy

Failing in this attempt we decided to abandon this method and consider alternative procedures. Remarkably, after reviewing the literature, we discovered that there was very little precedence for the amination of indole halides at the 3-position and only a few other viable procedures were identified.

#### 5.3.1. Attempting a Buchwald-Hartwig Reaction procedure.

Amongst the few procedures we had identified as being a probable alternative for the synthesis of our amino indole compound was a more conventional Buchwald-Hartwig type reaction method.<sup>122</sup> In this instance the brominated indole **103** was coupled with a substituted aniline, such as *N*-methylaniline or diphenylamine, in the presence of  $Pd(dba)_2$ , tri-*tert*-butylphosphine and sodium *tert*-butoxide leading to the 3-amino indole **104** (Scheme 47).

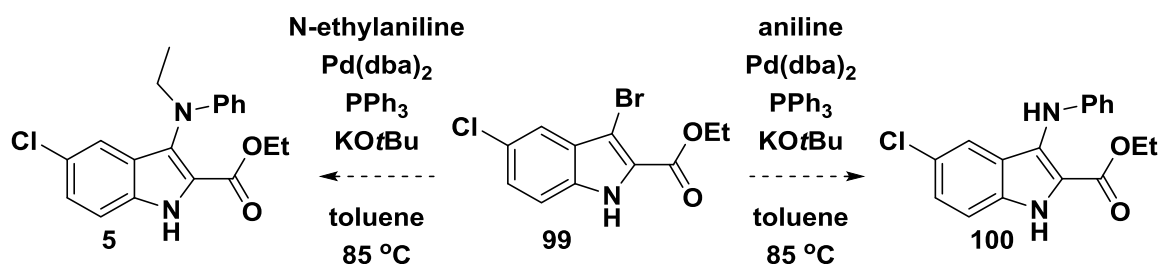
## Chapter 5: The Design and Synthesis of a 3-Aminoindole-Based Scaffold as an Extension of a Lead Compound



Scheme 47

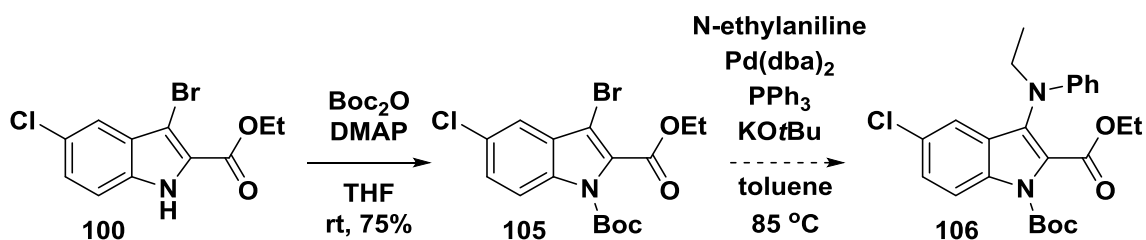
This methodology certainly looked promising for the synthesis of our target compound **4**, but unfortunately we did not have the specific tri-*tert*-butyl phosphine ligand on hand. Therefore, we substituted this with conventional triphenylphosphine. We hoped that even without the correct ligand we would be able to produce some product even if in not in the high yields reported in the paper.<sup>122</sup>

Our initial attempts at this reaction involved trying to couple **99** to *N*-ethylaniline (Scheme 48) to afford the desired compound **5**. Although we had argued previously that aniline may be more reactive, we were tempted to give the reaction a chance due to the fact that in the paper more sterically crowded amines such diphenylamine were employed successfully. However, when this reaction failed we attempted it again using aniline in an attempt to form compound **100**. Unfortunately, even in this instance, the reaction afforded complex mixtures from which any product was impossible to isolate.



Scheme 48

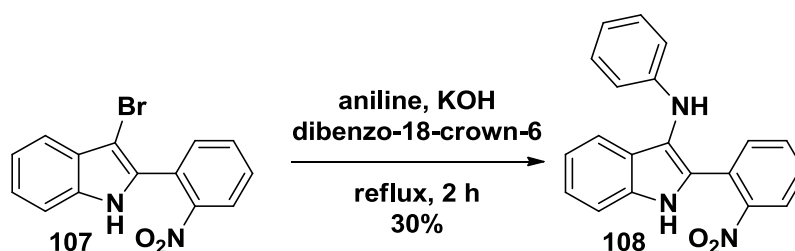
At this point, we considered that perhaps the unprotected indole nitrogen was impeding the reaction by acting as a competing nucleophile or, as a second possibility, rendering the C-Br bond too stable by virtue of electron donation. To test this hypothesis we introduced a Boc protecting group onto **99**. This was readily achieved affording compound **105** in good yield (Scheme 49). However, upon attempting the amination to form compound **106** we found that the Boc group made no difference to the end result, as the reaction continued to produce a complex mixture of products.



Scheme 49

### 5.3.2. A final attempt to obtain compound **4** employing a coupling reaction procedure.

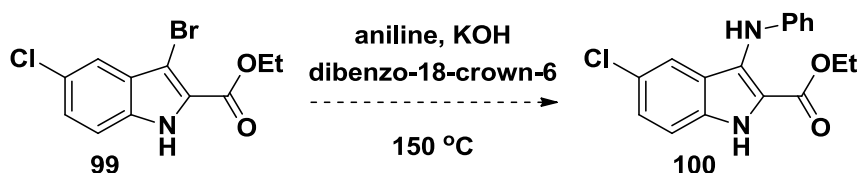
As a final resort we turned to a procedure described by Barraja *et al.* Here, they made use of the respective amine as the solvent and carried out the reaction under phase transfer catalysis conditions to achieve displacement of the bromine on position 3 of the indole. For example, under these conditions they converted compound **107** to **108**, albeit in a modest yield (Scheme 50).<sup>123</sup>



Scheme 50

According to Barraja *et al.* the presence of a protecting group on the indole nitrogen reduced the ability for nucleophilic substitution to occur, therefore, we decided to keep the indole nitrogen unprotected. Furthermore, although we expected that our ester could be hydrolysed in the presence of KOH we did not consider this to be a problem as we could easily re-esterify at a later stage.

With these considerations in mind we attempted the reaction by heating **99** in aniline, in the presence of KOH and dibenzo-18-crown-6 as the phase transfer catalyst (Scheme 51). However, as was becoming the trend with this scaffold, the reaction did not proceed at all and none of the desired product was obtained.

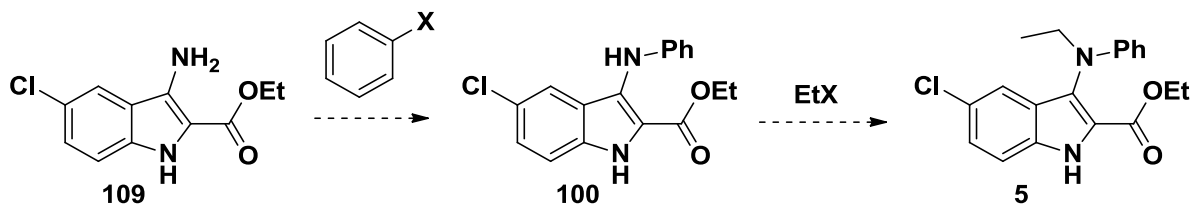


Scheme 51

## 5.4. Changing direction in our synthetic strategy

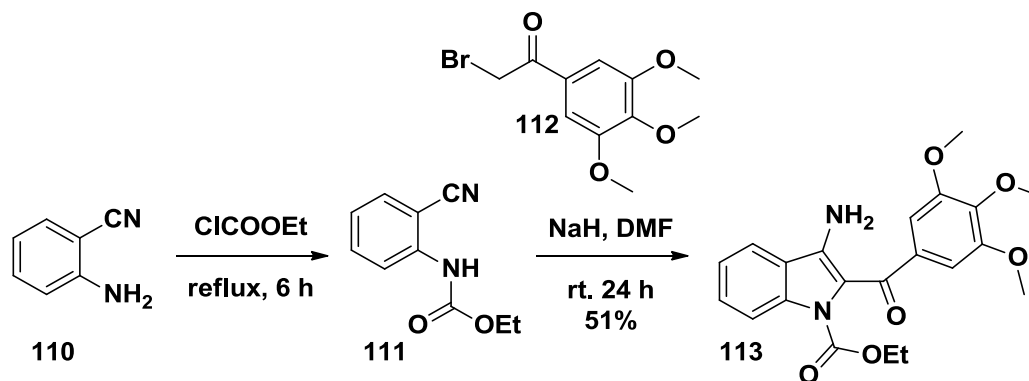
At this point we decided to abandon this strategy of trying to aminate the brominated indole and began to consider the fact that we may have been approaching the synthesis of our target compound the wrong way around. We considered that perhaps it would be simpler to first install the amine at the 3-position, to form **109** (Scheme 52) and then build onto the scaffold by introducing the phenyl **100** and alkyl groups **5** individually.

## Chapter 5: The Design and Synthesis of a 3-Aminoindole-Based Scaffold as an Extension of a Lead Compound



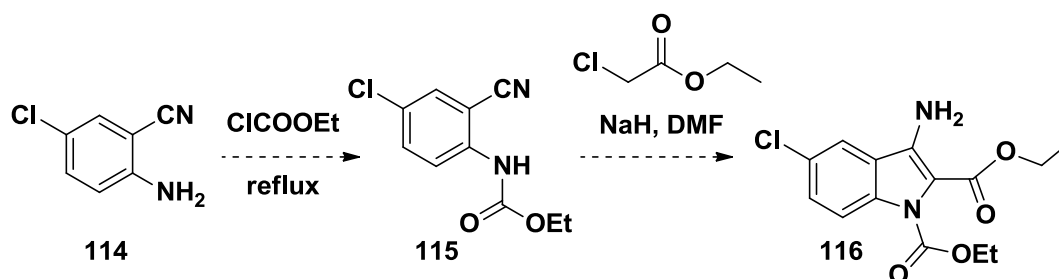
Scheme 52

A major consideration was that, having searched the literature, we realized that the entire indole scaffold would need to be constructed in order to achieve the desired substitution pattern for **109**. Fortunately, we could employ methodology described by Romagnoli *et al.*, and this would require only two steps to get to the desired indole scaffold **109**.<sup>124</sup> The first step in the reaction sequence involves the formation of *N*-ethoxycarbonylaniline **111** from 2-aminobenzonitrile **110** treated with ethyl chloroformate, followed by a condensation reaction with bromoethanone **112** and cyclization to form the indole **113** (Scheme 53).<sup>124</sup>



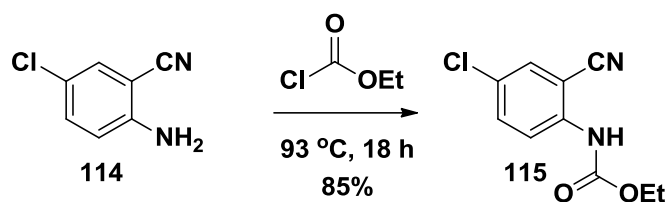
Scheme 53

For our reaction sequence we needed a somewhat different substitution as we would ultimately require an ester at the 2-position (Scheme 54). In order to achieve this, it was decided that we could carry out the condensation reaction with ethyl chloroacetate instead of bromoethanone. Furthermore, we could employ commercially available 2-amino-5-chlorobenzonitrile **114** as our starting material as we envisaged that the presence of the halogen at this position would not cause conflict with subsequent steps in the synthesis of compounds **115** and **116**, and would directly deliver the chloro at the 5-position of the indole.

Scheme 54 Our synthetic strategy based on the methodology described by Romagnoli *et al.*<sup>124</sup>

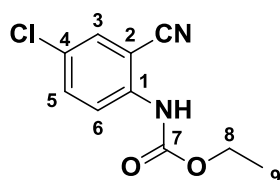


## Chapter 5: The Design and Synthesis of a 3-Aminoindole-Based Scaffold as an Extension of a Lead Compound

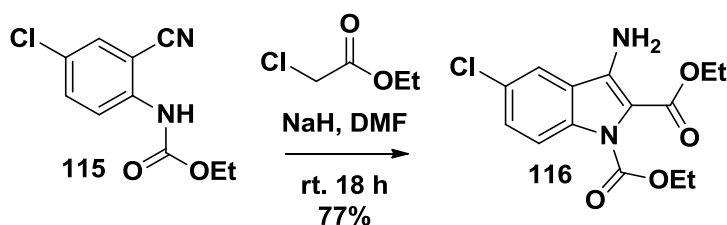
5.4.1. Synthesis of ethyl (4-chloro-2-cyanophenyl)carbamate (**115**)

Scheme 55

Following the reaction sequence carried out by Romagnoli *et al.* the first step of this synthetic strategy involved the formation of carbamate **115** (Scheme 55). This was readily achieved by heating 5-chloro-2-aminobenzonitrile under reflux in the presence of ethyl chloroformate for 18 hours. For this reaction no purification was required and the crude product was obtained in high yields.

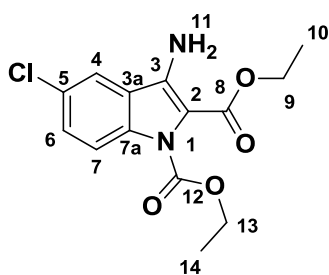


Analysis of the  $^1\text{H}$  NMR spectrum revealed a clear quartet integrating for 2H and a triplet integrating for 3H at 4.29 ppm and at 1.37 ppm respectively. These signals are indicative of the successful introduction of the carbamate on compound **115**. Furthermore, a broad singlet integrating for 1H at 7.13 ppm corresponds to the expected N-H. Mass spectral analysis revealed a mass of 225.0426 amu which coincides with the expected mass of 225.0431 amu.

5.4.2. Synthesis of diethyl 3-amino-5-chloro-1H-indole-1,2-dicarboxylate (**116**)

Scheme 56

The subsequent condensation between carbamate **115** and ethyl chloroacetate, followed by intramolecular cyclization in the presence of NaH in DMF at ambient temperature proceeded with ease and resulted in the formation of indole **116** in good yields.



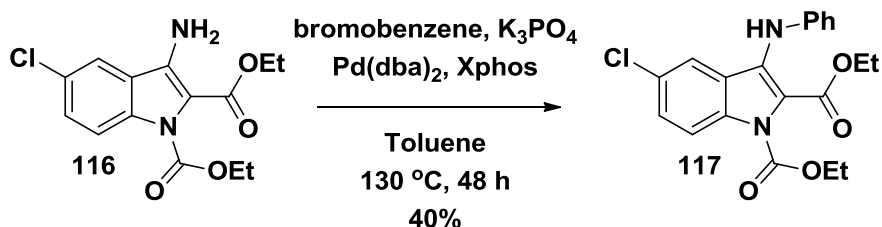
The presence of two multiplets at 4.30 ppm and at 1.31 ppm, integrating for 4H and 6H respectively, coincides with the two ethyl groups on the carbamate and ester functionalities. A broad singlet at 5.07 ppm which integrates for 2H is indicative of the presence of the amine at the three position of the indole.

## 5.5. Functionalizing the Amine

With the desired 3-amino indole **116** in hand we enthusiastically began our attempts to functionalize the amine. We had decided that we would first attempt to introduce the phenyl group onto the amine prior to the alkyl chain by employing a Buchwald-Hartwig type of methodology. We envisaged that if we attempted to introduce the larger phenyl group subsequent to the alkyl chain we could run into some complications based on steric effects.

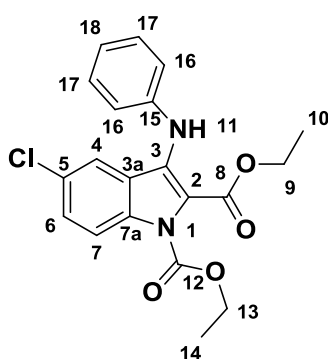
### 5.5.1. Synthesis of diethyl 5-chloro-3-(phenylamino)-1*H*-indole-1,2-dicarboxylate (**117**)

The Buchwald-Hartwig method we decided upon involved heating under reflux a mixture of **116** and an excess of bromobenzene in the presence of potassium phosphate, Pd(dba)<sub>2</sub> and 2-dicyclohexylphosphino-2',4',6'-triisopropylbiphenyl (Xphos) in toluene for 48 hours at 130 °C (Scheme 57).<sup>125</sup>



Scheme 57

This reaction we found was inexplicably inconsistent. Our initial attempts afforded product **117** in low to moderate yields ranging between 20% and 40% despite various attempts at optimizing the reaction conditions. Interestingly, when we attempted to carry out the reaction at higher concentrations in an effort to optimize our yields we found that the carbamate group was removed. Although this result was not desired at this point due complications that the free indole nitrogen might provide with subsequent steps in the synthesis, it did provide us with a possible means to remove the carbamate at a later stage. Despite the inconsistencies experienced with this reaction we were able to moderately improve the yields at higher concentrations and produce enough product **117** to continue on with the synthesis.



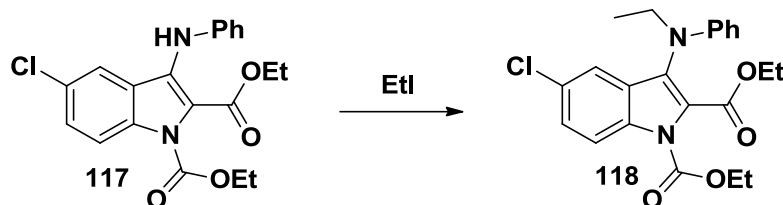
The signals in the aromatic region integrate for 8H which coincides with the presence of the protons on the phenyl ring as well as on the aryl part of the indole. Furthermore, a broad singlet belonging to the amine proton 11, integrating for 1H was observed at 7.71 ppm.

## Chapter 5: The Design and Synthesis of a 3-Aminoindole-Based Scaffold as an Extension of a Lead Compound

## 5.5.2. Synthesis of diethyl 5-chloro-3-(ethyl(phenyl)amino)-1H-indole-1,2-dicarboxylate (118)

Having synthesized compound **117** we could move on to the second last step in our synthetic strategy which entailed introducing the ethyl chain onto the amine. As before we envisaged that we could simply deprotonate the amine with a suitable strong base and then introduce the ethyl chain using an alkyl halide. Our initial attempt entailed heating **117** in the presence of  $K_2CO_3$  (Table 8). However, this reaction was unsuccessful and the full amount of starting material was recovered. We then considered attempting alkylation of the amine using a stronger base such as NaH. In this instance, we observed the formation of a product which we were able to isolate only in a very poor yield of 7%. Analysis of the  $^1H$  NMR suggested that this could be the desired product **118** due to the fact that 6 proton signals comprising of 3 quartets integrating for 2H and 3 triplets integrating for 3H were observed which indicated that three ethyl chains were present on the structure. However, as the yield was so poor, which could impede our progress, we decided to attempt to optimize the reaction conditions. Initially we changed the solvent from DMF to THF, however, in this environment no reaction occurred.

Table 8



Attempt	Base	Solvent	Temperature	Yield
1 <sup>126</sup>	$K_2CO_3$	DMF	80 °C	-
2 <sup>127</sup>	NaH	DMF	rt	7%
3	NaH	THF	rt	-

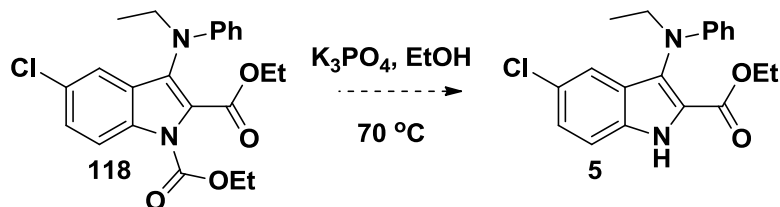
At this point, we decided that while we attempted to improve upon the yields of this reaction we would take the little material we had managed to isolate and advance to the next step in the synthesis as it was the final step. This step entailed the removal of the carbamate group from the indole nitrogen.

## 5.5.3. An attempted deprotection to afford our target compound (5)

In the paper by Romagnoli *et al.* the carbamate was removed by alkaline hydrolysis in the presence of NaOH in aqueous ethanol.<sup>124</sup> On our scaffold these conditions would inevitably result in the hydrolysis of the ester functionality at the 2-position in addition to the removal of the carbamate. In order to reduce the number of steps by keeping the ester intact and avoid losing the precious little product we had, we sought an alternative strategy. We knew that a Boc group could be removed in the presence of an excess amount of  $K_3PO_4$  and we knew that the carbamate could be removed in the same manner due to the accidental discovery made when

## Chapter 5: The Design and Synthesis of a 3-Aminoindole-Based Scaffold as an Extension of a Lead Compound

attempting to introduce the phenyl group in a too concentrated solution as mentioned previously. Unfortunately when we attempted to remove the carbamate under these conditions no reaction occurred and we struggled to retrieve the starting material **118**.



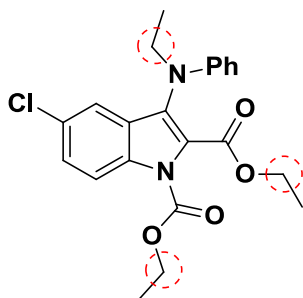
Scheme 58

#### 5.5.4. A last attempt to optimize the alkylation reaction

While we were still struggling to improve the yields of the alkylation reaction using sodium hydride we had, fortunately, come across another procedure for the reaction which employed potassium *tert*-butoxide in DMF.<sup>128</sup> When we carried out the alkylation using the alternative base, we noticed the distinct formation of a second product in addition to the product we had isolated using sodium hydride previously. We were intrigued by this second product as it had stained similarly to the first product on TLC. Having toyed with the idea that the carbamate, somehow, had been removed during the reaction we endeavoured to isolate both products which were subsequently purified using column chromatography and afforded in equally low yields of about 10%.

Surprisingly, the  $^1\text{H}$  NMR spectra of the two products revealed a number of similarities. The most prominent being the fact that for both spectra, 6 signals indicating the presence of three ethyl chains, was observed.

In the chemical shift region corresponding to the methylene protons of the three ethyl chains we can see the similarity quite clearly between the two products. For each spectrum three distinct quartets are observed each integrating for 2H.



## Chapter 5: The Design and Synthesis of a 3-Aminoindole-Based Scaffold as an Extension of a Lead Compound

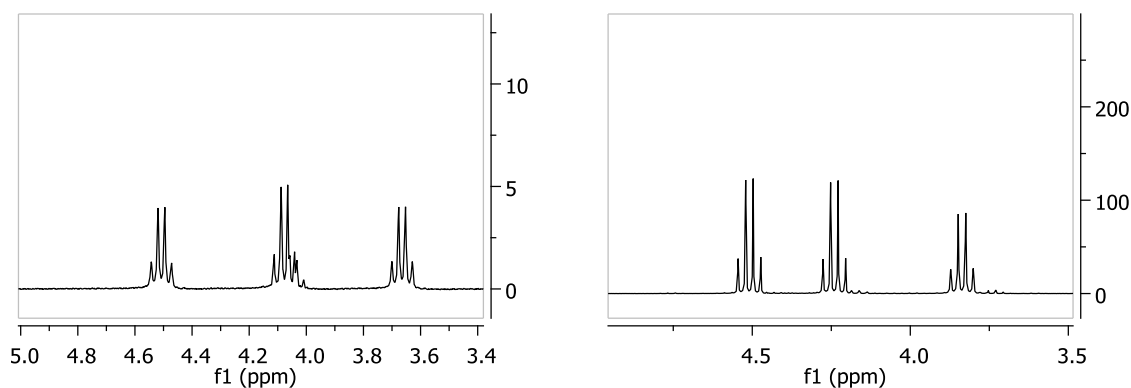


**Figure 55** Expanded region of  $^1\text{H}$  NMRs of products 1 (left) and 2 (right) showing signals corresponding to the three methylene groups

However, when we looked at the chemical shift region showcasing the signals belonging to the methyl protons a more distinctive difference between the two spectra was observed. For the newly formed product the methyl signals overlap slightly whereas the methyl signals for the first product we isolated don't overlap at all. This observation was important as it suggested that the original product we had isolated may have been the wrong product. This was based on the fact that for the starting product **117** a similar overlap for the methyl signals was observed. We could not imagine that introducing the ethyl chain onto the amine would affect the chemical shifts of the carbamate and ester signals so drastically, if at all.

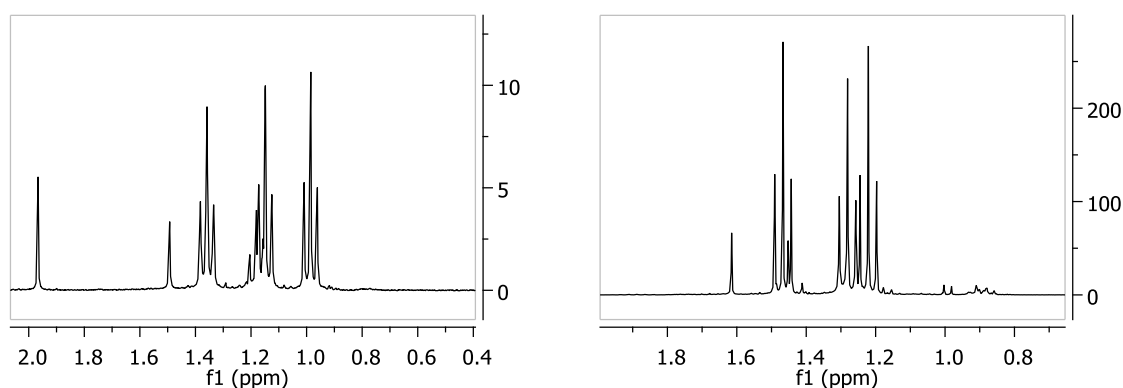
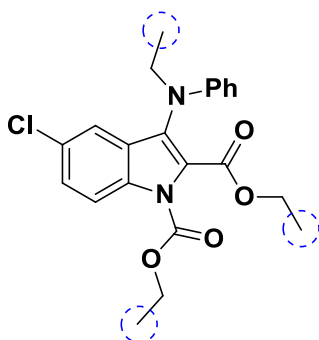
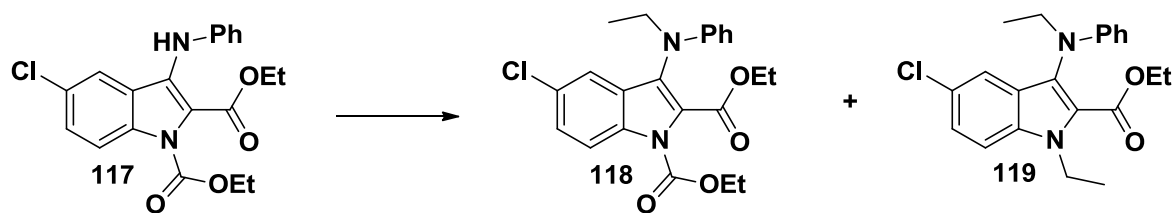


**Figure 56** Expanded region of  $^1\text{H}$  NMRs of products 1 (left) and 2 (right) showing signals corresponding to the three methyl groups

It was at this point that we hypothesized that during the alkylation step the carbamate had, in fact, been cleaved by the potassium *tert*-butoxide and had been replaced with the ethyl group.

## Chapter 5: The Design and Synthesis of a 3-Aminoindole-Based Scaffold as an Extension of a Lead Compound

As a result, we had formed a doubly alkylated product **119** in addition to the desired product **118** (Scheme 59). We feared that in the case of sodium hydride, the stronger base lead to the formation of only the doubly alkylated product, which would explain why the deprotection reaction hadn't worked.

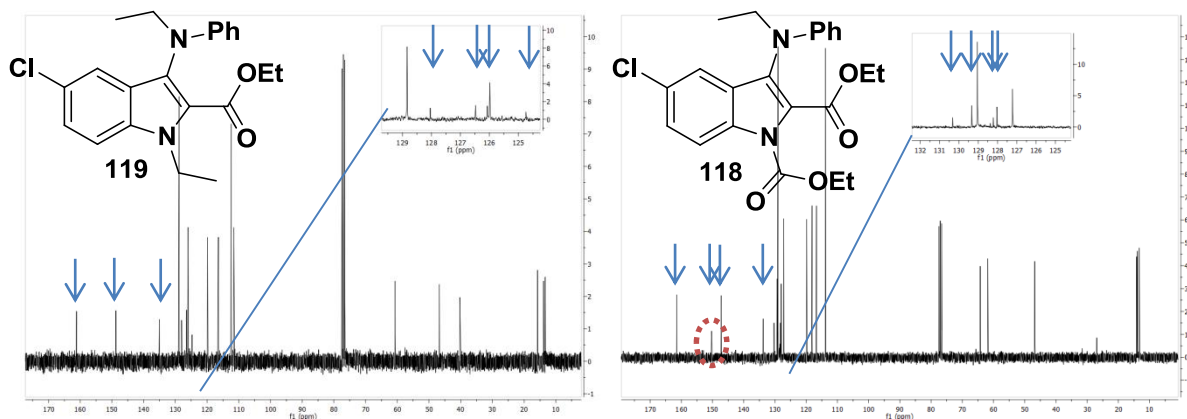


Scheme 59

### 5.6. Identifying the two products

In order to test our hypothesis and ascertain which product was which, we decided to compare the  $^{13}\text{C}$  NMR spectra. We could not compare the  $^1\text{H}$  NMR spectra of the two products as the spectra would, of course, be very similar. However, the  $^{13}\text{C}$  NMR would provide us with the answer as the spectrum for the desired compound **118** would have an extra carbon when compared with the doubly alkylated product **119**.

Figure 57 shows the  $^{13}\text{C}$  spectrum for the first product we isolated, whereupon we suspected alkylation had occurred at the amine as well as onto the indole nitrogen. If this had occurred, we would expect to observe only 19 signals of which 7 would represent quaternary carbon centres. Analysis of the  $^{13}\text{C}$  spectrum revealed that the number of carbon signals observed coincides with what was expected for the doubly alkylated product **119**.

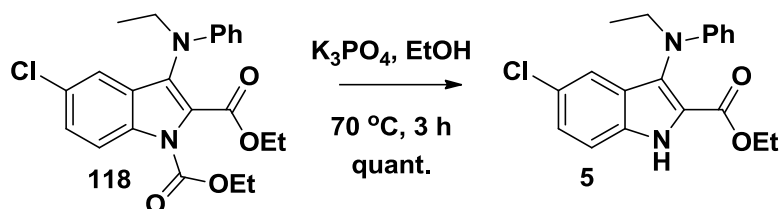
Figure 57  $^{13}\text{C}$  spectrum of products 1 (left) and 2 (right)

The  $^{13}\text{C}$  spectrum for the second product isolated which we now anticipated to be the desired product **118**. In this instance we had expected to observe one additional signal downfield corresponding to the carbonyl of the carbamate. As expected 20 carbon signals are observed of which 8 correspond to quaternary carbons with the additional carbonyl signal situated at 150 ppm (Figure 57).

## Chapter 5: The Design and Synthesis of a 3-Aminoindole-Based Scaffold as an Extension of a Lead Compound

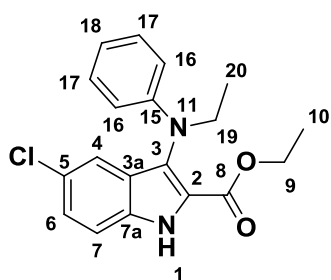
**5.6.1. Another attempt at the deprotection to yield ethyl 5-chloro-3-(ethyl(phenyl)amino)-1H-indole-2-carboxylate (5)**

Having now successfully isolated and identified the correct product we could once again attempt the deprotection of the carbamate using the same conditions we had employed for the incorrect product.



Scheme 60

For the deprotection reaction, the indole **118** and potassium phosphate were taken up in ethanol and heated to 70 °C for 3 hours. Subsequently purification by column chromatography afforded the desired product **5** in quantitative yield.



Analysis of the  $^1\text{H}$  NMR of **5** revealed that the deprotection reaction had proceeded successfully due to the presence of a singlet at 9.16 ppm integrating for 1H which was indicative of the unprotected indole nitrogen 1. Furthermore, only two methylene signals, both integrating for 2H at 4.26 ppm and at 3.81 ppm, as well as two methyl signals at 1.23 ppm and 1.16 ppm integrating altogether for 6H were observed. Analysis of the  $^{13}\text{C}$  NMR spectrum further justified our observations that the reaction had

been successful. Finally mass spectral analysis confirmed that **5** had a mass of 343.1200 amu which was in accordance with the calculated mass of 343.1213 amu.

**5.7. Efficacy results.**

Having finally arrived at our target compound **5**, we could now assess the compounds efficacy against HIV and compare it to the efficacy of the lead compound.

Figure 58 reveals the activity results for compound **5**. Although compound **5** showed some activity against HIV RT with an  $\text{IC}_{50}$  value of 1.2  $\mu\text{M}$  and a  $\text{CC}_{50}$  value of 22.8  $\mu\text{M}$  it was, disappointingly, nowhere near as active as the lead compound with an  $\text{IC}_{50}$  value of 1 nM.

## Chapter 5: The Design and Synthesis of a 3-Aminoindole-Based Scaffold as an Extension of a Lead Compound

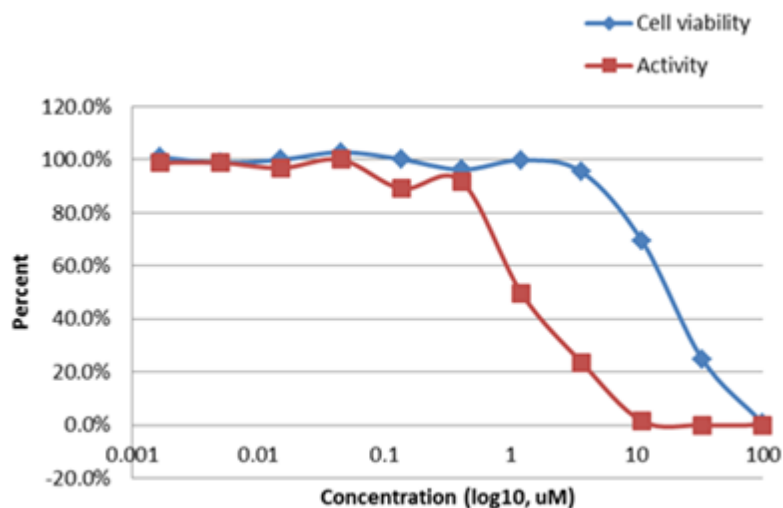
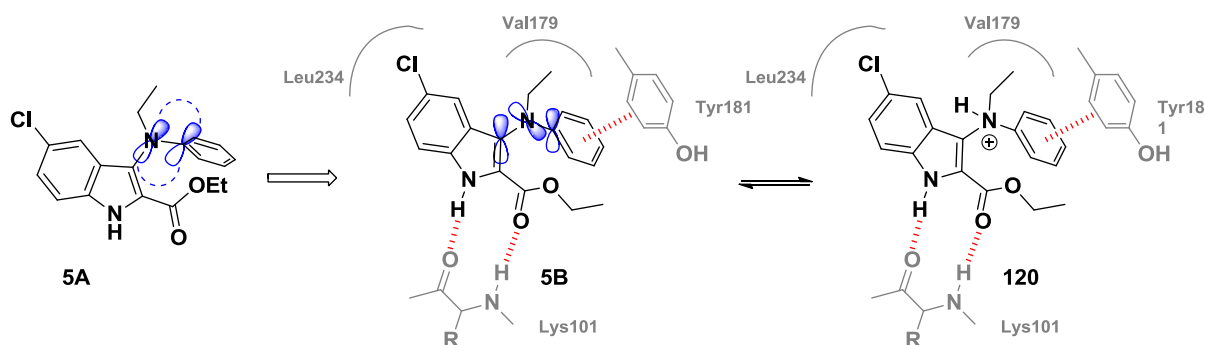


Figure 58

In an attempt to explain the poor activity of our target compound, we considered two possibilities. The first pertained to the problem observed with regards to the binding configuration of our compound as described earlier in the chapter. Upon binding to the allosteric pocket, the aromatic amine is forced out of plane with the adjacent aryl ring, **5B** (Scheme 61). The danger presented here is that without the favourable p-orbital overlap between the nitrogen and the adjacent aromatic systems, **5A**, the nitrogen may revert to an  $sp^3$  hybridization state. This occurrence would not only change the geometry of the nitrogen from trigonal planar to trigonal pyramidal but would also result in the nitrogen becoming basic. Although the change in geometry may still be well accommodated in the Val179 pocket, the basicity of the nitrogen would mean that *in vivo* at a pH of 7.4 the nitrogen would become protonated **120** and, as a result, no longer have as much of an affinity for the hydrophobic binding pocket. In addition, by forcing the compound into a less favourable position would result in a large energy penalty which, in essence, means that the molecule upon binding no longer can occupy a lowest energy configuration.



Scheme 61

The second possibility to explain the lack of activity of our compound relates to the electron rich nitrogen centre which, we hypothesized, could reduce the hydrogen bonding potential of the indole N-H.



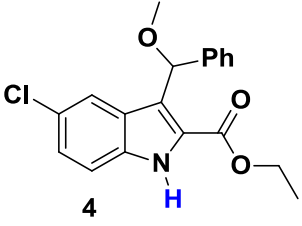
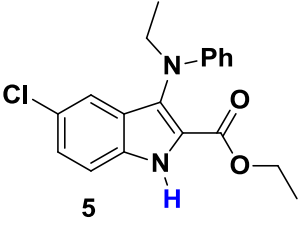
## Chapter 5: The Design and Synthesis of a 3-Aminoindole-Based Scaffold as an Extension of a Lead Compound

We resolved to investigate whether the amine at the 3-position could have an effect on the indole N-H. To do this we first decided to compare the  $^1\text{H}$  NMR spectra of our target compound **5** with compound **4** and, in particular, focus on the position of the indole N-H signal. If the nature of the functional group at the 3-position of the indole had any effect on the N-H we would expect a fairly obvious difference between the chemical shifts of the N-H peaks for both compounds. However, upon examination of both spectra we did not observe any significant difference in chemical shift between the indole N-H signal for both compounds. The small difference in chemical shift we reasoned could, more likely, be attributed to the fact that the position of the interchangeable N-H proton signal could vary depending on the concentration of the sample, as a result, this approach proved to be not entirely reliable.

A second strategy to investigate if the amine had any effect on the hydrogen bonding character of the indole N-H was to carry out some density functional theory (DFT) calculations in order to determine the partial charges on the indole N-H proton for both compounds. Again, if the presence of the amine at the 3-position had any direct effect on the bonding character of the indole N-H we would expect that the positive partial charge on the N-H proton would be greater than for the N-H proton on the methoxy-indole scaffold.

Table 9 displays the results of the DFT calculations carried out in both water and in a vacuum. Unfortunately, in either environment, there was no distinctive difference between the partial charges calculated for the N-H proton on compounds **4** and **5**. These observations, along with the observed similarity between the chemical shifts of the N-H proton for both compounds suggest that the hypothesis that the electron rich amine reduces the hydrogen bonding character of the indole is possibly incorrect.

**Table 9**

Compound		
<b>Calc. Mulliken Charge (H<sub>2</sub>O)</b>	0.383	0.384
<b>Calc. Mulliken Charge (Vacuum)</b>	0.381	0.383

Having ruled out this possibility, it would appear that the orbital problem as the primary suspect to explain the low activity of our target compound.

Although this compound had such poor activity it was worth investigating in an attempt to overcome the issue of instability with regards to the methoxy-indole compound.

## Chapter 6: Conclusion

In this project we set out to investigate the potential of novel scaffolds as NNRTIs. To this end we strategized the design and synthesis of three different scaffolds.

The first of these involved a library of small, flexible triazole containing NNRTIS whose design was based on the promising drug candidate lersivirine. To this end we managed to synthesis a library of 15 compounds using three different forms of Click chemistry to obtain three different triazole regioisomers. Unfortunately, all of these showed little or no activity against whole cell HIV-1 despite their structural similarity to lersivirine. As a result, we concluded that the triazole ring was perhaps an unsuitable core scaffold for the design of NNRTIs.

The second strategy involved the design and synthesis of a completely novel concept. Using an indole as our scaffold we sought to functionalize the 2 and 4-positions with appropriate functional groups in order to achieve  $\pi$ - $\pi$  interactions with Trp229 and Tyr188 respectively, as well as hydrogen bonding interactions with the backbone of Lys101. To this end we were able to synthesis the indole scaffold. However, when attempts were made to functionalize the 3-position with an alkyl chain we ran into problems as we were unaware of the electronic effects that would cause the alkyl chain to be introduced at the 7-position of the indole as opposed to the desired 3-position. At this point we had decided to evaluate the scaffold for efficacy against HIV as a proof-of-concept before attempting to solve the problem of putting on the alkyl group. However, we found that the basic scaffold had no activity against HIV. We were concerned that perhaps our aspirations to achieve the interactions to both regions of the NNIBP were not possible and as a result, we decided to remove the ester functionality in order to test this theory. We were able to successfully remove the ester by first albeit with low yields however, upon testing we found that even without the ester our compound had no activity against whole cell HIV-1. This was a somewhat baffling result and warrants further attention in a follow-up project.

The third and final part of this project involved improving on the stability of a lead compound by replacing the problematic methoxy functionality with a suitable bioisostere. With the aid of molecular modelling we were able to design a 3-aminoindole derivative of the lead compound. We were able to successfully synthesize our desired 3-aminoindole target however, despite promising docking results this compound was found to have an  $IC_{50}$  value of only 1.2  $\mu$ M, which was significantly less potent than the 1 nM  $IC_{50}$  value of the lead compound.

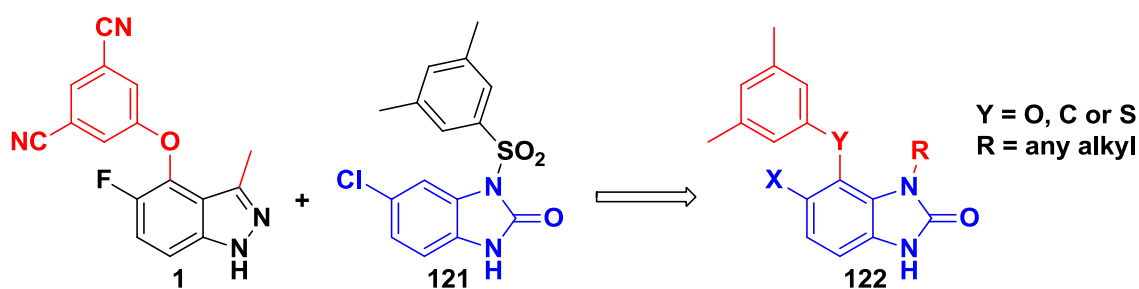
Overall, we were successful in synthesizing all target scaffolds but ascertained that in their current forms they were not to be pursued.

## Chapter 7: Future Work

### 7.1. A revision of our 4-hydroxyindole target

Despite having had no success in targeting both Trp229 and Lys101 simultaneously using the 4-hydroxyindole scaffold discussed in chapter 4, we reasoned that it would still be worthwhile to pursue other scaffold options based on the 4-hydroxyindazole compound **1**, synthesized by Jones *et al.*<sup>57</sup> Once again using this compound as a starting point we envisaged that a hybrid of the indazole compound **1** with benzimidazolone compound such as compound **121** could create a novel compound with the desired efficacy to both wild-type and drug resistance HIV-1 (Scheme 62). The discovery of benzimidazolone compound **121** as a potent NNRTI was first reported by Barreca *et al.* in 2007.<sup>129</sup> Using this core in NNRTI drug design is not novel and this particular compound was found to have a low toxicity and activity profile comparable to efavirenz.<sup>129, 130</sup>

Therefore, in a similar molecular hybridization approach as for our 4-hydroxyindole compound we envisaged we could introduce the aryl functionality of **1** to the 4-position of an imidazolone scaffold to afford compound **122** (Scheme 62). Once again, with the aryl functionality at this position we would be able to achieve  $\pi$ - $\pi$  stacking interactions with conserved residue Trp229 and Tyr188. Ideally the linker atom between the aryl functionality and the imidazolone core will be an oxygen however, we imagined that we could explore other options such as a carbon or sulphur atom as the linker atom. Additional features would include the introduction of an alkyl group at position 3, and a halogen at position 5. Furthermore, the presence of the carbonyl at the 2-position is advantageous as it renders the N-H proton to be more acidic and, therefore a better hydrogen bond donor.



Scheme 62

### 7.2. Exploring a variety of bioisosteres to improve the stability of a lead compound

For future work on this project it remains imperative that we maintain our focus on improving the stability of the potent indole compound **4**, due to its promising activity against wild type HIV-1 and mutant strains of the virus. Fortunately, we had not yet completely explored the scope of possible bioisosteres we could introduce to replace the acid labile methoxy functionality at the 3-position of the indole. Therefore, it was evident to us that this would be a good point to start in terms of future work.

To this end we proposed that the simplest option would entail replacing the problematic methoxy functionality of the lead compound **4** with an ethyl chain **123** (Figure 59). Not only would this ethyl chain occupy the same space in the Val179 pocket as the methoxy group but it would completely remove the possibility that elimination could occur at this position.

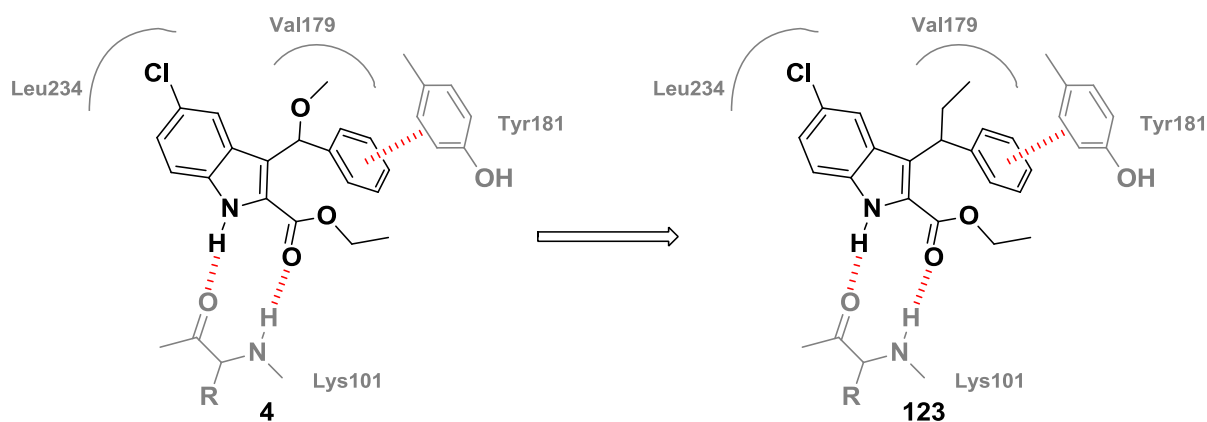
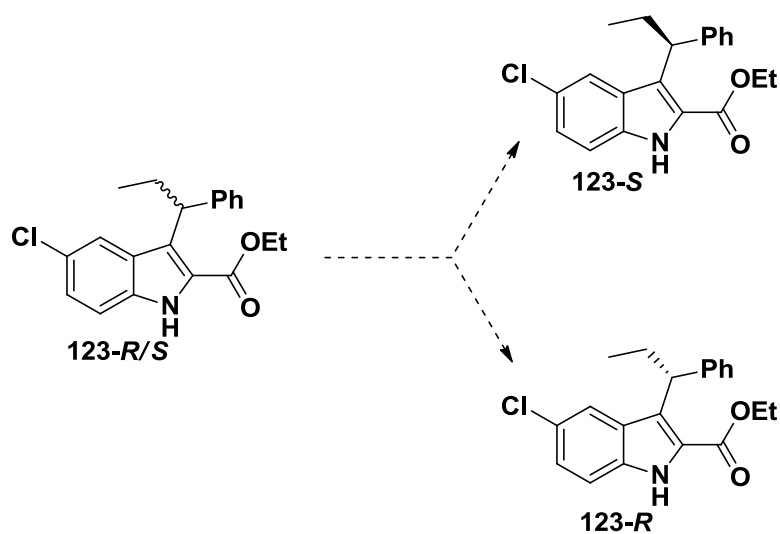


Figure 59

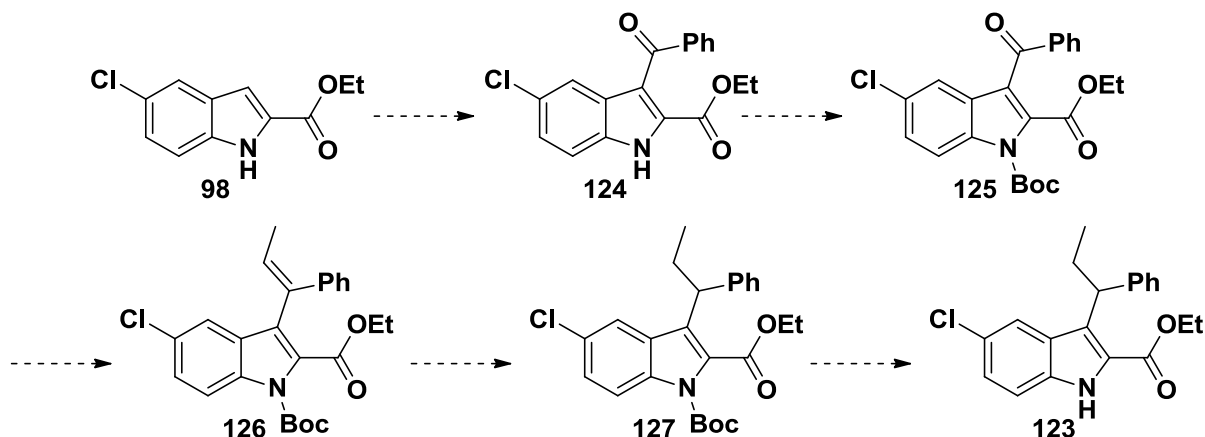
If we are able to synthesize the ethyl chain derivative and it is shown to have promising activity against whole cell HIV-1 then we would have to take into consideration that we would produce a racemic mixture of products. As a result, we would have to explore options to separate out the two diastereomers in order to test them separately (Scheme 63).



Scheme 63

We envisaged that we would be able to synthesize the ethyl derivative by first acylating ethyl 5-chloro-indole-2-carboxylate **98** with benzoyl chloride to yield the acylated product **124**. We knew that we could selectively acylate the 3-position on this particular scaffold as this was the same first step employed in the synthesis of lead compound **4**. Subsequently we could carry out a Wittig reaction with methylmagnesium bromide on a Boc protected indole **125** and then

reduce the resulting alkene **126** to the desired ethyl chain derivative **127**. This would be followed by removal of the Boc group to yield the desired product **123** (Scheme 64).



Scheme 64 Proposed synthetic strategy for the synthesis of compound 2

### 7.3. Getting creative and introducing an oxetane ring.

Another strategy that we are particularly keen to explore involves replacing the methoxy functionality of the lead compound **4** with an oxetane ring **128** (Figure 60). The oxetane ring is of particular interest due to its ability to be chemically robust in both basic and acidic environments.<sup>131</sup> Furthermore, by introducing the oxetane ring at this position we eliminate the problem of forming a racemic mixture of products whilst maintaining a similar pharmacophore to our lead compound. If we were to be successful in our endeavour to synthesize the oxetane compound **128** we would be breaking into new ground as no oxetane rings have been reported in the literature with regards to NNRTIs.

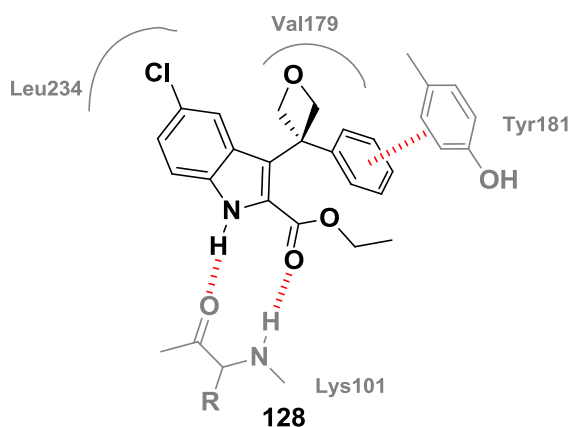


Figure 60

## Chapter 8: Experimental

### 8.1. General Procedures.

#### 8.1.1. Purification of Reagents and Solvents

The chemicals used in the following experiments were purchased from Merck or Sigma Aldrich. Solvents used for chromatographic purposes were distilled by means of conventional distillation procedures. Solvents used for reaction purposes were dried over the appropriate drying agents and then distilled under nitrogen gas. Tetrahydrofuran was distilled from sodium metal, using benzophenone as an indicator. Dichloromethane, dichloroethane, dimethylformamide and acetonitrile were distilled from calcium hydride. Ethanol was distilled from magnesium turnings and iodine. Diethyl ether and dioxane were purchased with a  $\geq 98\%$  purity grade from Sigma Aldrich and then dried on activated 3Å molecular sieves.

#### 8.1.2. Chromatography

Thin layer chromatography was performed using Merck silica gel 60 F254 coated on aluminium sheets. Visualization was performed with a UV lamp, using iodine on silica, or by spraying with a Cerium Ammonium Molybdate (CAM) or p-anisaldehyde or ninhydrin (NIN) or potassium permanganate ( $\text{KMnO}_4$ ) solution followed by heating. Column chromatography was performed on Merck silica gel 60 (particle size 0.040-0.063 mm) using one of or combinations of hexane, EtOAc, or MeOH as the mobile phase.

#### 8.1.3. Spectroscopic and physical data

NMR spectra ( $^1\text{H}$ ,  $^{13}\text{C}$ ) were recorded on a 300 MHz Varian VNMRS (75 MHz for  $^{13}\text{C}$ ), a 400 MHz Varian Unity Inova (101 MHz for  $^{13}\text{C}$ ), or a 600 MHz Varian Unity Inova (150 MHz for  $^{13}\text{C}$ ). Chemical shifts ( $\delta$ ) are reported in ppm and J-values are given in Hz. Chemical shifts were recorded using the residual solvent peak or external reference. All spectra were obtained at 25 °C unless otherwise reported. Spectroscopic data were processed using MestReNova v6.0.2.

Mass spectrometry was performed on a Waters SYNAPT G2. Infrared spectra were recorded on a Thermo Nicolet Nexus 470 by means of Attenuated Total Reflectance (ATR) mode. Melting points were obtained using a Gallenkamp Melting Point Apparatus and are uncorrected.

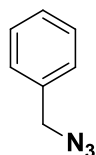
#### 8.1.4. Other general procedures

All reactions were performed under a positive pressure of 5.0 grade  $\text{N}_2$  or Ar unless water was used as a solvent. The glassware was flame-dried while under vacuum or oven dried overnight before being purged with  $\text{N}_2$  gas. Condensers were pre-dried at 120 °C for a minimum of two hours. Standard Schlenk techniques were employed when necessary. Solvents were removed

using a rotary evaporator followed by the removal of trace amounts of solvent using a high vacuum pump at *ca.* 0.08 mm Hg.

## 8.2. Experimental Procedures Pertaining to Chapter 3

### 8.2.1. Synthesis of (azidomethyl)benzene (7)

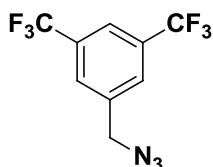


Sodium azide (570 mg, 8.78 mmol) was added to a solution of benzylbromide (0.70 mL, 5.9 mmol) in a mixture of acetone (6 mL) and water (4 mL). The reaction was left to carried out for 18 h at room temperature, after which the reaction mixture was taken up in ethyl acetate and washed with water. The organic layer was isolated and dried over magnesium sulphate and then concentrated *in vacuo* to yield a crude yellow oil. The crude material was then purified on silica by column chromatography (2% EtOAc/Hexane) to yield a colourless oil (697 mg, 5.24 mmol, 90%). ( $R_f$  = 0.53, 10% EtOAc/Hexane)

The spectroscopic data for this product correlated with the literature.<sup>132</sup>

**$^1\text{H NMR}$  (400 MHz, Chloroform-*d*)**  $\delta$  7.47 - 7.40 (m, 3H, *ArH*), 7.39 - 7.33 (m, 2H, *ArH*), 4.36 (s, 2H, *CH*<sub>2</sub>)

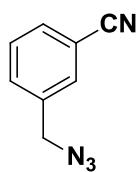
### 8.2.2. Synthesis of 1-(azidomethyl)-3,5-bis(trifluoromethyl)benzene (9)



The same procedure used for the synthesis of compound 7 was utilized for the synthesis of 9. The following equivalents were used: 3,5-bis(trifluoromethyl)benzyl bromide (0.30 mL, 1.7 mmol), sodium azide (161 mg, 2.48 mmol), acetone (8 mL) and water (2 mL). This reaction yielded a colourless oil (532 mg, 1.98 mmol, quant.). ( $R_f$  = 0.66, 20% EtOAc/Hexane).

The spectroscopic data for this product correlated with the literature.<sup>133</sup>

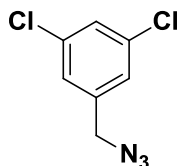
**$^1\text{H NMR}$  (300 MHz,  $\text{CDCl}_3$ )**  $\delta$  7.86 (s, 1H), 7.79 (s, 2H), 4.55 (s, 2H, *CH*<sub>2</sub>).

**8.2.3. Synthesis of 3-(azidomethyl)benzonitrile (11)**

The same procedure used for the synthesis of compound **7** was utilized for the synthesis of **11** but using DMF (10 mL) as the solvent. The following equivalents were used: 3-(bromomethyl)benzonitrile (1.0 g, 5.1 mmol) and sodium azide (3.32 g, 51.0 mmol). This reaction yielded a yellow oil (728 mg, 4.60 mmol, 90%). ( $R_f = 0.33$ , 20% EtOAc/Hexane)

The spectroscopic data for this product correlated with the literature.<sup>134</sup>

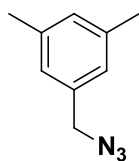
**$^1\text{H NMR}$  (400 MHz,  $\text{CDCl}_3$ )  $\delta$**  7.59 (dd,  $J = 6.5, 1.5$  Hz, 2H, ArH), 7.54 (dt,  $J = 7.8, 1.4$  Hz, 1H, ArH), 7.50 - 7.46 (m, 1H, ArH), 4.39 (s, 2H,  $\text{CH}_2$ ).

**8.2.4. Synthesis of 1-(azidomethyl)-3,5-dichlorobenzene (14)**

3,5-Dichlorobenzyl alcohol (300 mg, 1.71 mmol), sodium azide (141 mg, 2.17 mmol) and triphenylphosphine (446 mg, 1.71 mmol) were suspended in DMF (10 mL) and the reaction mixture was heated to 90 °C under reflux. Carbon tetrachloride (4 mL) was then added and the reaction was allowed to carried out for 5 h. The reaction mixture was then cooled to room temperature and taken up in diethyl ether. The organic layer was washed with cold water. The organic layer was separated and dried over magnesium sulphate. The solvent was then removed in vacuo. The resulting crude oil was purified by silica gel chromatography (2% EtOAc/Hex) to yield a yellow oil (218 mg, 1.08 mmol, 68%). ( $R_f = 0.45$ , 2% EtOAc/Hexane)

The spectroscopic data for this product correlated with the literature.<sup>135</sup>

**$^1\text{H NMR}$  (400 MHz,  $\text{CDCl}_3$ )  $\delta$**  7.33 (s, 1H, ArH), 7.21 (d,  $J = 0.7$  Hz, 2H, ArH), 4.32 (s, 2H,  $\text{CH}_2$ ).

**8.2.5. Synthesis of 1-(azidomethyl)-3,5-dimethylbenzene (23)**

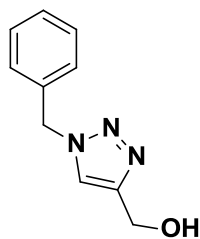
The same procedure used for the synthesis of compound **14** was utilized for the synthesis of **23**. The following equivalents were used: 3,5-methylbenzyl alcohol (500 mg, 3.67 mmol), sodium azide (287 mg, 4.41 mmol) and triphenylphosphine (960 mg, 3.67 mmol). This reaction yielded a colourless oil (327 mg, 2.03 mmol, 55%). ( $R_f = 0.68$ , 20% EtOAc/Hexane)

The spectroscopic data for this product correlated with the literature.<sup>135</sup>

**$^1\text{H NMR}$  (400 MHz,  $\text{CDCl}_3$ )  $\delta$**  7.01 (s, 1H, ArH), 6.96 (s, 2H, ArH), 4.28 (s, 2H,  $\text{CH}_2$ ), 2.36 (s, 6H,  $\text{CH}_3$ ).



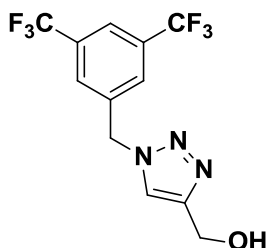
### 8.2.6. Synthesis of (1-benzyl-1H-1,2,3-triazol-4-yl)methanol (**29**)



Copper iodide (46 mg, 0.24 mmol) was added to a solution of **7** (500 mg, 3.76 mmol), propargyl alcohol (0.139 mL, 2.35 mmol) and DIPEA (0.90 mL, 4.9 mmol) in acetonitrile (2.5 mL). The reaction mixture was carried out at room temperature for 5 h after which the mixture was diluted with ethyl acetate and quenched with water. The organic and aqueous layers were separated and the organic layer was dried over magnesium sulphate and then concentrated *in vacuo* yielding a pink solid. The crude material was purified on a silica gel column (1% MeOH/EtOAc) to yield a white solid (354 mg, 1.87 mmol 80%). ( $R_f$  = 0.36, 1% MeOH/EtOAc)

**Mp** 85-87 °C.  **$^1\text{H NMR}$  (300 MHz,  $\text{CDCl}_3$ )**  $\delta$  7.37 (s, 1H, NCHC), 7.33 - 7.29 (m, 3H, ArH), 7.23 - 7.20 (m, 2H, ArH), 5.46 (s, 2H,  $\text{CH}_2$ ), 4.71 (d,  $J$  = 5.9 Hz, 2H,  $\text{CH}_2$ ), 2.07 (t,  $J$  = 6.0 Hz, 1H, OH).  **$^{13}\text{C NMR}$  (75 MHz,  $\text{CDCl}_3$ )**  $\delta$  148.28 (CHCN), 134.51 (ArC), 129.10 (ArC), 128.75 (ArC), 128.11 (ArC), 121.81 (NCHC), 56.14 ( $\text{CH}_2$ ), 54.16 ( $\text{CH}_2$ ). **HRMS-TOF MS ES+**:  $m/z$  [ $\text{M}+\text{H}$ ] $^+$  calcd for  $\text{C}_{10}\text{H}_{12}\text{N}_3\text{O}$ : 190.0980; found: 19.0973.

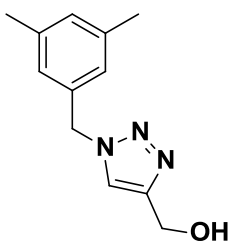
### 8.2.7. Synthesis of 1-(azidomethyl)-3,5-bis(trifluoromethyl)benzene (**30**)



The same procedure used for the synthesis of compound **29** was utilized for the synthesis of **30**. The following equivalents were used: **9** (405 mg, 1.53 mmol), propargyl alcohol (60  $\mu\text{L}$ , 0.96 mmol), DIPEA (0.35 mL, 2.0 mmol), CuI (18 mg, 0.10 mmol) and MeCN (2 mL). The reaction yielded a white solid (284 mg, 0.880 mmol, 92%). ( $R_f$  = 0.52, 3% MeOH/EtOAc)

**Mp** 127-129 °C.  **$^1\text{H NMR}$  (300 MHz,  $\text{CDCl}_3$ )**  $\delta$  7.82 (s, 1H, NCHC), 7.67 (s, 2H, ArH), 7.49 (s, 1H, ArH), 5.59 (s, 2H,  $\text{CH}_2$ ), 4.76 (s, 2H,  $\text{CH}_2$ ), 1.98 (s, 1H, OH).  **$^{13}\text{C NMR}$  (75 MHz, DMSO)**  $\delta$  149.02 (CHCN), 139.91 (ArC), 131.04 (q,  $J$  = 32.9 Hz  $\text{CF}_3$ ), 129.51 (ArC), 125.40 (CCN), 123.70 (ArC), 122.53 (ArC), 55.46 ( $\text{CH}_2$ ), 51.81 ( $\text{CH}_2$ ). **HRMS-TOF MS ES+**:  $m/z$  [ $\text{M}+\text{H}$ ] $^+$  calcd for  $\text{C}_{12}\text{H}_{10}\text{N}_3\text{OF}_6$ : 326.0728; found: 326.0737.

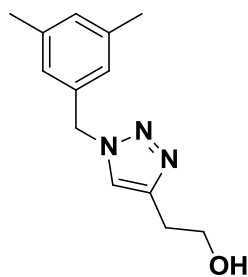
### 8.2.8. Synthesis of (1-(3,5-dimethylbenzyl)-1H-1,2,3-triazol-4-yl)methanol (**31**)



The same procedure used for the synthesis of compound **29** was utilized for the synthesis of **31**. The following equivalents were used: **23** (122 mg, 0.757 mmol), propargyl alcohol (30  $\mu\text{L}$ , 0.47 mmol), DIPEA (0.20 mL, 0.99 mmol), CuI (10 mg, 0.047 mmol) and MeCN (2 mL). The reaction yielded a white solid (100 mg, 0.460 mmol, 98%). ( $R_f$  = 0.60, 3% MeOH/EtOAc)

**Mp** 101-103 °C  **$^1\text{H NMR}$  (300 MHz,  $\text{CDCl}_3$ )**  $\delta$  7.46 (s, 1H, NCHC), 7.02 (s, 1H, ArH), 6.92 (s, 2H, ArH), 5.46 (s, 2H,  $\text{CH}_2$ ), 4.81 (d,  $J$  = 5.8 Hz, 2H,  $\text{CH}_2$ ), 2.33 (d,  $J$  = 0.6 Hz, 6H,  $\text{CH}_3$ ).  **$^{13}\text{C NMR}$  (75 MHz,  $\text{CDCl}_3$ )**  $\delta$  138.86 (NCHC), 134.29 (ArC), 130.43 (ArC), 125.98 (ArC), 121.46 (ArC), 56.79 ( $\text{CH}_2$ ), 54.22 ( $\text{CH}_2$ ), 21.20 ( $\text{CH}_3$ ). **HRMS-TOF MS ES+**:  $m/z$  [ $\text{M}+\text{H}$ ] $^+$  calcd for  $\text{C}_{12}\text{H}_{16}\text{N}_3\text{O}$ : 218.1293; found: 218.1295

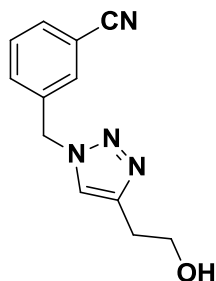
### 8.2.9. Synthesis of 2-(1-(3,5-dimethylbenzyl)-1H-1,2,3-triazol-4-yl)ethanol (**32**)



The same procedure used for the synthesis of compound **29** was utilized for the synthesis of **32** but using but-3-yn-1-ol as the alkyne. The following equivalents were used: **23** (130 mg, 0.807 mmol), but-3-yn-1-ol (40  $\mu$ L, 0.50 mmol), DIPEA (0.20 mL, 1.1 mmol), CuI (10 mg, 0.050 mmol) and MeCN (2 mL). The reaction yielded a white solid (100 mg, 0.432 mmol, 86%). ( $R_f$  = 0.75, 3% MeOH/EtOAc).

**$^1\text{H NMR}$  (300 MHz,  $\text{CDCl}_3$ )**  $\delta$  7.32 (s, 1H, NCHC), 7.02 (s, 1H, ArH), 6.93 (d,  $J$  = 5.6 Hz, 2H, ArH), 5.44 (s, 2H,  $\text{CH}_2$ ), 3.97 (q,  $J$  = 6.0 Hz, 2H,  $\text{CH}_2$ ), 3.00 - 2.89 (m, 2H,  $\text{CH}_2$ ), 2.58 (t,  $J$  = 6.1 Hz, 1H, OH), 2.33 (t,  $J$  = 1.7 Hz, 6H,  $\text{CH}_3$ ).

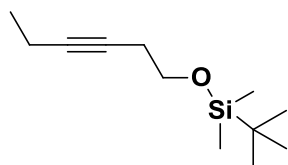
### 8.2.10. Synthesis of 3-((4-(2-hydroxyethyl)-1H-1,2,3-triazol-1-yl)methyl)benzonitrile (**33**)



The same procedure used for the synthesis of compound **29** was utilized for the synthesis of **33**. The following equivalents were used: **11** (247 mg, 1.86 mmol), but-3-yn-1-ol (70  $\mu$ L, 0.98 mmol), DIPEA (0.40 mL, 2.1 mmol), CuI (19 mg, 0.098 mmol) and MeCN (2 mL). The reaction yielded a white solid (102 mg, 0.45 mmol, 46%). ( $R_f$  = 0.21, 2% MeOH/EtOAc).

**Mp** 129-131  $^\circ\text{C}$ .  **$^1\text{H NMR}$  (300 MHz, DMSO)**  $\delta$  7.70 - 7.65 (m, 1H, ArH), 7.59 - 7.55 (m, 1H, ArH), 7.54 - 7.50 (m, 2H, ArH), 7.40 (s, 1H, NCC), 5.57 (s, 2H,  $\text{CH}_2$ ), 3.98 (q,  $J$  = 5.9 Hz, 2H,  $\text{CH}_2$ ), 3.02 - 2.93 (m, 2H,  $\text{CH}_2$ ), 2.42 (t,  $J$  = 5.9 Hz, 1H, OH).  **$^{13}\text{C NMR}$  (75 MHz, DMSO)**  $\delta$  148.01 (CCN), 140.88 (ArC), 135.96 (ArC), 134.97 (ArC), 134.65 (ArC), 133.13 (ArC), 125.89 (NCHC), 121.52 (CCN), 114.72 (ArC), 63.33 ( $\text{CH}_2$ ), 54.74 ( $\text{CH}_2$ ), 32.22 ( $\text{CH}_2$ ). **HRMS-TOF MS ES+**:  $m/z$  [ $\text{M}+\text{H}$ ] $^+$  calcd for  $\text{C}_{12}\text{H}_{13}\text{N}_4\text{O}$ : 229.1089; found: 229.1092

### 8.2.12. Synthesis of *tert*-butyl(hex-3-yn-1-yloxy)dimethylsilane (**38**)



Imidazole (1.53 g, 22.4 mmol) was added to a solution of 3-hexyn-1-ol (1.1 mL, 10 mmol) in DMF (10 mL) at 0  $^\circ\text{C}$ . Once all the imidazole had been fully dissolved, *tert*-butyldimethylsilyl chloride (1.84 g, 12.2 mmol) was added to the reaction mixture and the reaction was allowed to warm to room temperature. The reaction was carried out for 3 h. EtOAc was added to the reaction mixture and the organic phase was washed with brine. The organic phase was separated and dried over  $\text{MgSO}_4$ , after which the solvent was removed *in vacuo*. The residue was purified by silica gel column chromatography (5% EtOAc/Hexane) to afford the product as a colourless oil (1.48 g, 6.97 mmol, 69%). ( $R_f$  = 0.56, 5% EtOAc/Hexane).

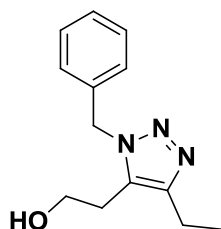
**$^1\text{H NMR}$  (300 MHz,  $\text{CDCl}_3$ )**  $\delta$  3.62 (t,  $J$  = 7.2 Hz, 2H,  $\text{CH}_2$ ), 2.35 - 2.23 (m, 2H,  $\text{CH}_2$ ), 2.16 - 2.01 (m, 2H,  $\text{CH}_2$ ), 1.04 (t,  $J$  = 7.5 Hz, 3H,  $\text{CH}_3$ ), 0.88 - 0.78 (m, 9H,  $\text{CH}_3$ ), 0.04 - -0.04 (m, 6H,  $\text{CH}_3$ ).  **$^{13}\text{C NMR}$  (75 MHz,  $\text{CDCl}_3$ )**  $\delta$  82.88 (CCC), 76.35 (CCC), 62.54 ( $\text{CH}_2$ ), 26.03 ( $\text{CH}_3$ ), 23.30 (SiCC), 18.48 ( $\text{CH}_2$ ), 14.34 ( $\text{CH}_3$ ), 12.53 ( $\text{CH}_2$ ), -5.15 ( $\text{CH}_3$ ). **HRMS-TOF MS ES+**:  $m/z$  [ $\text{M}+\text{H}$ ] $^+$  calcd for  $\text{C}_{12}\text{H}_{25}\text{OSi}$ : 213.1675; found: 213.1662

### 8.2.13. Synthesis of 2-(1-benzyl-4-ethyl-1H-1,2,3-triazol-5-yl)ethanol (43A) and 2-(1-benzyl-5-ethyl-1H-1,2,3-triazol-4-yl)ethanol (43B)

Toluene (5 mL) was thoroughly degassed for approximately 15 minutes before the ruthenium catalyst Cp\*RuCl(COD) (17 mg, 0.045 mmol) was added and the solvent was degassed again. This was followed by the addition of the alkyne **38** (478 mg, 2.25 mmol) and finally the benzyl azide **7** (300 mg, 2.25 mmol). After a final degassing of the reaction was heated to 60°C and was allowed to carried out for 18 h. The reaction was allowed to cool to room temperature before being concentrated under reduced pressure. The material was then taken to the next step crude.

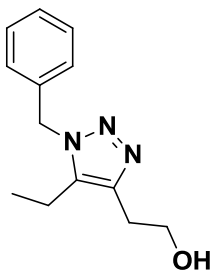
To a solution of the crude protected triazole products in MeOH (5 mL), was added 6N HCl (0.60 mL, 3.6 mmol) and the reaction was allowed to stir at room temperature for 1.5 h. The reaction mixture was then concentrated *in vacuo*, taken up in EtOAc and washed with distilled water. The crude products were purified and isolated using column chromatography on silica gel (60% EtOAc/Hexane).

**43A** was isolated as a white solid (61 mg, 0.26 mmol, 22%). ( $R_f = 0.40$ , 2% MeOH/EtOAc).



**Mp** 96-98 °C. **<sup>1</sup>H NMR (300 MHz, CDCl<sub>3</sub>)**  $\delta$  7.37 - 7.32 (m, 3H, ArH), 7.21 - 7.17 (m, 2H, ArH), 5.61 (s, 2H, CH<sub>2</sub>), 3.64 (dd,  $J = 11.8, 6.4$  Hz, 2H, CH<sub>2</sub>), 2.80 (t,  $J = 6.5$  Hz, 2H, CH<sub>2</sub>), 2.69 (q,  $J = 7.6$  Hz, 2H, CH<sub>2</sub>), 1.65 (t,  $J = 5.4$  Hz, 1H, OH), 1.32 (t,  $J = 7.6$  Hz, 3H, CH<sub>3</sub>). **<sup>13</sup>C NMR (101 MHz, CDCl<sub>3</sub>)**  $\delta$  147.52 (CCN), 135.70 (ArC), 130.41 (CCN), 129.14 (ArC), 128.40 (ArC), 127.32 (ArC), 61.20 (CH<sub>2</sub>OH), 52.29 (CH<sub>2</sub>), 26.24 (CH<sub>2</sub>), 18.70 (CH<sub>2</sub>), 14.17 (CH<sub>3</sub>). **HRMS-TOF MS ES+**:  $m/z$  [M+H]<sup>+</sup> calcd for C<sub>13</sub>H<sub>18</sub>N<sub>3</sub>O: 232.1450; found: 232.1447

**43B** was isolated as a white solid (25.0 mg, 0.11 mmol, 9%). ( $R_f = 0.26$ , 2% MeOH/EtOAc).

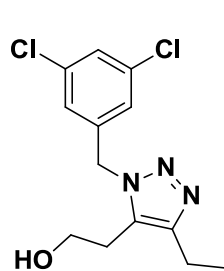


**Mp** 75-77 °C. **<sup>1</sup>H NMR (300 MHz, CDCl<sub>3</sub>)**  $\delta$  7.35 (dd,  $J = 6.9, 5.1$  Hz, 3H, ArH), 7.23 - 7.17 (m, 2H, ArH), 5.52 (s, 2H, CH<sub>2</sub>), 4.02 (q,  $J = 6.0$  Hz, 2H, CH<sub>2</sub>), 3.02 (t,  $J = 6.3$  Hz, 1H, OH), 2.87 (t,  $J = 5.8$  Hz, 2H, CH<sub>2</sub>), 2.57 (q,  $J = 7.6$  Hz, 2H, CH<sub>2</sub>), 1.00 (t,  $J = 7.6$  Hz, 3H, CH<sub>3</sub>). **<sup>13</sup>C NMR (75 MHz, CDCl<sub>3</sub>)**  $\delta$  142.78 (CCN), , 135.16 (ArC), 128.96 (ArC), 128.30 (ArC), 128.11 (CCN), 127.11 (ArC), 61.60 (CH<sub>2</sub>OH), 51.95 (CH<sub>2</sub>), 27.98 (CH<sub>2</sub>), 15.94 (CH<sub>2</sub>), 13.18 (CH<sub>3</sub>). **HRMS-TOF MS ES+**:  $m/z$  [M+H]<sup>+</sup> calcd for C<sub>13</sub>H<sub>18</sub>N<sub>3</sub>O: 232.1450; found: 232.1662

### 8.2.14. Synthesis of 2-(1-(3,5-dichlorobenzyl)-4-ethyl-1*H*-1,2,3-triazol-5-yl)ethanol (44A) and 2-(1-(3,5-dichlorobenzyl)-5-ethyl-1*H*-1,2,3-triazol-4-yl)ethanol (44B)

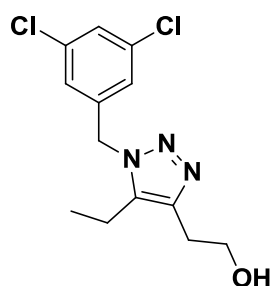
The same procedure used for the synthesis of compounds of **43A** and **43B** was utilized for the synthesis of **44A** and **44B**. The following equivalents were used: **14** (309 mg, 1.53 mmol), **38** (325 mg, 1.53 mmol), Cp\*RuCl(COD) (12 mg, 0.031 mmol) and toluene (5 mL), then 6*N* HCl (0.20 mL, 1.3 mmol) and MeOH (5 mL).

The reaction yielded a yellow solid (46 mg, 0.15 mmol, 37%). (*R*<sub>f</sub> = 0.28, 2% MeOH/EtOAc).



**Mp** 153-155 °C. <sup>1</sup>H NMR (300 MHz, CDCl<sub>3</sub>) δ 7.22 (t, *J* = 1.8 Hz, 1H, Ar*H*), 6.97 (d, *J* = 1.8 Hz, 2H, Ar*H*), 5.47 (s, 2H, CH<sub>2</sub>), 3.69 (t, *J* = 6.1 Hz, 2H, CH<sub>2</sub>), 2.69 (t, *J* = 6.1 Hz, 2H, CH<sub>2</sub>), 2.57 (q, *J* = 7.6 Hz, 2H, CH<sub>2</sub>), 1.22 (t, *J* = 7.6 Hz, 3H, CH<sub>3</sub>). <sup>13</sup>C NMR (75 MHz, CDCl<sub>3</sub>) δ 147.23 (CCN), 138.79 (ArC), 135.62 (ArC), 130.66 (CCN), 128.51 (ArC), 125.68 (ArC), 61.23 (CH<sub>2</sub>OH), 50.85 (CH<sub>2</sub>), 25.85 (CH<sub>2</sub>), 18.48 (CH<sub>2</sub>), 13.90 (CH<sub>3</sub>). **HRMS-TOF MS ES<sup>+</sup>: *m/z* [M+H]<sup>+</sup>** calcd for C<sub>13</sub>H<sub>16</sub>N<sub>3</sub>OCl<sub>2</sub>: 300.0670; found: 300.0669

The reaction yielded a yellow solid (15 mg, 0.050 mmol, 12%). (*R*<sub>f</sub> = 0.21, 2% MeOH/EtOAc).

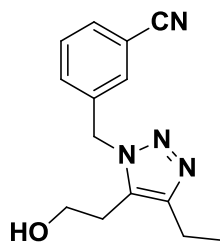


**Mp** 112-114 °C. <sup>1</sup>H NMR (300 MHz, CDCl<sub>3</sub>) δ 7.34 (t, *J* = 1.8 Hz, 1H, Ar*H*), 7.08 (d, *J* = 1.8 Hz, 2H, Ar*H*), 5.44 (s, 2H, CH<sub>2</sub>), 4.02 (t, *J* = 5.7 Hz, 2H, CH<sub>2</sub>), 2.89 (t, *J* = 5.9 Hz, 2H, CH<sub>2</sub>), 2.60 (q, *J* = 7.6 Hz, 2H, CH<sub>2</sub>), 2.48 (s, 1H, OH), 1.07 (t, *J* = 7.6 Hz, 3H, CH<sub>3</sub>). <sup>13</sup>C NMR (75 MHz, CDCl<sub>3</sub>) δ 143.00 (CCN), 138.40 (ArC), 135.74 (ArC), 135.23 (CCN), 128.71 (ArC), 125.58 (ArC), 61.55 (CH<sub>2</sub>OH), 50.64 (CH<sub>2</sub>), 27.93 (CH<sub>2</sub>), 15.98 (CH<sub>2</sub>), 13.37 (CH<sub>3</sub>). **HRMS-TOF MS ES<sup>+</sup>: *m/z* [M+H]<sup>+</sup>** calcd for C<sub>13</sub>H<sub>16</sub>N<sub>3</sub>OCl<sub>2</sub>: 300.0670; found: 300.0676

### 8.2.15. Synthesis of 3-((4-ethyl-5-(2-hydroxyethyl)-1*H*-1,2,3-triazol-1-yl)methyl)benzonitrile (45A) and 3-((5-ethyl-4-(2-hydroxyethyl)-1*H*-1,2,3-triazol-1-yl)methyl)benzonitrile (45B)

The same procedure used for the synthesis of compounds of **43A** and **43B** was utilized for the synthesis of **45A** and **45B**. The following equivalents were used: **11** (351 mg, 2.22 mmol), **38** (470 mg, 2.22 mmol), Cp\*RuCl(COD) (42 mg, 0.11 mmol) and toluene (5 mL), then 6*N* HCl (0.30 mL, 1.8 mmol) and MeOH (5 mL).

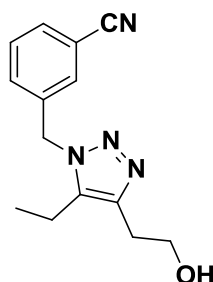
The reaction yielded a white solid (43 mg, 0.17 mmol, 29%). (*R*<sub>f</sub> = 0.36, 2% MeOH/EtOAc).



**Mp** 137-139 °C. <sup>1</sup>H NMR (300 MHz, CDCl<sub>3</sub>) δ 7.65 - 7.59 (m, 1H, Ar*H*), 7.53 - 7.40 (m, 3H, Ar*H*), 5.66 (s, 2H, CH<sub>2</sub>), 3.78 (t, *J* = 6.0 Hz, 2H, CH<sub>2</sub>), 2.78 (t, *J* = 6.0 Hz, 2H, CH<sub>2</sub>), 2.66 (q, *J* = 7.6 Hz, 2H, CH<sub>2</sub>), 2.19 (s, 1H, OH), 1.30 (t, *J* = 7.6 Hz, 3H, CH<sub>3</sub>). <sup>13</sup>C NMR (75 MHz, CDCl<sub>3</sub>) δ 147.16 (CCN), 137.17 (ArC), 131.89 (ArC), 131.80 (ArC), 130.87 (CCN), 130.73 (ArC), 129.83 (ArC), 118.21 (CN), 113.04 (ArC), 61.13 (CH<sub>2</sub>OH), 51.06 (CH<sub>2</sub>), 25.91 (CH<sub>2</sub>), 18.46 (CH<sub>2</sub>), 13.91 (CH<sub>3</sub>). **HRMS-TOF MS ES<sup>+</sup>: *m/z* [M+H]<sup>+</sup>** calcd for C<sub>14</sub>H<sub>17</sub>N<sub>4</sub>O:

257.1402; found: 257.1398

The reaction yielded a white solid (19 mg, 0.074 mmol, 13%). ( $R_f = 0.22$ , 2% MeOH/EtOAc).

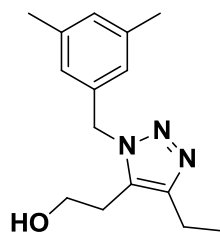


**Mp** 85-87 °C.  $^1\text{H NMR}$  (300 MHz,  $\text{CDCl}_3$ )  $\delta$  7.67 - 7.62 (m, 1H, ArH), 7.46 (ddd,  $J = 10.1, 9.2, 4.6$  Hz, 3H, ArH), 5.53 (s, 2H,  $\text{CH}_2$ ), 4.01 (t,  $J = 5.9$  Hz, 2H,  $\text{CH}_2$ ), 2.88 (t,  $J = 6.0$  Hz, 2H,  $\text{CH}_2$ ), 2.58 (t,  $J = 7.6$  Hz, 2H,  $\text{CH}_2$ ), 1.04 (t,  $J = 7.6$  Hz, 3H,  $\text{CH}_3$ ).  $^{13}\text{C NMR}$  (75 MHz,  $\text{CDCl}_3$ )  $\delta$  143.08 (CCN), 136.83 (ArC), 135.28 (CCN), 132.10 (ArC), 131.51 (ArC), 130.53 (ArC), 129.98 (ArC), 118.11 (CN), 113.24 (ArC), 61.54 ( $\text{CH}_2\text{OH}$ ), 50.83 ( $\text{CH}_2$ ), 27.96 ( $\text{CH}_2$ ), 15.96 ( $\text{CH}_2$ ), 13.40 ( $\text{CH}_3$ ). **HRMS-TOF MS ES+**:  $m/z$   $[\text{M}+\text{H}]^+$  calcd for  $\text{C}_{14}\text{H}_{17}\text{N}_4\text{O}$ : 257.1402; found: 257.1401

### 8.2.16. Synthesis of 2-(1-(3,5-dimethylbenzyl)-4-ethyl-1H-1,2,3-triazol-5-yl)ethanol (46A) and 2-(1-(3,5-dimethylbenzyl)-5-ethyl-1H-1,2,3-triazol-4-yl)ethanol (46B)

The same procedure used for the synthesis of compounds of **43A** and **43B** was utilized for the synthesis of **46A** and **46B**. The following equivalents were used: **23** (200 mg, 1.24 mmol), **38** (264 mg, 1.24 mmol),  $\text{Cp}^*\text{RuCl}(\text{COD})$  (9.4 mg, 0.025 mmol) and toluene (5 mL), then 6N HCl (0.10 mL, 0.79 mmol) and MeOH (5 mL).

The reaction yielded a white solid (43 mg, 0.17 mmol, 29%). ( $R_f = 0.50$ , 2% MeOH/EtOAc).



**Mp** 151-153 °C.  $^1\text{H NMR}$  (300 MHz,  $\text{CDCl}_3$ )  $\delta$  6.94 (s, 1H, ArH), 6.80 (s, 2H, ArH), 5.50 (s, 2H,  $\text{CH}_2$ ), 3.65 (d,  $J = 5.8$  Hz, 2H,  $\text{CH}_2$ ), 2.79 (t,  $J = 6.3$  Hz, 2H,  $\text{CH}_2$ ), 2.67 (q,  $J = 7.4$  Hz, 2H,  $\text{CH}_2$ ), 2.28 (s, 6H,  $\text{CH}_3$ ), 1.83 (s, 1H, OH), 1.31 (dd,  $J = 8.1, 7.1$  Hz, 3H,  $\text{CH}_3$ ).  $^{13}\text{C NMR}$  (75 MHz,  $\text{CDCl}_3$ )  $\delta$  138.56 (ArC), 135.34 (ArC), 129.84 (ArC), 124.89 (ArC), 61.14 ( $\text{CH}_2\text{OH}$ ), 52.06 ( $\text{CH}_2$ ), 26.00 ( $\text{CH}_2$ ), 21.22 ( $\text{CH}_3$ ), 18.54 ( $\text{CH}_2$ ), 14.03 ( $\text{CH}_3$ ). **HRMS-TOF MS ES+**:  $m/z$   $[\text{M}+\text{H}]^+$  calcd for  $\text{C}_{15}\text{H}_{22}\text{N}_3\text{O}$ : 260.1763; found: 260.1765

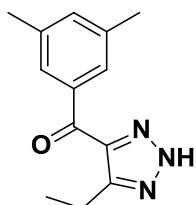
Unfortunately we were unable to isolate the desired 1,4-regioisomer **46B**.

### 8.2.17. Synthesis of (3,5-dimethylphenyl)(5-ethyl-2H-1,2,3-triazole-4-yl)methanone (54)

3,5-dimethylbenzoic acid (300 mg, 2.00 mmol) was dissolved in thionyl chloride (1.2 mL, 16 mmol) and the reaction was heated to 80 °C under reflux. The reaction was carried out for 18 h, allowed to cool down and the thionyl chloride was then aprotroped off with an excess of toluene. The crude product was taken to the next step without further purification.

An unknown amount of 1-butyne gas was condensed in a 3-necked r.b.f. at -50 °C, after which THF (5 mL) was added dropwise. This was followed by the slow addition of n-BuLi (1.2 mL, 1.7 mmol) at -50 °C. The reaction mixture was warmed to -20 °C before  $\text{ZnCl}_2$  (228 mg, 1.67 mmol) in THF (5 mL) was added slowly. The reaction mixture was then warmed to 0 °C and allowed to stir for approximately 10min before the addition of  $\text{Pd}[\text{P}(\text{Ph})_3]_4$  (4.00 mg, 3.34  $\mu\text{mol}$ ). The reaction was then warmed to 15 °C and the crude 3,5-dimethylbenzoyl chloride was added dropwise. After approximately 5 minutes the reaction had appeared to carried out to completion. The reaction mixture was diluted with diethyl ether and added to a saturated

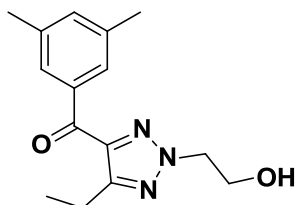
solution of sodium bicarbonate. Liquid ammonia was then added and the reaction was shaken up vigorously. The phases were separated and the aqueous layer was washed once more with diethyl ether. The organic phases were then combined and dried over  $\text{MgSO}_4$ . The organic solvent was removed *in vacuo* and the remaining brown crude material was again taken to the next step without purification.



The crude alkyne (292 mg, 1.57 mmol) was taken up in DMF (5 mL). Sodium azide (122 mg, 1.88 mmol) was then added to the reaction mixture and the reaction was left to carried out for 7 h at room temperature. The reaction mixture was then poured onto ice and acidified with a 6N HCl solution until a pH of 2 or 3 was achieved. The product was then extracted with EtOAc and washed with distilled water and brine. The organic solvent was dried over  $\text{MgSO}_4$  and concentrated *in vacuo*. The crude product was purified by silica gel chromatography (20% EtOAc/Hexane) to yield the triazole product as an orange solid (245 mg, 1.07 mmol, quant.). ( $R_f$  = 0.11, 20% EtOAc/Hexane).

**$^1\text{H}$  NMR (300 MHz,  $\text{CDCl}_3$ )**  $\delta$  7.82 (s, 2H, ArH), 7.23 (s, 1H, ArH), 3.10 (q,  $J$  = 7.5 Hz, 2H,  $\text{CH}_2$ ), 2.38 (s, 6H,  $\text{CH}_3$ ), 1.34 (t,  $J$  = 7.5 Hz, 3H,  $\text{CH}_3$ ).  **$^{13}\text{C}$  NMR (75 MHz,  $\text{CDCl}_3$ )**  $\delta$  182.88 (CO), 150.32 (CCN), 150.24 (CCN), 137.98 (ArC), 137.42 (ArC), 134.79 (ArC), 128.04 (ArC), 21.29 ( $\text{CH}_3$ ), 18.62 ( $\text{CH}_2$ ), 12.76 ( $\text{CH}_3$ ).

#### 8.2.18. Synthesis of (3,5-dimethylphenyl)(5-ethyl-2-(2-hydroxyethyl)-2H-1,2,3-triazol-4-yl)methanone (55)

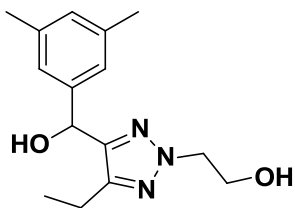


2-bromoethanol (100  $\mu\text{L}$ , 1.61 mmol) was added to a mixture of **54** (245 mg, 1.07 mmol) and  $\text{K}_2\text{CO}_3$  (295 mg, 2.14 mmol) in DMF (5 mL) at  $-8^\circ\text{C}$ . The reaction was allowed to warm to room temperature and was left to carried out for 18 h. Once completed the reaction mixture was quenched with distilled water and extracted with EtOAc. The organic layer was washed with brine and dried over  $\text{MgSO}_4$  and then concentrated *in vacuo*. The crude material was purified by silica gel column chromatography (20% EtOAc/Hexane - 60% EtOAc/Hexane) to yield the product as a yellow solid (197 mg, 0.72 mmol, 68%). ( $R_f$  = 0.30, 40% EtOAc/Hexane).

**$^1\text{H}$  NMR (300 MHz,  $\text{CDCl}_3$ )**  $\delta$  7.74 (dd,  $J$  = 1.4, 0.8 Hz, 2H, ArH), 7.25 (d,  $J$  = 0.7 Hz, 1H, ArH), 4.66 - 4.58 (m, 2H,  $\text{CH}_2$ ), 4.23 - 4.12 (m, 2H,  $\text{CH}_2$ ), 3.04 (q,  $J$  = 7.5 Hz, 2H,  $\text{CH}_2$ ), 2.83 (t,  $J$  = 6.5 Hz, 1H, OH), 2.41 (d,  $J$  = 0.6 Hz, 6H,  $\text{CH}_3$ ), 1.33 (t,  $J$  = 7.5 Hz, 3H,  $\text{CH}_3$ ). **HRMS-TOF MS ES+**:  $m/z$  [ $\text{M}+\text{H}$ ] $^+$  calcd for  $\text{C}_{15}\text{H}_{20}\text{N}_3\text{O}_2$ : 274.1556; found: 274.1555



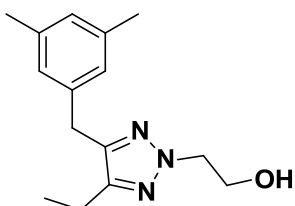
### 8.2.19. Synthesis of 2-(4-((3,5-dimethylphenyl)(hydroxyl)methyl)-5-ethyl-2H-1,2,3-triazol-2-yl)ethanol (**56**)



Triazole **55** (197 mg, 0.721 mmol) was dissolved in EtOH (5 mL). Sodium borohydride (109 mg, 2.88 mmol) was then added to the reaction mixture at 0 °C and the reaction was allowed to warm to room temperature and carried out for 4 h. The reaction mixture was then quenched with H<sub>2</sub>O and extracted twice with EtOAc. The organic layers were washed with brine and then dried over MgSO<sub>4</sub> before being concentrated *in vacuo* to yield the product as a white solid (177 mg, 0.648 mmol, 89%). No further purification was required. (*R*<sub>f</sub> = 0.10, 40% EtOAc/Hexane).

**<sup>1</sup>H NMR (300 MHz, CDCl<sub>3</sub>)** δ 6.99 (s, 2H, ArH), 6.93 (s, 1H, ArH), 5.87 (d, J = 4.6 Hz, 1H, CHOH), 4.52 - 4.43 (m, 2H, CH<sub>2</sub>), 4.07 (dd, J = 9.9, 6.1 Hz, 2H, CH<sub>2</sub>), 3.06 (d, J = 6.4 Hz, 1H, OH), 2.63 (d, J = 4.8 Hz, 1H, OH), 2.51 (q, J = 7.6 Hz, 2H, CH<sub>2</sub>), 2.30 (d, J = 0.5 Hz, 6H, CH<sub>3</sub>), 1.12 (t, J = 7.6 Hz, 3H, CH<sub>3</sub>). **<sup>13</sup>C NMR (75 MHz, CDCl<sub>3</sub>)** δ 141.49 (NCC), 138.17 (ArC), 130.30 (ArC), 129.65 (ArC), 124.21 (ArC), 69.18 (CHOH), 61.07 (CH<sub>2</sub>), 56.38 (CH<sub>2</sub>), 21.33 (CH<sub>3</sub>), 18.34 (CH<sub>2</sub>), 13.17 (CH<sub>3</sub>).

### 8.2.20. Synthesis of 2-(4-(3,5-dimethylbenzyl)-5-ethyl-2H-1,2,3-triazol-2-yl)ethanol (**47**)

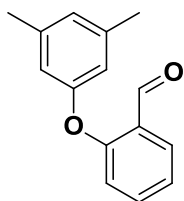


Trifluoroacetic acid (1 mL) was added to a suspension of **56** (177 mg, 0.648 mmol) in triethylsilane (1.2 mL, 7.2 mmol). The reaction was carried out for two h at room temperature, after which the reaction mixture was quenched with sodium bicarbonate solution and extracted twice with EtOAc. The organic layer was washed with brine, dried over MgSO<sub>4</sub>, concentrated *in vacuo* and then purified by silica gel chromatography (20% EtOAc/Hexane - 60% EtOAc/Hexane) to yield the product as a white solid (105 mg, 405 μmol, 63%). (*R*<sub>f</sub> = 0.42, 70% EtOAc/Hexane).

**Mp** 63-65 °C. **<sup>1</sup>H NMR (300 MHz, CDCl<sub>3</sub>)** δ 6.86 (s, 1H, ArH), 6.82 (d, J = 0.6 Hz, 2H, ArH), 4.51 - 4.45 (m, 2H, CH<sub>2</sub>), 4.12 - 4.04 (m, 2H, CH<sub>2</sub>), 3.92 (s, 2H, CH<sub>2</sub>), 3.24 (d, J = 6.5 Hz, 1H, OH), 2.56 (q, J = 7.6 Hz, 2H, CH<sub>2</sub>), 2.29 (d, J = 0.5 Hz, 6H, CH<sub>3</sub>), 1.18 (t, J = 7.6 Hz, 3H, CH<sub>3</sub>). **<sup>13</sup>C NMR (75 MHz, CDCl<sub>3</sub>)** δ 147.41 (CCN), 144.17 (CCN), 138.48 (ArC), 138.03 (ArC), 128.04 (ArC), 126.25 (ArC), 61.18 (CH<sub>2</sub>), 56.09 (CH<sub>2</sub>), 30.79 (CH<sub>2</sub>), 21.26 (CH<sub>3</sub>), 18.11 (CH<sub>2</sub>), 13.24 (CH<sub>3</sub>). **HRMS-TOF MS ES<sup>+</sup>: *m/z* [M+H]<sup>+</sup>** calcd for C<sub>15</sub>H<sub>22</sub>N<sub>3</sub>O: 260.1763; found: 260.1769

### 8.3. Experimental Procedures Pertaining to Chapter 4

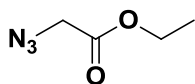
#### 8.3.1. Synthesis of 2-(3,5-dimethylphenoxy)benzaldehyde (69)



Dioxane (20 mL) was added to a Schlenk tube and degassed for approximately 10 min. To this was added 2-bromobenzaldehyde (3.2 mL, 27 mmol), 3,5-dimethylphenol (13.2 g, 108 mmol), N,N-dimethylglycine hydrochloride (1.13g, 8.10 mmol), cesium carbonate (13.2 g, 40.5 mmol) and copper iodide (516 mg, 2.71 mmol). The reaction mixture was heated to 97 °C and carried out for 43 h. The reaction mixture was then cooled to room temperature and then diluted with EtOAc and washed with a cold 1 N NaOH solution. The NaOH solution was removed and the organic layer was washed with brine. The organic phase was removed *in vacuo* and the residue was purified on silica gel by column chromatography (3% EtOAc/Hexane - 10% EtOAc/Hexane) to yield a yellow oil (4.10 g, 18.1 mmol, 67%). ( $R_f$  = 0.52, 20% EtOAc/Hexane).

$^1\text{H NMR}$  (300 MHz,  $\text{CDCl}_3$ )  $\delta$  10.53 (s, 1H, CHO), 7.96 (dd,  $J$  = 7.8, 1.4 Hz, 1H, ArH), 7.53 (ddd,  $J$  = 9.8, 8.2, 1.8 Hz, 1H, ArH), 7.23 - 7.15 (m, 1H, ArH), 6.93 (d,  $J$  = 8.4 Hz, 1H, ArH), 6.85 (s, 1H, ArH), 6.71 (s, 2H, ArH), 2.34 (d,  $J$  = 0.5 Hz, 6H,  $\text{CH}_3$ ).  $^{13}\text{C NMR}$  (75 MHz,  $\text{CDCl}_3$ )  $\delta$  189.46 (CHO), 160.22 (ArC), 156.37 (ArC), 140.00 (ArC), 135.71 (ArC), 128.26 (ArC), 126.83 (ArC), 126.03 (ArC), 123.09 (ArC), 118.64 (ArC), 117.04 (ArC), 21.31 ( $\text{CH}_3$ ). HRMS-TOF MS ES+:  $m/z$  [M+H] $^+$  calcd for  $\text{C}_{15}\text{H}_{15}\text{O}_2$ : 227.1072; found: 227.1076

#### 8.3.2. Synthesis of ethyl azidoacetate (64)

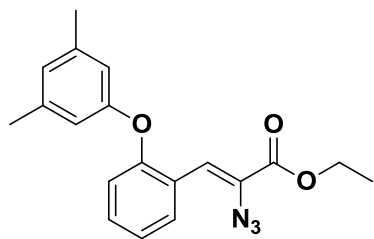


Ethyl chloroacetate (0.90 mL, 8.2 mmol) and tetrabutylammonium hydrogensulfate (277 mg, 0.816 mmol) were added to sodium azide (1.06 g, 16.3 mmol) suspended in a 1:1 mixture of dichloromethane (10 mL) and distilled water (10 mL). The reaction mixture was carried out for 18 h at room temperature. The aqueous layer was separated from the organic layer and washed with dichloromethane. The organic layers were combined and dried over  $\text{MgSO}_4$ . The solvent was removed *in vacuo* and no further purification was required. This reaction yielded a brown oil (929 mg, 7.20 mmol, 89%). ( $R_f$  = 0.47, 20% EtOAc/Hexane).

The spectroscopic data for this product correlated well with the literature.<sup>136</sup>

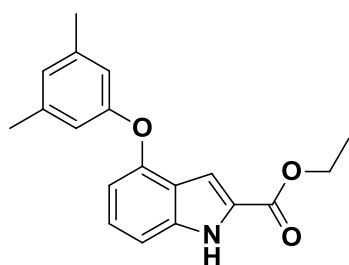
$^1\text{H NMR}$  (300 MHz,  $\text{CDCl}_3$ )  $\delta$  4.23 (q, 2H,  $\text{CH}_2$ ), 3.86 (s, 2H,  $\text{CH}_2$ ), 1.28 (t, 3H,  $\text{CH}_3$ ).  $^{13}\text{C NMR}$  (75 MHz,  $\text{CDCl}_3$ )  $\delta$  168.25 (CO), 61.75 ( $\text{CH}_2$ ), 50.24 ( $\text{CH}_2$ ), 14.00 ( $\text{CH}_3$ ).



**8.3.3. Synthesis of (Z)-ethyl 2-azido-3-(2-(3,5-dimethylphenoxy)phenyl)acrylate (68)**

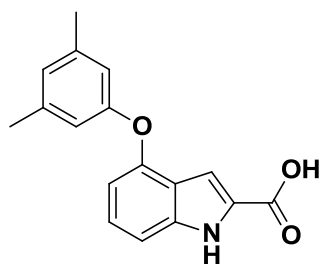
Sodium (364 mg, 15.8 mmol) was added to stirring ethanol (10 mL). Once all the sodium had dissolved, ethyl azidoacetate (2.28 g, 17.7 mmol) and ethyl trifluoroacetate (2.1 mL, 15 mmol) in a 1:2 mixture of EtOH (2 mL) and THF (4 mL) were added slowly dropwise at -8 °C. After which, benzaldehyde **69** (1.00 g, 4.42 mmol) in EtOH (2 mL) and THF (4 mL) was added dropwise at -8 °C. The reaction was allowed to carried out for 18 h at room temperature. The solvent was then removed *in vacuo*. The resulting residue was quenched with saturated ammonium chloride solution and extracted with EtOAc. The organic solvent was dried over MgSO<sub>4</sub>, concentrated *in vacuo*, and purified on silica gel by column chromatography (5% EtOAc/Hexane) to yield a yellow solid (969 mg, 2.87 mmol, 65%). (*R<sub>f</sub>* = 0.61, 20% EtOAc/Hexane).

**<sup>1</sup>H NMR (400 MHz, CDCl<sub>3</sub>)** δ 8.32 - 8.26 (m, 1H, ArH), 7.35 (s, 1H, CHCN), 7.29 - 7.22 (m, 1H, ArH), 7.13 (t, *J* = 7.5 Hz, 1H, ArH), 6.84 (t, *J* = 8.2 Hz, 1H, ArH), 6.76 (s, 1H, ArH), 6.61 (s, 2H, ArH), 4.33 (q, *J* = 7.1 Hz, 2H, CH<sub>2</sub>), 2.29 (s, 6H, CH<sub>3</sub>), 1.35 (dd, *J* = 7.5, 6.7 Hz, 3H, CH<sub>3</sub>). **<sup>13</sup>C NMR (101 MHz, CDCl<sub>3</sub>)** δ 163.79 (CO), 157.29 (ArC), 155.98 (ArC), 139.94 (ArC), 130.76 (ArC), 130.85 (ArC), 126.35 (ArC), 125.51 (ArC), 124.82 (CCN<sub>3</sub>), 123.15 (CCHC), 119.06 (ArC), 118.56 (ArC), 116.88 (ArC), 62.41 (CH<sub>2</sub>), 21.52 (CH<sub>3</sub>), 14.38 (CH<sub>3</sub>). **HRMS-TOF MS ES<sup>+</sup>: *m/z* [M+Na]<sup>+</sup>** calcd for C<sub>19</sub>H<sub>19</sub>N<sub>3</sub>O<sub>3</sub>Na: 360.1324; found: 360.1314

**8.3.4. Synthesis of ethyl 4-(3,5-dimethylphenoxy)-1H-indole-2-carboxylate (77)**

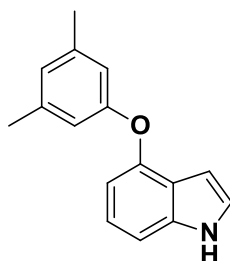
**68** (1.52 g, 4.51 mmol) was dissolved in toluene (10 mL) and added slowly dropwise to toluene (30 mL) stirred at 130 °C under reflux. The reaction was allowed to carried out for 18 h, after which the reaction was cooled to room temperature. The toluene was removed *in vacuo* and the residue was purified on silica gel by column chromatography (5% EtOAc/Hexane) to yield the product as a yellow solid (965 mg, 3.12 mmol, 69%). (*R<sub>f</sub>* = 0.40, 20% EtOAc/Hexane).

**Mp** 135-137 °C. **<sup>1</sup>H NMR (300 MHz, CDCl<sub>3</sub>)** δ 8.94 (s, 1H, NH), 7.25 (ddd, *J* = 9.6, 6.1, 5.2 Hz, 2H, ArH), 7.18 (dt, *J* = 8.3, 1.0 Hz, 1H, ArH), 6.78 (d, *J* = 0.7 Hz, 1H, ArH), 6.71 (d, *J* = 0.6 Hz, 2H, ArH), 6.63 (dd, *J* = 7.4, 1.0 Hz, 1H, ArH), 4.46 - 4.36 (m, 2H, CH<sub>2</sub>), 2.30 (d, *J* = 0.6 Hz, 6H, CH<sub>3</sub>), 1.47 - 1.36 (m, 3H, CH<sub>3</sub>). **<sup>13</sup>C NMR (75 MHz, CDCl<sub>3</sub>)** δ 162.01 (CO), 157.38 (ArC), 151.95 (ArC), 139.72 (ArC), 138.81 (ArC), 127.22 (ArC), 126.32 (ArC), 125.24 (ArC), 120.86 (ArC), 116.62 (ArC), 108.64 (ArC), 107.16 (ArC), 106.42 (ArC), 61.25 (CH<sub>2</sub>), 21.54 (CH<sub>3</sub>), 14.59 (CH<sub>3</sub>). **HRMS-TOF MS ES<sup>+</sup>: *m/z* [M+H]<sup>+</sup>** calcd for C<sub>19</sub>H<sub>20</sub>NO<sub>3</sub>: 310.1443; found: 310.1444

**8.3.5. Synthesis of 4-(3,5-dimethylphenoxy)-1H-indole-2-carboxylic acid (88)**

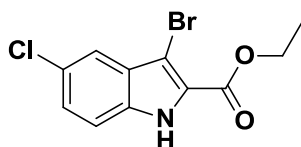
KOH (126 mg, 2.25 mmol) was added to a mixture of **77** (231 mg, 0.75 mmol) in EtOH (10 mL) and the reaction was allowed to stir at room temperature for 24 h. The solvent was then removed *in vacuo* and the residue was taken up in DCM and washed with water. The aqueous layer was then acidified with HCl and extracted with EtOAc. The organic layer was then washed with brine and dried over MgSO<sub>4</sub>. The organic layer was then once again concentrated *in vacuo* to afford **88** as a yellow solid (201 mg, 0.72 mmol, 95%).

**<sup>1</sup>H NMR (300 MHz, DMSO)** δ 11.94 (s, 1H, NH), 7.27 - 7.16 (m, 2H, ArH), 6.81 (d, *J* = 2.2 Hz, 1H, ArH), 6.77 (s, 1H, ArH), 6.64 (s, 2H, ArH), 6.57 (dd, *J* = 6.5, 1.9 Hz, 1H, ArH), 2.23 (s, 6H, CH<sub>3</sub>). **HRMS-TOF MS ES+**: *m/z* [M+H]<sup>+</sup> calcd for C<sub>17</sub>H<sub>16</sub>NO<sub>3</sub>: 282.1130; found: 282.1122

**8.5.6. Synthesis of 4-(3,5-dimethylphenoxy)-1H-indole (89)**

A catalytic amount of cupric oxide (5.00 mg, 0.063 mmol) was added to a solution of **88** (200 mg, 0.63 mmol) in quinoline (6 mL) and the reaction mixture was heated to 200 °C. The reaction was allowed to be carried out for 18 h after which the reaction was cooled and diluted with EtOAc. The organic phase was washed with dilute HCl solution, washed with water and finally with brine. The organic phase was then dried over MgSO<sub>4</sub> and concentrated *in vacuo*.

**<sup>1</sup>H NMR (300 MHz, CDCl<sub>3</sub>)** δ 8.22 (s, 1H, NH), 7.23 - 7.11 (m, 3H, ArH), 6.75 (dd, *J* = 1.4, 0.7 Hz, 1H, ArH), 6.72 (d, *J* = 0.6 Hz, 2H, ArH), 6.52 (ddd, *J* = 3.1, 2.1, 0.9 Hz, 1H, ArH), 2.30 (d, *J* = 0.6 Hz, 5H, CH<sub>3</sub>). **<sup>13</sup>C NMR (101 MHz, CDCl<sub>3</sub>)** δ 157.98 (ArC), 150.30 (ArC), 139.53 (ArC), 138.15 (ArC), 124.70 (ArC), 123.69 (ArC), 122.84 (ArC), 120.82 (ArC), 116.29 (ArC), 108.89 (ArC), 106.83 (ArC), 100.44 (ArC), 21.55 (CH<sub>3</sub>).

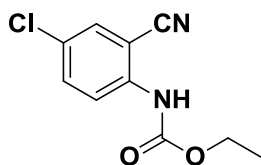
**8.4. Experimental Procedures Pertaining to Chapter 5****8.4.1. Synthesis of ethyl 3-bromo-5-chloro-1H-indole-2-carboxylate (99)**

*n*-Bromosuccinamide (191 mg, 1.07 mmol) was added to ethyl 5-chloro-2-indolecarboxylate (200 mg, 0.89 mmol) in THF (20 mL) at 0 °C. The reaction was carried out for 18 h after which the reaction mixture was quenched with water. The aqueous layer was then washed with EtOAc and the organic phase was then separated and dried over MgSO<sub>4</sub> and concentrated *in vacuo*. The crude residue was purified by silica gel column chromatography (5% - 40% EtOAc/Hexane) to yield the product as a yellow powder (214 mg, 0.705 mmol, 79%). (*R*<sub>f</sub> = 0.31, 20% EtOAc/Hexane).

**Mp** 192-194 °C. **<sup>1</sup>H NMR (300 MHz, DMSO)** δ 12.47 (s, 1H, NH), 7.58 - 7.55 (m, 1H, ArH), 7.53 (d, *J* = 0.6 Hz, 1H, ArH), 7.40 (dd, *J* = 8.8, 2.1 Hz, 1H, ArH), 4.41 (q, *J* = 7.1 Hz, 2H, CH<sub>2</sub>), 1.40 (t, *J* = 7.1 Hz, 3H, CH<sub>3</sub>). **<sup>13</sup>C NMR (75 MHz, DMSO)** δ 165.06 (CO), 139.47 (ArC), 133.00 (ArC), 131.46

(ArC), 131.08 (ArC), 130.65 (ArC), 124.28 (ArC), 120.23 (ArC), 100.18 (ArCBr), 66.29 (CH<sub>2</sub>), 19.43 (CH<sub>3</sub>). **HRMS-TOF MS ES<sup>+</sup>: m/z [M+H]<sup>+</sup>** calcd for C<sub>11</sub>H<sub>10</sub>NO<sub>2</sub>ClBr: 301.9583; found: 301.9591

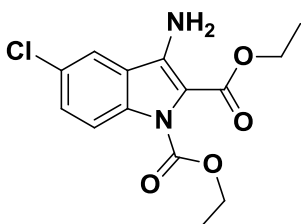
#### 8.4.2. Synthesis of ethyl (4-chloro-2-cyanophenyl)carbamate (115)



2-amino-5-chlorobenzonitrile (1.00 g, 6.55 mmol) was suspended in ethyl chloroformate (3.1 mL, 33 mmol) and heated to 93 °C. The reaction was carried out for 18 h, cooled to room temperature and then worked up with a saturated solution of sodium bicarbonate and EtOAc. No further purification was required. The reaction yielded an orange solid (1.25 g, 5.56 mmol, 85%). (*R<sub>f</sub>* = 0.30, 20% EtOAc/Hexane).

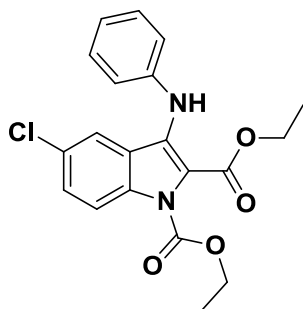
**Mp** 136-138 °C. **<sup>1</sup>H NMR (300 MHz, CDCl<sub>3</sub>) δ** 8.29 - 8.22 (m, 1H, ArH), 7.59 - 7.52 (m, 2H, ArH), 7.13 (s, 1H, NH), 4.29 (q, *J* = 7.1 Hz, 2H, CH<sub>2</sub>), 1.36 (t, *J* = 7.1 Hz, 3H, CH<sub>3</sub>). **<sup>13</sup>C NMR (75 MHz, CDCl<sub>3</sub>) δ** 152.68 (CO), 139.68 (ArC), 134.47 (ArC), 131.44 (ArC), 128.14 (ArC), 120.59 (ArC), 117.64 (CCN), 115.11 (ArC), 62.27 (CH<sub>2</sub>), 14.37 (CH<sub>3</sub>). **HRMS-TOF MS ES<sup>+</sup>: m/z [M+H]<sup>+</sup>** calcd for C<sub>10</sub>H<sub>10</sub>N<sub>2</sub>O<sub>2</sub>Cl: 225.0431; found: 225.0426

#### 8.4.3. Synthesis of diethyl 3-amino-5-chloro-1*H*-indole-1,2-dicarboxylate (116)



Sodium hydride (107 mg, 4.45 mmol) was added to a stirring solution of ethyl (4-chloro-2-cyanophenyl)carbamate (500 mg, 2.23 mmol) at °C. The reaction was then allowed to stir for 1 hour before ethyl chloroacetate (0.24 mL, 2.2 mmol) was added dropwise at 0 °C. The reaction was allowed to warm to room temperature. After 18 h the reaction mixture was quenched with distilled water and then extracted twice with dichloromethane. The organic layer was washed with brine and dried over MgSO<sub>4</sub> before being concentrated *in vacuo*. The crude residue was purified by silica gel column chromatography (5% - 40% EtOAc/Hexane) to yield the product as a colourless oil (1.11g, 3.57 mmol, 82%). (*R<sub>f</sub>* = 0.20, 20% EtOAc/Hexane).

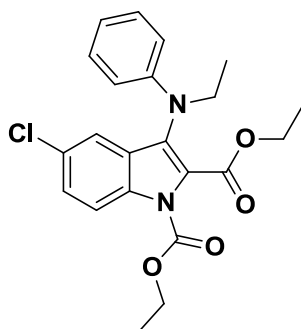
**Mp** 75-78 °C. **<sup>1</sup>H NMR (300 MHz, CDCl<sub>3</sub>) δ** 7.90 (dd, *J* = 8.9, 0.5 Hz, 1H, ArH), 7.42 (dd, *J* = 2.1, 0.5 Hz, 1H, ArH), 7.33 (dd, *J* = 8.9, 2.1 Hz, 1H, ArH), 5.07 (s, 2H, NH<sub>2</sub>), 4.30 (m, *J* = 10.3, 7.1 Hz, 4H, CH<sub>2</sub>), 1.35 - 1.28 (m, 6H, CH<sub>3</sub>). **<sup>13</sup>C NMR (75 MHz, CDCl<sub>3</sub>) δ** 162.55 (CO), 151.83 (CO), 140.31 (ArC), 136.64 (ArC), 129.09 (ArC), 128.33 (ArC), 123.24 (ArC), 118.65 (ArC), 116.74 (ArC), 108.34 (ArC), 63.42 (CH<sub>2</sub>), 60.49 (CH<sub>2</sub>), 14.50 (CH<sub>3</sub>), 14.24 (CH<sub>3</sub>). **HRMS-TOF MS ES<sup>+</sup>: m/z [M+H]<sup>+</sup>** calcd for C<sub>14</sub>H<sub>16</sub>N<sub>2</sub>O<sub>4</sub>Cl: 311.0799; found: 311.0802

**8.4.4. Synthesis of diethyl 5-chloro-3-(phenylamino)-1H-indole-1,2-dicarboxylate (117)**

Diethyl 3-amino-5-chloro-1H-indole-1,2-dicarboxylate (533 mg, 1.38 mmol) was taken up in toluene (5 mL) and degassed. Bromobenzene (0.22 mL, 2.1 mmol) was then added followed by the addition of Pd(dba)<sub>2</sub> (790 µg, 0.138 mmol), Xphos (132 mg, 0.276 mmol) and K<sub>3</sub>PO<sub>4</sub> (586 mg, 2.76 mmol). The reaction mixture was then added to 130 °C. As the reaction mixture heated up it changed colour from yellow to red, indicative of a ligand exchange occurring with the palladium catalyst. The reaction was carried out for 2 days. The reaction mixture was allowed to cool to room

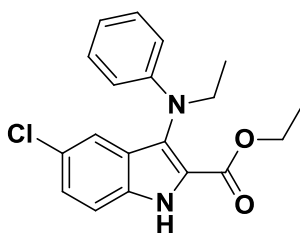
temperature, carried out through celite and then concentrated *in vacuo*. The residue was then purified by silica gel column chromatography (5% - 20% EtOAc/Hexane) to yield the product as a yellow solid (239 mg, 0.618 mmol, 32%). (*R*<sub>f</sub> = 0.32, 20% EtOAc/Hexane).

**<sup>1</sup>H NMR (300 MHz, CDCl<sub>3</sub>)** δ 8.05 (dd, *J* = 9.0, 0.5 Hz, 1H, *ArH*), 7.72 (s, 1H, *NH*), 7.40 (ddd, *J* = 7.6, 6.5, 1.8 Hz, 2H, *ArH*), 7.36 - 7.29 (m, 2H, *ArH*), 7.21 (dd, *J* = 2.1, 0.5 Hz, 1H, *ArH*), 7.07 - 7.01 (m, 2H, *ArH*), 4.42 (m, *J* = 22.1, 7.1 Hz, 4H, *CH*<sub>2</sub>), 1.49 - 1.34 (m, 6H, *CH*<sub>3</sub>). **<sup>13</sup>C NMR (75 MHz, CDCl<sub>3</sub>)** δ 162.53 (CO), 141.41 (CO), 136.04 (ArC), 135.30 (ArC), 130.08 (ArC), 129.23 (ArC), 128.50 (ArC), 128.36 (ArC), 128.00 (ArC), 123.34 (ArC), 123.16 (ArC), 122.15 (ArC), 120.43 (ArC), 116.25 (ArC), 63.78 (CH<sub>2</sub>), 61.05 (CH<sub>2</sub>), 14.33 (CH<sub>3</sub>), 14.24 (CH<sub>3</sub>).

**8.4.5. Synthesis of diethyl 5-chloro-3-(ethyl(phenyl)amino)-1H-indole-1,2-dicarboxylate (118)**

Sodium *tert*-butoxide (82 mg, 0.85 mmol) was added to **117** (200 mg, 0.568 mmol) in DMF (3 mL) at 0 °C. Ethyl iodide (90 µL, 1.1 mmol) was added to the reaction mixture which was then allowed to warm to room temperature. The reaction was left to carried out for 18 h and then diluted with EtOAc and quenched with water. The organic phase was separated, dried over MgSO<sub>4</sub> and concentrated *in vacuo*. The residue was then purified on silica using column chromatography (5% EtOAc/Hexane) to yield the product as a yellow oil (25 mg, 0.60 mmol, 11%). (*R*<sub>f</sub> = 0.61, 20% EtOAc/Hexane).

**<sup>1</sup>H NMR (300 MHz, CDCl<sub>3</sub>)** δ 7.50 (dd, *J* = 2.0, 0.6 Hz, 1H, *ArH*), 7.40 (dd, *J* = 8.9, 0.5 Hz, 1H, *ArH*), 7.35 - 7.30 (m, 1H, *ArH*), 7.18 - 7.10 (m, 2H, *ArH*), 6.72 - 6.64 (m, 1H, *ArH*), 6.60 - 6.53 (m, 2H, *ArH*), 4.61 (q, *J* = 7.1 Hz, 2H, *CH*<sub>2</sub>), 4.18 (q, *J* = 7.1 Hz, 2H, *CH*<sub>2</sub>), 3.77 (q, *J* = 7.1 Hz, 2H, *CH*<sub>2</sub>), 1.45 (td, *J* = 7.1, 4.4 Hz, 3H, *CH*<sub>3</sub>), 1.29 - 1.21 (m, 3H, *CH*<sub>3</sub>), 1.09 (t, *J* = 7.1 Hz, 3H, *CH*<sub>3</sub>). **<sup>13</sup>C NMR (75 MHz, CDCl<sub>3</sub>)** δ 161.17 (CO), 148.77 (CO), 148.65 (ArC), 135.00 (ArC), 128.84 (ArC), 128.04 (ArC), 126.48 (ArC), 126.07 (ArC), 125.99 (ArC), 124.74 (ArC), 119.83 (ArC), 116.43 (ArC), 112.35 (ArC), 111.53 (ArC), 60.70 (CH<sub>2</sub>), 46.72 (CH<sub>2</sub>), 40.23 (CH<sub>2</sub>), 15.75 (CH<sub>3</sub>), 13.86 (CH<sub>3</sub>), 13.34 (CH<sub>3</sub>).

**8.4.6. Synthesis of ethyl 5-chloro-3-(ethyl(phenyl)amino)-1H-indole-2-carboxylate (5)**

A mixture of **118** (25 mg, 0.060 mmol) and  $K_3PO_4$  (26 mg, 0.12 mmol) in EtOH (1 mL) was heated to 70 °C and allowed to be carried out for 3.5 h. The reaction was then cooled to room temperature and filtered over celite. The filtrate was then concentrated *in vacuo* and purified by silica gel column chromatography (5% EtOAc/Hexane - 20% EtOAc/Hexane) to yield the product as a yellow powder (22 mg, 0.64 mmol, quant.). ( $R_f$  = 0.31, 20% EtOAc/Hexane).

**Mp** 162-164 °C.  **$^1H$  NMR (400 MHz,  $CDCl_3$ )**  $\delta$  9.16 (s, 1H, NH), 7.48 - 7.22 (m, 3H, ArH), 7.14 (dd,  $J$  = 8.0, 7.4 Hz, 2H, ArH), 6.70 (dd,  $J$  = 7.2, 6.6 Hz, 1H, ArH), 6.62 (d,  $J$  = 8.6 Hz, 2H, ArH), 4.26 (dt,  $J$  = 14.0, 7.0 Hz, 2H,  $CH_2$ ), 3.80 (q,  $J$  = 7.1 Hz, 2H,  $CH_2$ ), 1.25 - 1.19 (m, 3H,  $CH_3$ ), 1.16 (q,  $J$  = 6.8 Hz, 3H,  $CH_3$ ).  **$^{13}C$  NMR (75 MHz,  $CDCl_3$ )**  $\delta$  161.33 (CO), 148.67 (ArC), 133.60 (ArC), 129.09 (ArC), 127.91 (ArC), 127.46 (ArC), 126.83 (ArC), 126.78 (ArC), 124.08 (ArC), 120.24 (ArC), 117.18 (ArC), 113.60 (ArC), 113.15 (ArC), 61.38 ( $CH_2$ ), 46.74 ( $CH_2$ ), 14.23 ( $CH_3$ ), 13.40 ( $CH_3$ ). **HRMS-TOF MS ES<sup>+</sup>:  $m/z$  [M+H]<sup>+</sup>** calcd for  $C_{19}H_{20}N_2O_2Cl$ : 343.1213; found: 343.1200

## Chapter 9: References

1. Gao, F.; Bailes, E.; Robertson, D. L.; Chen, Y.; Rodenburg, C. M.; Michael, S. F.; Cummins, L. B.; Arthur, L. O.; Peeters, M.; Shaw, G. M.; Sharp, P. M.; Hahn, B. H. Origin of HIV-1 in the chimpanzee *Pan troglodytes troglodytes*. *Nature* **1999**, 397, 436-441.
2. Barré-Sinoussi, F.; Chermann, J. C.; Rey, F.; Nugeyre, M. T.; Chamaret, S.; Gruest, J.; Dautuet, C.; Axler-Blin, C.; Vézinet-Brun, F.; Rouzioux, C.; Rozenbaum, W.; Montagnier, L. Isolation of a T-Lymphotropic Retrovirus from a Patient at Risk for Acquired Immune Deficiency Syndrome (AIDS). *Science* **1983**, 220, 868-871.
3. Gallo, R. C. The early years of HIV/AIDS. (Viewpoint: Historical Essay). *Science* **2002**, 298, 1728-1730.
4. Gallo, R. C. A reflection on HIV/AIDS research after 25 years. *Retrovirology* **2006**, 3, 72-7.
5. Gallo, R. C. M. D.; Montagnier, L. M. D. The Discovery of HIV as the Cause of AIDS. *The New England Journal of Medicine* **2003**, 349, 2283-2285.
6. Stangl, A. L.; Lloyd, J. K.; Brady, L. M.; Holland, C. E.; Baral, S. A systematic review of interventions to reduce HIV-related stigma and discrimination from 2002 to 2013: how far have we come? *Journal of the International AIDS Society* **2013**, 16, 18734-18747.
7. Gallo, R. C.; Montagnier, L. Historical essay: Prospects for the future. *Science* **2002**, 298, 1730-1731.
8. UNAIDS. *Global report: UNAIDS report on the global AIDS epidemic 2013*; Geneva, Switzerland, 2013.
9. Thurlow, J.; Gow, J.; George, G. HIV/AIDS, growth and poverty in KwaZulu-Natal and South Africa: an integrated survey, demographic and economy-wide analysis. *Journal of the International AIDS Society* **2009**, 12, 18-30.
10. WHO, U., UNAIDS. *Global update on HIV treatment 2013: Results, impact and opportunities*; Geneva, Switzerland, 2013.
11. Shattock, R. J.; Moore, J. P. Inhibiting sexual transmission of HIV-1 infection. *Nature reviews. Microbiology* **2003**, 1, 25-34.
12. Sattentau, Q. J. HIV gp120: double lock strategy foils host defences. *Structure* **1998**, 6, 945-949.
13. Freed, E. O. HIV-1 replication. *Somatic Cell and Molecular Genetics* **2000**, 26, 13-33.
14. Reynolds, C.; de Koning, C. B.; Pelly, S. C.; van Otterlo, W. A. L.; Bode, M. L. In search of a treatment for HIV - current therapies and the role of non-nucleoside reverse transcriptase inhibitors (NNRTIs). *Chemical Society Reviews* **2012**, 41, 4657-4670.
15. Kohl, N. E.; Emini, E. A.; Schleif, W. A.; Davis, L. J.; Heimbach, J. C.; Dixon, R. A. F.; Scolnick, E. M.; Sigal, I. S. Active Human Immunodeficiency Virus Protease is Required for Viral Infectivity. *Proceedings of the National Academy of Sciences of the United States of America* **1988**, 85, 4686-4690.
16. Wensing, A. M. J.; van Maarseveen, N. M.; Nijhuis, M. Fifteen years of HIV Protease Inhibitors: raising the barrier to resistance. *Antiviral Research* **2010**, 85, 59-74.
17. Coffin, J. M. HIV population dynamics in vivo: Implications for genetic variation, pathogenesis, and therapy. *Science* **1995**, 267, 483-489.
18. WHO. *Consolidated guidelines on the use of antiretroviral drugs for treating and preventing HIV infection: Recommendations for a public health approach*; Geneva, Switzerland, 2013.
19. De Clercq, E. Anti-HIV drugs: 25 compounds approved within 25 years after the discovery of HIV. *International Journal of Antimicrobial Agents* **2009**, 33, 307-320.



20. Goody, R. S.; Müller, B.; Restle, T. Factors contributing to the inhibition of HIV reverse transcriptase by chain-terminating nucleotides in vitro and in vivo. *FEBS Letters* **1991**, 291, 1-5.
21. Sneader, W. *Drug Discovery: A History*. 2006; p 1-468.
22. Yorchoan, M. The History of Zidovudine (AZT): Partnership and Conflict. <http://www.scribd.com/doc/92129927/The-History-of-Zidovudine-AZT-Partnership-and-Conflict>
23. Larder, B. A.; Kemp, S. D. Multiple mutations in HIV-1 reverse transcriptase confer high-level resistance to zidovudine (AZT). *Science* **1989**, 246, 1155-1158.
24. Mansky, L. M.; Bernard, L. C. 3'-Azido-3'-Deoxythymidine (AZT) and AZT-Resistant Reverse Transcriptase Can Increase the In Vivo Mutation Rate of Human Immunodeficiency Virus Type 1. *Journal of Virology* **2000**, 74, 9532-9539.
25. Flexner, C. HIV drug development: the next 25 years. *Nat Rev Drug Discov* **2007**, 6, 959-966.
26. Mehellou, Y.; De Clercq, E. Twenty-six years of anti-HIV drug discovery: Where do we stand and where do we go? *Journal of Medicinal Chemistry* **2010**, 53, 521-538.
27. Flexner, C.; Bate, G.; Kirkpatrick, P. Tipranavir. *Nature Reviews Drug Discovery* **2005**, 4, 955-956.
28. Di Santo, R. Inhibiting the HIV Integration Process: Past, Present, and the Future. *Journal of Medicinal Chemistry* **2013**, 57, 539-566.
29. Deeks, S. G.; Kar, S.; Gubernick, S. I.; Kirkpatrick, P. Raltegravir. *Nature Reviews Drug Discovery* **2008**, 7, 117-118.
30. Klibanov, O. M. Elvitegravir, an oral HIV integrase inhibitor, for the potential treatment of HIV infection. *Current Opinion in Investigational Drugs* **2009**, 10, 190-200.
31. Di Santo, R. Inhibiting the HIV integration process: Past, present, and the future. *Journal of Medicinal Chemistry* **2014**, 57, 539-566.
32. Osterholzer, D. A.; Goldman, M. Dolutegravir: A next-generation integrase inhibitor for treatment of HIV infection. *Clinical Infectious Diseases* **2014**, 59, 265-271.
33. Dando, T. M.; Perry, C. M. Enfuvirtide. *Drugs* **2003**, 63, 2755-2766.
34. Barmania, F.; Pepper, M. S. C-C chemokine receptor type five (CCR5): An emerging target for the control of HIV infection. *Applied & Translational Genomics* **2013**, 2, 3-16.
35. Kuritzkes, D.; Kar, S.; Kirkpatrick, P. Maraviroc. *Nature Reviews Drug Discovery* **2008**, 7, 15-16.
36. Kohlstaedt, L. A.; Wang, J.; Friedman, J. M.; Rice, P. A.; Steitz, T. A. Crystal Structure at 3.5 Å Resolution of HIV-1 Reverse Transcriptase Complexed with an Inhibitor. *Science* **1992**, 256, 1783-1790.
37. Das, K.; Clark, A. D.; Lewi, P. J.; Heeres, J.; de Jonge, M. R.; Koymans, L. M. H.; Vinkers, H. M.; Daeyaert, F.; Ludovici, D. W.; Kukla, M. J.; De Corte, B.; Kavash, R. W.; Ho, C. Y.; Ye, H.; Lichtenstein, M. A.; Andries, K.; Pauwels, R.; de Béthune, M.-P.; Boyer, P. L.; Clark, P.; Hughes, S. H.; Janssen, P. A. J.; Arnold, E. Roles of conformational and positional adaptability in structure-based design of TMC125-R165335 (etravirine) and related non-nucleoside reverse transcriptase inhibitors that are highly potent and effective against wild-type and drug-resistant HIV-1 variants. *Journal of Medicinal Chemistry* **2004**, 47, 2550-2560.
38. Prajapati, D. G.; Ramajayam, R.; Yadav, M. R.; Giridhar, R. The search for potent, small molecule NNRTIs: A review. *Bioorganic & Medicinal Chemistry* **2009**, 17, 5744-5762.
39. Sluis-Cremer, N.; Tachedjian, G. Mechanisms of inhibition of HIV replication by non-nucleoside reverse transcriptase inhibitors. *Virus Research* **2008**, 134, 147-156.
40. Lansdon, E. B.; Brendza, K. M.; Hung, M.; Wang, R.; Mukund, S.; Jin, D.; Birkus, G.; Kutty, N.; Liu, X. Crystal Structures of HIV-1 Reverse Transcriptase with Etravirine (TMC125) and Rilpivirine (TMC278): Implications for Drug Design. *Journal of Medicinal Chemistry* **2010**, 53, 4295-4299.

41. Ren, J.; Milton, J.; Weaver, K. L.; Short, S. A.; Stuart, D. I.; Stammers, D. K. Structural basis for the resilience of efavirenz (DMP-266) to drug resistance mutations in HIV-1 reverse transcriptase. *Structure* **2000**, *8*, 1089-1094.
42. Jochmans, D. Novel HIV-1 reverse transcriptase inhibitors. *Virus Research* **2008**, *134*, 171-185.
43. Gupta, R. K.; Pillay, D. HIV resistance and the developing world. *International Journal of Antimicrobial Agents* **2007**, *29*, 510-517.
44. Sarafianos, S. G.; Das, K.; Hughes, S. H.; Arnold, E. Taking aim at a moving target: designing drugs to inhibit drug-resistant HIV-1 reverse transcriptases. *Current Opinion in Structural Biology* **2004**, *14*, 716-730.
45. Hsiou, Y.; Ding, J.; Das, K.; Clark Jr, A. D.; Boyer, P. L.; Lewi, P.; Janssen, P. A. J.; Kleim, J.-P.; Rösner, M.; Hughes, S. H.; Arnold, E. The Lys103Asn mutation of HIV-1 RT: a novel mechanism of drug resistance. *Journal of Molecular Biology* **2001**, *309*, 437-445.
46. Ren, J.; Stammers, D. K. Structural basis for drug resistance mechanisms for non-nucleoside inhibitors of HIV reverse transcriptase. *Virus Research* **2008**, *134*, 157-170.
47. Fattorusso, C.; Gemma, S.; Butini, S.; Huleatt, P.; Catalanotti, B.; Persico, M.; De Angelis, M.; Fiorini, I.; Nacci, V.; Ramunno, A.; Rodriguez, M.; Greco, G.; Novellino, E.; Bergamini, A.; Marini, S.; Coletta, M.; Maga, G.; Spadari, S.; Campiani, G. Specific Targeting Highly Conserved Residues in the HIV-1 Reverse Transcriptase Primer Grip Region. Design, Synthesis, and Biological Evaluation of Novel, Potent, and Broad Spectrum NNRTIs with Antiviral Activity. *Journal of Medicinal Chemistry* **2005**, *48*, 7153-7165.
48. Jacobo-Molina, A.; Ding, J.; Nanni, R. G.; Clark, A. D., Jr.; Lu, X.; Tantillo, C.; Williams, R. L.; Kamer, G.; Ferris, A. L.; Clark, P.; Amnon, H.; Hughes, S. H.; Arnold, E. Crystal Structure of Human Immunodeficiency Virus Type 1 Reverse Transcriptase Complexed with Double-Stranded DNA at 3.0 Å Resolution Shows Bent DNA. *Proceedings of the National Academy of Sciences of the United States of America* **1993**, *90*, 6320-6324.
49. Pelemans, H.; Esnouf, R.; De Clercq, E.; Balzarini, J. Mutational Analysis of Trp-229 of Human Immunodeficiency Virus Type 1 Reverse Transcriptase (RT) Identifies This Amino Acid Residue as a Prime Target for the Rational Design of New Non-Nucleoside RT Inhibitors. *Molecular Pharmacology* **2000**, *57*, 954-960.
50. Pelemans, H.; Esnouf, R.; Min, K.-L.; Parniak, M.; De Clercq, E.; Balzarini, J. Mutations at Amino Acid Positions 63, 189, and 396 of Human Immunodeficiency Virus Type 1 Reverse Transcriptase (RT) Partially Restore the DNA Polymerase Activity of a TRP229TYR Mutant RT. *Virology* **2001**, *287*, 143-150.
51. Mowbray, C. E.; Burt, C.; Corbau, R.; Perros, M.; Tran, I.; Stuppel, P. A.; Webster, R.; Wood, A. Pyrazole NNRTIs 1: Design and initial optimisation of a novel template. *Bioorganic and Medicinal Chemistry Letters* **2009**, *19*, 5599-5602.
52. Vernazza, P.; Wang, C.; Pozniak, A.; Weil, E.; Pulik, P.; Cooper, D. A.; Kaplan, R.; Lazzarin, A.; Valdez, H.; Goodrich, J.; Mori, J.; Craig, C.; Tawadrous, M. Efficacy and safety of lersivirine (UK-453,061) versus efavirenz in antiretroviral treatment-naive HIV-1-infected patients: Week 48 primary analysis results from an ongoing, multicenter, randomized, double-blind, phase IIb trial. *Journal of Acquired Immune Deficiency Syndromes* **2013**, *62*, 171-179.
53. Corbau, R.; Mori, J.; Phillips, C.; Fishburn, L.; Martin, A.; Mowbray, C.; Panton, W.; Smith-Burchnell, C.; Thornberry, A.; Ringrose, H.; Knöchel, T.; Irving, S.; Westby, M.; Wood, A.; Perros, M. Lersivirine, a nonnucleoside reverse transcriptase inhibitor with activity against drug-resistant human immunodeficiency virus type 1. *Antimicrobial Agents and Chemotherapy* **2010**, *54*, 4451-4463.
54. Jones, L. H.; Allan, G.; Corbau, R.; Middleton, D. S.; Mowbray, C. E.; Newman, S. D.; Phillips, C.; Webster, R.; Westby, M. Comparison of the Non-Nucleoside Reverse Transcriptase Inhibitor Lersivirine with its Pyrazole and Imidazole Isomers. *Chemical Biology & Drug Design* **2011**, *77*, 393-397.



55. Tucker, T. J.; Sisko, J. T.; Tynebor, R. M.; Williams, T. M.; Felock, P. J.; Flynn, J. A.; Lai, M.-T.; Liang, Y.; McGaughey, G.; Liu, M.; Miller, M.; Moyer, G.; Munshi, V.; Perlow-Poehnel, R.; Prasad, S.; Reid, J. C.; Sanchez, R.; Torrent, M.; Vacca, J. P.; Wan, B.-L.; Yan, Y. Discovery of 3-{5-[(6-Amino-1H-pyrazolo[3,4-b]pyridine-3-yl)methoxy]-2-chlorophenoxy}-5-chlorobenzonitrile (MK-4965): A Potent, Orally Bioavailable HIV-1 Non-Nucleoside Reverse Transcriptase Inhibitor with Improved Potency against Key Mutant Viruses. *Journal of Medicinal Chemistry* **2008**, *51*, 6503-6511.
56. Côté, B.; Burch, J. D.; Asante-Appiah, E.; Bayly, C.; Bédard, L.; Blouin, M.; Campeau, L. C.; Cauchon, E.; Chan, M.; Chefson, A.; Coulombe, N.; Cromlish, W.; Debnath, S.; Deschênes, D.; Dupont-Gaudet, K.; Falguyret, J. P.; Forget, R.; Gagné, S.; Gauvreau, D.; Girardin, M.; Guiral, S.; Langlois, E.; Li, C. S.; Nguyen, N.; Papp, R.; Plamondon, S.; Roy, A.; Roy, S.; Selinotakis, R.; St-Onge, M.; Ouellet, S.; Tawa, P.; Truchon, J. F.; Vacca, J.; Wrona, M.; Yan, Y.; Ducharme, Y. Discovery of MK-1439, an orally bioavailable non-nucleoside reverse transcriptase inhibitor potent against a wide range of resistant mutant HIV viruses. *Bioorganic and Medicinal Chemistry Letters* **2014**, *24*, 917-922.
57. Jones, L. H.; Allan, G.; Barba, O.; Burt, C.; Corbau, R.; Dupont, T.; Knöchel, T.; Irving, S.; Middleton, D. S.; Mowbray, C. E.; Perros, M.; Ringrose, H.; Swain, N. A.; Webster, R.; Westby, M.; Phillips, C. Novel indazole non-nucleoside reverse transcriptase inhibitors using molecular hybridization based on crystallographic overlays. *Journal of Medicinal Chemistry* **2009**, *52*, 1219-1223.
58. Li, D.; Zhan, P.; De Clercq, E.; Liu, X. Strategies for the design of HIV-1 non-nucleoside reverse transcriptase inhibitors: lessons from the development of seven representative paradigms. *Journal of Medicinal Chemistry* **2012**, *55*, 3595-3613.
59. Müller, R.; Mulani, I.; Basson, A. E.; Pribut, N.; Hassam, M.; Morris, L.; van Otterlo, W. A. L.; Pelly, S. C. Novel indole based NNRTIs with improved potency against wild type and resistant HIV. *Bioorganic & Medicinal Chemistry Letters* **2014**, *24*, 4376-4380.
60. Agalave, S. G.; Maujan, S. R.; Pore, V. S. Click Chemistry: 1,2,3-Triazoles as Pharmacophores. *Chemistry – An Asian Journal* **2011**, *6*, 2696-2718.
61. Gomtsyan, A. Heterocycles in drugs and drug discovery. *Chemistry of Heterocyclic Compounds* **2012**, *48*, 8-10.
62. Kharb, R.; Sharma, P. C.; Yar, M. S. Pharmacological significance of triazole scaffold. *Journal of Enzyme Inhibition and Medicinal Chemistry* **2011**, *26*, 1-21.
63. Kolb, H. C.; Sharpless, K. B. The growing impact of click chemistry on drug discovery. *Drug Discovery Today* **2003**, *8*, 1128-1137.
64. Moyle, G.; Boffito, M.; Stoehr, A.; Rieger, A.; Shen, Z.; Manhard, K.; Sheedy, B.; Hingorani, V.; Raney, A.; Nguyen, M.; Nguyen, T.; Ong, V.; Yeh, L.-T.; Quart, B. Phase 2a Randomized Controlled Trial of Short-Term Activity, Safety, and Pharmacokinetics of a Novel Nonnucleoside Reverse Transcriptase Inhibitor, RDEA806, in HIV-1-Positive, Antiretroviral-Naïve Subjects. *Antimicrobial Agents and Chemotherapy* **2010**, *54*, 3170-3178.
65. Kolb, H. C.; Finn, M. G.; Sharpless, K. B. Click Chemistry: Diverse Chemical Function from a Few Good Reactions. *Angewandte Chemie International Edition* **2001**, *40*, 2004-2021.
66. Bunz, U. F. Adventures of an occasional click chemist. *Synlett* **2013**, *24*, 1899-1909.
67. Nwe, K.; Brechbiel, M. W. Growing applications of "click chemistry" for bioconjugation in contemporary biomedical research. *Cancer Biotherapy and Radiopharmaceuticals* **2009**, *24*, 289-302.
68. Campbell-Verduyn, L.; Elsinga, P. H.; Mirfeizi, L.; Dierckx, R. A.; Feringa, B. L. Copper-free 'click': 1,3-dipolar cycloaddition of azides and arynes. *Organic and Biomolecular Chemistry* **2008**, *6*, 3461-3463.
69. Tahtaoui, C.; Parrot, I.; Klotz, P.; Guillier, F.; Galzi, J.-L.; Hibert, M.; Ilien, B. Fluorescent Pirenzepine Derivatives as Potential Bitopic Ligands of the Human M1 Muscarinic Receptor. *Journal of Medicinal Chemistry* **2004**, *47*, 4300-4315.

70. Appel, R. Tertiary Phosphane/Tetrachloromethane, a Versatile Reagent for Chlorination, Dehydration, and P–N Linkage. *Angewandte Chemie International Edition in English* **1975**, 14, 801-811.
71. van Kalker, H. A.; van Delft, F. L.; Rutjes, F. P. J. T. Catalytic Appel reactions. *Pure and Applied Chemistry* **2013**, 85, 817-828.
72. Vidya Sagar Reddy, G.; Venkat Rao, G.; Subramanyam, R. V. K.; Iyengar, D. S. A new novel and practical one pot methodology for conversion of alcohols to amines. *Synthetic Communications* **2000**, 30, 2233-2237.
73. Rostovtsev, V. V.; Green, L. G.; Fokin, V. V.; Sharpless, K. B. A Stepwise Huisgen Cycloaddition Process: Copper(I)-Catalyzed Regioselective “Ligation” of Azides and Terminal Alkynes. *Angewandte Chemie International Edition* **2002**, 41, 2596-2599.
74. Tornøe, C. W.; Christensen, C.; Meldal, M. Peptidotriazoles on solid phase: [1,2,3]-Triazoles by regiospecific copper(I)-catalyzed 1,3-dipolar cycloadditions of terminal alkynes to azides. *Journal of Organic Chemistry* **2002**, 67, 3057-3064.
75. Bock, V. D.; Hiemstra, H.; van Maarseveen, J. H. Cu-Catalyzed Alkyne–Azide “Click” Cycloadditions from a Mechanistic and Synthetic Perspective. *European Journal of Organic Chemistry* **2006**, 2006, 51-68.
76. Meldal, M.; Tomøe, C. W. Cu-catalyzed azide - Alkyne cycloaddition. *Chemical Reviews* **2008**, 108, 2952-3015.
77. Hein, C. D.; Liu, X. M.; Wang, D. Click chemistry, a powerful tool for pharmaceutical sciences. *Pharmaceutical Research* **2008**, 25, 2216-2230.
78. Bernard, S.; Defoy, D.; Dory, Y. L.; Klarskov, K. Efficient synthesis of nevirapine analogs to study its metabolic profile by click fishing. *Bioorganic & Medicinal Chemistry Letters* **2009**, 19, 6127-6130.
79. Claridge, T. D. W. Chapter 8 - Correlations through space: The nuclear Overhauser effect. In *Tetrahedron Organic Chemistry Series*, Timothy, D. W. C., Ed. Elsevier: 2009; Vol. Volume 27, 247-302.
80. Gupta, R. K.; Kohli, A.; McCormick, A. L.; Towers, G. J.; Pillay, D.; Parry, C. M. Full-length HIV-1 gag determines protease inhibitor susceptibility within in-vitro assays. *AIDS* **2010**, 24, 1651-1655.
81. Parry, C. M.; Kohli, A.; Boinett, C. J.; Towers, G. J.; McCormick, A. L.; Pillay, D. Gag determinants of fitness and drug susceptibility in protease inhibitor-resistant human immunodeficiency virus type 1. *Journal of Virology* **2009**, 83, 9094-9101.
82. Ehlers, I.; Maity, P.; Aubé, J.; König, B. Modular synthesis of triazole-containing triaryl  $\alpha$ -helix mimetics. *European Journal of Organic Chemistry* **2011**, 2474-2490.
83. Ohmatsu, K.; Kiyokawa, M.; Ooi, T. Chiral 1,2,3-Triazoliums as New Cationic Organic Catalysts with Anion-Recognition Ability: Application to Asymmetric Alkylation of Oxindoles. *Journal of the American Chemical Society* **2011**, 133, 1307-1309.
84. Zhang, L.; Chen, X.; Xue, P.; Sun, H. H. Y.; Williams, I. D.; Sharpless, K. B.; Fokin, V. V.; Jia, G. Ruthenium-Catalyzed Cycloaddition of Alkynes and Organic Azides. *Journal of the American Chemical Society* **2005**, 127, 15998-15999.
85. Boren, B. C.; Narayan, S.; Rasmussen, L. K.; Zhang, L.; Zhao, H.; Lin, Z.; Jia, G.; Fokin, V. V. Ruthenium-Catalyzed Azide–Alkyne Cycloaddition: Scope and Mechanism. *Journal of the American Chemical Society* **2008**, 130, 8923-8930.
86. Majireck, M. M.; Weinreb, S. M. A Study of the Scope and Regioselectivity of the Ruthenium-Catalyzed [3 + 2]-Cycloaddition of Azides with Internal Alkynes. *The Journal of Organic Chemistry* **2006**, 71, 8680-8683.
87. Chen, Y.; Liu, Y.; Petersen, J. L.; Shi, X. Conformational control in the regioselective synthesis of N-2-substituted-1,2,3-triazoles. *Chemical Communications* **2008**, 3254-3256.
88. Davies, K. A.; Abel, R. C.; Wulff, J. E. Operationally Simple Copper-Promoted Coupling of Terminal Alkynes with Benzyl Halides. *The Journal of Organic Chemistry* **2009**, 74, 3997-4000.

89. Verkruijsse, H. D.; Heus-Kloos, Y. A.; Brandsma, L. Efficient methods for the preparation of acetylenic ketones. *Journal of Organometallic Chemistry* **1988**, 338, 289-294.
90. Tsai, C.-W.; Yang, S.-C.; Liu, Y.-M.; Wu, M.-J. Microwave-assisted cycloadditions of 2-alkynylbenzotriazoles with sodium azide: selective synthesis of tetrazolo[5,1-a]pyridines and 4,5-disubstituted-2H-1,2,3-triazoles. *Tetrahedron* **2009**, 65, 8367-8372.
91. Wang, X.-j.; Sidhu, K.; Zhang, L.; Campbell, S.; Haddad, N.; Reeves, D. C.; Krishnamurthy, D.; Senanayake, C. H. Bromo-Directed N-2 Alkylation of NH-1,2,3-Triazoles: Efficient Synthesis of Poly-Substituted 1,2,3-Triazoles. *Organic Letters* **2009**, 11, 5490-5493.
92. Carey, F. A.; Tremper, H. S. Carbonium ion-silane hydride transfer reactions. I. Scope and stereochemistry. *Journal of the American Chemical Society* **1968**, 90, 2578-2583.
93. Baer, H. H.; Zamkane, M. Stereospecific synthesis of (-)-anisomycin from D-galactose. *Journal of Organic Chemistry* **1988**, 53, 4786-4789.
94. Gevorgyan, V.; Liu, J.-X.; Rubin, M.; Benson, S.; Yamamoto, Y. A novel reduction of alcohols and ethers with a HSiEt<sub>3</sub>catalytic B(C<sub>6</sub>F<sub>5</sub>)<sub>3</sub> system. *Tetrahedron Letters* **1999**, 40, 8919-8922.
95. Williams, T. M.; Ciccarone, T. M.; MacTough, S. C.; Rooney, C. S.; Balani, S. K.; Condra, J. H.; Emini, E. A.; Goldman, M. E.; Greenlee, W. J.; Kauffman, L. R.; O'Brien, J. A.; Sardana, V. V.; Schleif, W. A.; Theoharides, A. D.; Anderson, P. S. 5-Chloro-3-(phenylsulfonyl)indole-2-carboxamide: A novel, non-nucleoside inhibitor of HIV-1 reverse transcriptase. *Journal of Medicinal Chemistry* **1993**, 36, 1291-1294.
96. Zhao, Z.; Wolkenberg, S. E.; Lu, M.; Munshi, V.; Moyer, G.; Feng, M.; Carella, A. V.; Ecto, L. T.; Gabryelski, L. J.; Lai, M.-T.; Prasad, S. G.; Yan, Y.; McGaughey, G. B.; Miller, M. D.; Lindsley, C. W.; Hartman, G. D.; Vacca, J. P.; Williams, T. M. Novel indole-3-sulfonamides as potent HIV non-nucleoside reverse transcriptase inhibitors (NNRTIs). *Bioorganic & Medicinal Chemistry Letters* **2008**, 18, 554-559.
97. Alexandre, F. R.; Amador, A.; Bot, S.; Caillet, C.; Convard, T.; Jakubik, J.; Musiu, C.; Poddesu, B.; Vargiu, L.; Liuzzi, M.; Roland, A.; Seifer, M.; Standing, D.; Storer, R.; Dousson, C. B. Synthesis and biological evaluation of aryl-phospho-indole as novel HIV-1 non-nucleoside reverse transcriptase inhibitors. *Journal of Medicinal Chemistry* **2011**, 54, 392-395.
98. Zhou, X.-J.; Pietropaolo, K.; Damphousse, D.; Belanger, B.; Chen, J.; Sullivan-Bólyai, J.; Mayers, D. Single-Dose Escalation and Multiple-Dose Safety, Tolerability, and Pharmacokinetics of IDX899, a Candidate Human Immunodeficiency Virus Type 1 Nonnucleoside Reverse Transcriptase Inhibitor, in Healthy Subjects. *Antimicrobial Agents and Chemotherapy* **2009**, 53, 1739-1746.
99. Zala, C.; St. Clair, M.; Dudas, K.; Kim, J.; Lou, Y.; White, S.; Piscitelli, S.; Dumont, E.; Pietropaolo, K.; Zhou, X.-J.; Mayers, D. Safety and Efficacy of GSK2248761, a Next-Generation Nonnucleoside Reverse Transcriptase Inhibitor, in Treatment-Naive HIV-1-Infected Subjects. *Antimicrobial Agents and Chemotherapy* **2012**, 56, 2570-2575.
100. Coowar, D.; Bouissac, J.; Hanbali, M.; Paschaki, M.; Mohier, E.; Luu, B. Effects of Indole Fatty Alcohols on the Differentiation of Neural Stem Cell Derived Neurospheres. *Journal of Medicinal Chemistry* **2004**, 47, 6270-6282.
101. Neagoie, C.; Vedrenne, E.; Buron, F.; Mérou, J.-Y.; Rosca, S.; Bourg, S.; Lozach, O.; Meijer, L.; Baldeyrou, B.; Lansiaux, A.; Routier, S. Synthesis of chromeno[3,4-b]indoles as Lamellarin D analogues : A novel DYRK1A inhibitor class. *European Journal of Medicinal Chemistry* **2012**, 49, 379-396.
102. Heaner Iv, W. L.; Gelbaum, C. S.; Gelbaum, L.; Pollet, P.; Richman, K. W.; DuBay, W.; Butler, J. D.; Wells, G.; Liotta, C. L. Indoles via Knoevenagel-Hemetsberger reaction sequence. *RSC Advances* **2013**, 3, 13232-13242.
103. Kunz, K.; Scholz, U.; Ganzer, D. Renaissance of Ullmann and Goldberg Reactions - Progress in Copper Catalyzed C-N-, C-O- and C-S-Coupling. *Synlett* **2003**, 2428-2439.
104. Monnier, F.; Taillefer, M. Catalytic C-C, C-N, and C-O Ullmann-Type Coupling Reactions: Copper Makes a Difference. *Angewandte Chemie International Edition* **2008**, 47, 3096-3099.

105. Monnier, F.; Taillefer, M. Catalytic C-C, C-N, and C-O Ullmann-Type Coupling Reactions. *Angewandte Chemie International Edition* **2009**, *48*, 6954-6971.
106. Marcoux, J. F.; Doye, S.; Buchwald, S. L. A general copper-catalyzed synthesis of diaryl ethers. *Journal of the American Chemical Society* **1997**, *119*, 10539-10540.
107. Ma, D.; Cai, Q. N,N-Dimethyl Glycine-Promoted Ullmann Coupling Reaction of Phenols and Aryl Halides. *Organic Letters* **2003**, *5*, 3799-3802.
108. Ju, Y.; Kumar, D.; Varma, R. S. Revisiting Nucleophilic Substitution Reactions: Microwave-Assisted Synthesis of Azides, Thiocyanates, and Sulfones in an Aqueous Medium. *The Journal of Organic Chemistry* **2006**, *71*, 6697-6700.
109. Bergman, J. A.; Hahne, K.; Song, J.; Hrycyna, C. A.; Gibbs, R. A. S-Farnesyl-Thiopropionic Acid Triazoles as Potent Inhibitors of Isoprenylcysteine Carboxyl Methyltransferase. *ACS Medicinal Chemistry Letters* **2011**, *3*, 15-19.
110. Cope, A. C. Condensation reactions. I. The condensation of ketones with cyanoacetic esters and the mechanism of the Knoevenagel reaction. *Journal of the American Chemical Society* **1937**, *59*, 2327-2330.
111. Hemetsberger, H.; Knittel, D.; Weidmann, H. Enazides, III: Thermolysis of  $\alpha$ -azido-cinnamates. Synthesis of indol carboxylates. *Monatshefte für Chemie* **1970**, *101*, 161-165.
112. Guchhait, S. K.; Kashyap, M.; Kamble, H. ZrCl<sub>4</sub>-mediated regio- and chemoselective Friedel-Crafts acylation of indole. *Journal of Organic Chemistry* **2011**, *76*, 4753-4758.
113. Baddeley, G.; Voss, D. The mechanism of Friedel-Crafts acylation. *Journal of the Chemical Society (Resumed)* **1954**, 418-422.
114. Huang, Z.; Jin, L.; Han, H.; Lei, A. The "kinetic capture" of an acylium ion from live aluminum chloride promoted Friedel-Crafts acylation reactions. *Organic and Biomolecular Chemistry* **2013**, *11*, 1810-1814.
115. Murakami, Y.; Tani, M.; Tanaka, K.; Yokoyama, Y. Synthetic Studies on Indoles and Related Compounds. XV. : An Unusual Acylation of Ethyl Indole-2-carboxylate in the Friedel-Crafts Acylation. *Chemical & pharmaceutical bulletin* **1988**, *36*, 2023-2035.
116. Ottoni, O.; De Neder, A. V. F.; Dias, A. K. B.; Cruz, R. P. A.; Aquino, L. B. Acylation of indole under Friedel - Crafts conditions - An improved method to obtain 3-acylindoles regioselectively. *Organic Letters* **2001**, *3*, 1005-1007.
117. Hassam, M.; Basson, A. E.; Liotta, D. C.; Morris, L.; van Otterlo, W. A. L.; Pelly, S. C. Novel cyclopropyl-indole derivatives as HIV non-nucleoside reverse transcriptase inhibitors. *ACS Medicinal Chemistry Letters* **2012**, *3*, 470-475.
118. Nyffeler, P. T.; Durón, S. G.; Burkart, M. D.; Vincent, S. P.; Wong, C.-H. Selectfluor: Mechanistic Insight and Applications. *Angewandte Chemie International Edition* **2005**, *44*, 192-212.
119. Parmerter, S. M.; Cook, A. G.; Dixon, W. B. The Synthesis of 4-Nitro-, 5-Nitro- and 7-Nitroindole. *Journal of the American Chemical Society* **1958**, *80*, 4621-4622.
120. Wu, G.; Robertson, D. H.; Brooks, C. L.; Vieth, M. Detailed analysis of grid-based molecular docking: A case study of CDOCKER—A CHARMM-based MD docking algorithm. *Journal of Computational Chemistry* **2003**, *24*, 1549-1562.
121. Hiremath, S. P.; Hiremath, D. M.; Purohit, M. G. Synthesis of Substituted Indolo[3,2-b][1,4]benzodiazepin-5-ones & 1-Arylimidazo[4,5-b]indol-2(1H)-ones. *Indian Journal of Chemistry Section B: Organic Chemistry including Medicinal Chemistry* **1987**, *26B*, 1042-1046.
122. Hooper, M. W.; Utsunomiya, M.; Hartwig, J. F. Scope and Mechanism of Palladium-Catalyzed Amination of Five-Membered Heterocyclic Halides. *The Journal of Organic Chemistry* **2003**, *68*, 2861-2873.
123. Barraja, P.; Diana, P.; Carbone, A.; Cirrincione, G. Nucleophilic reactions in the indole series: displacement of bromine under phase transfer catalysis. *Tetrahedron* **2008**, *64*, 11625-11631.

124. Romagnoli, R.; Baraldi, P. G.; Sarkar, T.; Carrion, M. D.; Cara, C. L.; Cruz-Lopez, O.; Preti, D.; Tabrizi, M. A.; Tolomeo, M.; Grimaudo, S.; Di Cristina, A.; Zonta, N.; Balzarini, J.; Brancale, A.; Hsieh, H. P.; Hamel, E. Synthesis and biological evaluation of 1-methyl-2-(3',4', 5'-trimethoxybenzoyl)-3-aminoindoles as a new class of antimetabolic agents and tubulin inhibitors. *Journal of Medicinal Chemistry* **2008**, 51, 1464-1468.
125. Goodacre, S. C. W., Karen; Price, Stephen; Dyke, Hazel Joan; Montana, John Gary; Stanley, Mark S; Bao, Liang; Lee, Wendy. Aza-Indolyl Compounds And Methods Of Use. WO2008/67481, 2008.
126. Ryabova, S. Y.; Alekseeva, L. M.; Granik, V. G. 2-formyl-3-arylaminoindoles in the synthesis of 1,2- and 1,4-dihydro-5H-pyrido[3,2-b]indole ( $\delta$ -carboline) derivatives. *Pharmaceutical Chemistry Journal* **1996**, 30, 579-584.
127. Zhang, X.; Raghavan, S.; Ihnat, M.; Thorpe, J. E.; Disch, B. C.; Bastian, A.; Bailey-Downs, L. C.; Dybdal-Hargreaves, N. F.; Rohena, C. C.; Hamel, E.; Mooberry, S. L.; Gangjee, A. The design and discovery of water soluble 4-substituted-2,6-dimethylfuro[2,3-d]pyrimidines as multitargeted receptor tyrosine kinase inhibitors and microtubule targeting antitumor agents. *Bioorganic & Medicinal Chemistry* **2014**, 22, 3753-3772.
128. Schmid, S.; Rottgen, M.; Thewalt, U.; Austel, V. Synthesis and conformational properties of 2,6-bis-anilino-3-nitropyridines. *Organic & Biomolecular Chemistry* **2005**, 3, 3408-3421.
129. Barreca, M. L.; Rao, A.; Luca, L. D.; Iraci, N.; Monforte, A.-M.; Maga, G.; Clercq, E. D.; Pannecouque, C.; Balzarini, J.; Chimirri, A. Discovery of novel benzimidazolones as potent non-nucleoside reverse transcriptase inhibitors active against wild-type and mutant HIV-1 strains. *Bioorganic & Medicinal Chemistry Letters* **2007**, 17, 1956-1960.
130. Monforte, A. M.; Logoteta, P.; De Luca, L.; Iraci, N.; Ferro, S.; Maga, G.; De Clercq, E.; Pannecouque, C.; Chimirri, A. Novel 1,3-dihydro-benzimidazol-2-ones and their analogues as potent non-nucleoside HIV-1 reverse transcriptase inhibitors. *Bioorganic & medicinal chemistry* **2010**, 18, 1702-10.
131. Wuitschik, G.; Rogers-Evans, M.; Müller, K.; Fischer, H.; Wagner, B.; Schuler, F.; Polonchuk, L.; Carreira, E. M. Oxetanes as promising modules in drug discovery. *Angewandte Chemie - International Edition* **2006**, 45, 7736-7739.
132. Campbell-Verduyn, L.; Elsinga, P. H.; Mirfeizi, L.; Dierckx, R. A.; Feringa, B. L. Copper-free 'click': 1,3-dipolar cycloaddition of azides and arynes. *Organic & Biomolecular Chemistry* **2008**, 6, 3461-3463.
133. Cinnamoyl inhibitors of transglutaminase. WO2008/144933, 2008.
134. Chen, G.; Zhou, Y.; Cai, C.; Lu, J.; Zhang, X. Synthesis and Antifungal Activity of Benzamidine Derivatives Carrying 1,2,3-Triazole Moieties. *Molecules* **2014**, 19, 5674-5691.
135. Tachykinin receptor antagonists. WO2005/821, 2005.
136. Golas, P. L.; Tsarevsky, N. V.; Matyjaszewski, K. Structure-Reactivity Correlation in "Click" Chemistry: Substituent Effect on Azide Reactivity. *Macromolecular Rapid Communications* **2008**, 29, 1167-1171.